UNIVERSITÉ DU LUXEMBOURG

PhD-FSTM-2025-092
The Faculty of Science, Technology and Medicine

DISSERTATION

Defence held on 03/10/2025 in Esch-sur-Alzette

to obtain the degree of

DOCTEUR DE L'UNIVERSITÉ DU LUXEMBOURG

EN *SCIENCES DE L'INGÉNIEUR*

by

Anna TOKAREVA
Born on 9 January 1991 in Almaty (Kazakhstan)

RECYCLING OF DEMOLITION WASTES FOR MANUFACTURING CO2-REDUCED CEMENT

Dissertation defence committee

Dr Danièle WALDMANN, dissertation supervisor
Professor, Technische Universität Darmstadt

Dr Joachim HANSEN, Chairman
Professor, Université du Luxembourg

Dr Jean-Frank WAGNER
Professor, Universität Trier

Dr Romain TRAUCHESSEC
Professor, Université de Lorraine

Dr Eduardus KOENDERS
Professor, Technische Universität Darmstadt

Acknowledgments

I would like to express my sincere gratitude to Prof. Danièle Waldmann (Technical University of Darmstadt) for her guidance and supervision throughout this research project. Her expertise and support were invaluable to the successful completion of this work.

I am also deeply grateful to the members of the thesis jury — Prof. Joachim Hansen (University of Luxembourg), Prof. Jean-Frank Wagner (Trier University), Prof. Romain Trauchessec (University of Lorraine), and Prof. Eddie Koenders (Technical University of Darmstadt) — for their constructive evaluation and insightful comments.

I extend special thanks to Prof. Joachim Hansen, Prof. Jean-Frank Wagner, and Prof. Romain Trauchessec for their helpful suggestions, critical feedback, and the valuable information they shared during various stages of this work.

I gratefully acknowledge the technical support and training provided by Mr. Marc Seil, Mr. Ed Weyer, Dr. Gilbert Klein, Mr. Mehdi Saeidi, Prof. Markus Schlienz, and Mrs. Zornitza Tosheva (University of Luxembourg); the team of the Laboratory of Ponts et Chaussées (Luxembourg); Dr. Claude Simon and Mr. Sven Jung (Cimalux, Luxembourg); Dr. Baptiste Luzu (University of Lorraine); and Dr. Neven Ukrainchyk (Technical University of Darmstadt). Their contributions were essential to the experimental aspects of this thesis.

I would like to thank the companies and individuals who kindly provided materials for this research: Mr. Robin Chapelle and Mr. Nicolas-Alexandre Eugene (Tradecowall, Belgium), Mr. Patrick Copus (Polygone Sàrl, Luxembourg), Mr. Cédric Langard (Xardel Demolition, Luxembourg), and Dr. Olivier Martinage (Groupe Vicat, France).

My heartfelt thanks go to my colleagues who became friends during this journey: Mrs. Suzanne Biwer, Dr. Sinan Kaassamani, Dr. Hooman Eslami, Dr. Tarik Camo, and Dr. Lorenc Bogoviku, for their camaraderie, kindness, and encouragement.

Above all, I wish to express my deepest gratitude to my mother, Natalya Tokareva, and my husband, Ludovic Zipsin, whose unwavering support, love, and patience have sustained me throughout this journey.

Abstract

The cement industry is one of the major contributors to global CO_2 emissions, primarily due to the limestone decarbonation and high energy consumption during clinker production. With increasing regulatory pressure to meet climate goals and the declining availability of traditional Supplementary Cementitious Materials (SCMs) like fly ash and blast furnace slag, there is a growing need to explore alternative, sustainable materials. This research addresses that need by investigating the recycling of fine construction and demolition waste (CDW) into viable SCMs for the production of CO_2-reduced cement.

The thesis is structured as a cumulative work comprising four peer-reviewed articles, each contributing to the overarching goal of assessing the technical feasibility and durability performance of CDW-derived SCMs. The study specifically focuses on fine fractions of recycled concrete and ceramic waste, two abundantly available yet underutilized by-products in the construction sector.

A key innovation in this research lies in the thermal treatment of hydrated cement paste within recycled concrete at moderate temperatures. This process successfully reactivates cementitious phases without decomposing carbonates, thus minimizing CO_2 emissions. Concrete fines were subjected to activation at two temperatures (400 and 500 °C), and their hydraulic reactivity, fresh and hardened properties, and microstructural characteristics were systematically evaluated. Similarly, the pozzolanic potential of finely ground ceramic waste, such as terracotta and porcelain, was studied in both ordinary blended cements and LC3 (limestone-calcined clay cement) formulations.

Comprehensive durability assessments were conducted, including 28 freeze-thaw cycles, fire resistance at 200, 300, 500 and 900 °C, 1% sulphuric acid solution attack, shrinkage, and capillary absorption. The findings indicate that incorporation of recycled concrete-based powders does not significantly affect the durability performance of mortars, neither before nor after thermal activation. By contrast, ceramic roofing wastes significantly enhance the long-term performance of blended cement systems when properly processed, due to the formation of densified microstructures through pozzolanic reactions.

Importantly, the study also explores the practicality of using unsorted mixed waste streams, providing insights into cost-effective and scalable industrial applications. The research outcomes

support the viability of a circular economy model in the cement and construction industries by offering environmentally sound, technically robust alternatives to traditional SCMs. Through statistical analysis, the work establishes correlations between chemical composition, particle treatment, and performance indicators, offering a scientifically grounded framework for industrial implementation.

This thesis contributes to the fields of materials science, environmental engineering, and construction technology by presenting a holistic approach to reducing the carbon footprint of cement through waste valorisation. The results not only pave the way for more sustainable building practices but also provide a strategic solution to the twin challenges of construction waste management and climate change mitigation.

List of abbreviations

SCM	Supplementary Cementitious Material
CDW	Construction and Demolition Waste
OPC	Ordinary Portland Cement
LC3	Limestone Calcined Clay Cement
CEM I	Portland Cement (EN 197-1 designation)
CS / MS / WM	Concrete Screenings / Mixed Screenings / Washing Mud
CSN / MSN / WMN	Dried in ambient conditions variants of above
CS105 / MS105 / WM105	Dried at 105 °C variants
CS400 / MS400 / WM400	Calcined at 400 °C variants
CS500 / MS500 / WM500	Calcined at 500 °C variants
RT / RP	Recycled Terracotta / Recycled Porcelain
RTU / RPU	Ultrafine Terracotta / Ultrafine Porcelain Powders
LRT / LRP / LRTU / LRPU	LC3-type mixes with respective ceramic
REF	Reference Portland cement mortar
SSA	Specific Surface Area
PSD	Particle Size Distribution
XRD	X-ray Diffraction
SEM	Scanning Electron Microscopy
TGA	Thermogravimetric Analysis
DTA	Differential Thermal Analysis
SAI	Strength Activity Index
w/b	Water-to-Binder Ratio
s/b	Sand-to-Binder Ratio
ANOVA	Analysis of Variance
MANOVA	Multivariate Analysis of Variance
LF	Limestone Filler

Structure of the Thesis

The present dissertation is structured as a cumulative thesis, comprising four peer-reviewed publications. The first three papers have been published in the globally renowned, top-ranking journal *Construction and Building Materials*. As of 2025, the journal has an Impact Factor of 7.4 and a CiteScore of 13.8, underscoring its high academic reputation. The thesis is divided into eight chapters, systematically presenting the research background, methodologies, findings, and implications.

Chapter 1 provides a general introduction to the dissertation, outlining the motivations behind the research, the primary objectives, and the contributions of each publication to the overall research goal. Furthermore, it establishes the interconnections between the four published papers, demonstrating their collective role in advancing the understanding of CO2-reduced cement production from demolition waste materials.

Chapter 2 presents a comprehensive literature review, offering background information on CO2 emissions in cement production and the role of blended cements. This chapter also discusses the potential of recycling demolition waste for sustainable cement production, elaborating on the environmental impact, composition, and mechanical properties of various waste-derived cement clinker substitutes, as well as their durability in cement-based materials.

Chapters 3 to 6 contain the core research findings, as presented in the four published scientific articles. These chapters detail the methodologies, experimental investigations, and analyses conducted to assess the viability of fine demolition waste materials for CO2-reduced cement production:

Chapter 3 and Chapter 5 focus on the characterization and performance of concrete-based demolition waste materials. Chapter 3 describes the evaluation of their hydraulic activity and mechanical properties, while Chapter 5 is dedicated to their durability aspects.

Chapter 4 and Chapter 6 explore ceramic demolition waste materials, examining their suitability as pozzolanic materials. Chapter 4 presents the analysis of their influence on fresh and hardened

cementitious systems and microstructural characteristics, and Chapter 6 gives the assessment of their durability performance.

Chapter 7 provides a general discussion, synthesizing the comparison of all investigated materials. It offers a comparative analysis of concrete and ceramic demolition waste materials, evaluates their compliance with standards requirements, and offer the comprehensive statistical analysis. Furthermore, it incorporates recent developments in the field that have emerged since the publication of these papers, ensuring the research remains current within the broader scientific discourse.

Finally, **Chapter 8** concludes the dissertation by summarizing the key insights gained from the research. It also highlights the contributions of the study to the field of CO2-reduced cement production, discusses the practical applications of the findings, and addresses the limitations of the study while suggesting directions for future research. These conclusions provide valuable insights for the advancement of sustainable construction materials and lay the foundation for future innovations in CO2-reduced cement technologies.

A visual representation of the overall thesis structure is provided in Fig. IV.1, offering a schematic overview of the dissertation's organization and logical progression.

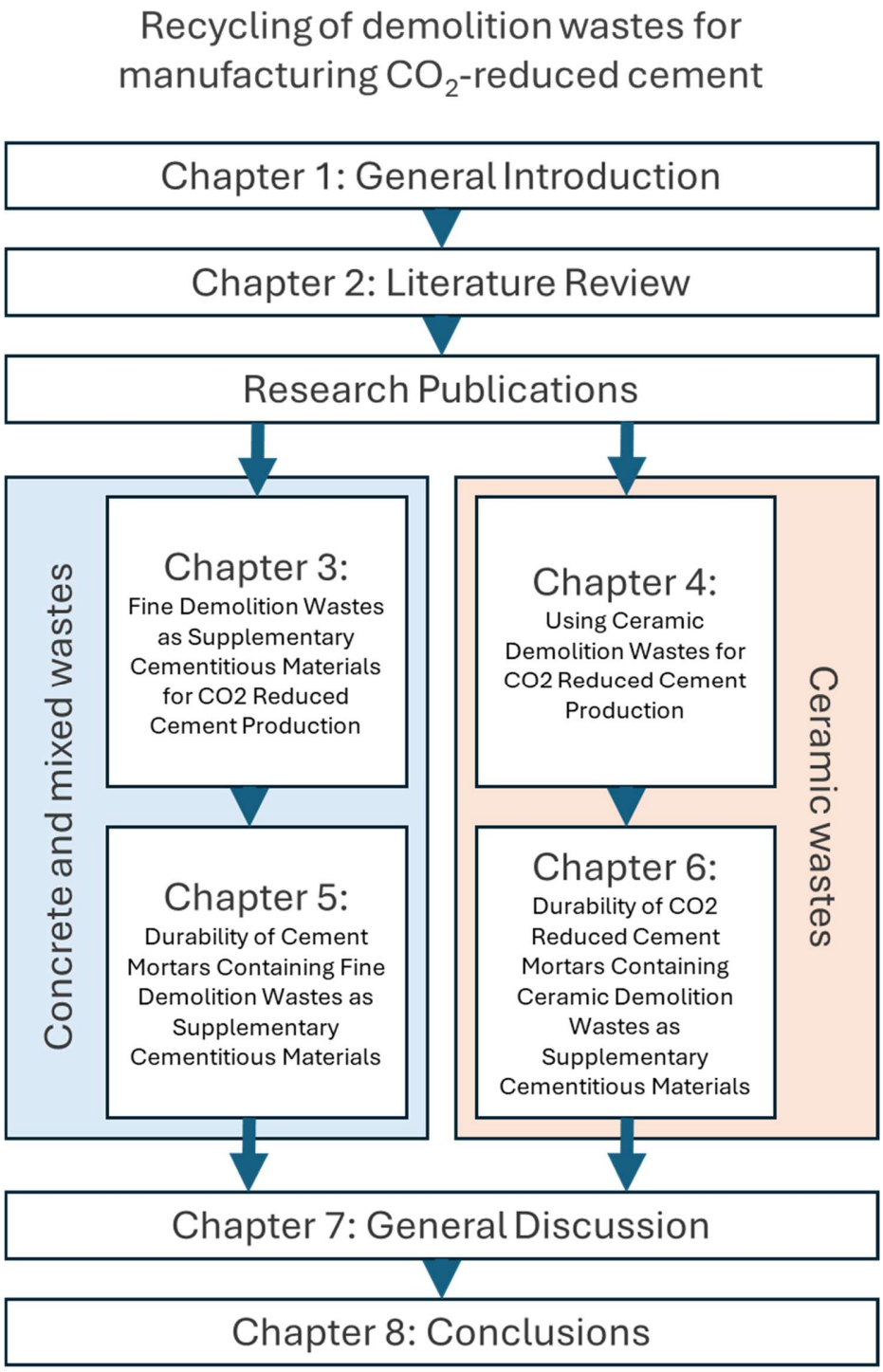

Fig. IV.1. Schematic overview of the thesis structure.

Table of Contents

Chapter 1: General introduction

1.1. The role of CO2-reduced cement in sustainable construction

Construction projects encompass a vast array of structural developments, including offshore infrastructure such as ports; hydropower structures like dams; sewage and wastewater treatment facilities; industrial complexes; water pipelines, reservoirs, and other water management facilities; transportation infrastructure including bridges, roads, highways, and drainage systems; residential and commercial buildings; and agro-industrial structures, among others. Each of these sectors has unique design specifications and material requirements. However, a common denominator across all construction activities is the reliance on cement and concrete as primary building materials due to their high strength, versatility, durability, and cost-effectiveness. However, cement production is highly energy-intensive and a major contributor to global carbon dioxide (CO_2) emissions.

The growing concern over climate change and environmental sustainability has led to heightened regulatory pressures, pushing industry toward more sustainable alternatives. In this context, CO_2-reduced cement has emerged as a promising solution to mitigate the environmental footprint of cement manufacturing. Transitioning to a low-carbon cement industry and adopting sustainable construction practices are now imperative steps toward minimizing carbon emissions and mitigating the adverse effects of climate change on human populations and ecosystems.

Currently, the most effective strategy for reducing CO_2 emissions from the cement industry is to decrease the clinker content in cement blends by incorporating Supplementary Cementitious Materials (SCMs). Clinker, the primary binding component in cement, is responsible for the bulk of emissions associated with cement production due to its energy-intensive calcination process, which releases large amounts of CO_2 after limestone decomposition. By partially replacing clinker with SCMs, it is possible to lower emissions while enhancing resource efficiency, promoting waste valorisation, and supporting circular economy principles.

The adoption of CO_2-reduced cement aligns with key global sustainability initiatives, including the Paris Agreement and the United Nations Sustainable Development Goals (SDGs). Specifically, it supports:

- SDG 9 (Industry, Innovation, and Infrastructure): By fostering advancements in green construction materials and promoting technological innovation in cement manufacturing.
- SDG 13 (Climate Action): By significantly reducing greenhouse gas emissions associated with the built environment and contributing to the broader goal of climate change mitigation.

Blended cements containing SCMs are already widely used across various construction sectors. However, their applicability remains limited in specific scenarios, particularly where rapid strength gain and high hydration rates are required, such as construction in extremely cold environments.

While the integration of SCMs into cement blends has made notable progress, the current rate of clinker substitution remains insufficient to meet global sustainability targets. Moreover, the primary SCMs currently used in cement production, such as blast furnace slag and fly ash, are becoming increasingly scarce due to changes in industrial practices. Improvements in steel production technology have reduced the usage of blast furnaces and as consequence, the generation of blast furnace slag, while the phase-out of coal-fired power plants has led to a decline in fly ash availability. This trend underscores the urgency of identifying and developing alternative SCMs to maintain progress toward low-carbon cement production. For this reason, researchers are actively exploring non-standard SCMs that could serve as viable alternatives. Promising materials include:

- Calcined clays
- Biogenic ashes, like rice husk ash or sugarcane bagasse ash
- Recycled inert wastes like construction and demolition waste

Despite their potential, these alternative SCMs face several practical and regulatory barriers. Many remain underutilized due to a lack of certification, variations in composition and local availability. Additionally, concerns regarding long-term durability and structural performance limit their widespread adoption.

A further increase in alternative SCM usage is necessary, but achieving this requires overcoming several technical, economic, and supply-related barriers:

1. Technical Challenges of Alternative SCMs

   The introduction of new SCMs into cement formulations also presents technical challenges. For instance, concretes incorporating these materials often exhibit lower early-age strength than traditional cementitious formulations. This can pose construction risks, particularly in applications requiring rapid formwork removal or early load-bearing capacity. To address these limitations, further research and optimization of mix designs are needed to enhance the performance of low-carbon cements.

2. Economic and Market Challenges

   The production costs of certain low-carbon cements can be higher due to additional processing requirements, logistical challenges, and limited supply chains for alternative SCMs. Achieving economies of scale and introducing financial incentives for sustainable materials will be essential to enhance market competitiveness.

3. Industry Scepticism and Resistance to Change

   The construction sector has traditionally relied on well-established SCMs, leading to scepticism toward newer alternatives. Comprehensive education, training programs, and pilot projects are necessary to build confidence in new CO_2-reduced cement and demonstrate its feasibility to industry professionals.

Achieving meaningful decarbonization in the cement and concrete industry will require a systemic, multi-stakeholder approach. While advancements in cement technology are crucial, a successful transition to low-carbon construction cannot rely solely on the cement industry. Key players such as construction contractors, architects, designers, policymakers and consumers must actively participate in the new materials integration into the cement industry. By addressing existing challenges and fostering innovation, the cement sector can play a pivotal role in creating a more sustainable, resilient, and low-carbon built environment.

1.2. Objectives of the research

The present study investigates the potential utilization of various construction and demolition wastes (CDW) as alternative SCMs. The construction industry generates vast quantities of CDW, a significant proportion of which remains unutilized, particularly the fine fraction resulting from the screening and washing of recycled aggregates. These fine wastes storage pose challenges on site such as dust generation during dry conditions and the formation of impassable mud in wet conditions. Simultaneously, traditional SCMs are becoming increasingly scarce, necessitating the exploration of alternative materials. This research aims to assess the viability of CDW as a

sustainable SCM, offering a solution to waste accumulation while reducing the environmental impact of cement production.

The primary objective of this research is to develop an effective approach for recycling CDW into viable SCMs, thereby promoting sustainability in the construction sector. The specific objectives include:

- Evaluating the suitability of fine CDW fractions as SCMs in cement production.
- Investigating the impact of thermal activation on the reactivity of concrete powders.
- Assessing the pozzolanic properties of recycled ceramics and their potential replacement of calcined clay in LC3 cements.
- Analysing the effects of mixed wastes (concrete and ceramics) on cement properties.
- Examining the influence of CDW-based SCMs on the durability and performance of eco-friendly cement formulations.

CDW were selected as the subject of the research for the following reasons:

1. Availability and Industrial Interest

   CDW is abundantly available near urban areas, reducing transportation costs and energy expenditures. The recycling aggregates industry generates large quantities of fine waste that currently lack applications, leading to their accumulation at processing sites. The integration of CDW into cement production provides a sustainable alternative, addressing both waste management and resource scarcity issues.
2. Environmental Considerations

   The global cement industry is a major contributor to carbon emissions and natural resource depletion. Traditional SCMs such as fly ash and slag are becoming less accessible due to declining coal-fired power plants and limited industrial by-products. Alternative SCMs such as natural pozzolans require quarrying, further impacting the environment. In contrast, CDW is an underutilized waste material that does not require additional extraction, making it a promising alternative with minimal ecological footprint.

The study is based on existing knowledge regarding the reactivity and potential of CDW-derived materials in cement applications:

- Hydrated cement can be reactivated by thermal treatment at temperatures above 400°C.
- Finely ground ceramics exhibit pozzolanic properties.

These fundamental principles form the basis for the hypotheses explored in this research:

Hypothesis 1. Heating concrete powders to approximately 500°C will be sufficient to reactivate hydrated cement phases while avoiding CO2 emissions associated with limestone and dolomite decomposition, which occurs at higher temperatures. Furthermore, the formation of free lime due to decomposition of portlandite will be minimized.

Hypothesis 2. The lack of free lime in the thermally activated recycled concrete wastes will contribute to the durability of the eco-cement, making it comparable to conventional Portland cement in terms of long-term performance.

Hypothesis 3. Finely ground ceramic waste possesses sufficient pozzolanic activity, allowing it to serve as a substitute for calcined clay in the production of LC3 cement.

Hypothesis 4. Cement incorporating recycled ceramics will exhibit improved durability due to the pozzolanic reactions and the resultant dense microstructure.

Additionally, the study will determine whether separating concrete and ceramic waste before processing is necessary or if a combined waste stream can be effectively utilized in cement production.

The study presents several novel aspects that distinguish it from existing research in the field of SCMs and recycling of CDW:

- Unlike traditional high-temperature calcination used for SCM activation, this study investigates a lower-temperature thermal treatment (up to 500 °C) to reactivate cementitious properties in waste concrete. This approach aims to avoid free lime formation and CO_2 emissions from limestone and dolomite decomposition, making the process more sustainable.
- Most studies separate different types of CDW before processing. This research examines whether mixed CDW can be effectively used without extensive sorting. This has practical implications for recycling facilities, potentially simplifying processing and reducing costs.
- LC3 cement typically uses calcined clay, which requires additional quarrying and energy-intensive processing. This study explores the potential of ground ceramic wastes as a direct substitute, leveraging their pozzolanic properties to enhance cement performance.
- While previous research has examined the fresh paste and mechanical properties of cements with reactivated recycled concrete powders and ceramics, this study investigates the long-term durability and performance of CDW-enhanced cement formulations.
- Many laboratory-scale studies use unrealistic processing conditions. This research aims to align closely with real-world industrial recycling methods, ensuring practical

implementation. The study minimizes additional energy consumption and suggests strategies that can be integrated into existing cement and recycling industries.

- Unlike other research, this study does not use laboratory-made concrete for reactivation but instead utilizes real CDWs. Furthermore, it compares different types of CDW, including concrete, concrete-ceramic mixtures, terracotta, and porcelain, providing a comprehensive evaluation of various waste streams.

The study primarily addresses the interests of:

- Recycling companies specializing in the production of recycled aggregates, providing them with an additional market for fine waste fractions.
- Cement manufacturers, who require sustainable SCM alternatives to reduce their carbon footprint and dependency on traditional SCMs.
- Construction companies, offering them access to eco-friendly cementitious materials with comparable performance to Portland cement.
- Regulatory bodies and environmental organizations, which can use the findings to promote policies that encourage circular economy practices in the construction sector.
- The general public, raising awareness about the benefits of sustainable construction materials in mitigating climate change and reducing industrial waste.

1.3. Contribution of each paper to the research goal and links between publications

Each article included in the dissertation verifies a specific hypothesis, contributing to the overarching research objective of assessing the potential of fine demolition waste materials for CO2-reduced cement production. All publications are essential for understanding the progressive development of the study, from material characterization to durability analysis and comparative evaluation.

Article I

A. Tokareva, S. Kaassamani, D. Waldmann, "Fine demolition wastes as supplementary cementitious materials for CO2 reduced cement production," *Construction and Building Materials*, 392 (2023) 131991, https://doi.org/10.1016/j.conbuildmat.2023.131991.

This paper investigates the composition and hydraulic activity of three demolition waste materials: concrete aggregates screening fines (CS), mixed aggregates screening fines (MS) and mud from recycled aggregates washing (WM), after undergoing four different treatments:

- Natural drying (CSN, MSN, WMN)
- Drying at 105°C (CS105, MS105, WM105)
- Heating at 400°C (CS400, MS400, WM400)
- Heating at 500°C (CS500, MS500, WM500)

The study evaluates the impact of these treatments on fresh paste properties, compressive strength, and microstructure of mortars incorporating 20% of each recycled powder.

Hypothesis Tested:

> Heating concrete powders to approximately 500°C will reactivate hydrated cement phases while avoiding CO2 emissions from limestone and dolomite decomposition, thus minimizing free lime formation.

Key Contributions:

- Assesses the suitability of fine concrete CDW as SCMs in cement production.
- Gives information about effect of mixed wastes on blended cement properties.
- Investigates the impact of thermal activation on the reactivity of concrete powders.
- Provides insights for the selection of optimal preparation conditions for further durability testing in Article III.

Article II

A. Tokareva, S. Kaassamani, D. Waldmann, "Using ceramic demolition wastes for CO2-reduced cement production," *Construction and Building Materials*, 426 (2024) 135980, https://doi.org/10.1016/j.conbuildmat.2024.135980.

This study examines the composition and pozzolanic activity of fine and ultrafine terracotta and porcelain powders (RT, RTU, RP, and RPU). The fresh paste properties, mechanical performance

(flexural and compressive strength), and microstructure of mortars incorporating 10%, 20% and 30% ceramic powders, as well as LC3 mixtures with the same ceramic content and 5%, 10% and 20% limestone are analysed.

Hypothesis Tested:

> Finely ground ceramic waste possesses sufficient pozzolanic activity to substitute calcined clay in LC3 cement production.

Key Contributions:

- Determines the suitability of different fine ceramic demolition wastes in cement production.
- Assesses the potential of recycled ceramics to replace calcined clay in LC3 cements.
- Provides guidance for the selection of optimal blended cement compositions for further durability testing in Article IV.

Article III

A. Tokareva, D. Waldmann, "Durability of cement mortars containing fine demolition wastes as supplementary cementitious materials," *Construction and Building Materials,* 477 (2025) 141316, https://doi.org/10.1016/j.conbuildmat.2025.141316.

This paper evaluates the durability characteristics of cement mortars incorporating 20% of CS, MS, and WM, focusing on freeze-thaw resistance, fire resistance, resistance to chemical sulfuric acid corrosion and also capillary adsorption and drying shrinkage.

Hypothesis Tested:

> The absence of free lime in thermally activated recycled concrete waste contributes to the durability of eco-cement, making it comparable to conventional Portland cement.

Key Contributions:

- Assesses the suitability of fine concrete CDW as SCMs in cement production.
- Establishes the effects of mixed wastes on cement properties.
- Complements the findings of Article I by providing durability assessments.

Article IV

A. Tokareva, D. Waldmann, "Durability assessment of cement mortars with recycled ceramic powders," *Materials,* 18 (2025) 4420, https://doi.org/10.3390/ma18184420.

This study evaluates the durability of cement mortars containing 20% fine and ultrafine terracotta powders (RT and RTU) and LC3 mortars with 20% ceramic powders and 10% limestone filler. The durability parameters investigated include freeze-thaw resistance, fire resistance, resistance to chemical sulfuric acid corrosion and also capillary adsorption and drying shrinkage.

Hypothesis Tested:

> Cement incorporating recycled ceramics will exhibit improved durability due to pozzolanic reactions and a dense microstructure.

Key Contributions:

- Confirms the suitability of fine ceramic demolition wastes for durable cement formulations.
- Complements the findings of Article II by providing durability assessments.

Synthesis and Interconnections Between Publications

The combined findings of all four publications enable a comprehensive comparison of the impact of different demolition waste materials on blended cement properties. The results support waste separation strategies and provide recommendations for optimal processing methods for their incorporation into cement production.

Although the general preparation and analysis process for waste materials was similar, some differences existed:

- Theoretically, ceramic wastes did not require thermal activation, as the initial materials had already been fired at high temperatures. However, achieving pozzolanic properties necessitated a very fine particle size.
- The reactivity of ceramic and concrete waste materials varied, requiring different analytical techniques (e.g., hydration heat measurements for concrete waste and portlandite consumption tests for ceramic waste).

The methodology used to study the durability of all mortars specimens was the same, enabling a comparative analysis of all the results in Chapter 7.

A general schematic representation of the preparation methodology for all waste materials is provided in Fig. 1.1.

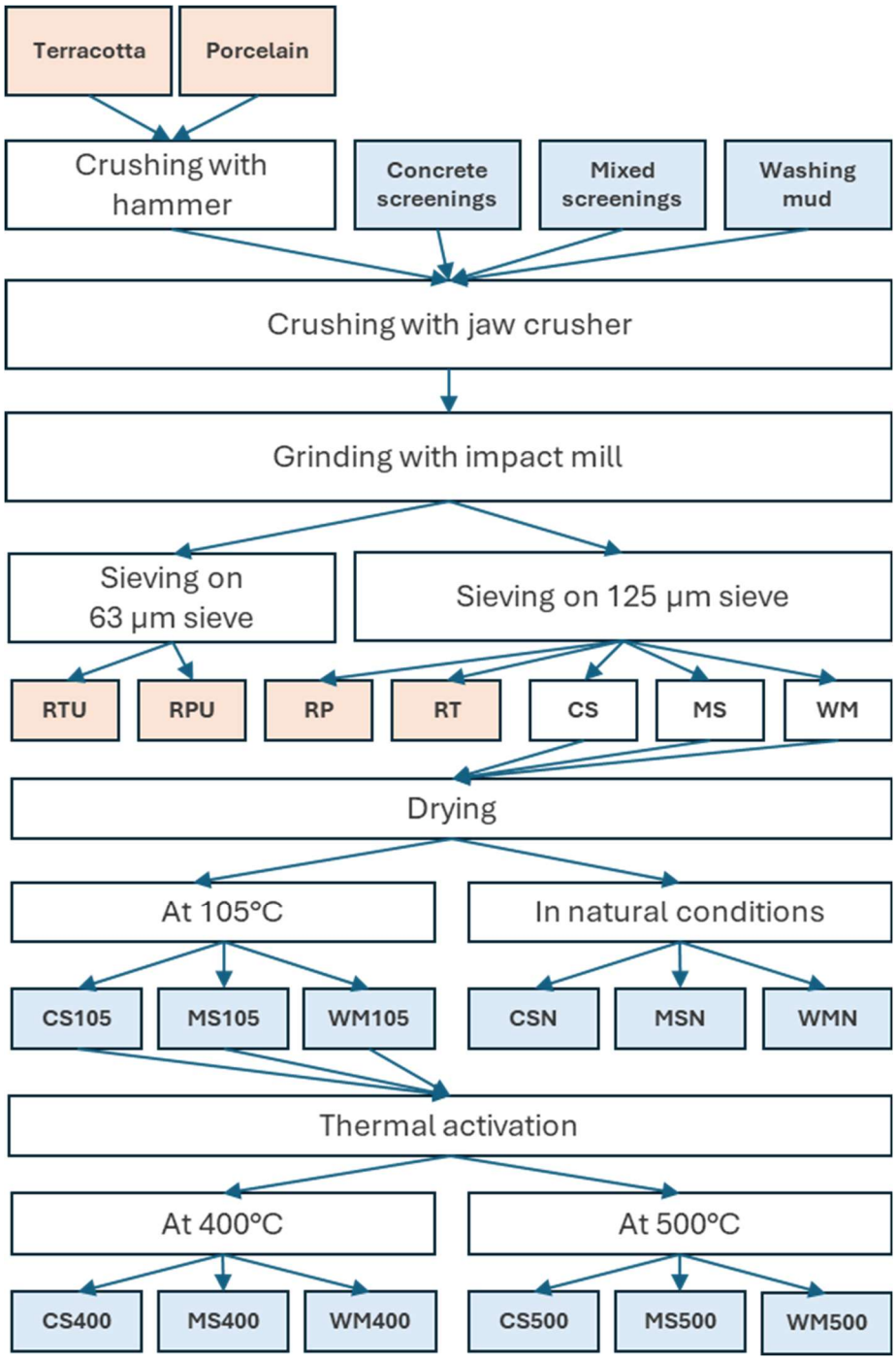

Fig. 1.1. Preparation methodology of all investigated waste materials.

Chapter 2: Literature review

2.1. CO2 Emissions in cement production

Cement is a fundamental material in modern construction, serving as the primary binding agent in concrete, the most widely used construction material globally, as well as in mortars, screeds, coatings, and soil stabilization. Its popularity is attributed to its wide availability, relatively low cost, and versatility.

The consumption of cement has increased substantially over the past decades, driven by population growth, urbanization, and infrastructure development. The proportion of the world's population living in urban areas has increased from 30% to 54% over the past 65 years and is projected to reach 66% by 2050 [1]. This demographic shift has led to a surge in construction material demand, particularly in developing economies, where infrastructure expansion often coincides with the need to replace aging structures. Consequently, cement consumption is growing at an unprecedented rate, with demand expected to rise by 12–23% above 2020 levels by 2050 [2]. As a result, global cement production is projected to reach 3.7–4.4 billion tons by 2050 [3].

Currently, the most commonly used cement is Ordinary Portland Cement (OPC), which consists of finely milled cement clinker with up to 5% gypsum. Cement clinker is produced in a rotary kiln through either a wet or dry process. The wet process is significantly less energy efficient and is now rarely used [4]. A schematic representation of a typical cement production process using the dry method is shown in Fig. 2.1.

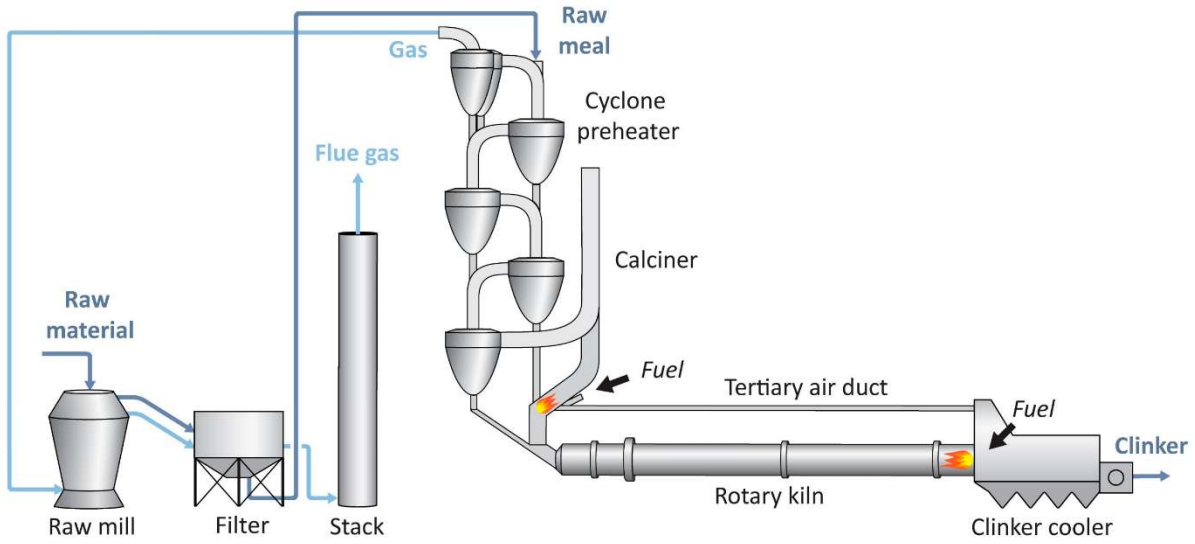

Fig. 2.1. Schematic of the cement clinker production process using the dry method [5].

The main steps of cement production are as follows [5]:

1. Raw Material Preparation:
    - Raw materials (such as limestone, clay, marl, and others) are fed into a raw mill, where they are ground into a fine powder known as raw meal.
    - Simultaneously, the raw meal is dried using hot flue gas from the preheater.
    - The flue gas and raw meal are then separated in a dust filter.
    - The raw meal is sent to the preheater, while the flue gas is released through the stack.
2. Preheating and Calcination:
    - In the preheater, the raw meal is heated by hot flue gas from both the calciner and the rotary kiln.
    - The meal and hot gases mix for efficient heat transfer, then separate in a series of cyclones arranged in a vertical cascade.
    - The preheated raw meal enters the calciner, where the majority of calcium carbonate ($CaCO_3$) decomposes into calcium oxide (CaO) and carbon dioxide (CO_2).
    - Approximately 60% of the total fuel input is consumed in the calciner, where the temperature reaches ~860°C to drive the endothermic decomposition of $CaCO_3$.

3. Clinker Formation in the Rotary Kiln:
    - The calcined raw meal is fed into the rotary kiln.
    - Any remaining unreacted limestone is fully calcined in the initial few meters of the kiln.
    - The main burner heats the kiln, consuming the remaining 40% of the total fuel input.
    - Clinker nodules form in the high-temperature zone of the kiln.
    - The solid material reaches 1450°C, while the gas phase can reach 2000°C.
4. Clinker Cooling and Heat Recovery:
    - The hot clinker exits the kiln and enters the clinker cooler, where it is rapidly cooled using ambient air.
    - Some of the resulting hot air is recovered and used as secondary air for combustion in the main burner and as tertiary air for combustion in the calciner.

One of the most pressing concerns regarding cement production is its significant contribution to global CO_2 emissions. These emissions primarily arise from two sources: the calcination process, which accounts for 50% of emissions, and the combustion of fuels for heating, which contributes around 40%. The remaining 10% of emissions originate from electricity consumption and transportation [3, 6]. On average, the production of one ton of cement releases approximately 866 kg of CO_2 into the atmosphere [7]. Cement manufacturing is one of the most carbon-intensive industrial processes, emitting approximately 1.57 billion tonnes of CO_2 in 2023, as shown in Fig. 2.2 [8].

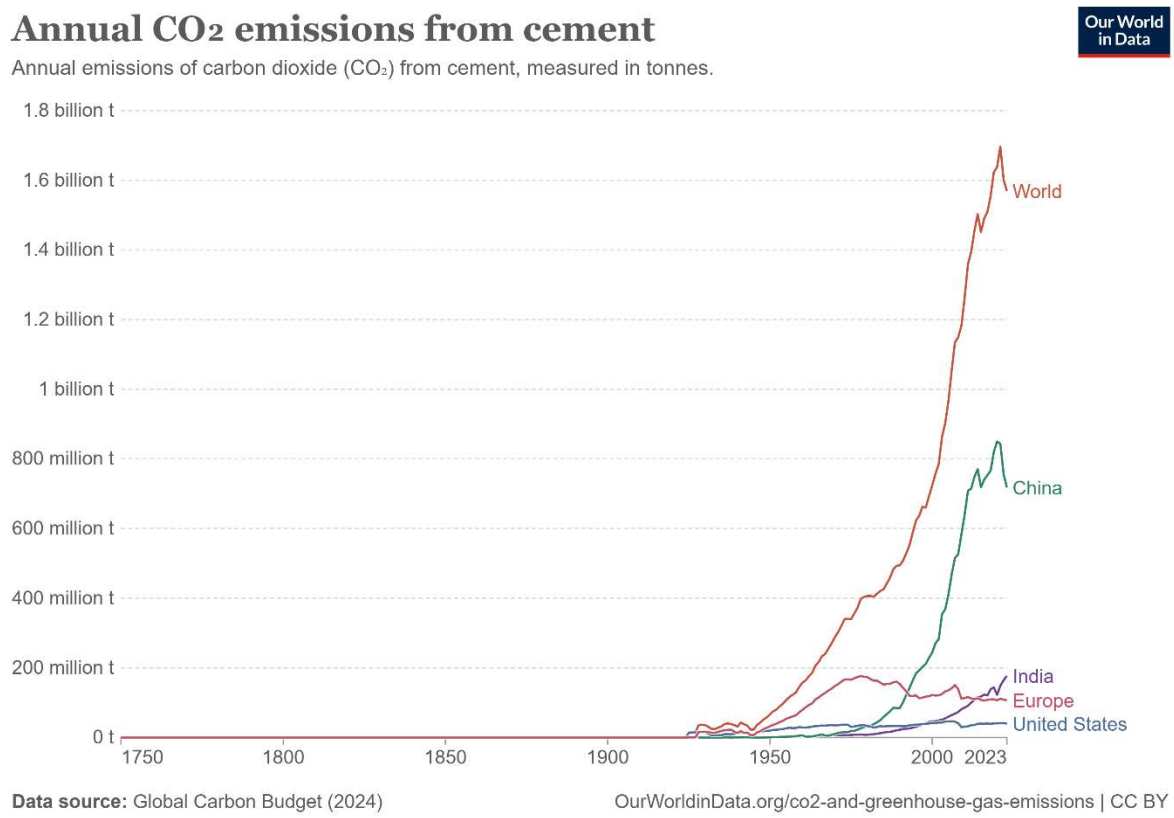

Fig. 2.2. Annual emissions of carbon dioxide from cement production [8].

Several strategies have been proposed and implemented to mitigate the carbon footprint of cement production:

- **Energy efficiency improvements**

Process optimization, automation, and upgrading manufacturing technologies contribute to reducing energy consumption and emissions [6, 9 - 11].

- **Use of alternative fuels**

The replacement of traditional fossil fuels with alternative fuels such as biomass, waste-derived fuels, and lower-carbon options can significantly reduce emissions. Biomass-based fuels, for example, produce about 20–25% less CO_2 compared to coal [6, 9 - 11].

- **Clinker substitution with Supplementary Cementitious Materials (SCMs)**

Since clinker production is the most carbon-intensive stage in cement manufacturing, replacing a portion of clinker with SCMs, such as fly ash, blast furnace slag, and limestone fillers, can lead to substantial emissions reductions [6, 9 - 11].

- **Development of novel cements**

Alternative cement formulations, including belite cements, calcium sulfoaluminate (CSA) cements, geopolymers, and carbonated calcium silicates, have been explored as potential replacements for Portland cement. These materials require lower production temperatures and emit less CO_2. However, large-scale adoption remains limited due to technical and economic barriers [6, 10].

- **Carbon Capture and Storage (CCS) and Carbon Capture and Utilization (CCU)**

CCS and CCU technologies involve capturing CO_2 emissions during cement production and either storing them underground or utilizing them in industrial processes. Despite their potential, these technologies face significant challenges, including high energy requirements, substantial investment costs, and the lack of infrastructure. Consequently, CCS and CCU are not yet widely implemented on a commercial scale [11, 12].

Among these strategies, the use of SCMs stands out as the most promising approach for reducing the carbon footprint of cement production. Since clinker production is both highly carbon-intensive and energy-consuming, reducing its proportion in cement can lead to significant emissions reductions and lower energy consumption. SCMs can replace a considerable fraction of clinker without compromising cement performance [10, 11]. Unlike CCS, which entails high investment and operational costs, SCM adoption does not require extensive modifications to existing cement plants. Additionally, SCMs are often industrial by-products, making them cost-effective and readily available [1]. Finally, SCMs promote circular economy principles by utilizing waste materials such as fly ash from coal power plants and blast furnace slag from steel production, thereby reducing landfill waste while simultaneously lowering the environmental impact of cement production [6].

2.2. Supplementary cementitious materials (SCMs)

As discussed in the previous chapter, the use of SCMs represents one of the most promising approaches to reducing the carbon footprint of the cement industry.

Currently, eight standard SCMs are utilized in cement production in proportions ranging from 6% to 95%, as specified in EN 197-1 [13]. These include blast furnace slag, silica fume, natural pozzolans, calcined natural pozzolans, siliceous fly ash, calcareous fly ash, burnt shale, and limestone.

SCMs can be categorized into three groups based on their chemical composition and reactivity: hydraulic, pozzolanic, and inert. Fig. 2.3 provides a summary of each classification.

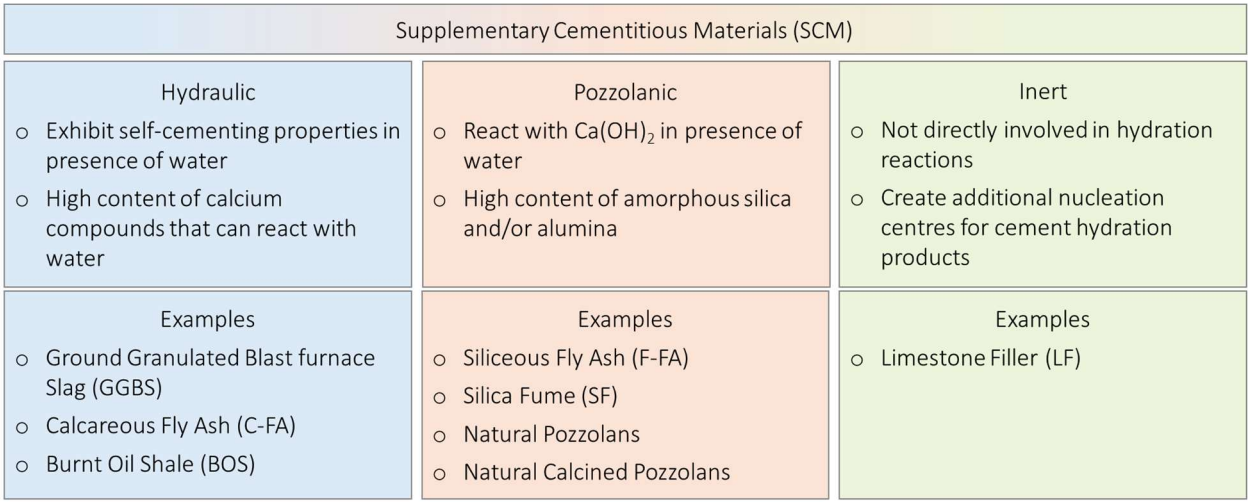

Fig. 2.3. Classification of SCMs.

Fig. 2.4 illustrates the distribution of standard SCMs within the $CaO–SiO_2–Al_2O_3$ ternary diagram, offering insight into their approximate chemical composition and variability. For instance, the composition of materials such as limestone and silica fume is relatively uniform, as indicated by their narrow regions on the diagram. In contrast, fly ash and natural pozzolans exhibit significant variability, reflected in their broader distribution.

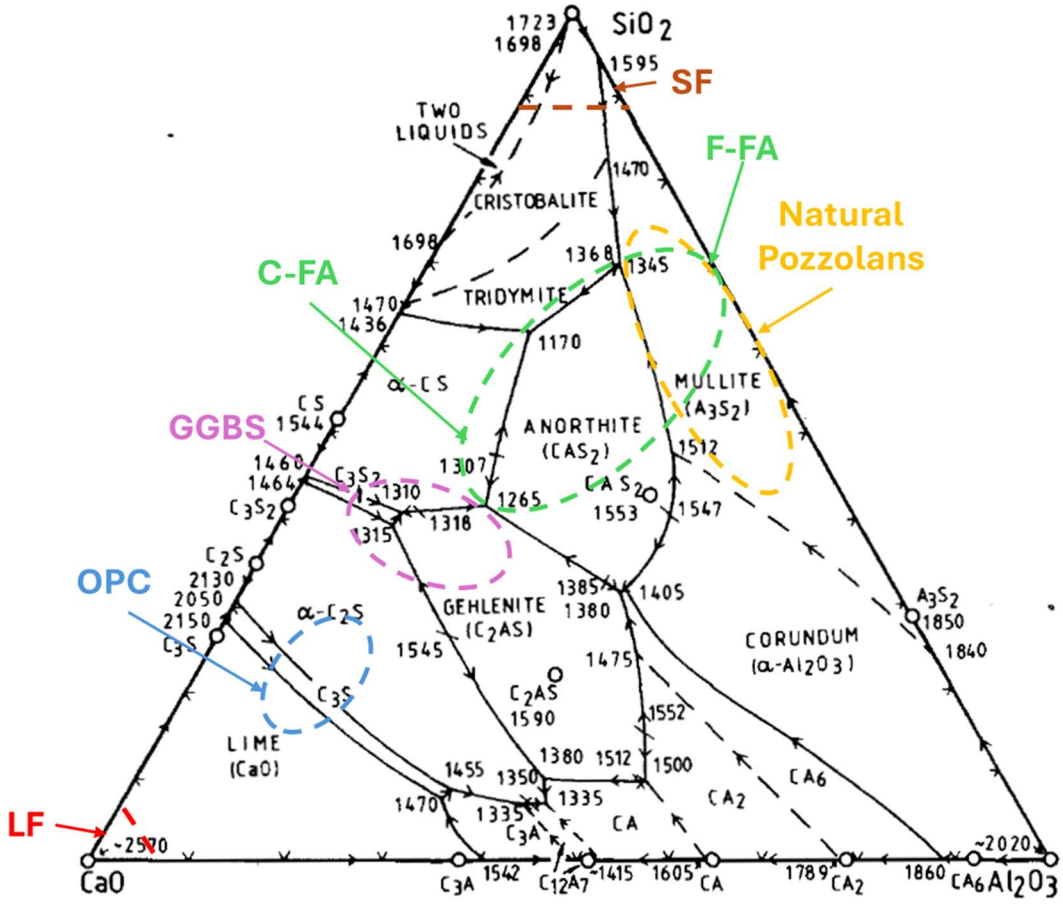

Fig. 2.4. $CaO–Al_2O_3–SiO_2$ ternary diagram of SCMs and Portland cement [14, 15]: Limestone Filler (LF), Ordinary Portland Cement (OPC), Ground Granulated Blast Furnace Slag (GGBS), Calcareous Fly Ash (C-FA), Silica Fume (SF), Siliceous Fly Ash (F-FA) and Natural Pozzolans.

This chapter provides a detailed examination of the primary SCMs, focusing on their hardening mechanisms and their influence on the properties of hardened cement and concrete.

2.2.1. Hydraulic SCMs

Hydraulic SCMs are finely dispersed materials that, like Portland cement, react with water to form hard and durable hydration products. This category includes Ground Granulated Blast Furnace Slag (GGBS), Calcareous Fly Ash (C-FA), and Burnt Oil Shale (BOS). These materials are characterized by a significant calcium content, but typically lower than that of Portland cement, and a high proportion of the amorphous phase [16 - 19].

The hydration of hydraulic SCMs produces similar hydrate phases to those formed during the hydration of Portland cement, with calcium silicate hydrate (C–S–H) as the dominant phase [20]. However, unlike Portland cement, hydraulic SCMs usually possess latent hydraulic properties

and require activation to initiate and accelerate hydration reactions. While they can develop cementitious properties without external activation, this process is slow, limiting their independent use [17, 19, 20]. Activation typically occurs in an alkaline environment created by the hydration products of Portland cement, particularly calcium hydroxide (portlandite, $Ca(OH)_2$ or CH), and by sulfates introduced through gypsum or anhydrite [17, 20].

Based on the $CaO–Al_2O_3–SiO_2$ ternary diagram (Fig. 2.4), the composition of OPC is conventionally represented by alite ($3CaO \cdot SiO_2$ or C_3S), its primary phase, while the composition of GGBS is approximated as gehlenite ($Ca_2Al[Al, SiO_7]$ or C_2AS) [20]. In this case, the general hydration mechanism of hydraulic SCMs can be outlined as follows [19, 22]:

- Primary reactions:
    - Hydration of OPC:

      $C_3S + H \rightarrow C\text{-}S\text{-}H + CH$
    - Activation and hydration of GGBS:

      $C_2AS + H + CH \rightarrow C\text{-}S\text{-}(A)\text{-}H$
- Secondary reactions (interaction of hydration products of OPC and GGBS): These reactions include further interaction between the hydration products of Portland cement and GGBS, leading to modification of the microstructure and properties of the hardened cement.

The hydration of GGBS follows a dissolution-precipitation mechanism. Initially, ions are released, followed by the formation of ettringite and C–S–H phases. Over time, the composition and structure of C–S–H evolve, influencing the final properties of the hardened cementitious system. Figure 2.4 illustrates the hydration mechanism of GGBS over time, detailing the formation and development of hydration products:

10 min:

- Dissolution of gypsum with release of Ca^{2+} and SO_4^{2-}.
- GGBS particles dissolves in the presence of OH^-, H_2O and SO_4^{2-} with release of Ca^{2+}, Si^{4+}, Al^{3+}, Mg^{2+}, K^+, Na^+, and S^{2-}.

4 h:

- Ettringite (1–5 µm) begins to form around GGBS particles due to the reaction of Al^{3+} with SO_4^{2-} from gypsum.
- A single uniform calcium-silicate-hydrate (C–S–H) phase starts to develop as hydration progresses.

12 h:

- The ettringite crystals grow larger (3–5 μm).
- The C–S–H phase continues to develop, forming a Ca-rich C–S–H layer around the GGBS particles.

48 h:

- The structure becomes more defined with a Ca-rich C–S–H phase and a Ca-poor, Mg- and Al-rich C–S–H phase.
- Ettringite remains present, and the hydration products contribute to the binding and hardening of the cement matrix.

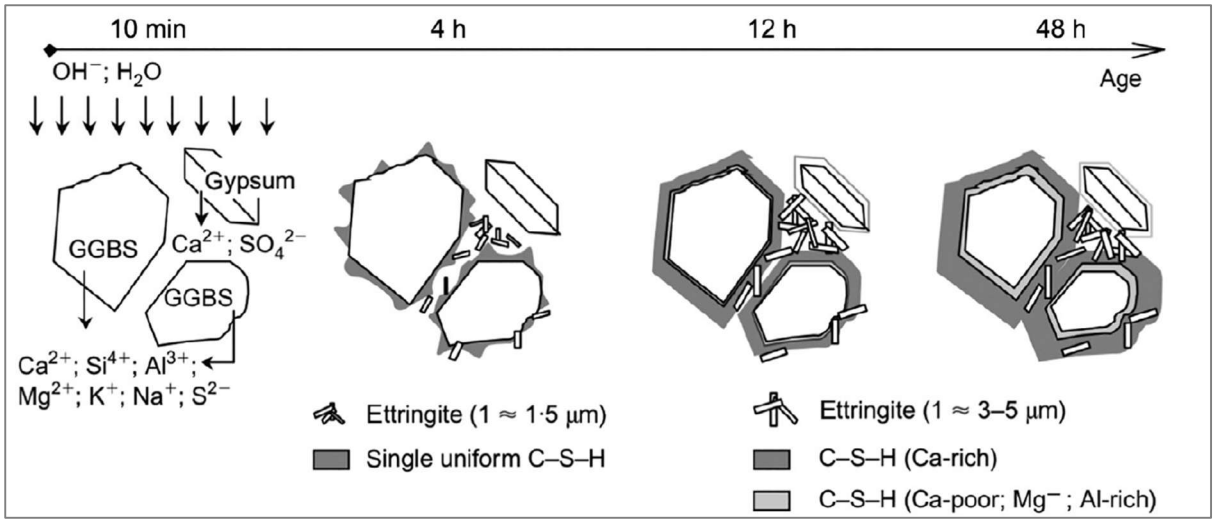

Fig. 2.5. Hydration scheme for the hardening of blended GGBS Portland cement [21].

Since cement hydration is an exothermic process, calorimetry is used to analyse hydration kinetics. Calorimetric curves provide insights into reaction kinetics and the effects of different SCMs on both early and late-stage hardening. A typical calorimetric curve for Portland cement hydration consists of five phases (Fig. 2.6) [17, 23, 24]:

I. Initial period (wetting): Rapid heat release immediately after water addition, associated with the dissolution of calcium silicate phases.

II. Induction period: A temporary slowdown in reaction rate.

III. Acceleration period: Intense heat release due to alite (C_3S) hydration and C-S-H formation.

IV. Deceleration period: Heat release rate declines after reaching the peak of alite hydration. An additional "aluminate peak" may appear, associated with the hydration of aluminates.

V. Slow continuing reaction period: Sustained heat release due to ongoing hydration and pozzolanic reactions.

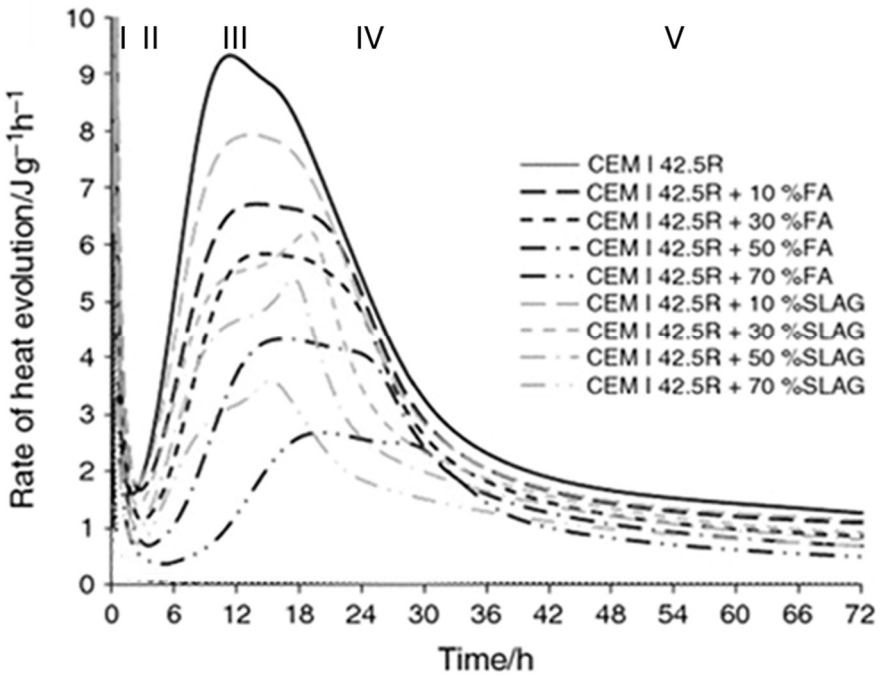

Fig. 2.6. Isothermal calorimetry curves at 20 °C for cement–fly ash and cement–slag binders [24].

The incorporation of SCMs to Portland cement alters hydration heat kinetics. The calorimetric curves of GGBS-containing cements typically show a reduction in total exothermicity compared to pure Portland cement due to the lower clinker content [23, 25]. Additionally, the "aluminate peak" appears earlier and more pronounced, particularly between 12 and 24 hours (Fig. 2.6), likely due to the reaction of GGBS once sufficient $Ca(OH)_2$ is available, which accelerates cement hydration [23, 26, 27].

Granulated Blast Furnace Slag (GGBS)

GGBS is the most widely used hydraulic SCM. It is a by-product of ironmaking in blast furnaces, obtained during the iron smelting process through the thermal reduction of iron ore. It consists mainly of calcium silicates and aluminosilicates [11, 16, 19, 21]. High-quality GGBS typically contains 85–95% amorphous phase. To achieve this, the molten slag is rapidly cooled (granulated), usually by high-pressure water jets. This process prevents the formation of large crystals and forms granular particles, usually no larger than 5 mm. The granulated slag is then dried and ground in a ball mill to produce a fine powder known as GGBS [16].

GGBS has a similar general chemical composition to ordinary Portland cement but in different proportions. Its main chemical components are CaO, SiO_2, Al_2O_3, and MgO [16, 21].

Slag cements are widely used in various applications around the world. Notable examples include the structural elements of the Groen Hart Tunnel in the Netherlands, the Rance tidal

power station, 142 piles of the new Mont Saint-Michel access bridge, and the Palais de Chaillot in France [21].

The use of GGBS can reduce water demand for a given workability due to the smooth surface of slag particles, which lowers internal friction [28]. Additionally, GGBS retards the setting time of cement mixtures [21]. Replacing OPC with GGBS reduces early-age heat generation [20, 21, 24], which is beneficial for massive concrete structures by minimizing the risk of thermal cracking. However, at low temperatures, the curing rate of GGBS-containing cement can be significantly slower [20].

GGBS promotes continued hydration over extended periods (beyond 28 days), leading to higher long-term strength development [19, 20]. It also contributes to a finer pore structure in hardened cement, reducing permeability and enhancing durability by improving resistance to aggressive chemicals such as chlorides and sulfates [16, 19]. Additionally, GGBS can help reduce shrinkage and creep in concrete [20].

However, advancements in energy and resource efficiency in the steel industry, particularly the increased use of scrap metal in electric arc furnaces, are leading to a decline in pig iron production from iron ore and, consequently, a reduction in GGBS availability [10].

Calcareous Fly Ash

Calcareous Fly Ash (Class C Fly Ash, C-FA) is a fine powder produced by burning lignite or brown coal in power plants. During combustion, mineral impurities in the coal melt and are carried out of the chamber with flue gases. As the molten material cools, it solidifies into spherical glassy particles, which are collected from flue gases using electrostatic precipitators or bag filters [16, 17, 20].

The primary chemical components of C-FA are SiO_2, Al_2O_3, and CaO. Compared to siliceous fly ash (Class F), C-FA contains significantly more CaO (11.6–29.0%) and less SiO_2 (23.1–50.5%) [16, 17].

The mineralogical composition of C-FA is more diverse than that of siliceous fly ash. In addition to aluminosilicate glass, its primary reactive component, C-FA may contain crystalline phases such as quartz, free CaO, mullite, gehlenite, anhydrite, and cementitious minerals, including tricalcium aluminate (C_3A), dicalcium silicate (C_2S), and calcium sulfoaluminate (C_4A_3S). The presence of these hydraulically active crystalline phases gives C-FA self-cementing properties [16, 17].

Burnt Oil Shale

If the organic matter content of the oil shale is sufficiently high, it can be burned for electricity generation or used as an alternative feedstock in Portland cement production. The resulting ash, known as Bottom Oil Shale Ash (BOS), exhibits both hydraulic and pozzolanic activity [17].

2.2.2. Pozzolanic SCMs

Pozzolanic SCMs are finely dispersed materials characterized by a high content of active (amorphous) silica or alumina. By themselves, these materials exhibit little or no cementitious properties; however, in a finely dispersed state and in the presence of moisture, they chemically react with calcium hydroxide, which is formed during the hydration of Portland cement. This reaction results in the formation of additional cementitious compounds, primarily calcium silicate hydrates (C-S-H) and calcium aluminosilicate hydrates (C-A-S-H). These chemical processes are collectively referred to as pozzolanic reactions [18, 19, 23, 28, 29]. Pozzolanic SCMs include Siliceous Fly Ash (F-FA), Silica Fume (SF), Natural Pozzolans, and Natural Calcined Pozzolans.

It is important to note that the low calcium content of pozzolans, compared to Portland cement, leads to the formation of hydrate phases that differ from those of Portland cement during hydration. This distinction significantly influences the resulting microstructure. In particular, the C-S-H produced in pozzolanic reactions exhibits a lower Ca/Si ratio than that formed in Portland cement hydration [14, 23, 28].

The fundamental equations representing pozzolanic reactions can be schematically expressed as follows [16, 18]:

- For siliceous pozzolans (e.g. microsilica - S):
  S + CH → C-S-H
- For aluminosilicate pozzolans (e.g. metakaolin - AS_2):
  AS2 + CH → C-A-S-H
- In the presence of calcium sulfate (CSs), calcium monosulfoaluminate (C_4ASsH_{12}) can be formed [18]:
  $AS_2 + 6.4\ CH + CSs + 13.6\ H_2O \rightarrow 2\ CSH_4 + C_4ASsH_{12}$

These reactions contribute to a reduction in calcium hydroxide content in hydrated cement while simultaneously generating additional C-S-H and C-A-S-H, which enhance both strength and durability [14, 23].

The mechanism of pozzolanic reactions, illustrated in Fig. 2.7, involves the dissolution of active pozzolan silicates and aluminates in the alkaline environment created by Portland cement hydration. The dissolved species subsequently interact with calcium ions, leading to the formation of low-basic calcium silicate hydroxides and/or calcium aluminosilicate hydroxides [14, 18, 23]. The rate of pozzolanic reactions is generally lower than that of the hydration of the primary clinker phases [18, 29].

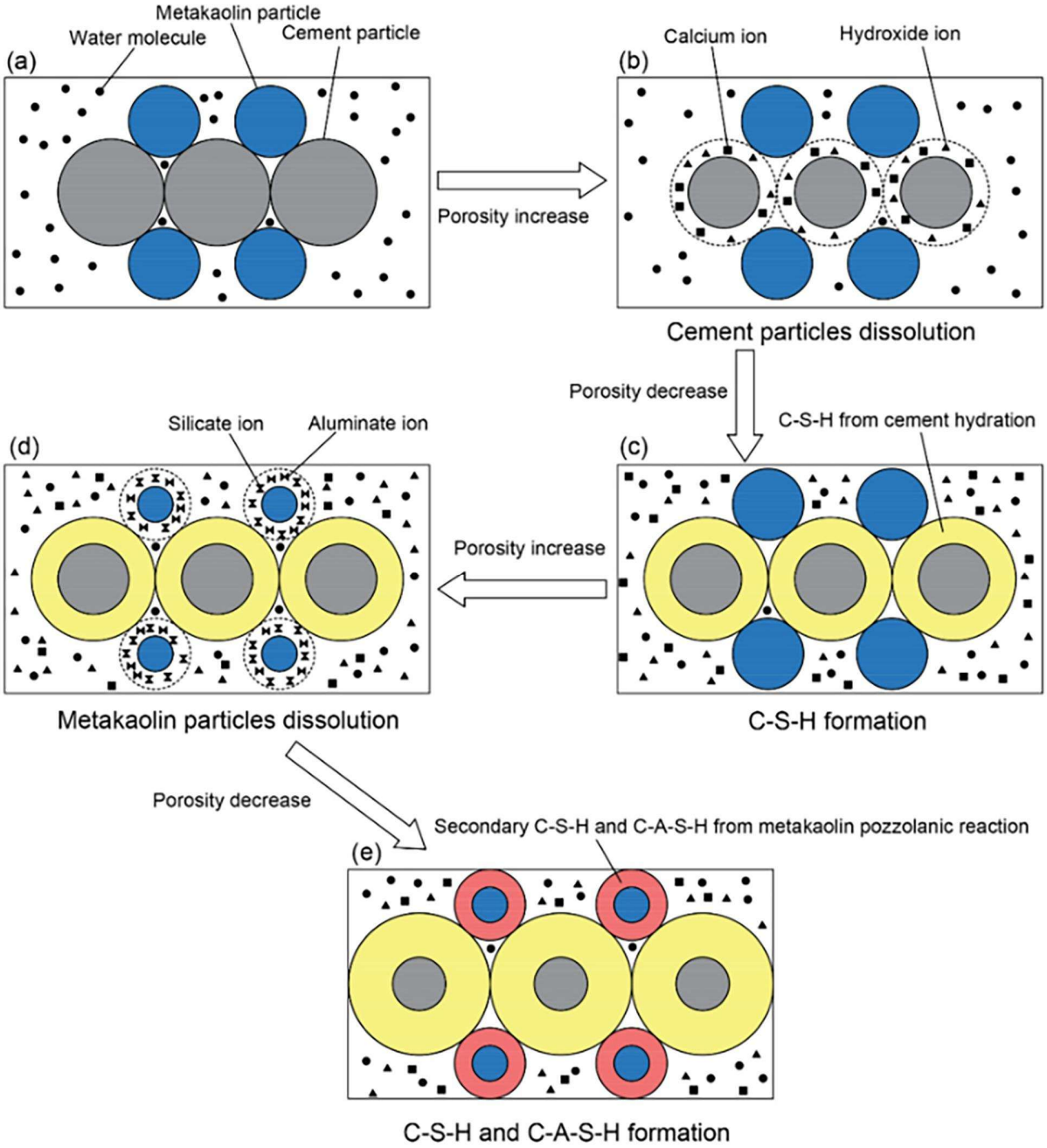

Fig. 2.7. Hydration scheme for the hardening of blended metakaolin-Portland cement [30].

The incorporation of pozzolanic SCMs can lead to variations in calorimetric curves, depending on the fineness and reactivity of the pozzolan. The following changes can be observed:

- Reduced exothermicity at early stages compared to pure Portland cement when clinker is partially replaced with a less reactive pozzolan [23, 24].
- Delay in the main peak of heat release (the acceleration period of alite hydration), which is dependent on the degree of clinker substitution and pozzolan reactivity [18]. However, in the case of highly fine pozzolans, an enhancement of the early peak may occur due to the nucleation effect [31].

Siliceous Fly Ash

Siliceous Fly Ash, also known as Class F fly ash (F-FA), is a fine, powdery material obtained from the combustion of pulverized coal in power plants. Unlike Class C fly ash (C-FA), it contains less calcium oxide and exhibits no hydraulic activity. Its pozzolanic activity is primarily determined by its high content of amorphous silica and alumina. The silica content of F-FA typically ranges from 45% to 64.4%, while the alumina content is approximately 19.6% to 30.1%, and the calcium oxide content varies from 0.7% to 7.5% [16].

Class F fly ash is generated when coal is burned in power plant boilers at temperatures between 1250°C and 1600°C [19]. During combustion, mineral impurities in the coal, such as clay, feldspar, quartz, and shale, melt into a slurry and are carried out of the combustion chamber with the flue gases. As this molten material rises, it cools and solidifies, forming spherical glassy particles known as fly ash. These fine particles, which range in size from less than 1 μm to 150 μm in diameter, are collected from the flue gases using electrostatic precipitators or bag filters [16].

Class C and Class F fly ash exhibit distinct effects on the properties of fresh paste and hardened cement. The following differences can be observed:

- *Workability and Air Content:* C-FA generally reduces workability and entrained air content in fresh concrete, while F-FA does not significantly affect these properties [32].
- *Consistency and Setting Time:* F-FA improves consistency more effectively than C-FA, whereas C-FA extends the setting time to a greater extent [33].
- *Hydration Heat:* C-FA does not impact early-age heat release but increases it at later stages, while F-FA reduces early-age hydration heat without significantly influencing later hydration [33].
- *Strength Development:* In hardened cement, both types of fly ash contribute to long-term strength gain. However, F-FA enhances compressive strength more significantly than C-FA [32]. The self-cementing nature of C-FA may lead to additional early-age strength development, whereas F-FA, being non-self-cementing, relies solely on the pozzolanic

reaction for strength enhancement. Since pozzolanic reactions occur more slowly than clinker hydration, F-FA results in lower early-age strengths but higher later-age strengths [34].

The durability and long-term performance of fly ash concrete have been demonstrated in several historical projects. The Lednock, Clatworthy, and Lubrech Dams, constructed in the 1950s in Scotland, incorporated fly ash as a partial cementitious material. After more than 70 years, these structures remain in excellent condition [19].

The availability of fly ash is declining due to the decreasing number of coal-fired power plants, as energy production shifts toward renewable sources. In Europe, coal combustion restrictions have further limited access to fly ash [10, 11, 16].

Silica Fume

Silica Fume, also known as microsilica or condensed silica, is a by-product of smelting processes in the production of metallic silicon or various silicon ferroalloys. It is an amorphous, fine material consisting almost exclusively of silicon dioxide and possessing high pozzolanic activity. Silica Fume particles are spherical in shape and range in diameter from 0.1 to 0.2 μm [14, 16, 17, 20, 29].

Silica Fume is formed by the high-temperature reduction of quartz at temperatures up to 2000°C using coal, coke, or wood chips as the reducing agent in electric arc furnaces. The reaction produces silica vapours which, as they rise to the upper, cooler parts of the furnace, are oxidized by oxygen and condense to form tiny spherical particles of amorphous silica. These particles are then collected from the exhaust gases using dust collectors such as bag filters [17, 19, 20].

The addition of Silica Fume to cement pastes or concrete usually results in decreased workability and an increased water requirement to maintain a constant slump. This is due to the very fine particle size and high specific surface area of SF. To compensate for this effect, Silica Fume is often used together with superplasticizers [16, 19, 20, 35]. It is also noted that the addition of microsilica can increase the setting time of cement pastes, especially at high percentages of the admixture. However, when adding 10% microsilica, the effect on setting time may be negligible [16]. Moreover, the addition of Silica Fume to high cement content mixtures can result in higher heat release during the initial stages of hydration, which subsequently slows down as reactivity decreases [19].

The incorporation of SF significantly enhances the compressive strength of concrete. This improvement is attributed to the better bond between the cement paste and aggregates, as well

as the filling of voids and pores inside the concrete with calcium hydrosilicates formed as a result of pozzolanic reactions [16, 19, 20]. The reduction in concrete porosity due to silica fume makes it more resistant to the penetration of liquids and gases such as chloride ions and sulphates, thereby enhancing its durability [16, 19, 20, 29]. Furthermore, Silica Fume reduces the porosity of the transition zone between the cement paste and aggregates, as well as at the interface of the cement matrix and steel reinforcement, improving adhesion and mechanical properties [16, 20].

High-performance concrete with Silica Fume has been successfully used in the construction of notable high-rise buildings, such as the 79-story office block at 311 South Wacker Drive in Chicago (USA) and the Petronas Towers in Kuala Lumpur (Malaysia) [19]. Silica Fume has also been employed in the construction of the Great Belt Bridge in Denmark, one of the longest bridges in the world, as well as in the Channel Tunnel and the Indianapolis International Airport [35].

Silica Fume is a very expensive material. Additionally, due to its high specific surface area and low density, its transportation and processing can be difficult and costly. This may limit its economically feasible use at large distances from production sites [20].

Natural Pozzolans

Natural pozzolans are materials of volcanic or sedimentary origin that possess suitable chemical and mineralogical composition. They primarily consist of amorphous or weakly crystalline siliceous compounds, which contribute to their pozzolanic activity [10, 17, 36]. Examples of natural pozzolans include volcanic ash, perlite, pumice, opal schists, tuffs and diatomaceous earths [17, 20, 36]. Historically, these materials were widely used in construction by ancient civilizations, particularly the Greeks and Romans, in combination with lime [23, 28, 29]. Roman-era constructions, such as the Colosseum, were built using natural pozzolanic materials [37].

Volcanic pozzolans typically contain more than 50% silica, followed by alumina, iron oxides and lime, and may have high alkali contents (up to 10%) [19]. The primary pozzolanic component in unaltered pyroclastic pumices and ashes is highly porous volcanic glass, predominantly of intermediate (52–66 wt.% SiO_2) or felsic (>66 wt.% SiO_2) compositions [17].

Tuffs, another category of volcanic pozzolans, are formed through the partial or complete alteration of volcanic glass into zeolitic compounds due to weathering [17, 19]. Zeolites, which are aluminosilicates with a three-dimensional open framework, often exhibit higher pozzolanic activity than glassy volcanic pozzolans [17, 20].

Sedimentary pozzolans rich in opal diatomites contain high silica amount [19, 29]. Diatomites consist primarily of siliceous skeletons of diatom microorganisms, which are composed of opal. The higher the opal content, the greater the pozzolanic activity of the material [17, 20].

Due to their typically irregular particle shape, natural pozzolans tend to increase water demand in concrete mixtures. This occurs because a larger surface area must be wetted and additional water is needed to fill voids between particles, which can negatively impact workability. The use of plasticizers is often necessary to mitigate this effect [11, 19, 28].

Concretes containing natural pozzolans exhibit enhanced resistance to chemical attack, particularly from sulphates and chlorides [17, 20].

Although natural pozzolans are available in significant global reserves, their distribution is regionally constrained by geological formations. The availability of natural pozzolans is dependent on the presence of specific deposits. As a result, transportation and logistical costs often pose challenges to their widespread use as cement clinker substitutes [10, 11, 17, 40].

Natural Calcined Pozzolans

Natural Calcined Pozzolans are natural materials of volcanic origin, clays, shales or sedimentary rocks that have been artificially activated by heat treatment. They usually include heat-treated clays. The heating process removes bound water and destroys the mineral structure, forming reactive silicon and aluminium compounds [10].

The most common clay minerals include kaolinite, smectite, illite, and chlorite. In their natural state, these clays exhibit low pozzolanic activity due to the stability of their crystalline structures [17].

Metakaolin (MK) is among the most well-known calcined natural pozzolans. It is produced by calcining kaolin clays within a temperature range of approximately 600°C to 800°C. During heating, kaolinite ($Al_2O_3 \cdot 2SiO_2 \cdot 2H_2O$) undergoes dehydroxylation, a process in which water is released, and the crystalline structure is destroyed. This results in the formation of an amorphous aluminosilicate ($Al_2O_3 \cdot 2SiO_2$) known as metakaolin or metakaolinite. The effectiveness of the pozzolanic material depends on achieving near-complete dehydroxylation while avoiding overheating. Excessive temperatures can lead to sintering and the formation of crystalline mullite, a refractory material that is non-reactive in pozzolanic reactions [10, 16 - 19, 38, 39].

Among all clay minerals, kaolin is the most suitable for producing pozzolanic materials due to its broad dehydroxylation temperature range without recrystallization. Other clays exhibit lower pozzolanic activity upon thermal activation. For example, although illite dehydroxylates at

relatively low temperatures, it does not fully transition into an amorphous state before recrystallizing into spinel and corundum. Consequently, calcined illite exhibits significantly lower pozzolanic activity than the less thermally stable smectite or kaolinite. Chlorite minerals require higher temperatures for dehydroxylation due to their elevated magnesium content [17, 18].

The incorporation of calcined clays into cementitious mixtures can increase water demand to achieve the desired rheological behaviour compared to ordinary Portland cement [28].

The addition of metakaolin enhances the mechanical properties and durability of concrete. It increases compressive strength while reducing permeability, thereby improving resistance to chloride ion diffusion and reinforcement corrosion. These benefits result from a favourable modification of the pore structure, characterized by an increase in the volume of fine pores (<0.01 μm) and a reduction in larger pores (>0.1 μm) [20, 28].

In 1932, calcined clays were used in the construction of bridges in San Francisco, USA. It is also used in the construction of many large dams in Brazil [11].

Although kaolin, the raw material for metakaolin production, is widely available in nature, high-purity metakaolin, commonly used as SCM, is quite expensive. Its cost is driven by the limited availability of high-quality kaolin and its competing demand in industries such as paper production and ceramics. Consequently, the price of metakaolin can be approximately three times higher than that of cement [19, 39, 40].

Other pozzolanic SCMs that are not yet standardized include ashes derived from the combustion of agricultural waste, such as rice husk ash and sugarcane bagasse ash. However, these materials are regionally specific, and their composition can vary significantly, affecting their consistency as pozzolanic additives.

2.2.3. Inert fillers

Inert fillers are finely dispersed materials that generally do not participate in hydration reactions but serve as additional nucleation sites for Portland cement hydration products. They also improve particle packing by filling the spaces between cement grains due to their fine granulometric composition [20, 28, 41]. Typical inert fillers include ground limestone, quartz, and granite [20, 41, 42].

The filler effect (Fig. 2.8) occurs when fine filler particles provide additional surfaces for the nucleation of hydrate phases such as calcium silicate hydrate (C-S-H). This increases the

availability of crystallization sites, which can accelerate the early hydration of cement [14, 42 - 45]. Additionally, the fine filler particles fill voids between larger cement grains, leading to increased packing density and reduced porosity in the fresh paste [20, 46].

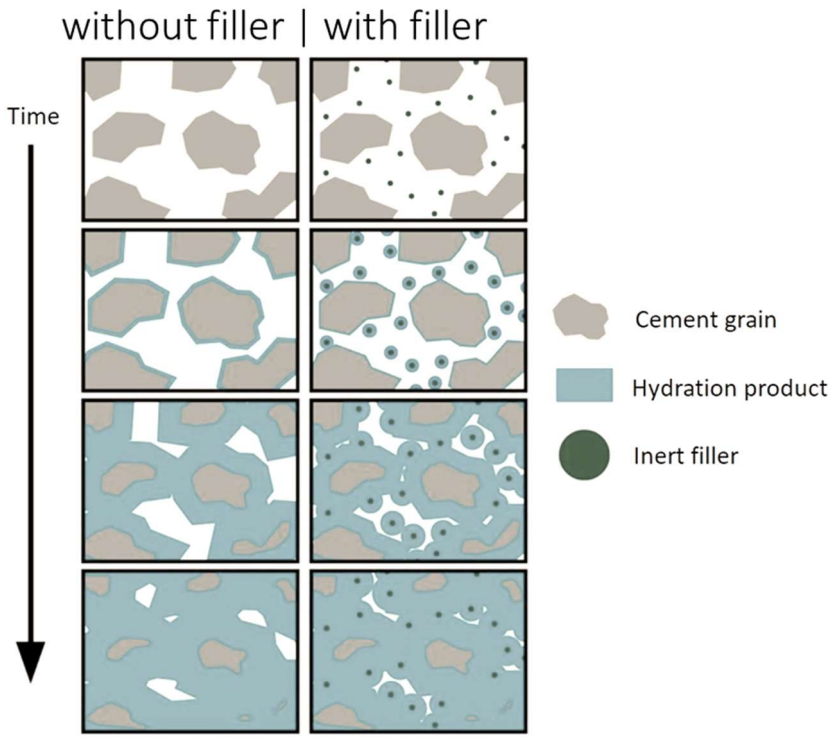

Fig. 2.8. Hydration scheme for the hardening of cement paste with inert filler [47].

The additional surface area provided by the filler can promote the nucleation of hydration products, which may result in accelerated early hydration and increased early heat release rates (Figure 2.9) [42, 44]. Limestone has a greater accelerating effect than quartz due to its higher nucleation potential and the ability to incorporate carbonate ions into C-S-H, resulting in the release of hydroxide ions and an increased driving force for C-S-H growth [42].

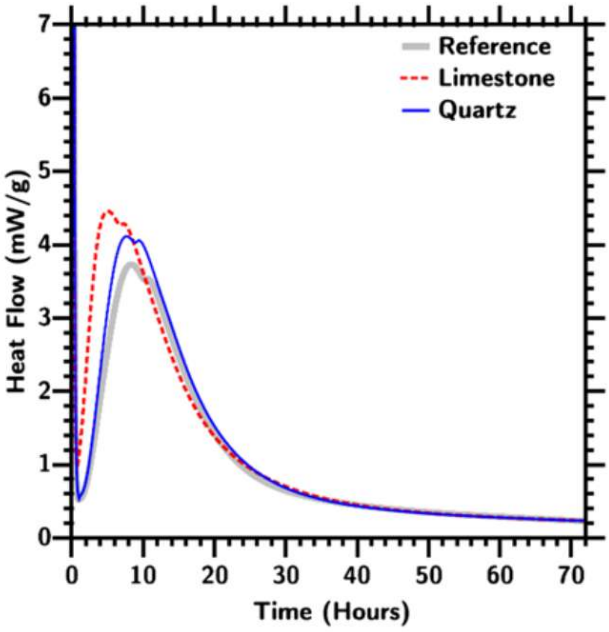

Fig. 2.9. Comparison of calorimetric curves of OPC, limestone-cement and quartz-cement binders [42].

Although inert fillers do not chemically react with cement hydration products, their physical presence and influence on the microstructure can enhance the mechanical properties and durability of hardened cement [20, 41, 48]. Fillers can also contribute to reducing the formation of microcracks [20].

The first known structure constructed using inert fillers is the Elephant Butte and Arrowrock Dams, built in the United States between 1912 and 1916. During their construction, 45-48% of the cement was replaced with ground granite and sandstone. The downcomer and spillway of Arrowrock Dam were repaired due to deterioration caused by a freeze in 1935, but no major repairs have been reported for Elephant Butte Dam in Texas. These dams, which are over 100 years old, are still in use [48].

2.2.4. Limestone calcined clay cement (LC3)

Although limestone filler has traditionally been regarded as an inert material, increasing evidence suggests that it can undergo chemical reactions during cement hydration, particularly in the presence of aluminates. These reactions result in the formation of carboaluminate phases, which contribute to the microstructural evolution of cementitious systems [11, 18, 20, 39, 49].

Recognizing this potential, researchers from the École Polytechnique Fédérale de Lausanne (EPFL) developed a novel class of blended cements known as Limestone Calcined Clay Cement

(LC3). This system partially replaces cement clinker with a combination of calcined clay and limestone filler to achieve comparable performance with reduced clinker content [39, 40, 49].

The most promising composition is LC3-50, which consists of 50% cement clinker, 30% calcined clay (preferably containing at least 40% kaolinite), 15% limestone filler, and 5% gypsum. This formulation enables the development of mechanical properties comparable to Ordinary Portland Cement (OPC) within just 7 days. In the LC3-X nomenclature, "X" represents the percentage of clinker in the blend [39, 40, 49].

In LC3 systems, calcium carbonate from limestone filler reacts with aluminates derived from hydration of Portland cement and calcined clay, forming carboaluminate hydrates [18, 20, 39, 49]. The dominant phases formed include hemicarboaluminate and monocarboaluminate [49]. These high-volume phases contribute to pore filling, densification of the cement paste, and improved strength development.

Thus, the development of strength in LC3 is driven by a synergistic effect involving [38, 39, 49]:

- Clinker hydration, leading to the formation of calcium silicate hydrate.
- The pozzolanic reaction of calcined clay with portlandite, forming additional C-S-H and C-A-S-H gels.
- The reaction of limestone with aluminates, forming carboaluminate hydrates, which enhance microstructural compactness and strength.

The early strength of LC3 can be comparable to that of OPC due to the physical effect of finely ground limestone and metakaolin, which accelerates alite hydration [49], and the enhanced particle packing, reducing porosity and increasing the rate of hydration [28].

The long-term strength continues to develop due to the sustained pozzolanic reaction, which further refines the microstructure and the ongoing formation of carboaluminate hydrates, which contribute to long-term durability [18, 49].

Despite significant progress in the study of LC3, several areas require further investigation:

- Optimization of LC3 formulations for different clay and limestone types. Further research is needed to assess how impurities in clays and limestones affect reactivity and performance.
- Long-term hydration mechanisms require deeper analysis to improve predictive models of durability and performance.

- Development of standardized test methods and regulatory frameworks to facilitate the widespread adoption of LC3 in the construction industry.
- Assessment of LC3's resistance to aggressive environments, such as sulphate attack, chloride penetration, and carbonation, to ensure long-term durability.
- Comprehensive life cycle analysis (LCA), considering regional variations in raw material availability and environmental impact, to refine sustainability assessments.

2.3. Recycling of demolition wastes for CO2-reduced cement production

As discussed in the previous chapter, the cement industry faces significant challenges related to the availability of traditional SCMs. For instance, the production of blast furnace slag is decreasing due to the transition of the iron and steel industry from blast furnace technology to electric arc furnaces, as well as the increasing implication of scrap metal for smelting. Similarly, the availability of fly ash has significantly declined as coal-fired power plants are being phased out in favor of more sustainable energy sources.

Moreover, other commonly used SCMs are either scarce, geographically limited, or economically unviable for widespread application. Microsilica, a byproduct of silicon and ferrosilicon production, has always been produced in limited quantities. Natural pozzolans are available only in specific regions with a history of volcanic activity, restricting their global use. High-quality metakaolin, while an effective SCM, is expensive and widely utilized in other industries, such as ceramics and polymer composites, making it less accessible for cement production.

Given these constraints, the cement industry must explore alternative SCM sources to continue reducing CO_2 emissions while maintaining material performance and availability. One promising avenue is the valorisation of construction and demolition waste (CDW). Properly processed CDW has the potential to serve as a sustainable SCM, contributing to circular economy practices and reducing the environmental impact of cement production.

2.3.1. Environmental impact of demolition wastes

Construction and demolition waste (CDW) is the largest category of solid waste in the world, with the construction sector accounting for more than one-third of all waste generated in Europe,

according to EUROSTAT (Figure 2.10). In 2022, the European Union produced approximately 848.5 million tonnes of CDW, corresponding to an average of 1,896.6 kg per capita. Over a lifetime, an average European generates more than 150 tonnes of CDW, highlighting the significant environmental impact of construction-related activities [50].

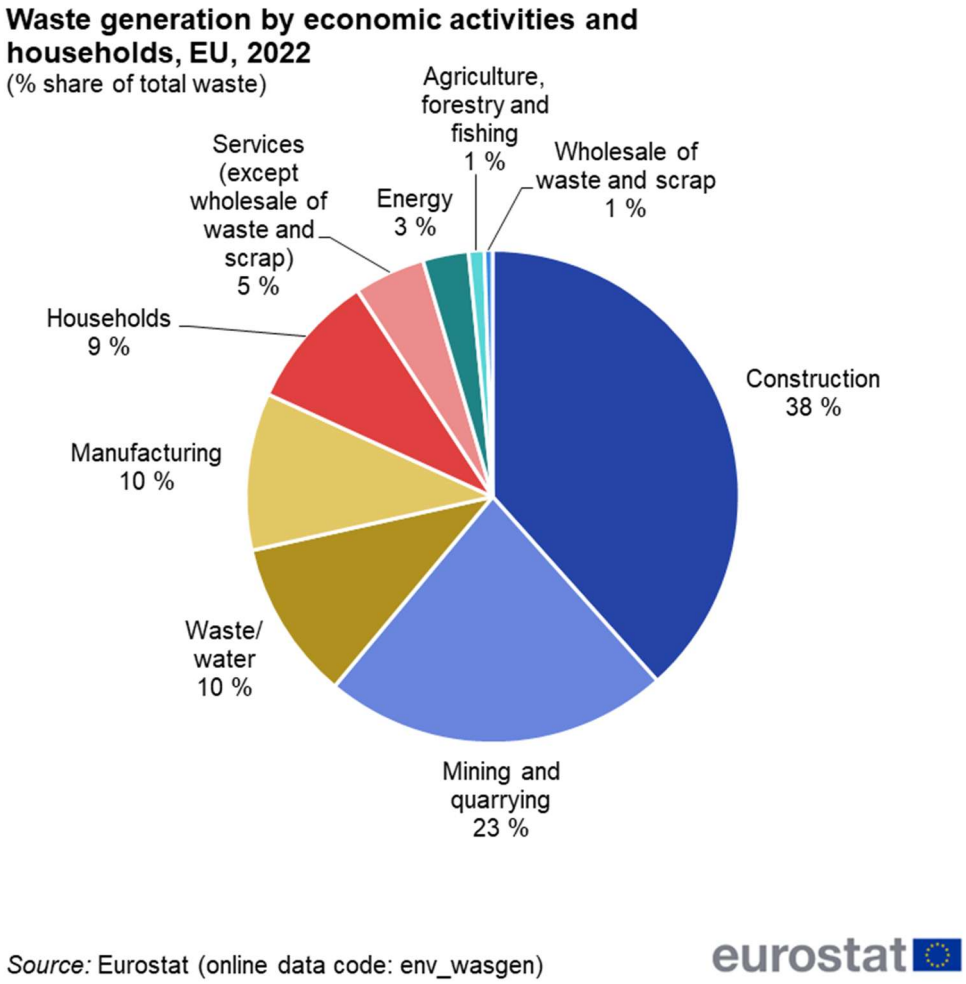

Fig. 2.10. Percentage share of waste generation by economic activities and households in the EU, 2022 [50].

To mitigate this impact, the EU Waste Framework Directive (2008/98/EC) established a target requiring Member States to recycle at least 70% of CDW from 2020. However, actual recycling rates remain well below this threshold, with only about half of CDW currently being recycled. These rates vary significantly across EU countries. For instance, nations such as the Netherlands, Denmark, and Germany achieve recycling rates of approximately 90%, demonstrating well-established recycling infrastructure and regulatory frameworks. In contrast, southern European countries lag behind: Spain recycles only around 15% of its CDW, Italy achieves an estimated 10%, and Portugal recycles as little as 4%, with the majority of CDW still being landfilled rather than reintegrated into the construction sector [51 - 53].

CDW is composed of a diverse range of materials. The majority (approximately 80%) consists of concrete and building ceramics, such as bricks and tiles. The remaining 20% includes wood, glass, plastic, insulation materials, metals, and other construction-related debris [51, 53 - 55]. Additionally, CDW encompasses excavated rock and soil generated during construction and demolition work [52].

The large volumes of CDW produced pose a significant environmental challenge. A substantial proportion of this waste is still disposed of in landfills or, in some cases, in uncontrolled dumps, leading to land consumption, environmental degradation, and resource loss [51, 52]. Moreover, in many European countries, including Italy, the Netherlands, and Denmark, geological and spatial constraints limit the feasibility of opening new landfill sites, necessitating a shift toward more sustainable waste management solutions [53].

Although a considerable share of CDW can be recycled or reused, various technical and regulatory barriers hinder its full valorisation. One major challenge is the structural integrity and quality of recycled concrete aggregates, which often fail to meet the performance requirements for high-grade concrete applications [56]. While clean concrete aggregates can technically be separated from mixed CDW and reused in new concrete production, this practice remains uncommon on a global scale. However, as natural aggregate reserves continue to deplete and environmental awareness grows regarding CDW accumulation, the demand for recycled aggregates is expected to rise [52].

Furthermore, current recycling efforts primarily focus on the coarse fraction of CDW, while the fine fraction—composed of cement paste, fine sand, and other particles—remains underutilized due to limited market demand and technical challenges associated with its reuse [51]. To enhance CDW recycling efficiency, it is crucial to prevent contamination from undesirable materials and to advance selective demolition techniques that allow for better material separation and recovery. The development and implementation of clear standards and specifications for the use of recycled materials are also essential to facilitate their integration into the construction industry and promote a more circular economy in the built environment.

2.3.2. Use of demolition wastes in constructure

Currently, the processing of CDW is primarily focused on the production of recycled aggregates. In practice, coarse recycled aggregates with a particle size between 4 and 63 mm, as defined by EN 12620:2002+A1:2008, are the most commonly used fraction [57]. However, the use of fine

recycled aggregates, with a particle size of 0.063 to 4 mm, is significantly restricted due to several drawbacks.

One major issue affecting fine recycled aggregates is the presence of gypsum plaster residues, which are often found on concrete surfaces before demolition. During the crushing process, a considerable portion of this plaster is transferred into the fine fraction, leading to an elevated sulphate content in the material. This, in turn, increases the risk of delayed ettringite formation, a phenomenon that can cause internal expansion and microcracking in concrete [58]. Additionally, fine recycled aggregates is characterized by a high content of porous particles, mainly originating from the residual cement paste and mortar. These porous particles significantly increase water demand in fresh concrete, making it difficult to maintain workability without excessive use of admixtures or additional cement. Furthermore, the irregular particle shape of fine recycled aggregates contributes to increased internal friction, further exacerbating the need for additional binder to achieve acceptable rheological and mechanical properties [59].

Coarse recycled aggregates are predominantly used in non-structural applications, including road construction, where they serve as sub-base material; asphalt production, as filler aggregate; cement-treated soil mixtures for infrastructure projects; prefabricated concrete elements, such as curbstones and paving slabs [51, 52, 58, 60]. For example, in Belgium, approximately 90% of recycled aggregates are used in road construction [51]. However, recycled aggregates can be incorporated into new concrete production for both structural and non-structural applications. Research has shown that replacing up to 20% of coarse natural aggregates with recycled aggregates does not significantly alter the properties of concrete [56, 61].

Several real-world projects have demonstrated the feasibility of using recycled aggregates in construction. In Ludwigshafen, Germany, a six-story residential and office building was successfully constructed using concrete containing 30% recycled aggregates instead of natural aggregates. The BBVA headquarters in Las Tablas, Spain, a 114,000 m^2 building complex, incorporated 20% recycled coarse aggregates in its footings, foundation slabs, structural and non-structural floors, and auditorium walls. The BBVA employee services building in Madrid, which houses a nursery, physical therapy clinic, fitness facility, and parking garage, was constructed with concrete, where 25% of the coarse aggregate consisted of recycled CDW [51, 60].

The classification of recycled aggregates varies between countries. Different national standards define aggregate types based on a range of characteristics, including chemical composition, physical and mechanical properties, strength, and the presence of contaminants or impurities.

Although classification systems differ, several national standards, including the Belgian PTV 406, British BS 8500-2, German DIN 4226-1, and Japanese JSCE guidelines, adopt principles derived from the RILEM classification system. In general, based on their origin and composition, recycled aggregates are categorized into three main types [62]:

- Recycled concrete aggregate (RCA) is derived from the crushing of concrete structural elements. Due to the heterogeneous nature of the parent concrete, which may include various types of cement, aggregates, admixtures, and degrees of carbonation, RCA is inherently non-homogeneous in its physical and chemical characteristics. Typical properties include density of 2.1–2.4 Mg/m^3 and water absorption of 4%–9% [62].

- Ceramic recycled aggregates (CRA) consist predominantly of fired clay-based materials such as bricks, tiles, and sanitary ware. These aggregates are characterized by density between 1.2 and 1.8 Mg/m^3 and water absorption between 6% and 25% [62]. They have higher water demand than RCA due to its porous microstructure and rough surface texture, which increase the absorption of mixing water. However, ceramic materials are rich in alumina and silica, which makes them capable of engaging in pozzolanic reactions when in contact with calcium hydroxide in the cement paste. These reactions enhance the adhesion between the aggregate and cement matrix [63, 64].

- Mixed recycled aggregates (MRA) are blend of various demolition materials and must contain a minimum of 50% concrete-derived material with density ≥ 2.1 Mg/m^3. The remaining fraction composed mainly of ceramics with density ≥ 1.6 Mg/m^3 [62].

In addition to the heterogeneity of composition, one of the most critical drawbacks of recycled aggregates is the presence of adhering cement mortar on the surface of the original (natural) aggregates. This residual mortar exhibits significantly higher porosity and water absorption than natural aggregates, which in turn increases the overall water absorption of the recycled aggregates. The consequence is a higher water demand during mixing and a reduction in mechanical strength and durability of the hardened concrete [51, 52, 56, 62]. Furthermore, the presence of a double interfacial transition zone (ITZ) significantly impairs the microstructural integrity of recycled aggregates. In conventional concrete, a single ITZ forms between the natural aggregate and the cement matrix. In recycled aggregates, however, two ITZs develop between the natural aggregate and the adhered old cement mortar, and between the old and the new cement matrix (Fig. 2.11). These interfaces are typically zones of weakness due to increased porosity and microcracking, which contribute to reduced bond strength and inferior mechanical performance [51 - 53, 62, 65].

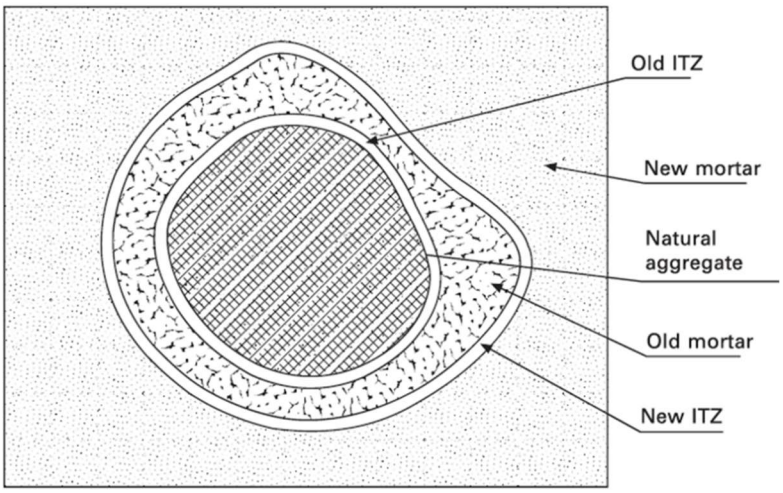

Fig. 2.11. Schematic representation of the double interfacial transition zone in recycled aggregate [55].

To improve the quality and performance of recycled aggregates, various mechanical, physical, and chemical treatments have been developed to remove the attached mortar and contaminants. These include [52 - 54]:

- Crushing and screening with intense attrition help remove weakly bonded old mortar.
- Impact crushing can be more effective in separating mortar from aggregate grains.
- Vibration can also help remove aggregates from cement.
- Water washing removes dust, fines, and partially soluble contaminants.
- Acid soaking can reduce the thickness of the adhered cement paste by partially dissolving its components, thereby facilitating its mechanical removal [66]. Nevertheless, this approach is associated with environmental risks and may require additional measures for safe implementation.

2.3.3. Fine demolition wastes as SCMs

Enhancing the quality of recycled aggregates by removing as much adhered hardened cement paste as possible improves their performance and expands their range of applications in construction. However, this process also generates secondary waste, such as screening fines and washing mud, which consist of fine particles. Due to their fine granulometry, these materials cannot be reused as aggregates, limiting their direct application in construction. As a result, a significant portion, approximately one-third, of CDW is not recycled and is instead sent to landfills. This fine fractions of CDW primarily consist of hardened cement paste, quartz, and ceramic particles, depending on the type of the processed recycled aggregates. Depending on

their mineralogical and chemical properties, these materials have the potential to be used as inert, hydraulic or pozzolanic SCMs.

2.3.3.1. Concrete powders as inert filler

Recycled concrete powder (RCP) is typically generated during the crushing and screening of CDW during production of recycled aggregates. This fine fraction, usually passing through a 0.125 mm or even 0.063 mm sieve [67 - 69], is composed of a mixture of hydrated cement paste, unreacted cement particles, and dust from the natural aggregates resulting from mechanical attrition [67]. Its particle size distribution may, in some cases, resemble that of cement or mineral fillers, which theoretically allows its use as a partial clinker replacement in blended cement or concrete mixtures.

Without preliminary activation RCP do not show significant pozzolanic or hydraulic activity. The original hydraulic phases in the cement (such as alite and belite) have already undergone hydration during the service life of the concrete, forming stable products such as calcium silicate hydrates, which no longer contribute to strength development upon reuse. The content of amorphous silica and alumina, key indicators of pozzolanic potential, is insufficient in recycled concrete, rendering the material chemically inert in terms of cementitious behaviour. Another characteristic feature of RCP is its high content of crystalline quartz, originating from the original fine and coarse aggregates present in the parent concrete. During the mechanical crushing process, these mineral particles are reduced in size and incorporated into the fine fraction. In addition, recycled concrete fines often exhibit a high degree of carbonation due to prolonged exposure to atmospheric CO_2. The large specific surface area of these particles facilitates the carbonation of Ca-bearing phases, leading to the formation of stable calcium carbonate. This makes the material close to the low-grade limestone filler [54, 67 - 72].

Despite its weak chemical reactivity, RCP may still serve a useful role as an inert filler in cementitious systems. When used in controlled proportions, fine recycled powder can contribute to improved particle packing and enhance the mechanical properties of concrete [67, 68, 72]. Moreover, partial replacement of cement clinker with inert powders allows for a reduction in CO_2 emissions associated with clinker production, thereby supporting the objectives of sustainable construction [67].

The utilization of fine RCP as an inert SCM has been validated by various experimental studies [67 - 70, 72, 73]. Results generally indicate that, although the mechanical properties of concrete

or mortar may decrease with increasing RCP content, moderate substitution levels (typically up to 10–15% by weight of cement) are feasible without significantly compromising or even with a slight improvement of performance. In some cases, the micro-filler effect of RCP can even enhance the compactness of the matrix and reduce porosity when optimized particle gradation is achieved.

2.3.3.2. Dehydrated concrete powders as hydraulic SCMs

During the study of concrete behaviour after exposure to fire, it was observed that, following water cooling, concrete largely regains its mechanical strength. This recovery is attributed to the partial restoration of the hydraulic properties of cement due to the rehydration of previously dehydrated cement hydration products, such as calcium silicate hydrates, portlandite, and ettringite [74].

Based on the endothermic peaks observed in the thermogravimetric (DTG) curve presented in Fig. 2.12, the decomposition of hydration products in recycled concrete can be divided into four main stages. The first stage, occurring between 0 and 105 °C, corresponds to the evaporation of free water and the decomposition of ettringite. The second stage, from 105 to 430 °C, is associated with the decomposition of C–S–H phases. The third stage, between 430 and 490 °C, corresponds to the decomposition of calcium hydroxide (portlandite). The final stage, with a DTG peak between 490 and 850 °C, is attributed to the decomposition of calcium carbonate (calcite) [75].

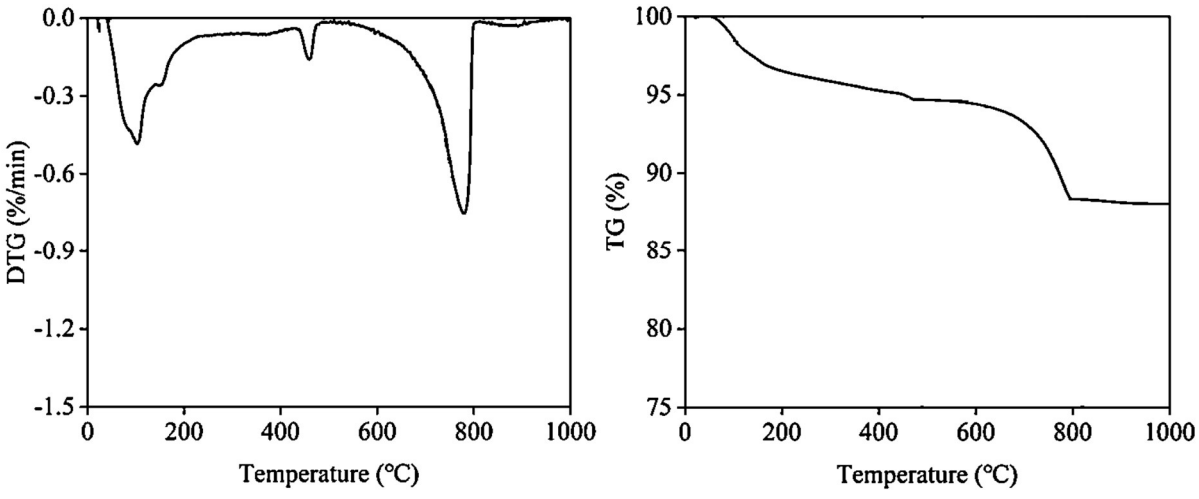

Fig. 2.12. DTG and TG curves of recycled concrete [75].

Above 200 °C, the formation of a new nesosilicate phase is initiated. At approximately 450 °C, C–S–H gel undergoes a progressive transformation, leading to the development of a modified gel structure [78]. Between 500 °C and 700 °C, C–S–H transforms into a highly reactive polymorph of

dicalcium silicate (C_2S) [76 - 78]. Additionally, above 450 °C, both portlandite and calcite decompose to form calcium oxide (lime, CaO), which retains the capacity to react with water [78].

Upon rehydration of the heat-treated recycled cement, recrystallisation of calcite, portlandite, and ettringite is observed. Moreover, C–S–H is reformed through the hydration of reactive C_2S phases [78].

The hydration kinetics of dehydrated cement differ significantly from those of OPC. These differences arise from changes in the phase composition and microstructure of the cement caused by the thermal activation process.

The main distinctions are as follows:

- Dehydrated cement exhibits very high initial reactivity upon contact with water [79, 80]. This behaviour is attributed to several factors:
    - The hydration of free lime formed during the thermal decomposition of portlandite and calcite. The hydration of CaO is extremely rapid and is accompanied by significant heat release, which is reflected as a pronounced initial peak in isothermal calorimetry measurements [65, 78, 80]. In OPC, free lime is typically absent.
    - The formation of reactive polymorphs of C_2S, such as α'H-C_2S and α'L-C_2S, during the dehydration of calcium silicate hydrate. These polymorphs may exhibit higher hydration rates in the early stages compared to β-C_2S, which is the dominant form in conventional OPC [77, 80, 81].
- Absence or low content of tricalcium silicate (C_3S). Unlike OPC, dehydrated cement derived from hydrated cement paste contains no or negligible amounts of C_3S, the principal phase responsible for early strength development in OPC. The absence or reduction of this phase implies that strength gain in dehydrated cement occurs through alternative mechanisms, primarily via the hydration of CaO and highly reactive C_2S polymorphs [80, 82].
- Although dehydrated cement demonstrates high early reactivity, its later-stage hydration rate is generally lower than that of OPC, largely due to the absence of C_3S [81, 82].

The rapid initial hydration of dehydrated cement also results in increased water demand to achieve standard consistency, as well as accelerated setting times compared to OPC [59, 79, 82].

The incorporation of dehydrated cement has a complex influence on the mechanical properties of cement mortars and concretes. This effect is governed by numerous factors, including the replacement level of OPC with dehydrated cement, the thermal activation temperature, the

fineness of grinding, the water-to-binder ratio, and the presence of other admixtures or supplementary materials [79, 83].

Numerous studies have reported a decline in both compressive and flexural strength with increasing proportions of dehydrated cement. However, at low replacement levels (typically up to 20–30%) the impact on mechanical properties may be negligible or even beneficial, depending on the specific mix design and processing conditions [67, 79, 82, 83].

The thermal activation temperature of the dehydrated cement is a critical parameter influencing its reactivity and the resulting mechanical performance. A temperature range between 600 and 800 °C is commonly cited as optimal for enhancing rehydration properties and facilitating strength development [67, 79].

Despite encouraging results, several aspects of thermally activated RCP remain underexplored. One promising direction is the optimisation of thermal treatment regimes to strike a balance between energy efficiency and the reactivity of the resulting material. Furthermore, existing research has largely concentrated on the recycling of clean, laboratory-prepared hydrated cement paste. Broader investigations are needed to assess the potential of various cementitious wastes as feedstock for thermally activated RCP. While the mechanical properties of rehydrated cement and its associated composites have received considerable attention, durability-related characteristics remain insufficiently studied. Future research should focus on evaluating how the incorporation of dehydrated RCP influences the pore structure, permeability, and overall transport properties of concrete, which are essential indicators of long-term performance.

2.3.3.3. Ceramic powders as pozzolanic SCMs

Ceramics are artificial stone-like materials produced through the sintering of clay-based raw materials. In the context of construction, ceramics encompass a variety of products such as bricks, sewer and drainage pipes, roof tiles, wall tiles, floor tiles, and sanitary ware. Broadly, construction ceramics can be divided into two main categories: red ceramics, also known as terracotta, and white ceramics, which include porcelain and the more porous faience also called earthenware. A schematic representation of the classification of ceramics used in construction is shown in Fig. 2.13.

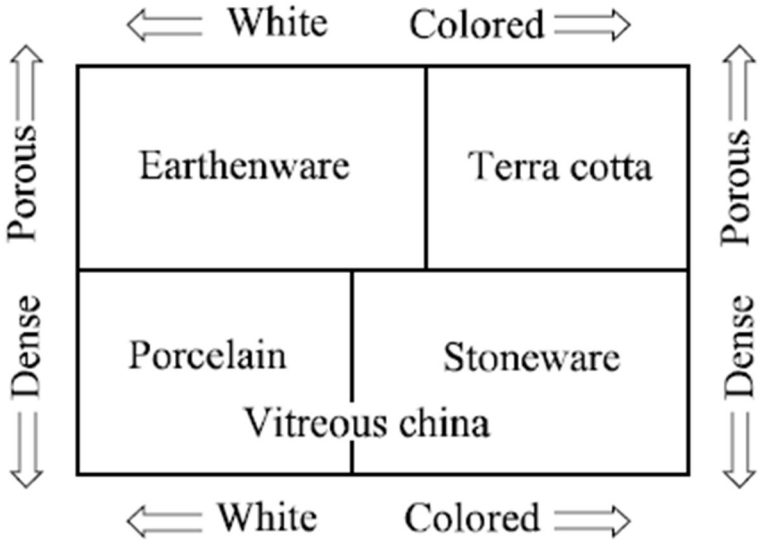

Fig. 2.13. Schematic representation of the traditional ceramic families [84].

Red ceramics are primarily manufactured from natural clays rich in iron oxides (Fe_2O_3), which impart the characteristic reddish colour to the fired product. These ceramics are widely used for structural and roofing applications, including bricks and roof tiles. The clays used are typically illitic or kaolinitic, but what fundamentally distinguishes red ceramics is the elevated iron content, which contributes to both the colour and sintering behaviour [84, 85].

Various additives may be incorporated into the clay mixture to enhance workability, control drying shrinkage, and improve mechanical or thermal properties:

- Non-plastic materials, such as quartz or grog (pre-fired ceramic fragments), help reduce shrinkage during drying and firing, improving dimensional stability [84, 85].

- Fluxing agents, such as feldspar, are added to lower the sintering temperature and encourage partial vitrification, contributing to strength and cohesion in the ceramic matrix [84, 85].

Typical firing temperatures for ceramic bricks and roof tiles range from 800°C to 1000°C [86].

White construction ceramics, such as porcelain stoneware tiles and faience tiles or sanitaryware, are made from refined clay-based mixtures designed to produce white or light-coloured, dense, and durable ceramic bodies. Kaolin is the key ingredient in porcelain, while faience often uses more plastic but less pure clays, such as illitic or calcareous clays, with low content of iron oxides. Besides, feldspar is used as flux to lower the melting point and promote vitrification, and quartz is added to control shrinkage and improve the mechanical resistance of the ceramics.

Firing temperatures of the white ceramics is higher than that of terracotta. Porcelain is fired at 1200-1300°C to ensure full vitrification and very low water absorption. Faience is produced at lower temperature between 950°C and 1150°C [84, 85].

White ceramics are produced from more refined clay compositions that yield light-coloured, dense, and often more vitrified ceramic bodies. They are used in applications requiring low porosity and high aesthetic or hygienic standards, such as floor and wall tiles, as well as sanitary ware.

Porcelain is based on high-purity kaolinitic clays, which contain minimal impurities such as iron oxides. This composition results in a white fired body with excellent mechanical strength, low water absorption, and a high degree of vitrification. Feldspar is used as a flux, and quartz is added to minimise shrinkage and enhance mechanical performance. Porcelain is typically fired at temperatures between 1200°C and 1300°C, ensuring almost full vitrification and very low water absorption (<0.5%) [84, 85].

Faience is generally more porous and less vitrified than porcelain. It is manufactured using more plastic but less pure clays, such as illitic or calcareous clays, which may contain small amounts of iron compounds. Firing temperatures for faience are somewhat lower, ranging from 950°C to 1150°C, resulting in a semi-vitrified product with higher water absorption than porcelain [84].

Terracotta is characterised by a mixture of mineral and amorphous phases. Its typical composition includes quartz (SiO_2), hematite (Fe_2O_3), mullite ($3Al_2O_3{\cdot}2SiO_2$), remnants of dehydroxylated clay minerals, and a limited glassy phase. As it is not fully vitrified, terracotta retains a greater proportion of crystalline minerals and unreacted clay components than porcelain [84].

Porcelain, in contrast, is more homogeneously vitrified. Its microstructure is composed primarily of mullite, quartz, and a significant amorphous glassy phase. Fine acicular (needle-like) mullite crystals are typically embedded within a dense glassy matrix, contributing to the material's high strength, low porosity, and translucency in some cases. Faience typically contains less mullite and glassy phase, but a higher amount of quartz and dehydroxylated clay minerals than porcelain, due to its lower firing temperature [84].

It is therefore evident that ceramics are, in essence, calcined clays. Although the firing temperature during ceramic production typically exceeds the transformation threshold for metakaolin formation (600–800 °C), resulting in partial recrystallisation of some phases, ceramics still retain pozzolanic properties, though to a lesser extent than pure metakaolin.

Moreover, ceramic materials often contain non-reactive mineral components such as quartz and feldspars, which dilute their overall pozzolanic potential.

Numerous studies have confirmed the pozzolanic activity of various ceramic waste types, including red clay bricks, ceramic tiles, and sanitary ware. These studies generally report that replacing up to 25 wt.% of Portland cement with finely ground ceramic waste yields compressive strengths that comply with the mechanical performance criteria established for pozzolanic SCMs [87 - 92].

Despite the well-documented pozzolanic behaviour of ceramic powders, their practical application in cementitious systems remains limited. This is primarily due to the absence of normative standards and the need for further targeted research. A major challenge is the high variability inherent in ceramic waste materials. Differences in raw material origin, chemical and mineralogical composition, firing temperatures, particle size distribution, and post-processing methods contribute to considerable heterogeneity in test results. Consequently, treating different types of ceramic waste with the same methodology oversimplifies its complex nature and leads to inconsistencies in the reported mechanical properties. To address this, it is essential to undertake systematic comparative studies focused on well-characterised, distinct types of ceramic waste. Establishing standardised protocols for material characterisation, along with predictive models that account for ceramic type would provide a robust foundation for broader implementation in construction materials.

Furthermore, there remains a significant knowledge gap concerning the long-term durability of cementitious composites incorporating ceramic powders. In particular, key performance indicators such as resistance to fire and frost, carbonation behaviour, sulphate and acid attack, alkali–silica reaction, and gas permeability have either been insufficiently investigated or not addressed in the literature. Comprehensive studies on these aspects are required to evaluate the long-term reliability of ceramic SCMs and to support their safe and effective utilisation in durable, sustainable concrete.

2.4. Durability of CO2-reduced cement mortars and concretes

In order to implement new SCMs in practical applications, it is essential to first assess their impact on the durability of concrete and mortars. Insufficient resistance to aggressive environmental conditions can compromise the integrity of structures and potentially lead to their

failure. Although concrete degradation due to environmental exposure typically occurs gradually and is often addressed through routine maintenance, it may still result in severe accidents.

A notable example is the partial collapse of the De la Concorde Overpass Bridge (Quebec, Canada) in 2006, which caused five fatalities and six injuries. One of the officially documented contributing factors was the inadequate durability of the concrete used in the bridge piers. The concrete was of poor quality and vulnerable to deterioration under freeze-thaw cycles and exposure to de-icing salts [93].

This chapter discusses key durability indicators and influence of various SCMs on these parameters.

2.4.1. Freeze-thaw resistance

Freeze-thaw resistance is a critical parameter for the durability of many engineering structures, particularly in cold climates where temperatures regularly fall below freezing and repeated freeze-thaw cycles occur. Such cycles can lead to concrete surface scaling, cracking, and eventual deterioration [94, 95].

The primary mechanism of freeze-thaw damage in concrete is the freezing of water retained in the pores of the cement paste and aggregates. Upon freezing, water expands by approximately 9% in volume [96]. This expansion generates internal stresses within the pore structure, primarily due to two types of pressure:

- *Hydraulic pressure*. When the degree of saturation in capillary pores exceeds approximately 91%, freezing causes water to be expelled into the gel pores, which are already saturated. This process generates hydraulic pressure that can exceed the tensile strength of the concrete, leading to internal cracking [95].
- *Osmotic pressure*. As part of the water in the capillary pores freezes into pure ice crystals, the concentration of soluble salts in the remaining liquid phase increases. A concentration gradient develops between the capillary water and the gel pores, which are separated by a semi-permeable structure. This results in osmotic pressure that further stresses the concrete matrix [95].

If the concrete lacks sufficient tensile strength to resist these internal pressures, surface scaling and microcracking occur [94]. Repeated freeze-thaw cycles lead to the progressive accumulation of damage, ultimately compromising the structural integrity of the concrete [95].

The freeze–thaw resistance of concrete is influenced by numerous factors related to both the material properties and the environmental conditions in which it operates:

- The higher the degree of water saturation within the concrete, the greater the likelihood of damage during freezing [16, 96].
- The characteristics and size distribution of pores in cement matrix significantly affect freeze–thaw resistance. A denser matrix with smaller, well-distributed, and isolated pores enhances resistance by limiting water ingress and reducing internal stresses during freezing [16, 19, 95].
- A lower water-to-cement (w/c) ratio generally results in a denser and less permeable concrete matrix. Reduced permeability limits water penetration into the pore system, thereby increasing freeze–thaw durability [94, 95]. The poor durability of concrete used in the De la Concorde Overpass Bridge was attributed to an excessively high w/c ratio (0.56 instead of the recommended 0.49) [93].
- The incorporation of air-entraining agents is a widely accepted method for enhancing freeze-thaw resistance. The intentionally introduced air voids act as pressure-relief zones, providing space for expanding water during freezing and thus mitigating internal stresses [94 - 96].
- The durability of coarse aggregates under freeze–thaw conditions is also critical. Unstable aggregates may undergo internal cracking or spalling upon freezing of entrapped water, leading to surface defects such as pop-outs and overall reduction in concrete performance [95, 96].

As discussed in Section 2.1.2, SCMs influence the type and morphology of hydration products in blended cements. They contribute to improved particle packing, refinement of the pore structure, and reduced pore connectivity. These effects decrease the permeability of the concrete and thereby enhance its resistance to freeze–thaw cycles [40].

2.4.2. Fire resistance

Fire resistance of concrete refers to the ability of concrete structures to retain their load-bearing capacity and functional integrity under fire conditions for a specified period of time [97]. Ensuring adequate fire protection is a critical aspect of structural design, as it directly impacts the safety of building occupants and emergency personnel during fire incidents.

During fire exposure, the surface temperature of concrete can range from 550 °C to 1200 °C, while the internal temperature remains significantly lower, depending on the depth from the exposed surface [98 - 100].

Concrete degradation typically begins at temperatures exceeding 300 °C, where the decomposition of hydration products such as calcium silicate hydrate, the thermal incompatibility between aggregate and cement paste, and the formation of microcracks due to stress concentrations become evident [97]. At approximately 450 °C, portlandite decomposes, while at 700–900 °C, carbonate phases undergo decarbonation. Beyond 1000 °C, melting of the cement matrix and aggregates occurs [97, 100, 101].

In addition to chemical decomposition, the build-up of vapour pressure within capillary pores can create tensile stresses that exceed the tensile strength of the concrete. This risk is particularly pronounced in concrete with high moisture content and under rapid heating conditions [100]. In severe cases, significant parts of the concrete structure may break away. High-strength concretes with low permeability are more susceptible to spalling due to the impeded escape of vapor [100]. Furthermore, uneven heating introduces thermal gradients, resulting in internal stresses caused by the differential thermal expansion of the cement matrix and aggregates [97].

Different SCMs have different effects on the fire resistance of concrete [101]:

- Concretes incorporating fly ash or slag materials generally exhibit higher residual strength after exposure to elevated temperatures than those made with ordinary Portland cement.
- Silica fume enhances mechanical properties up to 300 °C, but leads to performance deterioration above 550 °C. At 800 °C, concrete containing 10% silica fume shows significantly increased porosity and average pore size compared to OPC concrete.
- Concretes with metakaolin display improved residual strength in the range of 200–400 °C; however, they tend to lose strength more rapidly between 400 °C and 800 °C, resulting in lower residual strength than OPC.
- At 300 °C, LC3 binder demonstrates higher relative strength than OPC. However, at 900 °C, its residual strength is lower—similar to concretes containing silica fume or metakaolin.

2.4.3. Sulphate attack

Sulphate resistance is an important property of concrete, as sulphate salts are often found in soils and groundwater. These salts can cause deleterious effects such as expansion, cracking, loss of strength, and eventual deterioration of concrete structures [16, 17, 96, 102].

The deterioration of concrete due to sulphate attack occurs through a series of chemical reactions, the most significant of which are as follows [16, 17, 96, 103]:

- Formation of gypsum through the reaction of sulphate ions with calcium hydroxide:
  $Ca(OH)_2 + SO_4^{2-} + 2H_2O \rightarrow CaSO_4 \cdot 2H_2O + 2OH^-$ (1)
  This reaction is accompanied by a volumetric expansion of approximately 2.2 times.
- Formation of ettringite through the reaction of sulphates with calcium aluminate phases in the hydrated cement paste:
  $Ca_4Al_2(OH)_{12} \cdot SO_4 \cdot 6H_2O + 2CaSO_4 + 20H_2O \rightarrow Ca_6Al_2(OH)_{12} \cdot (SO_4)_3 \cdot 26H_2O$ (2)
  This reaction also results in substantial expansion (1.2–2.2 times compared to the original reactants).
- In the presence of magnesium sulphate ($MgSO_4$), in addition to forming gypsum and ettringite, magnesium ions react with the calcium silicate hydrate gel ($CaO \cdot 2SiO_2 \cdot nH_2O$), leading to its decomposition and the formation of brucite ($Mg(OH)_2$) and silica:
  $3CaO \cdot 2SiO_2 \cdot nH_2O + 3MgSO_4 + 7H_2O \rightarrow 3CaSO_4 \cdot 2H_2O + 3Mg(OH)_2 + 2SiO_2 + nH_2O$ (3)
  This process compromises the binding capacity of the cement paste, accelerating structural degradation.

The formation of expansive products such as gypsum and ettringite generates internal stresses within the concrete, leading to cracking, spalling, and eventual loss of strength. Furthermore, sulphate attack may promote the leaching of calcium from the C–S–H gel, weakening the gel's rigidity and contributing to the progressive degradation of the cement matrix [16, 17, 96].

The cement phase most vulnerable to sulphate attack is tricalcium aluminate (C_3A). Therefore, sulphate-resistant cements typically contain no more than 5% C_3A [16, 19, 38, 96, 104].

The incorporation of pozzolanic SCMs improves sulphate resistance through multiple mechanisms. Firstly, pozzolanic reactions consume calcium hydroxide, thereby reducing the availability of $Ca(OH)_2$ for reaction with sulphates. Secondly, the partial replacement of OPC by SCMs reduces the total C_3A content in blended cements. Finally, when properly proportioned, SCMs refine the pore structure by filling spaces between cement particles and generating

additional C–S–H, thus reducing permeability and slowing the ingress of sulphate ions [16, 17, 19, 94].

2.4.4. Chloride penetration

Concrete structures are exposed to chlorides in environments affected by seawater, de-icing salts, and saline groundwater. Seawater contains considerable concentrations of both chloride and sulphate ions, which pose a significant threat to the durability of concrete. The ingress of chlorides can result in several detrimental effects, including enhanced leaching of calcium hydroxide and consequent increased porosity of the cement matrix and reduction in the mechanical strength of the concrete [17, 19, 96, 103]. In reinforced concrete, a particularly critical issue is the increase in the chloride-to-hydroxide ion ratio ($Cl^-/(OH)^-$), which may lead to depassivation of the steel reinforcement and initiate corrosion. The corrosion of reinforcement generates cracks within the concrete, thereby compromising the integrity and load-bearing capacity of the structure [17, 96, 105].

The deterioration process begins with the penetration of chloride ions through the pores and microcracks of the concrete. When the chloride ion concentration at the reinforcement surface reaches a critical threshold, the protective oxide layer on the steel is destabilised, initiating electrochemical corrosion. The products of corrosion occupy a greater volume than the original steel, generating internal tensile stresses within the surrounding concrete. These stresses lead to cracking and spalling of the concrete cover, which, in turn, facilitates the further ingress of chlorides, oxygen, and moisture, thereby accelerating the corrosion cycle [17, 19, 96, 105]. Additionally, salts crystallisation within the concrete pores can induce further pressure, contributing to material degradation [17].

It is evident that reducing the permeability of concrete slows down the ingress of chloride ions. Furthermore, as with sulphate attack, the tricalcium aluminate content in Portland cement influences chloride resistance, since C_3A can react with chloride ions to form calcium chloroaluminate [19].

The incorporation of SCMs into the concrete mix contributes to reduced permeability. Consequently, the use of high-quality SCMs, in combination with appropriate concrete mix design and adequate concrete cover over the reinforcement, significantly enhances the durability of the structure [19, 38, 40, 94, 101].

2.4.5. Acid attack

Concrete structures may be exposed to a variety of acidic environments. Such conditions can arise due to industrial pollution, for instance in mining areas or chemical plants. In natural settings, acidic environments can develop in marshy soils that contain marcasite or pyrite, which, upon oxidation, produce sulphuric acid [96, 104]. Similar processes occur in certain shale formations, such as alum shales, which contain the unstable iron sulphide pyrrhotite. When these rocks are crushed and weathered, pyrrhotite rapidly oxidises, resulting in the formation of iron sulphates and sulphuric acid [104]. Of particular concern is the problem of biogenic sulphuric acid corrosion, which is commonly observed in sewer systems. In these systems, microbial activity leads to the release of hydrogen sulphide, which subsequently oxidises to sulphuric acid, aggressively attacking the concrete [16, 96].

The mechanism of concrete degradation in acidic environments involves the dissolution of components within the cement matrix. Initially, acids react with calcium hydroxide, a hydration product of cement, to form soluble salts that are leached from the concrete. Sulphuric acid reacts with calcium hydroxide to produce gypsum. This reaction is associated with a substantial increase in the volume of the solid phase, generating internal stresses that contribute to cracking [16, 96].

In addition to reacting with calcium hydroxide, acids can also attack calcium silicate hydrates, which constitute the primary binding phase in concrete. This reaction leads to the breakdown of the C–S–H gel and the formation of silica gel ($SiO_2 \cdot nH_2O$), a weak product that does not support the structural integrity of concrete [96]:

$$3CaO \cdot 2SiO_2 \cdot 3H_2O + 6H^+ + nH_2O \rightarrow 3Ca^{2+} + 2(SiO_2 \cdot nH_2O) + 6H_2O \quad (4)$$

As a result, porosity and permeability increase, facilitating the further ingress of aggressive agents and accelerating the deterioration process.

Pozzolanic materials react with calcium hydroxide in the cement matrix to form additional calcium silicate hydrates. This reaction lowers the $Ca(OH)_2$ content of the concrete, thereby reducing its susceptibility to acid attack by decreasing the amount of material available for dissolution. Furthermore, the generation of additional C–S–H gel contributes to the densification of the concrete microstructure, lowering its permeability and limiting acid penetration [16, 38, 94, 96].

2.4.6. Carbonation

Carbonation is a process in which calcium hydroxide present in the pores of concrete reacts with carbon dioxide from the atmosphere to form calcium carbonate [40]:

$$Ca(OH)_2 + CO_2 \rightarrow CaCO_3 + H_2O \quad (5)$$

This reaction leads to a reduction in the pH of the concrete pore solution from a highly alkaline level (typically around 12.5–13.5) to values below 9. The high alkalinity of concrete is essential for maintaining the passivity of steel reinforcement, thereby protecting it from corrosion. However, the reduction in pH caused by carbonation destroys this passive film, rendering the steel vulnerable to corrosion, particularly in the presence of moisture and oxygen. The corrosion of reinforcement results in an increase in its volume, which generates internal stresses within the surrounding concrete. These stresses cause cracking, which can ultimately compromise the integrity and durability of the structure [19, 40].

As with other forms of chemical degradation, the incorporation of pozzolanic SCMs enhances the resistance of concrete to carbonation by reducing its permeability [19, 38, 40, 94].

Chapter 3: Fine demolition wastes as supplementary cementitious materials for CO2 reduced cement production

Abstract

Construction and demolition waste accounts for a significant amount of the total solid waste produced worldwide, and its recycling is challenging. Although some demolition waste is processed into recycled sand and rubble, the finer fractions resulting from screening and washing of recycled aggregates are not used. This research investigates the potential of use of real demolition wastes, namely concrete screening fines (CS), mixed concrete-ceramic screening fines (MS), and mud from recycled aggregates washing (WM), as supplementary cementitious materials (SCMs) in eco-efficient blended cement. The study employed various experimental methods, such as isothermal calorimetry, thermogravimetric analysis (TGA), and setting time tests, to evaluate the hydraulic activity of waste materials and the Chapelle test and TGA to assess their pozzolanic activity. The mechanical properties and microstructure of mortars containing 20% of waste powders were evaluated using compressive strength tests and scanning electron microscopy (SEM). The results showed that thermal treatment of waste materials at 500°C improved the mechanical properties of mortars, increasing Strength Activity Index (SAI) by 10% for CS and MS and by 6% for WM after 90 days of curing. All three waste types achieved similar mechanical properties, with compressive strengths of at least 37.93 MPa, 46.25 MPa, and 51.33 MPa after 7, 28, and 90 days of curing, respectively. The contribution of waste powders to mortar strength was due to filler effect and partially dehydrated C-S-H products. However, pozzolanic ceramic inclusions in waste powders did not affect mortar strength at a 20% substitution rate. Therefore, the research findings indicate that waste materials derived from demolition can potentially be used as environmentally friendly materials in construction. Their use as SCMs with a substitution rate of 20% can reduce the CO2 emissions of cement production by at least 10.7%.

3.1. Introduction

Worldwide, construction and demolition waste (CDW) accounts for 30–40% of the total solid waste produced [106, 107]. A large part of these wastes are inert materials such as concrete and ceramics, and although they are not hazardous, their recycling is quite challenging. Currently, part of the demolition waste is successfully processed into recycled sand and recycled rubble, which are used as aggregates in road works [107]. In addition, there is a growing interest in exploring the possibility of using these materials to create high-strength and long-lasting concrete and mortar [108 - 110]. The use of recycled aggregates for concrete production faces a major challenge of adherent hydrated cement, resulting in a double interfacial zone between the aggregate and the new cement matrix [111 - 115]. This causes a decline in the strength of concrete made with recycled aggregates. Hence, to enhance aggregates quality, it is necessary to clean them of the old cement matrix. Numerous studies have explored methods to improve the quality of recycled aggregates [116 - 118] including mechanical [119], thermal [110, 120] and chemical [112 - 124] approaches. Nevertheless, in practice, processing plants primarily utilize screening and washing to remove small, non-conforming fractions from the aggregates. However, even this method generates a large amount of secondary wastes such as screening fines and washing sludge, which are still not used. Thus, more than two thirds of CDW are disposed in the landfills [125], which not only disfigure the landscape, but can also change the composition of the soil and groundwater and thereby lead to the disruption of ecosystems [55, 106]. In addition, dusty waste from screening and washing in dry weather conditions forms aerosols, that adversely affects air quality.

Recently, due to the threat of global climate change, studies on the possibility of using CDW as Supplementary Cementitious Materials (SCMs) [91, 126 - 133] and as an alternative raw material for the production of cement clinker [129, 134 - 138] have been increasingly conducted since the production of Ordinary Portland cement is associated with high CO_2 emissions. For the countries of the European Union, the use of CDW as a cement substitution is a promising area of research, since traditional SCMs such as natural pozzolans, fly ash and granulated blast furnace slag have limited availability [11, 139]. On the other hand, according to the analysis performed on the example of Luxembourg by Bogoviku and Waldmann [140], construction and demolition waste should cover the demand for materials to produce new cement for at least the next 80 years.

In addition, studies of the characteristics of concrete after a fire have shown that, after contact with water, concrete that has lost its strength under the influence of high temperatures is capable

of rehydration and partial restoration of mechanical properties [74, 78, 141, 142]. This gave impetus to research on the possibility of reactivating cement-based waste for use as a hydraulic binder or hydraulic SCM. Thus, according to Splittgerber and Mueller [141], the hydration of pure clinker is a completely reversible process. However, during the dehydration of cement containing gypsum additional intermediate phases are formed, such as ye'elimite. Zhang et al. [76] and Shi et al. [143] also state that when hydrated cement paste is calcined at temperatures above 500°C, the resulting product includes β-C2S, which is a component of Portland cement, and lime. However, other studies [77, 79 - 81, 144, 145] have shown that β-C2S is only formed at temperatures above 800°C. At lower temperatures, depolymerization of C-S-H resulted in the formation of α-C2S, which is a more reactive polymorph of C2S than β-C2S. This explains the higher initial strength of heat-treated cement pastes compared to Portland cement, as well as the non-linear increase in the strength of samples from processed cement depending on the processing temperature. Thus, 600-750°C was named as the optimal range of activation temperatures [79, 81, 144, 145]. On the other hand, Wang et al. [146] state that the optimum treatment temperature for hydrated cement is 450°C, at which partial dehydration of C-S-H has already taken place, but decarbonization of calcite particles has not yet begun, that provided filler and nucleation effect. It also should be noted that C3S is not formed during the thermal treatment of hydrated cement [80 - 83].

In general, according to the literature, the processes occurring during the heat treatment of hydrated cement can be considered as follows [11, 80, 82, 144, 147 - 150]:

- 20 – 130°C: elimination of evaporable water and a part of the bound water.
- 110 – 200°C: dehydration of ettringite and gypsum.
- 140 – 450°C: dehydration of calcium silicate hydrates and carboaluminate hydrates.
- 450 – 650°C: formation of lime due to portlandite dehydroxilation, and formation of α-C2S due to calcium silicates depolymerization.
- 600 – 900°C: formation of lime due to calcite decarbonization, and polymorphic transformation of α-C2S to β-C2S.
- Above 1000°C: melting.

The study of the rehydration of heat-treated cement carried out by Bogas et al. [77, 80], Real et al. [145] and Carriço et al. [79] showed the formation of C-S-H, portlandite and ettringite, similar to those found in Portland cement. In addition, calcium carboaluminate hydrates and AFm phases were detected already after 8 hours of rehydration. Moreover, the recycled cement showed higher degree of hydration in the early stages due to the high reactivity of α-C2S and CaO, but by the 28th

day, the hydration was significantly reduced compared to Portland cement, leading to weaker strength gain.

It is important to note that all the above studies on thermal activation of demolition waste focus on research conducted on laboratory-made hydrated paste and concrete as the precursor material. This approach eliminates the influence of impurities and allows for more controlled and accurate results. However, it is crucial to investigate the thermal activation of actual demolition waste as it may differ significantly from laboratory-prepared samples. The presence of impurities and contaminants, such as calcite and quartz derived from aggregates, as well as high levels of carbonization resulting from prolonged service life, can greatly impact the thermal activation process. Understanding the thermal activation of real demolition waste is crucial for the development of effective and sustainable waste management strategies and for reducing the environmental impact of construction and demolition activities.

3.2. Goals and significance of the research

This paper presents the results of a study investigating the recycling potential of fine waste generated during the production of recycled aggregates. The study focuses on the thermal activation of real demolition waste, which has not been extensively studied in previous comparable works. A comparative table of available works on the use of dehydrated cement in the production of binders is provided in the appendix to this article.

The materials studied in this paper are waste from the processing of recycled aggregates, which have already been exposed to an entire life cycle in a structure and thus have a high degree of carbonation and high impurities. Screening fines and wash mud, that are the final wastes from recycled aggregates processing, have not yet found a practical application due to their substandard granulometry and high concentration of organic impurities and gypsum.

The main objective of the research is to understand whether the investigated materials possess hydraulic activity, or they can be used as inert fillers, which are important properties for the use of waste materials in the production of blended cement. The study aims to identify the possibility of using these fines generated from the processing of demolition waste in the production of cement with reduced CO_2 emissions. As discussed in section 1, the process of decarbonization in concrete-containing waste typically starts at around 600°C, while the breakdown of hydration products and the activation of hydrated cement can occur as low as 450°C. To avoid excessive CO2 emissions from the decarbonization of raw materials and fuel combustion, this study has

chosen to utilize treatment temperatures no higher than 500°C to minimize the environmental impact of the treatment process while still achieving the desired outcomes.

The novelty of the study lies in the fact that it considers the mud from the washing of recycled aggregates, which has not yet been studied, and the effect of thermal activation on mixed demolition waste, including the pozzolanic activity of ceramic inclusions. This can be an important factor, since according to Bogas et al. [80], the high amount of CaO found in dehydrated cement quickly reacts with water, providing ample CH for pozzolanic reactions. The combination of pozzolanic admixtures with thermally activated cement may address some of the main issues reported in the literature, such as short setting time and high water demand.

The present research aims to contribute to the growing body of knowledge on the use of real demolition waste in the production of cement. The study will provide valuable information on the feasibility of using wash mud and mixed demolition waste in the production of cement with reduced CO_2 emissions and will fill the gap in the existing literature on the topic.

3.3. Materials

3.3.1. Raw materials description

The materials investigated in this study were three types of fine demolition waste provided by the Belgian company Tradecowall, which processes inert waste into recycled aggregates and sand. During processing, the aggregates go through several screening stages, as a result of which they are separated into different fractions. Substandard fractions sifted out in the screening process cannot be used as aggregates and are considered as final waste which is stored on site. After screening, the recycled aggregates are washed forming a wash mud which is also stored on site.

Approximately 30 kg of three types of demolition waste fines were sampled:

- Screening waste from concrete (CS) aggregates processing consisted of concrete fines mixed with a minor proportion of impurities, including metal reinforcement debris.
- Screening waste from mixed (MS) aggregates processing consisted of about 60% of concrete, 30% of ceramics, glass and stones with minor impurities of organic materials such as wood, bitumen, polymers and fabrics.

- Mud from recycled aggregates washing (WM), which was a dark grey mass with a light petroleum-like odour.

According to the manufacturer, the size of the screening waste and wash mud used in this study was 0/8 mm and 0/63 μm respectively. Moisture content in the screening wastes was about 13 mass-%, while in the wash mud was 22 mass-%.

Besides the investigated wastes in the research, a Portland cement CEM I 52.5 R with specific gravity of 3.05 g/cm^3 and Blaine specific surface area of 5418 cm^2/g provided by the French manufacturer Vicat, CEN Standard Sand according to EN 196-1 [150], and tap water were used for the mortar specimens mixing.

3.3.2. Materials preparation

After sampling in the field, the materials were separated into two groups and dried in two different modes: at room temperature and at 105°C to constant mass. Dried materials were subjected twice to crushing. Preliminary crushing was carried out in a jaw crusher, and the final crushing was performed in an impact mill with a bottom sieve of 2 mm mesh size. After crushing, the wastes were sieved on a 125 μm mesh sieve for their separation into two fractions: 0.125/2 mm and 0/125 μm. Regardless of the drying method, the finer fraction of CS and MS accounted for one third of the total material, while in the case of WM, three quarters of the material consisted of particles smaller than 125 μm. The discrepancy of the WM fineness declared by the manufacturer can be explained by the partial cementation of the material during storage and drying, as well as by its contamination with larger debris. Fraction of 0.125/2 mm can potentially be used as recycled sand. In this study, only the 0/125 μm fraction was used.

Thus, after drying, grinding and sieving, 6 investigated powders were obtained: concrete fines, mixed fines and wash mud dried in natural conditions (CSN, MSN and WMN), and dried at 105°C (CS105, MS105 and WM105). Furthermore, the materials dried at 105°C were calcined in a muffle furnace at 400°C and 500°C for 2 hours with heating mode 10°C/min without ventilation and subsequent natural cooling in a closed furnace. As a result, 6 more materials were obtained: CS400, MS400, WM400, CS500, MS500 and WM500.

3.4. Experimental methods

3.4.1. Characterization of investigated wastes

Dried in ambient conditions and crushed materials underwent thermal DTA/TGA analysis with a STA 449 F5 Jupiter thermal analyser at air atmosphere and with a heating rate of 20°C/min. After materials preparation, the changes in their mineralogical composition, density and fineness depending on the treatment temperature were investigated. Mineralogical composition was studied using D2 PHASER X-ray diffractometer with following parameters: Cu-Kα radiation, 10 mA, 30 kV, rotation between 5° and 70° with a 0.02° 2θ step and a step time of 0.6 s, and measured by Rietveld method using Profex software. The pycnometer method with petrol as liquid was used to determine the density. Fineness of the materials was determined by Blaine method for air permeability specific surface area measurement as well as by particle size distribution analysis obtained with HELOS & RODOS laser granulometer.

3.4.2. Evaluation of hydraulic activity

The change in the hydraulic activity depending on the treatment temperature of the investigated powders was estimated by the measurement of the hydration heat using micro DSC 7 evo isothermal calorimeter. TGA of pastes made of 100% WMN and WM500 and w/b ratio of 0.5 after 90 days curing and drying at 50°C until weight constancy was carried out to check if the hydration products formed at later stages. In addition, the measurement of the setting time of binder pastes using a Vicat apparatus in accordance with the European standard EN 196-3 [151] was used, except that the pastes were not immersed in water. The dry part of paste mixtures consisted of 0.8 parts Portland cement and 0.2 parts SCM, the water content in the pastes was determined by standard consistency test in accordance with EN 196-3 standard [151].

3.4.3. Evaluation of pozzolanic activity

The Chapelle test combined with the TGA were used to estimate the pozzolanic activity of the investigated materials.

For the Chapelle test, 1 g of investigated powder, 2 g of calcium oxide and 250 ml of distilled water were placed in a 500 ml Erlenmeyer flask. The flask with magnetic stir bar and laboratory condenser was placed on a magnetic-stirrer hot plate heated to a temperature of 85°C. The mixture was stirred for 16 hours. After cooling to a room temperature, the solution was mixed with 250 ml of saccharose syrup (0.7 M) and stirred for 30 minutes to extract unreacted lime. Then, the mixture was filtered on a filter paper and 25 ml of the filtrate were titrated with 0.1 N solution of hydrochloric acid using phenolphthalein as an indicator. To calculate the amount of fixed lime a blank test without pozzolan was carried out. The pozzolanic activity was calculated according to the formula:

$$mg\ of\ Ca(OH)_2 fixed = 2*((V_1-V_2)/V_1)*(M_{Ca(OH)2}/M_{CaO})*100 \quad (6)$$

where V_1 is the volume of HCl solution consumed in the blank test, V_2 is the volume of HCl solution consumed in the pozzolan test, $M_{Ca(OH)2}$ is the molar mass of calcium hydroxide (74 g/mol), M_{CaO} is the molar mass of calcium oxide (56 g/mol).

TGA was carried out only on the paste samples with 20% of MSN and MS500 and w/b ratio of 0.4 after 90 days curing and drying at 50°C until weight constancy to check if there are differences in portlandite consumption by ceramic particles.

3.4.4. Evaluation of compressive strength

To assess the suitability of the materials for use as SCMs, their effect on the compressive strength of 40x40x160 mm mortar bars in accordance with the ISO 679:2009 [152] international standard was studied. The water-to-binder (w/b) and sand-to-binder (s/b) ratios of all mixtures were fixed at 0.5 and 3 respectively. Portland cement substitution rate was set at 20%. This substitution rate was selected for the possibility of assessing Strength Activity Index (SAI) according to the ASTM C311/C311M standard [153]. The use of SAI is favourable for evaluating the effect of investigated materials on mortar strength and their suitability for use as SCMs. The specimens were cured in the moisture chamber at 20°C during 7, 28 and 90 days before testing on a hydraulic press. Compressive strength test results of reference specimens and specimens containing 20% SCMs were used to calculate SAI using the following formula:

$$SAI = (R/R_{ref})*100\% \quad (7)$$

where R is the average strength of the mortar bars with 20% of investigated SCMs, R_{ref} is the average strength of the referenced mortar.

3.4.5. Microstructure of mortar specimens

After undergoing strength tests for 90 days of curing, the fragments remaining from the reference mortar specimens, as well as the mortar specimens CS500, MS500 and WM500, were stored in plastic bags for a year. To analyse the microstructure, they were coated with a 4 nm layer of gold and examined with a field emission scanning electron microscope JEOL JSM-6010LA.

3.5. Results and discussion

3.5.1. Characterization of investigated wastes

The chemical composition of the investigated materials and cement obtained by X-Ray Fluorescence analysis is given in the Table 3.1. The main oxides of all wastes are SiO_2 and CaO, followed by Al_2O_3, Fe_2O_3, K_2O and MgO. As expected, MS and WM contain more silica, alumina, and iron oxides than CS due to ceramics and glass presence. However, the content of pozzolanic oxides in all the studied wastes is less than 70% that is not high enough to consider them as materials with significant pozzolanic activity. Nevertheless, the higher content of these oxides in MS and WM suggests some difference in the rehydration of these materials compared to pure concrete. The loss on ignition of concrete fines is noticeably higher than that of the other two materials, which indicates a higher content of cement hydration and carbonation products in CS.

Table 3.1. Oxide composition of the investigated materials, mass-%.

	SiO_2	Al_2O_3	Fe_2O_3	CaO	MgO	TiO_2	MnO	Na_2O	K_2O	P_2O_5	SO_3	LOI*
CS	28.42	5.90	4.12	33.29	1.63	0.45	0.12	0.35	1.25	0.17	0.80	23.50
MS	41.94	8.10	5.51	21.24	1.11	0.77	0.11	0.47	2.15	0.44	2.56	15.60
WM	44.60	9.42	5.83	17.76	1.37	0.81	0.11	0.30	2.30	0.34	1.27	15.90
CEM I	16.07	3.91	3.58	66.72	1.45	0.37	0.08	0.26	1.18	0.39	3.88	2.10

* Loss on ignition at 950 °C

The X-ray diffraction patterns of the investigated materials shown in Fig. 3.1, indicate the presence of high levels of quartz and calcite in all three samples. However, compared to CS, which contains approximately equal amounts of both minerals, MS and WM have reduced levels

of calcite and elevated levels of muscovite, which can be attributed to the presence of ceramic particles and lower concrete content. The presence of dolomite was detected in CS and WM, but not in MS. Furthermore, small amounts of gypsum were observed in MS and WM, with MS exhibiting a higher concentration. Clay minerals, chlorites, were exclusively detected in CS. The presence of a faint amorphous halo between 20 and 40 degrees, especially in sample CS, and broad peaks indicates the presence of some moderate amount of amorphous phase in the materials.

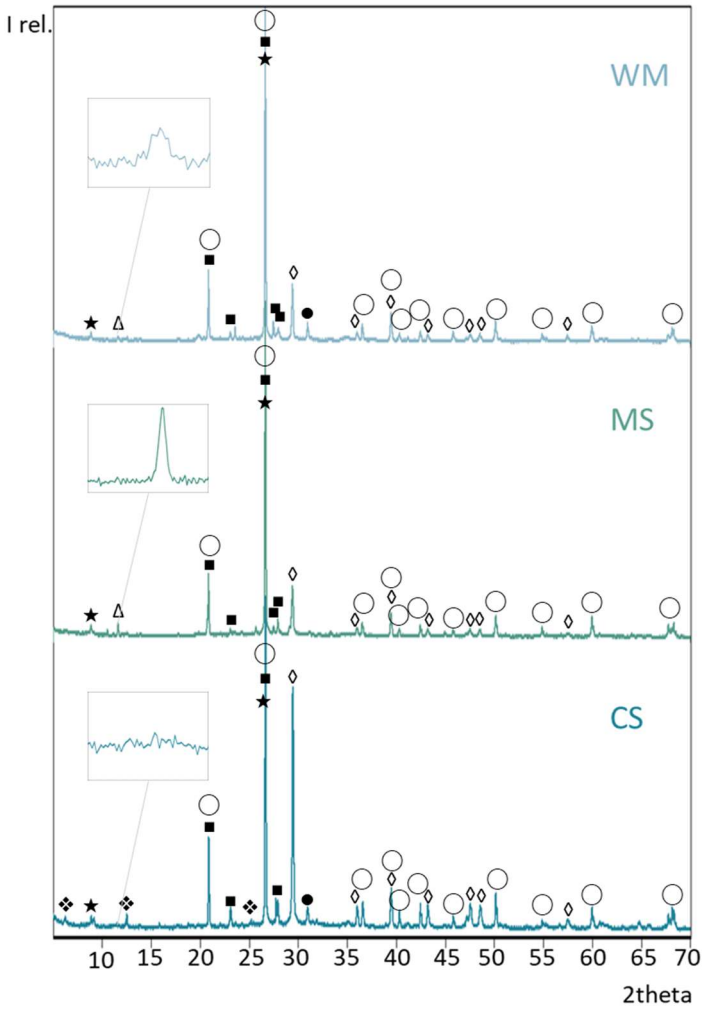

Fig. 3.1. XRD patterns of the investigated materials: ◯ – quartz, ◊ – calcite, ■ – feldspars, ★ – muscovite, ● – dolomite, ❖ – chlorites, Δ – gypsum.

Unlike the data of Gastaldi et al. [135], Florea et al. [127] and Shui et al. [147], mineralogical analysis of all investigated materials did not show the presence of portlandite and ettringite that have the main peaks at 18.0° 2θ and 9.1° 2θ respectively. The absence of these phases in the investigated materials is explained by their transformation into calcite over time as a result of carbonation processes. It should be noted that portlandite and ettringite are the phases that are

important for reactivation of recycled cement by thermal treatment due to their dehydration and dehydroxylation, and the non-availability of these phases in the investigated wastes may indicate the ineffectiveness of heat treatment for their activation.

The results of the mineralogical analysis were confirmed by DTA/TGA analysis. Three main endothermic and two exothermic peaks are observed on the DTA curves of all materials shown in the Fig. 3.2. The first endothermic between 100°C and 200°C, accompanied by a weight loss of about 5% for CS and 2.5% for MS and WM, refers to the removal of free water and dehydration of calcium silicate hydrates. The second endothermic peak with a maximum at 570°C, which is not accompanied by a weight change, is related to the polymorphic transformation of α-quartz into β-quartz. The third endothermic peak around 800°C related to the decarbonization processes is accompanied by a loss in mass of 13%, 8.5% and 7.5% for CS, WM and MS respectively. The wide exothermic peak between 150°C and 350°C refers to the organic impurities burning processes, and the exothermic peak at 820 – 860°C refers to the crystallization of wollastonite as a result of sintering of silicon oxide with calcium oxide released during calcite decarbonization. Portlandite dehydroxylation process was not detected for any material.

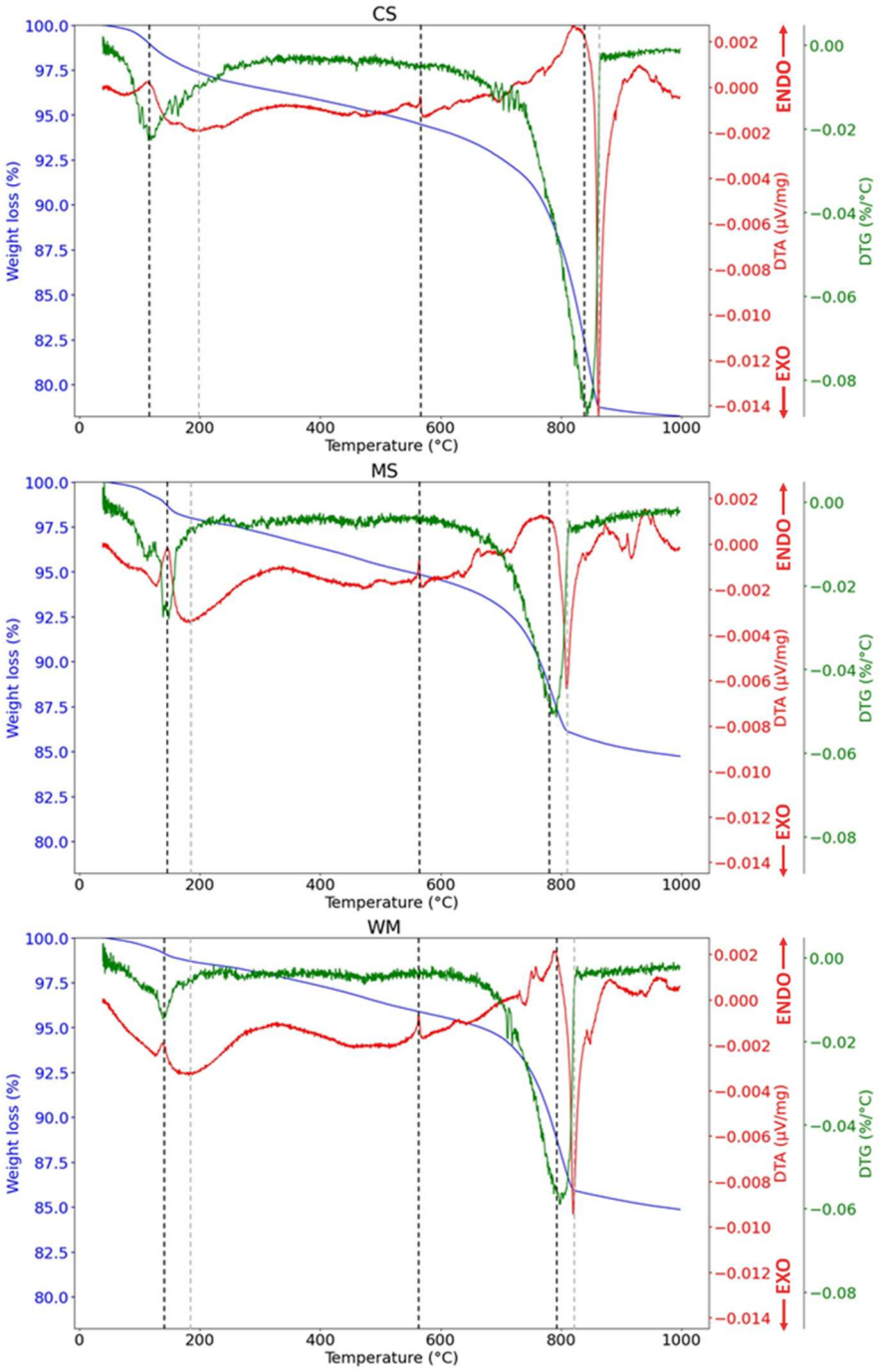

Fig. 3.2. TGA/DTG/DTA curves of investigated materials.

Since the thermal decomposition of cement hydration products, which should facilitate waste grinding, takes place already at a temperature of 100 – 200°C, it can be expected that materials dried at increased temperature followed by grinding will have a higher fineness than materials dried in natural conditions. On the other hand, Carriço et al. [83] noticed that fine thermoactivated cement particles tend to agglomerate, which decreases their fineness. Also, considering that when materials are heated to a temperature of 500°C, further decomposition of hydration products occurs as well as oxidation processes and organic matter burnout. Thus, it

can be assumed that the thermal treatment of powders can affect their density, granulometric and mineralogical composition.

Fig. 3.3 shows the results of measuring the specific gravity and specific surface area (SSA) of the investigated materials. As expected, samples crushed after drying at elevated temperatures have a higher SSA than samples dried at room temperature. For CS, MS and WM this increase is from 5216, 5009 and 4888 to 5620, 5316 and 5436 respectively. However, after calcination, the fineness of the powders decreases from 5620, 5316 and 5436 cm^2/g to 5539, 5049 and 5105 cm^2/g for CS, MS and WM respectively. These data are confirmed by particle size distribution plots obtained using laser granulometry (Fig. 3.4). This can be explained by the agglomeration of particles due to melting of low-melting inclusions. However, the difference in SSA and particle size distribution of all powders seems insignificant, and these values are quite close to those of Portland cement.

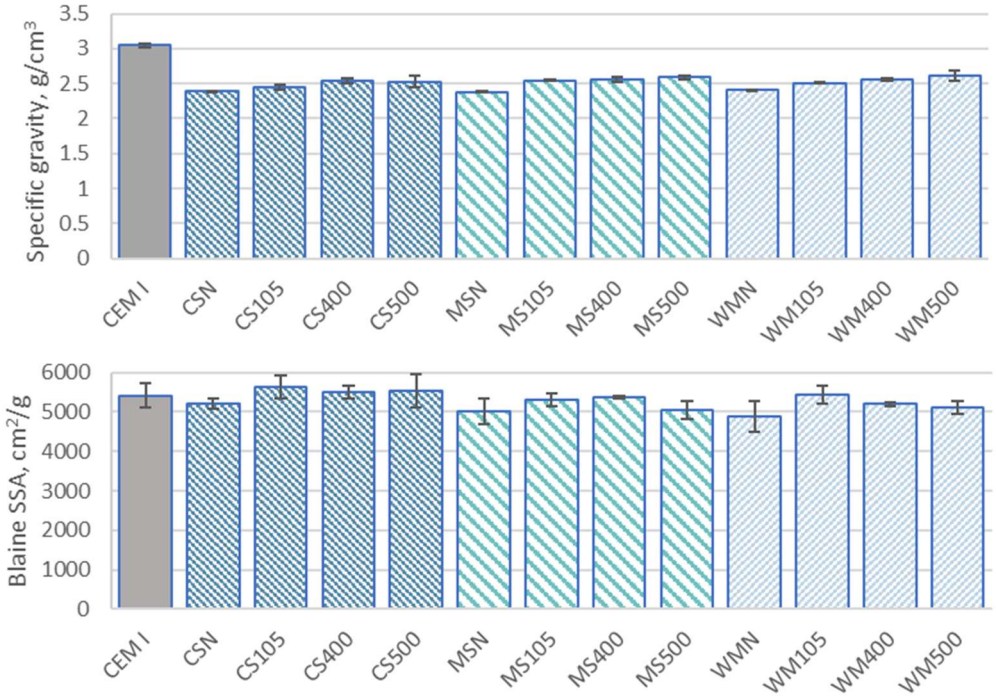

Fig. 3.3. Physical properties of powders treated at different temperatures.

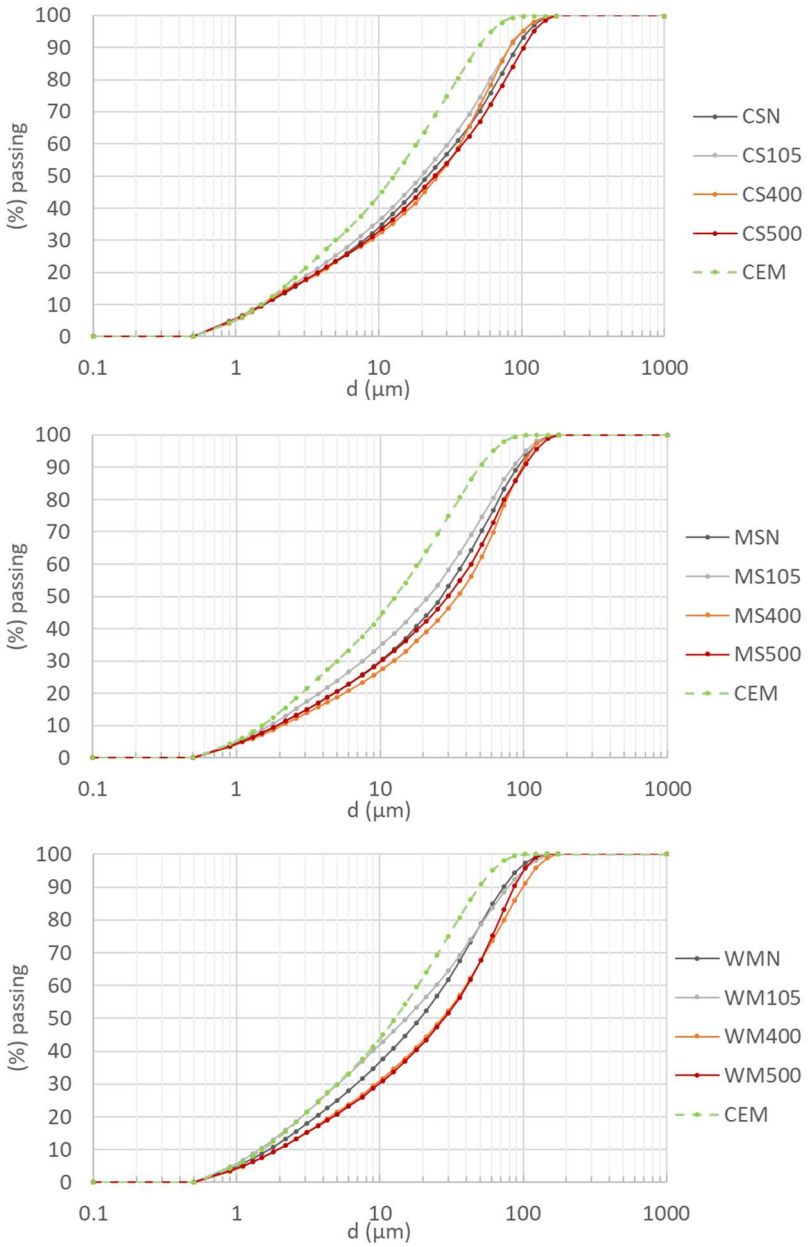

Fig. 3.4. Particle size distribution of powders treated at different temperatures (CS – concrete fines, MS – mixed fines, WM – wash mud, CEM – Portland cement CEM I 52.5 R).

Regarding the change in density, from the Figure 3.3, it can be seen that with an increase of treatment temperature, the density of materials slightly increases. Thus, after heating CS from room temperature to 500°C, its density increased from 2.40 g/cm^3 to 2.53 g/cm^3 (5.4%), while the density of MS and WM increased from 2.38 g/cm^3 to 2.59 g/cm^3 (8.8%) and from 2.42 g/cm^3 to 2.61 g/cm^3 (7.9%) respectively. This increase in specific gravity is due to elimination of chemically bonded water and combustion of organic impurities present in the demolition wastes that have low density.

The mineral composition of the waste samples remained largely unchanged with increasing treatment temperatures, as indicated in Fig. 3.5 and Table 3.2. The only notable change was the disappearance of gypsum peaks in MS and WM and a decrease in chlorites peaks in CS. As a result of its partial dihydroxylation, the content of chlorites presented dropped from 5.6 % in the unheated sample to 1.5% in the sample treated at 500°C. Since no portlandite was detected in the starting material, and the heating temperatures were below the decarbonization point of calcite and dolomite, no peaks of free lime were observed on the X-ray diffraction patterns of the calcined materials. Similarly, no patterns showed C2S polymorphs, a product of C-S-H dehydration that gives a broad peak between 30 and 35° 2theta, as this phase seems to form at higher heating temperatures, according to various studies [77, 79 - 81, 127, 145, 147]. However, it is worth noting that some dehydration products may still be present in the amorphous phase, which cannot be indicated by XRD.

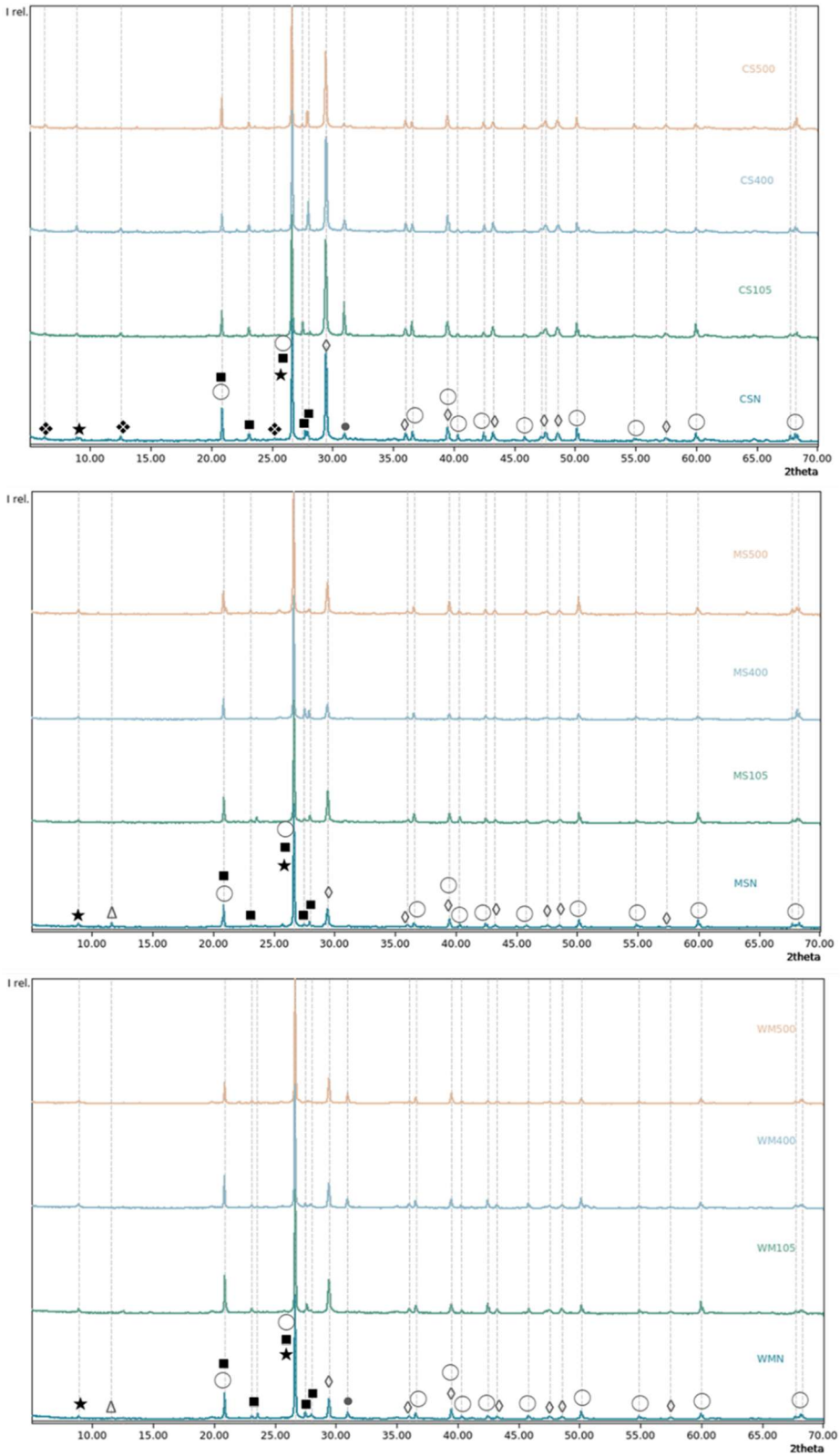

Fig. 3.5. XRD patterns of investigated materials before and after thermal treatment: ◯ – quartz, ◊ – calcite, ■ – feldspars, ★ – muscovite, ● – dolomite, ❖ – chlorites, Δ – gypsum.

Table 3.2. Mineralogical composition of the investigated materials before and after thermal treatment, mass-%.

	Quartz	Calcite	Feldspars	Muscovite	Dolomite	Chlorites	Gypsum
CSN	35.2	33.6	13.4	5.7	6.5	5.6	-
CS105	30.4	38.7	13.1	5.2	7.7	4.9	-
CS400	26.9	35.2	18.4	8.2	7.5	3.8	-
CS500	38.0	35.9	13.3	5.8	5.5	1.5	-
MSN	52.7	20.1	13.0	10.0	-	-	4.2
MS105	54.6	23.6	14.7	7.1	-	-	-
MS400	56.7	20.1	15.0	8.2	-	-	-
MS500	58.4	20.9	12.4	8.3	-	-	-
WMN	46.4	17.1	15.5	12.7	6.2	-	2.1
WM105	47.6	25.4	13.1	12.2	1.7	-	-
WM400	45.2	18.2	17.3	12.4	6.9	-	-
WM500	47.7	19.0	10.6	12.4	10.3	-	-

3.5.2. Hydraulic activity

The microcalorimetric analysis of the investigated pure waste materials revealed a heat flux only within the first 2 hours of hydration for all samples, irrespective of the treatment temperature (see Fig.3.6). These findings are consistent with the calorimetry results reported by Zhang et al. [154] for real demolition waste. However, they differ from the results of the analyses conducted on laboratory-made samples dehydrated at 450°C, as reported by Wang et al. [146], as well as from those of laboratory-made samples dehydrated at higher temperatures, as reported by Splittgerber and Mueller [141], Bogas et al. [77, 80] and Carriço et al. [79], who observed a heat flux peak between 10 and 20 hours of hydration.

Xu et al. [144] attributed the initial heat release during the hydration of thermally activated recycled cement to the hydration of free lime. However, the materials investigated in this study do not contain free lime. Therefore, the initial heat release during hydration may have been caused by other factors, such as the dissolution of soluble compounds and the high reactivity of C-S-H dehydration products [77, 79, 80].

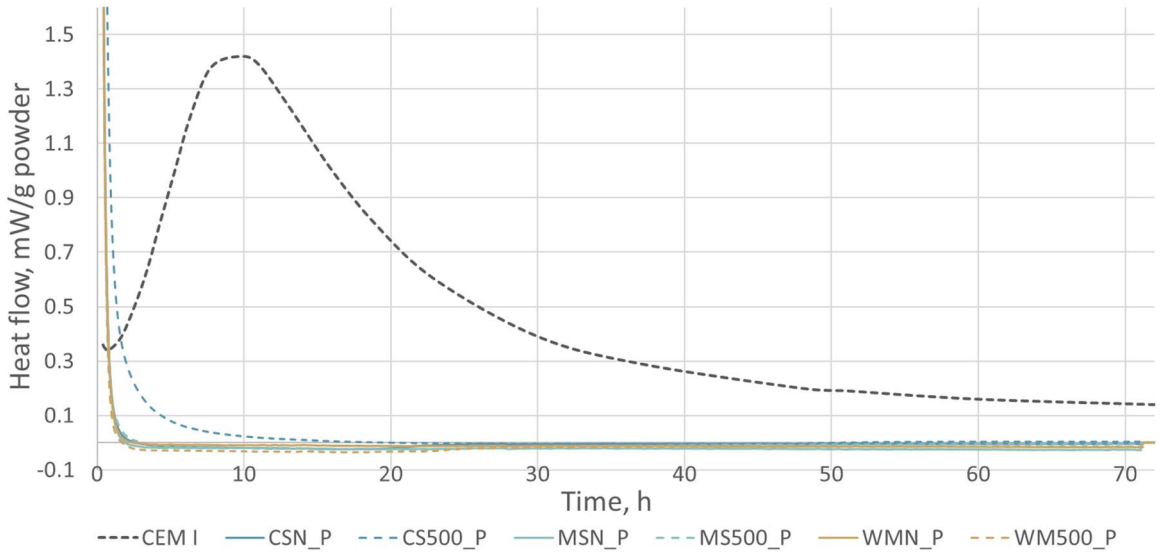

Fig. 3.6. Heat flows of pure pastes: CEM I is paste consisted of 100% Portland cement; CSN_P, MSN_P, WMN_P, CS500_P, MS500_P, WM500_P are pastes consisted of 100% waste powder.

Fig. 3.7 shows TGA/DTG curves for pastes consisting of 100% WMN and WM500. These curves confirm that the sample made from thermally treated powder contains a higher amount of C-S-H rehydration products than the sample made from unheated powder. Thus, according to DTG curves, during heating, the WM500 sample lost up to 0.026% of its mass per 1°C at temperatures between 100°C and 400°C due to dehydration of ettringite and calcium silicate hydrates. In contrast, the WMN sample only lost up to 0.019%/°C. This indicates that the thermally treated powder has slightly greater hydraulic activity.

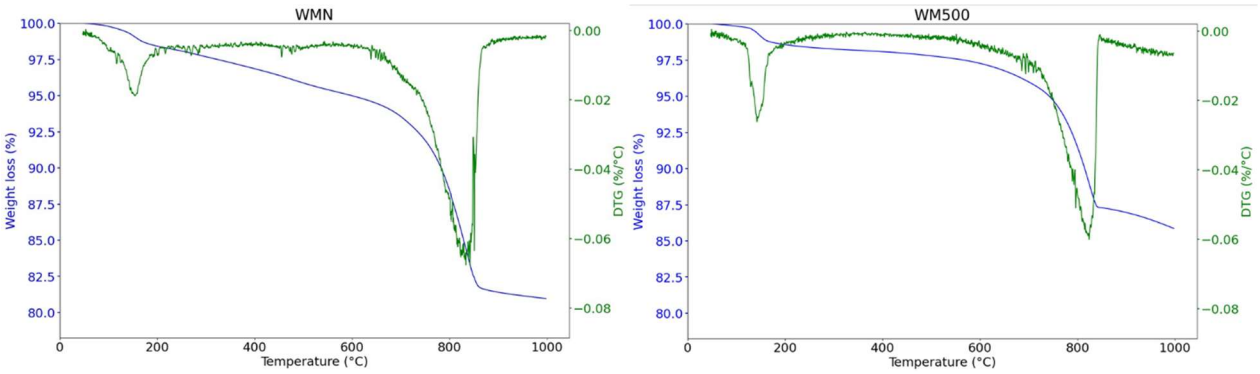

Fig. 3.7. TGA/DTG curves of pastes consisted of 100% WMN and WM500 after 90 days curing.

To evaluate the effect of waste powders on cement hydration, microcalorimetry was performed on pastes containing 80% Portland cement and 20% waste powders. The resulting heat flow curves, normalized per gram of cement, are shown in Fig. 3.8 and indicate that the addition of waste powders enhances the cement hydration process, that can be attributed to their filler effect.

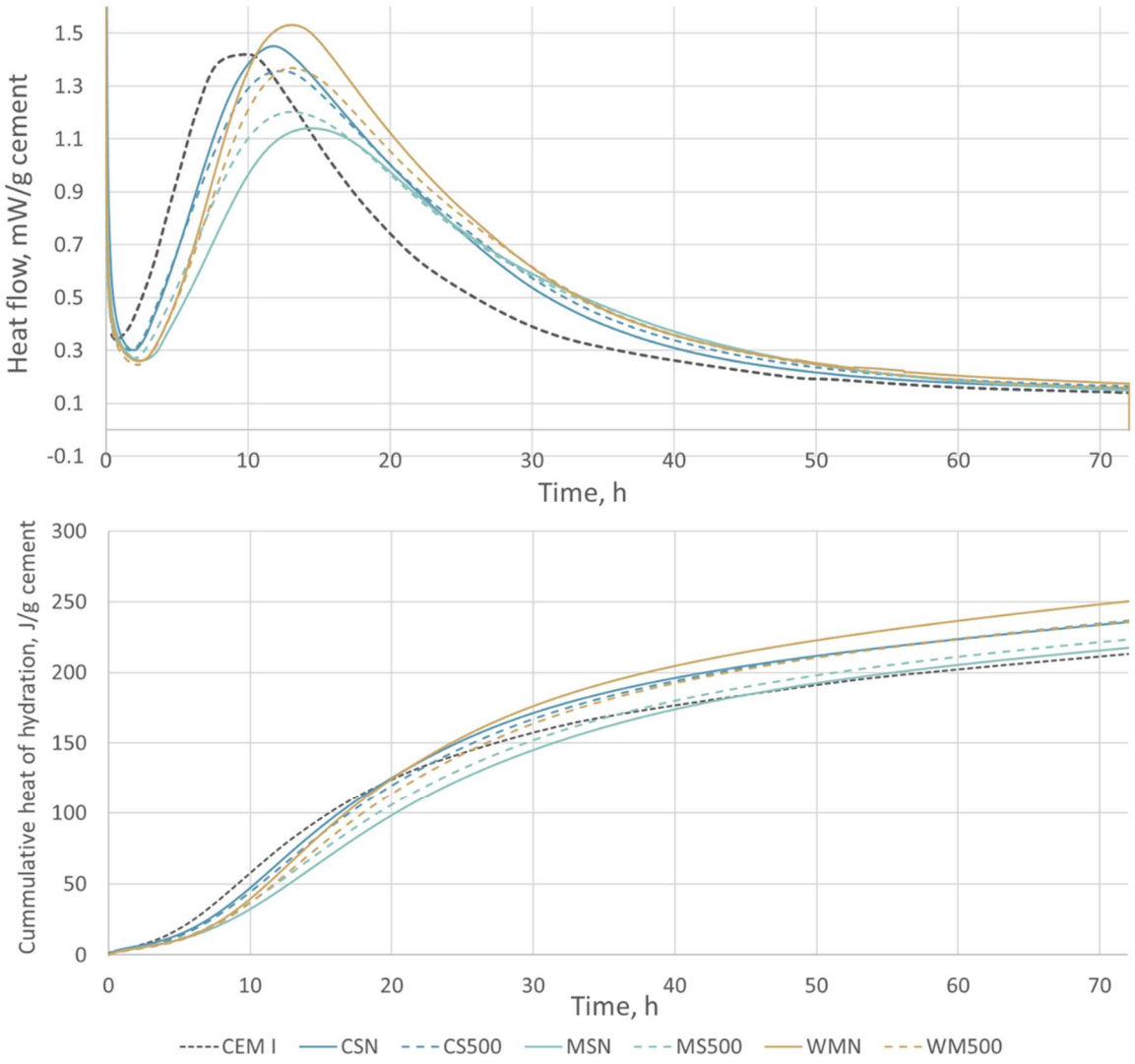

Fig. 3.8. Heat flows and cumulative heat of hydration of pastes: CEM I is paste consisted of 100% Portland cement; CSN, MSN, WMN, CS500, MS500, WM500 are pastes containing 80% of Portland cement and 20% of waste powder.

The incorporation of waste powders can influence the water demand and setting time of the binder. Xu et al. [144] and Carriço et al. [83] identified specific factors of dehydrated cement that increase water demand, including specific surface area, porous morphology of dehydrated compounds, and high free lime content. The comparison of standard consistency (Fig. 3.9) of the pure Portland cement pastes with pastes containing 20% of investigated wastes showed an increase in water demand with the addition of waste powders, particularly in the case of MS and WM, where this increase is 7% and 11% for MSN and WM105 respectively. Additionally, all pastes containing waste treated at 400°C showed a decrease in water demand, with a subsequent increase for waste treated at 500°C. Since the materials do not contain free CaO and the fineness

of waste powders is comparable to the used cement, this can be explained only by particles morphology and high reactivity of the C-S-H dehydration products.

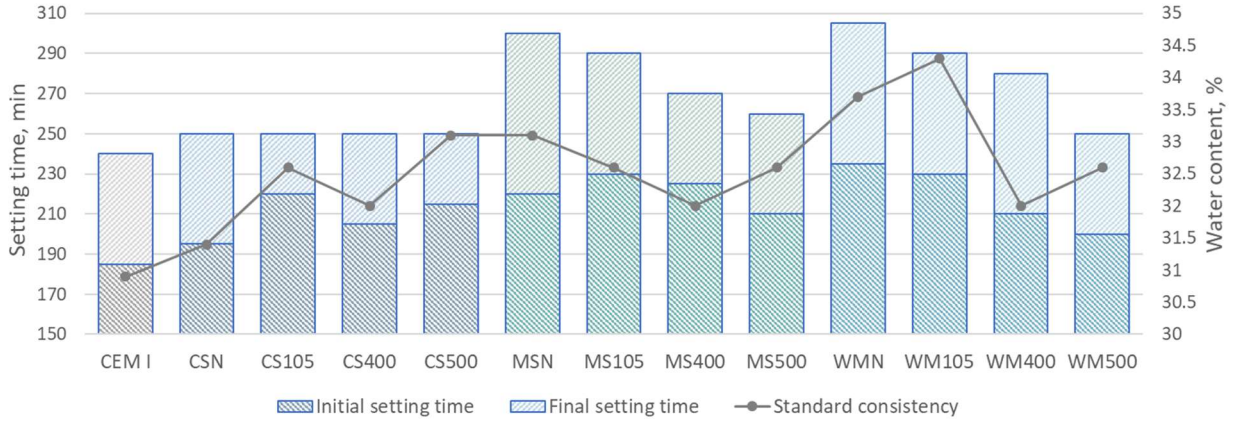

Fig. 3.9. Standard consistency, initial and final setting times of pastes with 20% of SCMs.

The previous studies have reported that thermally activated recycled cement generally exhibits shorter setting times than ordinary Portland cement [83, 144], which can have a negative effect on the fresh properties of the materials and their durability. However, Xu et al. [144] caution that this may be due to a false setting phenomenon resulting from the rapid reaction between free lime and water, leading to the formation of portlandite in the absence of gypsum.

However, the results of measuring the setting time of pastes with 20% thermally activated materials (Fig. 3.9) showed no acceleration of setting since the materials do not contain free lime and contain a small amount of gypsum. This also can be explained by the lower activation temperature as it was noted by Vysvaril et al. [154], who observed an increase in the setting time of pastes made of recycled cement dehydrated at 200–400°C.

Although, as shown in Table 3.1, MS and WM contain more alkali, which act as set accelerators [155, 156] than CS, results of setting time measurement shown on Fig. 3.9 indicates that pastes with untreated MS and WM powders have a significantly longer setting time compared to those with untreated CS. This difference diminishes as waste treatment temperature increases, and at 500°C, the initial and final setting times of pastes containing different wastes differ by no more than 10 minutes. Therefore, since in the investigated wastes, alkalis are in an insoluble state in the composition of muscovite and glass particles, they do not affect the setting time.

In contrast, gypsum, present in MS and WM but not in CS, acts as a retarder by reacting with C3A to form ettringite [157 - 159]. This likely explains the longer setting time of pastes with untreated MS and WM powders. When heated, gypsum dehydrates, and at temperatures above 300°C, insoluble β-anhydrite (natural anhydrite, anhydrite II) forms [160, 161]. This compound, as

evidenced by numerous studies [157 - 159], accelerates cement setting and explains the observed decrease in setting time of the pastes with MS and WM subjected to heat treatment.

3.5.3. Pozzolanic activity

In general terms, it is known that after mixing cement with water, in the first instance C-S-H gel and portlandite are formed as a result of hydration of C3S and C2S, and ettringite as a result of the reaction of C3A with gypsum [162]. Afterwards, portlandite reacting with amorphous silica and alumina, transforms into strong hydrated calcium silicates and aluminates, while ettringite, reacting with alumina, forms monosulfoaluminate of hydrated calcium [163]. Reactions occurring between SiO_2, Al_2O_3 and cement hydration products with the formation of strong compounds are called pozzolanic. The phases formed as a result of pozzolanic reactions reduce the average pore size in the binder matrix, thereby improving the mechanical properties and durability of concrete [163]. In addition, Fe_2O_3 also reacts with portlandite to form hydrated C-F-H and C-F-S-H gel, as well as enhances the pozzolanic reactions [164].

Section 3.5.1 already pointed out that the materials under study cannot be classified as pozzolanic, as their SiO_2, Al_2O_3, and Fe_2O_3 contents are insufficient. Nonetheless, MS and WM contain ceramic inclusions that may possess weak pozzolanic properties. Thus, by subjecting these materials to thermal activation, the ceramic particles can be separated from the hydrated cement adhering to them, increasing their availability for reactions with cement hydration products. Therefore, the goal of this section is not to demonstrate that demolition wastes are pozzolanic, but rather to distinguish between the effects on cement hydration of pure concrete waste and mixed waste containing ceramic and glass inclusions.

To evaluate the pozzolanic properties of the studied wastes after thermal treatment, the Chapelle test was conducted, with CS serving as a reference material without any pozzolanic activity (Fig. 3.10). The results demonstrate that, unlike CS, the reactivity of MS and WM gradually improves with increasing treatment temperature from 301 and 208 mg/g for MSN and WMN to 395 and 353 mg for MS500 and WM500 respectively. Furthermore, MS exhibits a slightly higher capacity for binding calcium hydroxide than WM. However, the reactivity of all investigated materials is not significant, as expected from their chemical composition, as the amount of $Ca(OH)_2$ fixed by 1 g of the material is lower than the threshold of 436 mg established by Raverdy et al. [165] for materials exhibiting pozzolanic activity.

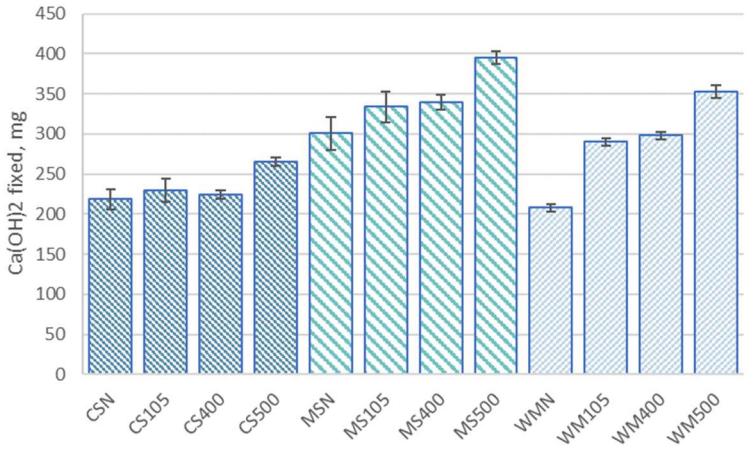

Fig. 3.10. Pozzolanic activity of investigated powders measured by modified Chapelle test.

The slightly improved activity of CS after calcination at 500°C can be attributed to the transformation of chlorites, which were present in small amounts in the material, into an amorphous phase, as it was showed by XRD analysis (Table 3.2 and Fig. 3.5). Additionally, a Chapelle test was conducted with pure magnetite or iron oxide (II, III) and hematite or iron oxide (III) to examine the influence of iron oxidation state on pozzolanic activity. The results indicate that magnetite only fixes 164.15±21.72 mg of $Ca(OH)_2$, while hematite binds 415.85±9.48 mg of $Ca(OH)_2$. Therefore, the increased activity of CS can also be attributed to the oxidation of less reactive compounds to more reactive ones in a redox system.

To investigate the influence of heat treatment on waste materials containing ceramic impurities on cement hydration, a TGA was performed on cement pastes containing 20% MSN and MS500 after a 90-day curing. The findings, depicted in Fig. 3.11, revealed that the quantity of portlandite in both samples was identical. Thus, according to the DTG curves, the weight loss in the temperature range of 400-600°C caused by the dehydroxylation of portlandite was up to 0.03%/°C in both samples. These results imply that, at this substitution rate, the marginal increase in pozzolanicity caused by the heat treatment of the mixed waste, as indicated by the Chapelle test, had no impact on cement hydration.

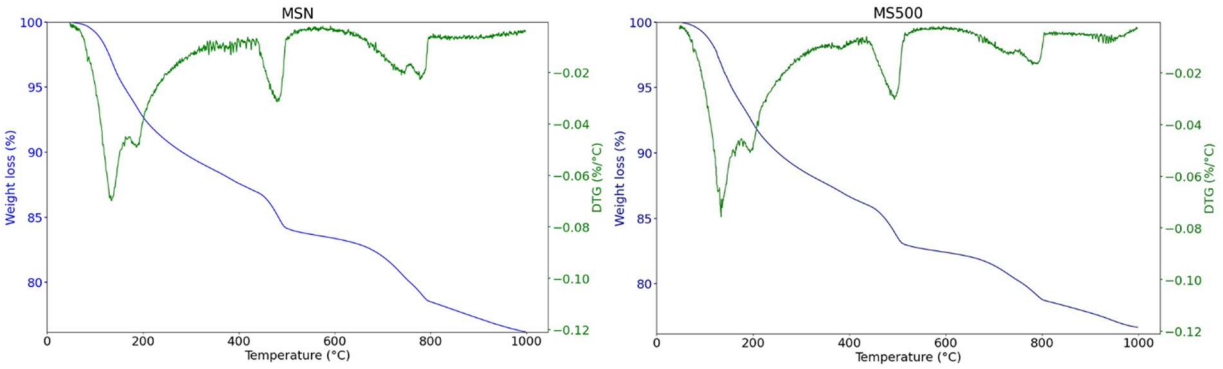

Fig. 3.11. TGA/DTG curves of pastes containing 20% of MSN and MS500 after 90 days curing.

3.5.4. Compressive strength

Fig. 3.12 presents the compressive strength values of the tested mortar and reference Portland cement mortar specimens. All investigated materials exhibited similar mechanical properties development. Thus, the strength of the mortars after 90 days of curing was 52.9±0.9, 51.3±0.4, and 52.6±0.9 for mortars containing CSN, MSN, and WMN, respectively, and 59.5±0.8, 57.9±0.5, and 56.4±0.5 for mortars containing CS500, MS500, and WM500, respectively. The strength of mortars containing CS and the other two materials did not show a significant difference, indicating that the presence of ceramic and glass impurities in waste powders does not affect the mechanical properties of the mortars at the substitution rate of 20%.

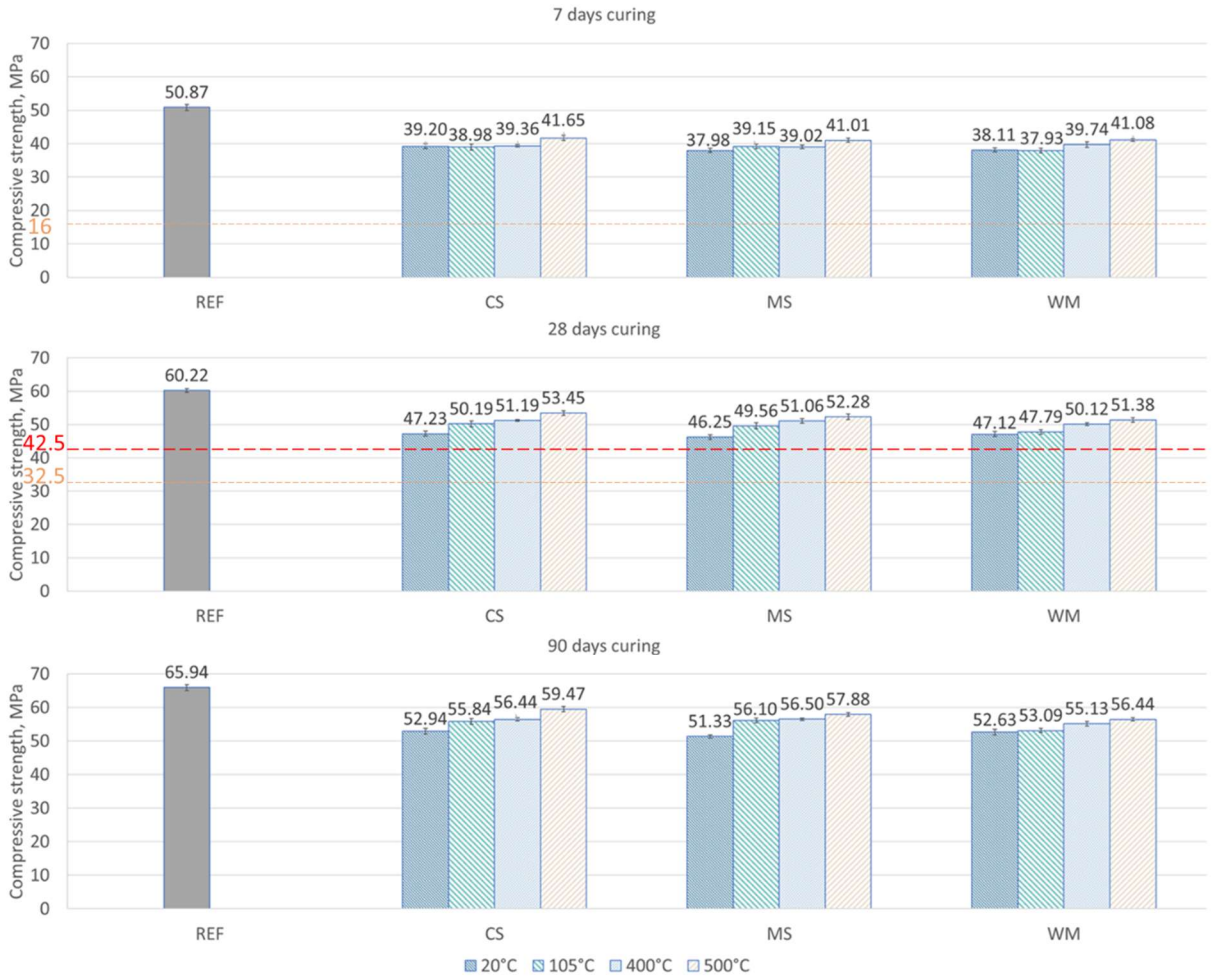

Fig. 3.12. Compressive strength of mortars containing 20% of SCMs treated at different temperatures.

All samples met the European standard EN 197-1 for blended cement, with a minimum strength of 32.5 MPa and an initial setting time threshold of ≥75 min. Additionally, they even met the strength class of 42.5 MPa, demonstrating that all materials can be used as SCMs for blended cement production. The waste powders contributed to the strength of the mortars due to the filler effect, and in the case of heat-treated materials, due to the combined action of the filler effect and rehydration of the products of partial C-S-H dehydration.

Fig. 3.13 shows the SAI of the mortar specimens. There is no single standard that defines the threshold, so the researchers usually use 75% as the threshold, as defined by the ASTM C311 standard [153] for fly ash and natural pozzolans. All investigated materials met this threshold, despite not being pozzolans. The SAI values of the studied materials were consistent with data obtained by other researchers for the substitution rate of 20% by recycled cement (RC), limestone filler (LF), and quartz filler (QF), which are given in Table 3.3. Thus, after 7 days of curing, the ranges of SAI values were 75-77% for unheated materials and 81-82% for materials treated at

500°C. For RC, LF, and QF, the SAI values were 77±11%, 85±6%, and 83±12%, respectively. After 28 days of curing, the SAI values were 77-78% for unheated materials, 85-89% for materials calcined at 500°C, and 72±6%, 81±6%, and 74±6% for RC, LF, and QF, respectively. Finally, after 90 days of curing, the SAI values were 78-80% for unheated materials, 86-90% for materials calcined at 500°C, and 72±8%, 83±1%, and 79±4% for RC, LF, and QF, respectively.

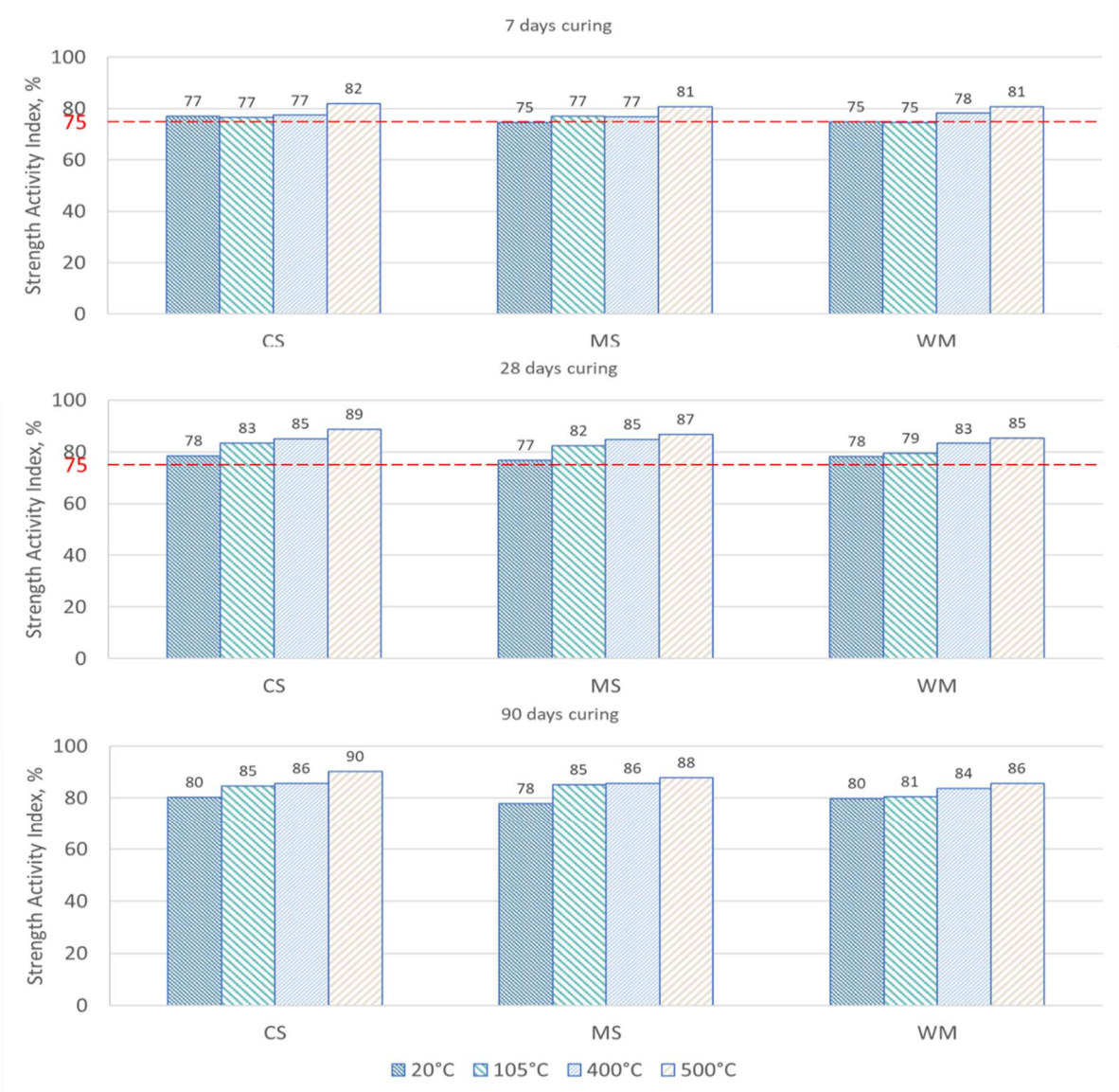

Fig. 3.13. Strength Activity Indices of mortars containing 20% of SCMs treated at different temperatures.

Table 3.3. SAI values for cement substitution rate of 20% by different materials: RC is recycled cement, LF is limestone filler, QF is quartz filler.

Additive material	Treatment temperature, °C	7 days SAI, %	28 days SAI, %	90 days SAI, %	Source
RC	500	-	77	-	[149]
RC	700	108	92	88	[79]
RC	-	81	74	-	[79]
RC	-	70	77	-	[127]
RC	500	66	68	-	[127]
RC	800	84	83	-	[127]
RC	-	74	69	75	[82]
RC	350	83	73	77	[82]
RC	650	88	78	78	[82]
RC	350	79	74	65	[82]
RC	650	85	79	82	[82]
RC	650	90	77	85	[82]
RC	650	92	88	95	[82]
Average SAI		77±11	72±6	72±8	
LF	-	95	87	-	[166]
LF	-	91	83	-	[166]
LF	-	88	82	-	[166]
LF	-	77	76	-	[166]
LF	-	90	87	-	[166]
LF	-	88	88	-	[166]
LF	-	80	78	-	[166]
LF	-	77	77	-	[166]
LF	-	80	81	-	[167]
LF	-	83	81	84	[168]
LF	-	85	66	84	[169]
LF	-	80	84	82	[170]
Average SAI		85±6	81±6	83±1	
QF	-	91	78	81	[171]
QF	-	74	69	76	[171]
Average SAI		83±12	74±6	79±4	

3.5.5. Microstructure of mortar specimens

To investigate the effect of waste powders on the microstructure development of cementitious mortars, scanning electron microscopy (SEM) analysis was employed. Fig. 3.14 shows the SEM micrographs of the reference mortar and mortars containing 20% waste materials calcined at 500°C after curing for 90 days and storage for approximately 1 year. EDX microanalysis of the mineralogical phases is given in the appendix to this article.

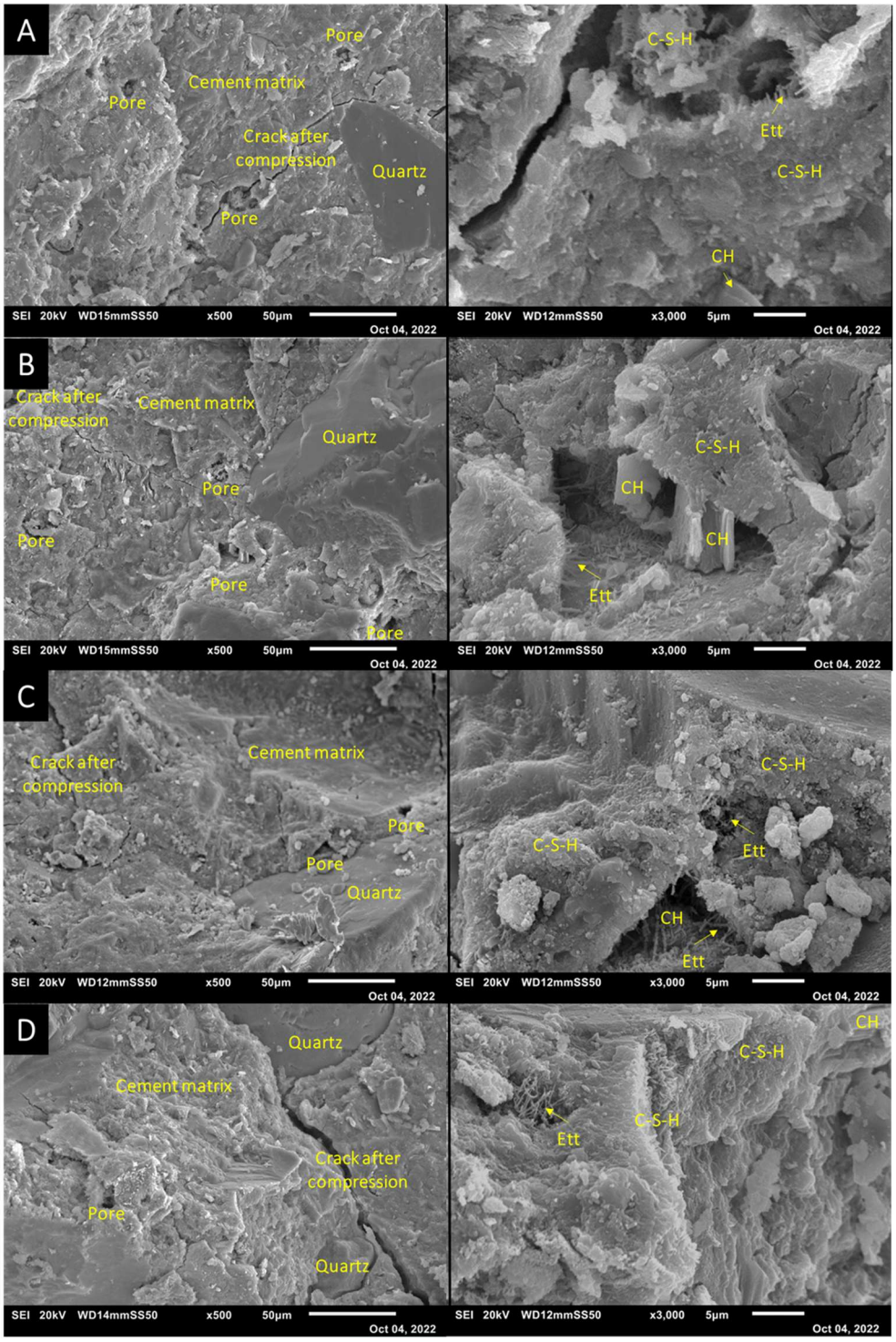

Fig. 3.14. SEM pictures of mortars with 20% of waste powder after 90 days curing and 1 year of storage: A – reference OPC mortar, B – CS500, C – MS500, D – WM500.

Observations of the microstructure of cement mortars confirmed that the waste powders were embedded perfectly in the cement matrix, forming a compact microstructure. There were no significant differences in the microstructure of the four specimens, except that the microstructure of the mortars with waste powders appeared slightly looser than that of the

reference mortar, which may explain the strength loss. However, the pictures show that the pores in the cement matrix with waste powders are filling with hydration products, which explains the growth of SAI with age.

3.5.6. Rationality of SCMs thermal treatment

To assess the rationality of thermal treatment of SCMs, as well as to compare the two drying methods from the economic and environmental aspects, approximate calculations of specific energy consumption and specific CO_2 emissions were made for the production of 1 kg of binder with a substitution rate of Portland cement of 20%. For the calculation, the following literature-based data valid for European Union countries were used:

- Energy demand for heating up to 1450°C: 1715 kJ per 1 kg of Portland cement clinker [172];

- Energy demand for drying of raw materials with moisture content of 10%: 2315 kJ per 1 kg of Portland cement clinker [172];

- CO_2 emissions related to limestone decarbonation: 0.53 kg CO_2 per 1 kg of Portland cement clinker [173];

- 65% of CO_2 emitted during cement production is associated with limestone decarbonation and 35% of CO_2 associated with fuel combustion [174, 175];

- 100% fossil fuel was taken as energy source.

The composition of Portland cement was considered as 95% clinker and 5% gypsum, the moisture content in CS and MS was assumed as 10%, and the moisture content in WM was 20%. Energy consumption for crushing, grinding and sieving was not taken into account. The calculation results are given in Table 3.4.

Table 3.4. Comparison of energy consumption and CO_2 emissions related to production of 1 kg ordinary Portland cement and 1 kg of blended binder with cement substitution rate of 20%.

Waste	Drying conditions	Calcination temperature, °C	Energy consumption, kJ/kg_{binder}	Energy consumption related to reference, %	CO_2 emissions, kg_{CO2}/kg_{binder}	CO_2 emissions related to reference, %
CS; MS	Ambient	-	3224	-20.0	0.624	-20.0
		400	3251	-17.6	0.631	-19.1
		500	3272	-17.0	0.632	-19.0
	105 °C	-	3614	-8.3	0.656	-15.9
		400	3714	-5.8	0.663	-15.0
		500	3735	-5.3	0.664	-14.9
WM	Ambient	-	3224	-20.0	0.624	-20.0
		400	3251	-17.6	0.631	-19.1
		500	3272	-17.0	0.632	-19.0
	105 °C	-	4081	+3.5	0.688	-11.8
		400	4177	+5.9	0.695	-10.9
		500	4198	+6.4	0.696	-10.7
Ordinary Portland cement			3944		0.780	

As it can be seen from Table 4, the drying of raw materials at elevated temperatures is the most energy-intensive process in the production of cement components. Moreover, the production of blended cement using WM dried by heating requires more energy than the production of ordinary Portland cement due to the high moisture content in the mud. In the case of ambient drying the energy consumption is significantly reduced.

Considering CO_2 emissions, all studied blended cements have an advantage over ordinary Portland cement, and the drying of raw materials without heating greatly enhances this advantage.

To assess the rationality of calcination the wastes at temperatures of 400°C and 500°C, the increase in energy consumption and CO_2 emissions was compared with the increase in strength of specimens containing 20% thermally treated SCMs after 28 days of curing relative to specimens containing unheated SCMs. The comparison results, given in Table 3.5, show that drying CS and MS at elevated temperatures improves the strength of the samples, but at the same time it is associated with an important increase in energy consumption and CO_2 emissions. Calcination of the wastes at 500°C significantly improves the strength of samples containing

SCMs, while the increase in energy consumption and CO_2 emissions is not much higher than for specimens with uncalcined wastes. In addition, the differences between the strengths of samples containing SCMs treated at 400°C and at 500°C are more pronounced than the differences in energy consumptions and CO_2 emissions for the same samples, which suggests that calcining the waste at 500°C is more appropriate.

Table 3.5. Comparison of changes in strength, energy consumption and CO2 emissions depending on the SCMs treatment temperature. Percentages are relative to their respective uncalcined SCMs dried at natural condition.

Waste	Drying conditions	Calcination temperature, °C	Strength gain with thermal treatment of SCMs, %	Energy consumption increase with thermal treatment of SCMs, %	CO_2 emissions increase with thermal treatment of SCMs, %	Energy effectiveness index	CO_2 reduction effectiveness index
CS	Ambient	400	8.4	0.8	1.1	10.5	7.6
		500	13.2	1.5	1.3	8.8	10.2
	105 °C	-	6.3	12.1	5.1	0.5	1.2
		400	8.4	15.2	6.3	0.6	1.3
		500	13.2	15.8	6.4	0.8	2.1
MS	Ambient	400	10.4	0.8	1.1	13.0	9.5
		500	13.0	1.5	1.3	8.7	10
	105 °C	-	7.2	12.1	5.1	0.6	1.4
		400	10.4	15.2	6.3	0.7	1.7
		500	13.0	15.8	6.4	0.8	2.0
WM	Ambient	400	6.4	0.8	1.1	8.0	5.8
		500	9.0	1.5	1.3	6.0	6.9
	105 °C	-	1.4	26.6	10.3	0.1	0.1
		400	6.4	29.6	11.4	0.2	0.6
		500	9.0	30.2	11.5	0.3	0.8

The energy effectiveness indices, which are the ratio of the strength gain with the associated energy consumption increase, as well as the CO_2 reduction effectiveness indices, which are the ratio of the strength gain with the associated CO_2 emission increase, both illustrate the advantage of drying at natural condition rather than at 105°C. While it is obvious that natural drying has a clear environmental advantage over drying by heating, this method is much more time consuming

and requires a lot of space, which is difficult to carry out on an industrial scale. Perhaps this problem could be solved by the use of mechanical drying methods such as centrifugal drying, or changes to the storage method for fine demolition wastes to reduce their moisture content. Calcining materials at relatively low temperatures up to 500°C contributes significantly less to energy consumption and CO_2 emissions than drying them by heating for a long time.

3.6. Conclusions

This study provides an assessment of the potential use of real demolition waste, including mixed concrete-ceramic screening fines and mud from recycled aggregate washing, in eco-cement production. The following conclusions are drawn based on the research:

(1) The XRD and DTA/TGA analysis of the investigated materials showed that all three samples are mainly composed of quartz and calcite. Small amounts of gypsum were observed in MS and WM, accounting for 4.2% and 2.1% of the respective samples crystalline phase weights. No portlandite was detected in any of the investigated materials due to its transformation into calcite over time as a result of carbonation processes.

(2) The investigated waste materials showed only an initial heat release during the first 2 hours of hydration. The addition of waste powders improved cement hydration due to their filler effect, but also increased water demand by 2% to 11% depending on the type of waste and treatment temperature. CS and calcined MS and WM had no significant impact on setting time, whereas uncalcined MS and WM caused retardation due to the presence of gypsum.

(3) The reactivity of MS and WM gradually improves with increasing treatment temperature, but remains low even at the highest treatment temperature. The amount of Ca(OH)2 fixed by 1 g of the material is lower than the threshold for materials exhibiting pozzolanic activity, ranging from 208 mg/g to 353 mg/g for unheated WM and WM calcined at 500°C, and from 301 mg/g to 395 mg/g for unheated MS and MS calcined at 500°C. The ceramic inclusions in the waste powders do not appear to affect the strength of mortars when the substitution rate is 20%.

(4) The mortars with 20% of all three waste types had similar mechanical properties and is at least 37.93 MPa, 46.25 MPa and 51.33 MPa after 7, 28 and 90 days of curing, respectively. Thermal treatment of wastes improves the mechanical properties of the mortars, and

increases the SAI after 90 days of curing at 10% for the mortars with CS and MS and at 6% for the mortars with WM. The contribution of waste powders to the strength of mortars is explained by their filler effect and the presence of partially dehydrated C-S-H products in the calcined materials.

(5) By using the CDW fines investigated as SCMs to replace 20% of Portland cement, CO2 emissions can be reduced by 10.7 to 20%. However, the process of drying wash mud by heating leads to higher energy consumption compared to the production of ordinary Portland cement due to the material's high moisture content. Therefore, alternative drying methods should be considered for this material.

The study showed that real demolition waste, despite containing high levels of inactive components like quartz, can be utilized to produce eco-efficient blended cement. However, it's crucial to assess the long-term properties and durability of building materials that contain these wastes when exposed to environmental factors. In addition, one of the main challenges of utilizing demolition waste in producing new building materials is uncertainty about the stability of their composition. Thus, conducting systematic studies comparing the properties and composition of different demolition waste, over time and across various locations, is essential. To carry out such studies, a comprehensive database is necessary, and continued research on demolition waste is required to expand and update this database.

Chapter 4: Using ceramic demolition wastes for CO2 reduced cement production

Abstract

This study focuses on assessing the pozzolanic potential of two types of ceramic demolition waste, namely terracotta roof tiles and sanitary porcelain, as substitutes for traditional calcined clays in blended and limestone calcined clay (LC3) cement production. Experimental methods employed include the modified Chapelle test and XRD for pozzolanic activity evaluation, flexural and compressive strength tests, capillary absorption measurements, and SEM for microstructure analysis. Mortars containing 10%, 20%, and 30% ceramic powders and 5%, 10%, or 15% limestone filler were tested. The findings showed that porcelain powders exhibited lower pozzolanic activity due to their lower surface area and higher firing temperature of the material. Up to 20% substitution of OPC with terracotta had minimal strength impact, with a 103% strength activity index (SAI) at 90 days. Ultrafine terracotta powder showed promise in LC3 production with up to 30% OPC substitution, achieving a 97% SAI after 90 days. The poor mechanical properties of porcelain-containing mortars were explained by surfactants present in sanitary porcelain. This research informs the cement and processing industries on the potential use of specific ceramic demolition waste materials in eco-cement production, offering insights into blended pozzolanic cements and LC3 formulations, with the goal of reducing the carbon footprint of cement manufacturing.

4.1. Introduction

The cement industry stands as a significant contributor to global carbon dioxide (CO_2) emissions, accounting for a substantial portion of the overall environmental footprint. These emissions arise mainly from the fuel combustion and decarbonation of limestone during clinker manufacturing, responsible for approximately 8% of global anthropogenic CO_2 emissions [176]. The urgency of this issue has driven extensive research and innovation in the search for sustainable alternatives to Ordinary Portland Cement (OPC). One promising approach to mitigate CO_2 emissions is the incorporation of supplementary cementitious materials (SCMs) into cement formulations. The

utilization of SCMs not only reduces environmental impact but also enhances the performance and durability of concrete structures.

Special emphasis is placed on pozzolanic SCMs rich in amorphous silica and alumina, which can react with calcium hydroxide (CH) to produce additional calcium hydrosilicates and hydroaluminates. The use of pozzolans in concrete production has a long history. Historical records show that pozzolans of volcanic origin, such as volcanic ash, tuff, and pumice, were employed in the construction of concrete structures in ancient Rome [177 - 180]. One notable characteristic of concretes incorporating pozzolans is their ability to withstand corrosion caused by salts present in seawater, attributed to their reduced CH content [180, 181].

Calcined clays also find utility as pozzolanic SCMs. When clay containing kaolinite is calcined, metakaolin is formed, which is essentially an amorphous aluminosilicate ($Al_2Si_2O_7$) that can react with CH like a pozzolan to form C-(A)-S-H and aluminate hydrates [182]. These products fill space and promote mechanical and durability properties. The optimal temperature range for firing kaolinite clays is 600 - 900 °C, within which kaolin undergoes complete transformation into metakaolin [39, 183, 184]. However, metakaolin is also used in paper processing and ceramic and refractory industries, where there are strict requirements for colour and purity. This means that it typically costs for about 5 times the price of cement [185]. Thus, the use of conventional metakaolin is not practical for the production of general-purpose cement.

Scientists from EPFL in Switzerland and UCLV in Cuba proposed replacing part of the cement with a mixture of calcined clay and limestone filler. This formula is called LC3 (limestone calcined clay cements) [39]. After studying 46 substandard clays from around the world for use in the production of LC3, they concluded that replacing 50% clinker with 30% fired clay, 15% limestone filler and 5% gypsum did not lead to a deterioration in the mechanical properties of the material.

Ceramics can also be considered as calcined clay, since it is clay with additives such as sand and feldspars, fired at a temperature of 800 - 1400 °C, and contains therefore amorphous matter [84, 186]. Thus, there is obvious economic and environmental advantage of using ceramic waste in the cement industry compared to using calcined clay, because there is no need to develop quarries, extract natural resources and consume energy for calcination. In addition, ceramic waste is widespread throughout the world and requires recycling.

Many studies have already been conducted to demonstrate the acceptability of using various ceramic wastes as pozzolanic SCMs. Thus, Asensio et al. [187] after measuring the reactivity of ceramic demolition waste with lime and comparing the values with other standard pozzolans concluded that the ceramic waste has a pozzolanicity above fly ash and below silica fume, and

after a year of reaction they bind almost all the lime. Wild et al. [188] proved the pozzolanic activity of 8 different brick powders collected in 4 countries using the Chappelle test, and Vejmelková et al. [189] obtained a Chapelle test result for ceramic powder of 840 mg($Ca(OH)_2$)/g, which is high enough for metakaolin. Lavat et al. [92] examined the reactivity of glazed and unglazed red roof tiles using the Fratini method and concluded that both ceramic materials had good pozzolanic properties.

However, most researchers use indirect methods to study the reactivity of ceramic powders, such as XRD and TGA to measure the consumption of portlandite, or the development of compressive strength, instead of direct chemical methods. All researchers who have studied the development of portlandite during the hydration of cements with ceramic powders noted an increase in the content of portlandite in the early stages up to 28 days due to the hydration of cement phases, but its gradual decrease at later stages due to pozzolanic reactions with ceramic particles, which was not observed in reference samples [92, 191 - 194]. This is also confirmed by the lower early strength of specimens made using ceramic powders compared to the strength of reference specimens due to cement dilution [126, 195], but comparable or even improved late strength at substitution rates up to 20% [89, 197 - 200]. Microstructure studies have shown pore refinement and matrix compaction in samples containing ceramic powders due to pozzolanic reactions [88, 90, 189, 192, 201], which leads to a decrease in water absorption [89, 193, 194, 197 - 199], chloride ions [89, 194, 201] and sulphate ions permeability [89]. Thus, the improvement of the microstructure, mechanical and durability properties of cements due to the pozzolanic properties of ceramic additives has been repeatedly proven. Among the available studies on this topic, only in that of Abreu et al. [202] on the use of ground electrical porcelain insulator as SCM, the hypothesis of its pozzolanic reactivity was rejected, which may be due to the too high firing temperature of the original porcelain material.

The pozzolanic properties of ceramics are intricately influenced by the firing temperature to which they are subjected. Within the temperature range of 600 - 900 °C, clay minerals undergo a transformative process, rendering them reactive. This thermal treatment leads to the creation of disordered, amorphous states of silica and alumina, fundamentally altering their crystalline networks. These altered clay minerals possess the ability to react when combined with lime and water, forming insoluble CSH- and CAH-type compounds [92, 184, 198, 203, 204]. However, it is essential to note that when firing temperatures exceed 900 °C, silica and alumina can reorganize into stable compounds, such as mullite and tridymite, with diminished reactivity [87, 184, 203, 204]. This makes firing temperature a critical factor in determining the pozzolanic potential of ceramic materials.

The firing temperature for porcelain is 1250 - 1400 °C, while terracotta ceramics and red bricks are fired at 950 - 1050 °C [186]. From the above, we can conclude that the pozzolanicity of red ceramics should exceed the reactivity of porcelain. However, for the moment there are not enough studies comparing the pozzolanic properties of different types of ceramics in uniform experimental settings, and the results of the few that are available contradict each other. Thus, Pitarch et al. [91], after comparing SAI and the amount of lime fixed by porcelain tiles, sanitary porcelain and red bricks powders, indeed confirmed the slightly lower reactivity of porcelain compared to red ceramics. Pacheco-Torgal and Jalali [205] reached similar conclusions. On the other hand, Pereira-de-Oliveira et al. [87] found a more active development of strength by cement mortars with terracotta tile powders fired at a temperature of 1100 - 1200 °C than by mortars with red bricks powder fired at a temperature of 800 - 1000 °C. Also, Lasseuguette et al. [190] in their study concluded that white ceramics have better pozzolanic activity than red ceramics. However, it is worth noting that the manufacturing temperature of the ceramics used in their study was not known and judging by the greater amount of mullite in the red ceramic samples, it can be assumed that the firing temperature of the white ceramics was lower than the red ones.

Despite the proven pozzolanic properties of ceramic waste, there has been no attempt to study different types of ceramic demolition waste as calcined clay in the LC3 formula. Mohit et al. [206], in their recent study, described the use of ceramic production waste to replace cement with a mixture of 15% limestone and 10, 20 and 30% ceramic. The results showed that samples containing 20% ceramic waste and 15% limestone filler had mechanical properties comparable to the reference specimen. The results of this study suggest that various ceramic demolition wastes can also be used to produce three-component limestone calcined clay cement.

4.2. Goals and significance of the research

The principal aim of this research is to investigate and compare the pozzolanic reactivity of two distinct types of ceramic demolition waste: specifically, terracotta roof tiles and a mixture of sanitary and tile porcelain collected after the renovation of sanitary rooms. The goal is to assess their potential suitability for use in LC3 as an alternative to traditional calcined clays. These materials have undergone minimal processing, avoiding washing and thermal treatment, aligning with a commitment to environmentally friendly and cost-effective procedures, tailored for industrial feasibility.

In the landscape of current research, there exists a noticeable gap in the comparative analysis of different ceramic waste types under standardized conditions. This void is highlighted by the finding that existing studies yield divergent results concerning the pozzolanic properties of these materials. Therefore, the present research endeavours to fill this knowledge gap and bring clarity to the intricate realm of ceramic waste utilization in cementitious applications.

In addition, while the pozzolanic potential of ceramic waste in cementitious formulations has been well-established, there has been a conspicuous absence of investigations regarding the applicability of various ceramic demolition wastes as substitutes for calcined clay within the LC3 framework. In this context, the present research stands at the forefront of exploration, aiming to assess the suitability of terracotta and porcelain demolition wastes as alternatives to conventional calcined clay.

This research carries the potential to offer a cost-effective and environmentally conscious alternative to natural raw materials for LC3 production, thereby reducing the industry's ecological footprint. The findings are anticipated to pave the way for sustainable and efficient cement production, aligning with the demands of a rapidly evolving world with an increasing focus on eco-friendly practices and resource conservation.

4.3. Materials

Two different types of demolition waste ceramics shown in Fig. 4.1 were used in the study: the terracotta roof tiles (RT) and the mix of white ceramic tiles and sanitary ware (RP). The materials were collected on different demolition sites in Luxembourg and North-East of France.

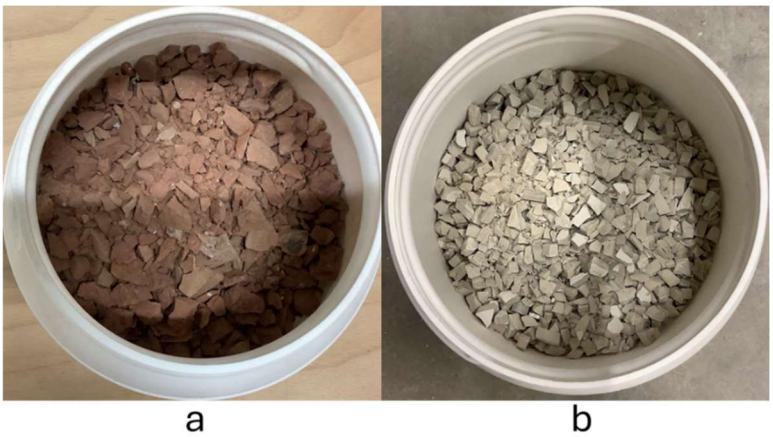

Fig. 4.1. Demolition waste ceramics used in the study: a – terracotta roof tiles; b – mix of sanitary ware and tiles.

After being collected, the wastes were broken with hammer to pieces of about 3 cm in size and crushed with jaw crusher. Then they were dried in natural conditions to the constancy of mass and ground in the impact mill with a bottom sieve of 2 mm mesh size. After grinding, a half of wastes was sieved on a 125 μm mesh sieve to obtain fine ceramic powders (RT and RP) and the other half was sieved on a 63 μm mesh sieve to obtain ultrafine ceramic powders (RTU and RPU).

Besides the investigated ceramics in the research, a Portland cement (OPC) CEM I 52.5 R and limestone filler (LF) provided by the French manufacturer Vicat, CEN Standard Sand according to EN 196-1 [150], and tap water were used for the mortar specimens mixing. Limestone filler was used for mixing LC3 mortars and pastes with ceramic powders named LRT, LRP, LRTU and LRPU for the mixtures of cement, limestone filler and RT, RP, RTU and RPU powders, respectively. The characteristics of the investigated materials, as well as OPC and LF are given in section 4.4.1.

4.4. Experimental methods

4.4.1. Materials characterization

The mineralogical composition of investigated ceramic powders was studied using D2 PHASER X-ray diffractometer with following parameters: Cu-Kα radiation, 10 mA, 30 kV, rotation between 5° and 70° with a 0.02° 2θ step and a step time of 0.6 s and measured by Rietveld method using Profex software. An approximate calculation of the amorphous phase was carried out by the amorphous halo method using a code written in the Python language.

The physical properties of ceramic, cement and limestone powders were also studied. The pycnometer method with petrol as liquid was used to determine the specific gravity of materials. Fineness of the powders was determined by Blaine method for air permeability specific surface area measurement as well as by particle size distribution analysis obtained with HELOS & RODOS laser granulometer. The chemical composition of the materials was investigated with Wave-Dispersive BRUKER S8-Tiger spectrometer.

4.4.2. Evaluation of pozzolanic activity

The modified Chapelle test [207] combined with the XRD were used to estimate the pozzolanic activity of the investigated materials.

For the Chapelle test, 1 g of ceramic powder, 2 g of calcium oxide and 250 ml of distilled water were placed in a 500 ml Erlenmeyer flask. The flask with magnetic stir bar and laboratory condenser was placed on a magnetic-stirrer hot plate heated to a temperature of 85 °C. The mixture was stirred for 16 hours. After cooling to a room temperature, the solution was mixed with 250 ml of saccharose syrup (0.7 M) and stirred for 30 minutes to extract unreacted lime. Then, the mixture was filtered on a filter paper and 25 ml of the filtrate was titrated with 0.1 N solution of hydrochloric acid using phenolphthalein as an indicator. To calculate the amount of fixed lime a blank test without pozzolan was carried out. The pozzolanic activity was calculated according to the formula:

$$m_{g\ of\ Ca(OH)2\ fixed} = 2 \cdot \frac{V_1 - V_2}{V_1} \cdot \frac{M_{Ca(OH)2}}{M_{CaO}} \cdot 100 \quad (8)$$

where V_1 is the volume of HCl solution consumed in the blank test, V_2 is the volume of HCl solution consumed in the pozzolan test, $M_{Ca(OH)2}$ is the molar mass of calcium hydroxide (74 g/mol), M_{CaO} is the molar mass of calcium oxide (56 g/mol).

XRD was carried out on the paste samples with 20% of ultrafine ceramic powders (RTU_20, RPU_20, LRTU_20 and LRPU_20) and w/b ratio of 0.4 after 90 days curing and drying at 50 °C until weight constancy to check if there are differences in portlandite consumption by pozzolans particles and in formation of carboaluminates.

4.4.3. Evaluation of fresh pastes properties

To investigate the properties of fresh pastes, the water demand for standard consistency and setting time of binder pastes were measured using a Vicat apparatus in accordance with European standard EN 196-3 [151], without immersing the pastes in water.

The dry part of the paste mixtures consisted of 0.8 parts OPC and 0.2 parts ceramic powders, and 0.7 parts OPC, 0.2 parts ceramic powders, and 0.1 parts limestone filler. The water content in the pastes was determined through the standard consistency test following EN 196-3 [151].

4.4.4. Evaluation of mechanical properties

The mechanical properties of the reference mortar and mortars containing ceramic powders were evaluated using flexural and compressive strength tests on 40x40x160 mm mortar bars in accordance with the ISO 679 international standard [152].

The water-to-binder (w/b) and sand-to-binder (s/b) ratios of all mixtures were set at 0.5 and 3, respectively. The content of ceramic powders in the binders was set at 10%, 20% and 30%, and the content of LF was set at 0.5 of ceramic powder weight. The design of the mortars is presented in Fig. 4.2. The specimens were cured in a moisture chamber at 20°C for 7, 28, and 90 days before being tested on a hydraulic press.

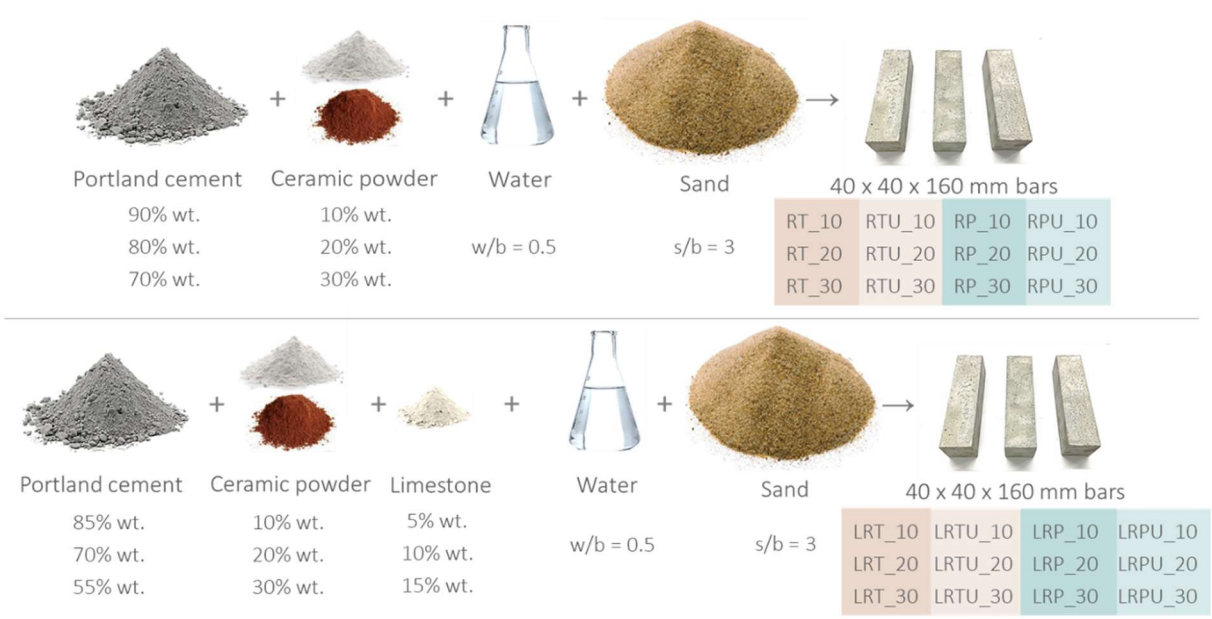

Fig. 4.2. Design of mortars containing ceramic powders.

Compressive strength test results of reference specimens and specimens containing SCMs were used to calculate Strength Activity Indices (SAI) using the following formula:

$$SAI = \frac{R}{R_{ref}} \cdot 100\% \quad (9)$$

where R is the average strength of the mortar bars with SCMs, R_{ref} is the average strength of the reference mortar.

4.4.5. Microstructure of mortar specimens

After undergoing strength tests for 90 days of curing, the fragments remaining from the mortar specimens containing 20% ultrafine ceramic powders (RTU_20, RPU_20, LRTU_20 and LRPU_20), were coated with a 4 nm layer of gold and examined with a field emission scanning electron microscope JEOL JSM-6010LA to analyse their microstructure.

4.4.6. Capillary absorption measurement

After 90 days curing, two specimens of each mortar containing 20% of ceramic powders as well as of reference mortar without additives were dried at 105 °C for 24 hours and immersed in water to the depth of 5 mm by the face of 40x40 mm size. The change in their mass was measured after 0.25, 0.5, 1, 2, 4, 6, 24, 48 and 168 hours. The value of capillary absorption was calculated using the following formula:

$$C_A = \frac{m - m_0}{1600} \quad (10)$$

where m_0 is the mass in grams of the dry specimen, m is the mass in grams of the specimen after the required absorption time, and 1600 is the surface of the specimen's bottom in mm^2.

4.5. Results and discussion

4.5.1. Materials characterization

The chemical composition of the materials is given in the Fig. 4.3(a). The main oxides of both ceramic samples are SiO_2 and Al_2O_3, followed by CaO, Fe_2O_3 and K_2O. The sum of contents of silica, alumina, and iron oxide, which are considered as pozzolanic oxides in RT and RP is 76.72% and 85.74%, respectively, which is higher than the minimum threshold of 70% established by ASTM C618 [208] standard for pozzolanic materials. In general, the materials investigated in this study have a composition that aligns with typical red and white ceramics, as indicated by the data in Fig. 4.3(b), based on an analysis of 121 samples gathered from various sources in the literature. The higher content of calcium in the studied porcelain can be explained by the presence of adhering cement on the tiles.

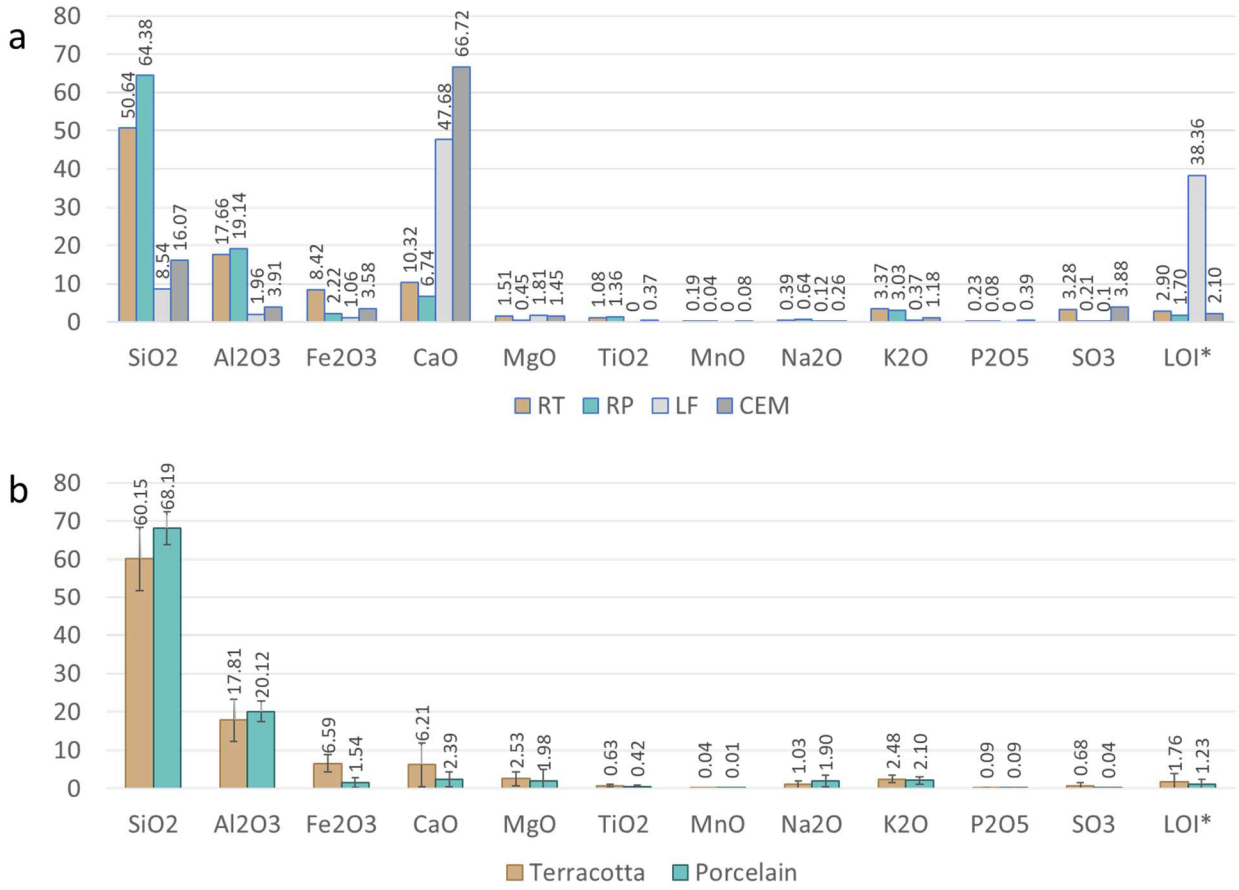

* Loss on ignition at 950 °C

Fig. 4.3. Oxide composition of the investigated materials (a) and the average composition of ceramic materials according to the literature review (b), mass %.

While the chemical composition of investigated ceramics corresponds to calcined clays, it can be highlighted that the pozzolanic oxides have to be present in an active amorphous state. Additionally, the materials need to be sufficiently fine, with a minimum of 66% of particles smaller than 45 μm [208], in order to ensure high reactivity.

The X-ray diffraction patterns and calculated mineralogical composition of the investigated ceramics, given in Fig. 4.4 and Table 4.1, respectively, indicate the presence of high levels of crystalline quartz in both samples. The approximate calculation of the amorphous phase by the amorphous halo method showed that the amount of glassy phase in RP was higher than in RT and was 40% and 28%, respectively. The presence of a high content of mullite, which is formed through the recrystallization of clay minerals when they are heated above 1000 °C [212 - 213], in the RP and its absence in the RT indicates the difference in firing temperatures between the two types of ceramics. In general, the mineralogical composition of the studied materials

corresponds to the typical composition of red and white ceramics [64, 90, 126, 188, 190, 209, 210, 214 - 216].

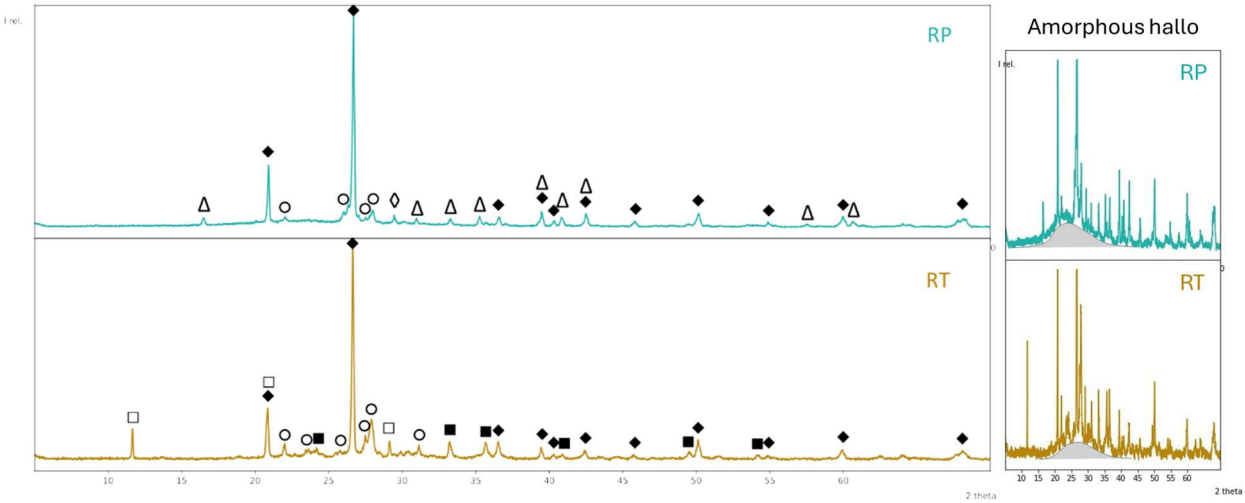

Fig. 4.4. XRD patterns of the investigated ceramics: ◆ - quartz, Δ – mullite, ◊ - calcite, □ - gypsum, ○ - feldspars, ■ - hematite.

Table 4.1. Mineralogical composition of investigated ceramics, mass-%.

	Quartz	Feldspars	Mullite	Calcite	Hematite	Gypsum	Amorphous phase
RT	32.4	29.9	-	-	5.2	4.5	28.0
RP	34.9	9.3	14.1	1.7	-	-	40.0

The specific gravities of the LF, RT (and RTU), RP (and RPU) and cement shown in Fig. 4.5 were determined to be 2.70, 2.42, 2.59, and 2.95 g/cm^3, respectively. After undergoing the same grinding and sieving procedure, it was observed that the terracotta powders were finer compared to the porcelain powders (Fig. 4.5). Thus, the specific surface area of RT and RTU was measured as 5239 and 6249 cm^2/g, respectively, while the corresponding values for RP and RPU were 3608 and 5543 cm^2/g, respectively. This difference can be attributed to the greater hardness of porcelain, which makes it more challenging to grind. The specific surface area of cement and limestone filler was 4887 and 10465 cm^2/g, respectively.

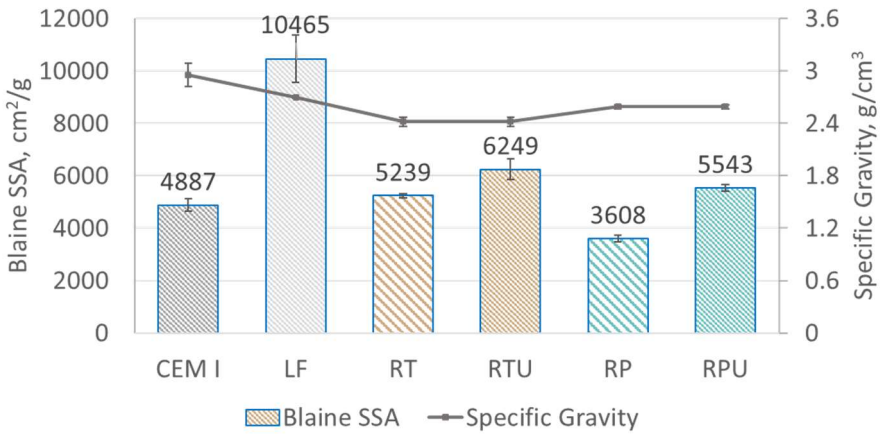

Fig. 4.5. Physical properties of powder materials.

Laser granulometry also confirmed these findings (Fig. 4.6). The particle size distribution curves revealed that the D10, D50, and D90 values for RT were determined as 1.55, 19.82, and 85.23 µm, respectively, whereas for RP, they were determined as 3.33, 31.97, and 95.71 µm, respectively. As for the ultrafine ceramic powders, the corresponding values were 1.19, 11.09, and 38.39 µm for RTU and 2.09, 17.87, and 49.91 µm for RPU. The distribution density curves clearly show that the limestone filler has a granulometry different from the other materials and contains notably higher amount of ultrafine particles with size <10 µm, which means that it can contribute to the packing density improvement.

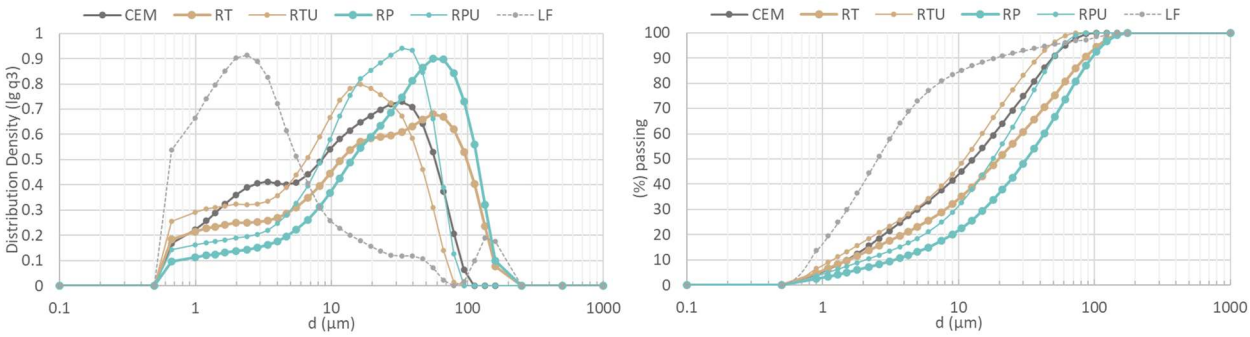

Fig. 4.6. Particle size distribution of powder materials.

4.5.2. Evaluation of pozzolanic activity

The results of the modified Chapelle test presented in Fig. 4.7(a) indicate that RP powder does not exhibit pozzolanic activity. The amount of $Ca(OH)_2$ fixed by 1 g of the material is lower than the threshold of 436 mg established by Raverdy et al. [217] for materials exhibiting pozzolanic activity. All other materials exceed this threshold, although they do not reach the 700 mg/g mark set for

metakaolin. Overall, the results of the Chapelle test are consistent with the data for ceramic materials collected from other studies (Fig. 4.7(b)). Unfortunately, there is currently a lack of sufficient studies in the literature regarding the pozzolanicity of ceramic powders using the Chapelle test, which prevents a reliable statistical analysis. Therefore, only four values, notably 595 mg $Ca(OH)_2$ given by Medeiros et al. [218] and 234, 409 and 512 mg $Ca(OH)_2$ given by Pereira et al. [219] could be used to characterize porcelain at this point.

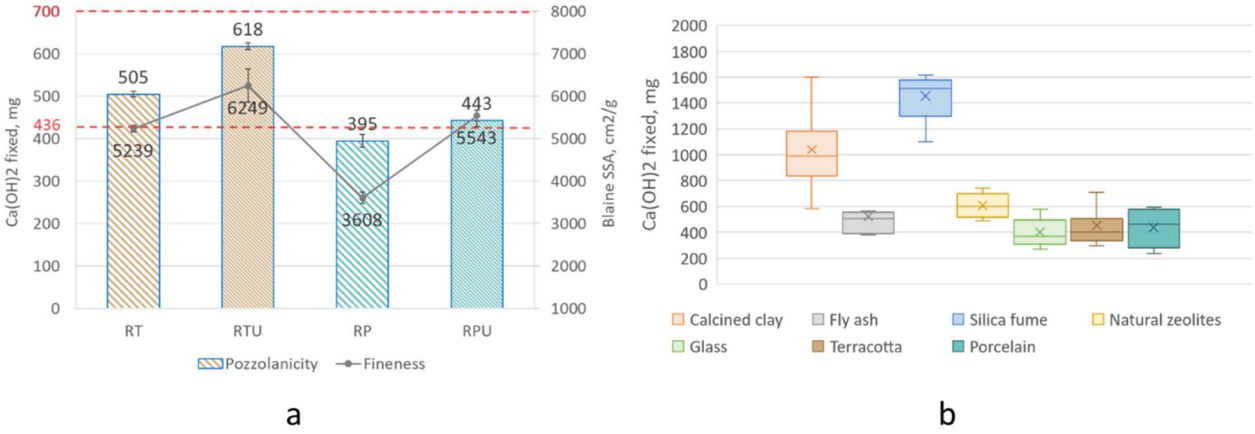

Fig. 4.7. Chapelle test results for pozzolanic activity: a – investigated ceramic powders; b – data collected from literature.

It is intriguing that porcelain powders, despite having a higher amorphous phase and pozzolanic oxide content, exhibit weaker pozzolanic behaviour compared to terracotta powders. This can be attributed to the lower specific surface area of porcelain powders, which may limit the availability of active sites for pozzolanic reactions. Additionally, the high firing temperature of porcelain may contribute to reduced reactivity of the amorphous phase. When clay is heated at temperatures higher than 1000°C, kaolinite undergoes recrystallization into mullite, and the change in the composition of the amorphous phase makes it less active for pozzolanic reactions [91, 211 - 213].

X-ray diffraction analysis of pastes containing 20% RTU and RPU after 90 days of curing, shown in Fig. 4.8 and Table 4.2, did not reveal a significant difference between samples made using RTU and samples made using RPU. As expected, the pastes with limestone filler contained more carboaluminates than the pastes without it, indicating reactions between the limestone and the pozzolanic ceramic powders. Both pastes with terracotta and porcelain contained the same amount of carboaluminates and calcite, which indicates the same degree of reaction of both ceramics with calcite. The RTU_20 paste contains 1.2% less portlandite than RPU_20. Moreover, RTU_20 includes 2.7% more amorphous phase, primarily composed, as is known, of hydration

products. These two observations confirm that RTU exhibits slightly better pozzolanic activity compared to RPU.

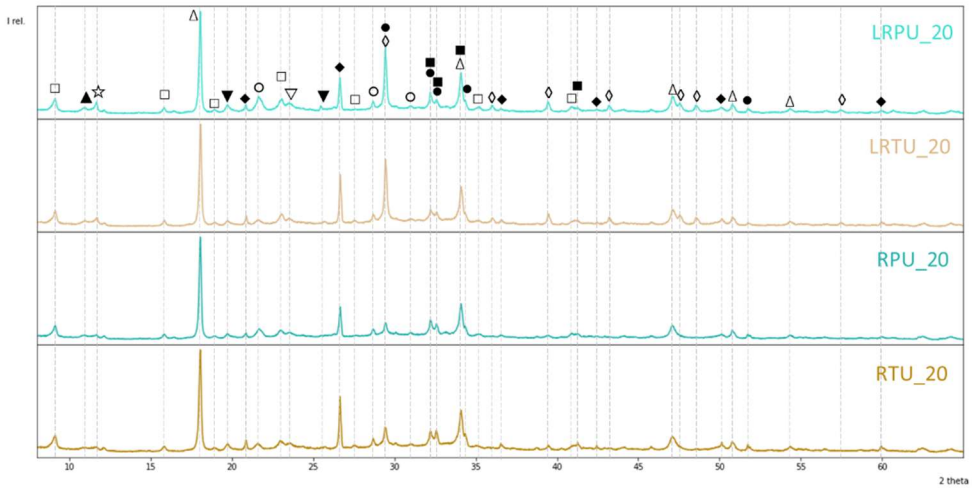

Fig. 4.8. XRD patterns of the pastes containing 20% of ceramic powders RTU and RPU after 90 days curing: Δ – portlandite ($Ca(OH)_2$), ◊ - calcite ($CaCO_3$), □ - ettringite ($Ca_6Al_2(SO_4)_3(OH)_{12}\cdot 26H_2O$), ○ - C-S-H ($CaSiO_3\cdot H_2O$), ● - alite ($Ca_3SiO_5$), ■ - belite ($Ca_2SiO_4$), ◆ - quartz ($SiO_2$), ▽ - ye'elimite ($Ca_4Al_6O_{12}SO_4$), ▼ - grossite ($CaAl_4O_7$), ☆ - monocarboaluminate ($Ca_4Al_2CO_9\cdot 11H_2O$), ▲- hemicarboaluminate ($Ca_8Al_4CO_{16}\cdot 22H_2O$).

Table 4.2. Mineralogical composition of the pastes containing 20% of ceramic powders after 90 days curing, mass. %.

	RTU_20	RPU_20	LRTU_20	LRPU_20
Portlandite	15.2	16.4	13.9	13.5
Calcite	1.9	1.7	6.4	6.5
Ettringite	6	6.9	6	6.4
C-S-H	5.8	6.8	6.4	6.9
Alite	6.2	6.3	4.9	4.2
Belite	6.1	6.8	5.3	5.4
Quartz	5.4	4.1	4.8	3.7
Ye'elimite	2.3	2.4	2.1	2.2
Grossite	1.2	0.9	0.9	0.9
Hemicarboaluminate	0.9	0.9	1.5	1.6
Monocarboaluminate	0.8	1.3	4.1	4.5
Amorphous phase	48.2	45.5	43.7	44.2

4.5.3. Evaluation of fresh pastes properties

Fig. 4.9 demonstrates that water demand increases after the addition of terracotta powders, which aligns with findings of Pitarch et al. [91]. Pereira-de-Oliveira et al. [87] attribute this to the higher specific surface area of the ceramic powder. Conversely, RPU has almost no effect, and the addition of RP leads to a decrease in water demand due to its low specific surface area, as powders with larger particles tend to have lower water demand [220]. Additionally, the decrease in water demand when adding limestone filler to the samples containing ceramic SCM can be attributed to an increase in the packing density of the dry mixture [221, 222]. The particle distribution curves shown in Fig. 4.6 clearly demonstrate that the particle size distribution of the limestone filler differs significantly from that of other materials. Consequently, the fine limestone particles fill the spaces between the cement and ceramic particles, reducing the available space for water.

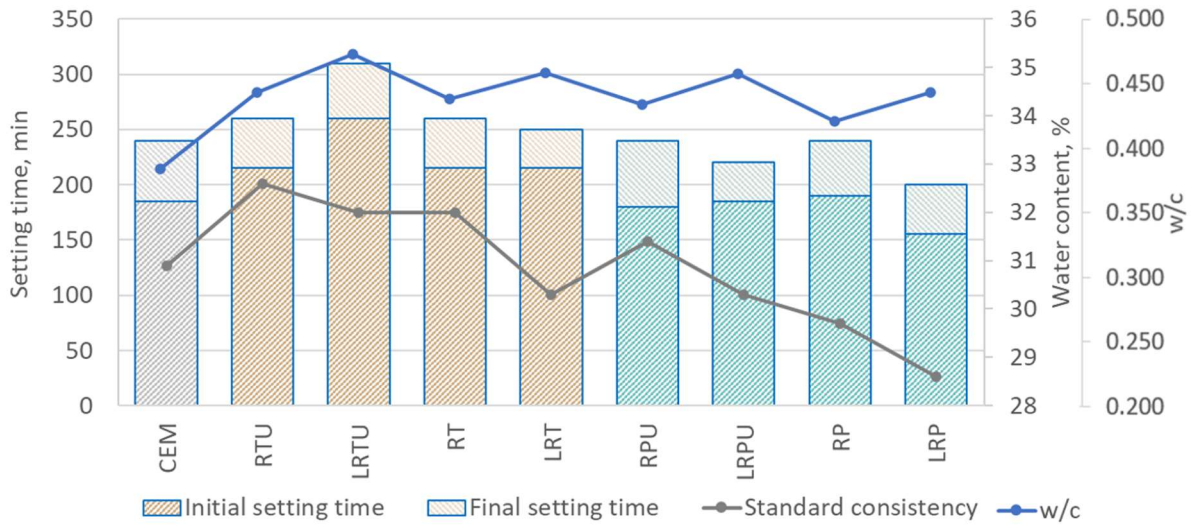

Fig. 4.9. Standard consistency, initial and final setting times of pastes with 20% of ceramic powders and 10% of limestone filler.

Regarding the setting time of cement pastes, it can be seen from Fig. 4.9 that the inclusion of terracotta powders resulted in an increase in both the initial and final setting time, while the addition of porcelain powders had negligible effects on the setting time. The delay of the setting can be explained by the dilution effect of cement phases, which are responsible for the early hydration. Moreover, a significant correlation between setting time and water demand was evident. Similar delays in setting have been reported by other researchers when incorporating ceramic powders [195, 206].

The addition of limestone filler had different effects on the setting time depending on the type of ceramic powder used. For pastes with porcelain powders, the inclusion of limestone filler reduced the initial and final setting time, with values of 155 and 200 minutes, respectively, observed for LRP. However, the paste LRTU exhibited the longest initial and final setting times, with values of 260 and 310 minutes, respectively. The impact of LF on cement setting time is multifaceted and depends on factors such as the amount of additive, particle size, and cement properties. On one hand, LF can accelerate setting by creating nucleation centres, thus promoting cement hydration. On the other hand, it can also retard setting due to the dilution effect of the cement.

The graphs demonstrate that LF increased the setting time of pastes containing RTU, which possesses a higher specific surface area, and had no significant effect on pastes with RT. At the same time, LF reduced the setting time of pastes with both types of porcelain powders. This can be attributed to LF acting as nucleation centres and as inert filler, facilitating cement hydration in some instances, while also potentially retarding setting due to the dilution effect of the cement.

4.5.4. Evaluation of mechanical properties

Fig. 4.10 illustrates the flexural strength of cement mortar samples incorporating ceramic powders and limestone filler after 7, 28, and 90 days of curing. The replacement of 10% of cement with terracotta powders (RT_10 and RTU_10) or 15% with a limestone-terracotta mix (LRT_10 and LRTU_10), regardless of the fineness of the ceramic powder, did not significantly impact the strength compared to the reference mortar. However, a more noticeable reduction in strength was observed with higher substitution rates. Nevertheless, after 90 days of curing, all samples containing terracotta powders exhibited good flexural strength, regardless of their fineness. The addition of limestone filler did not significantly affect the late-stage curing flexural strength, but it did decrease the early strength in high-substitution rate specimens.

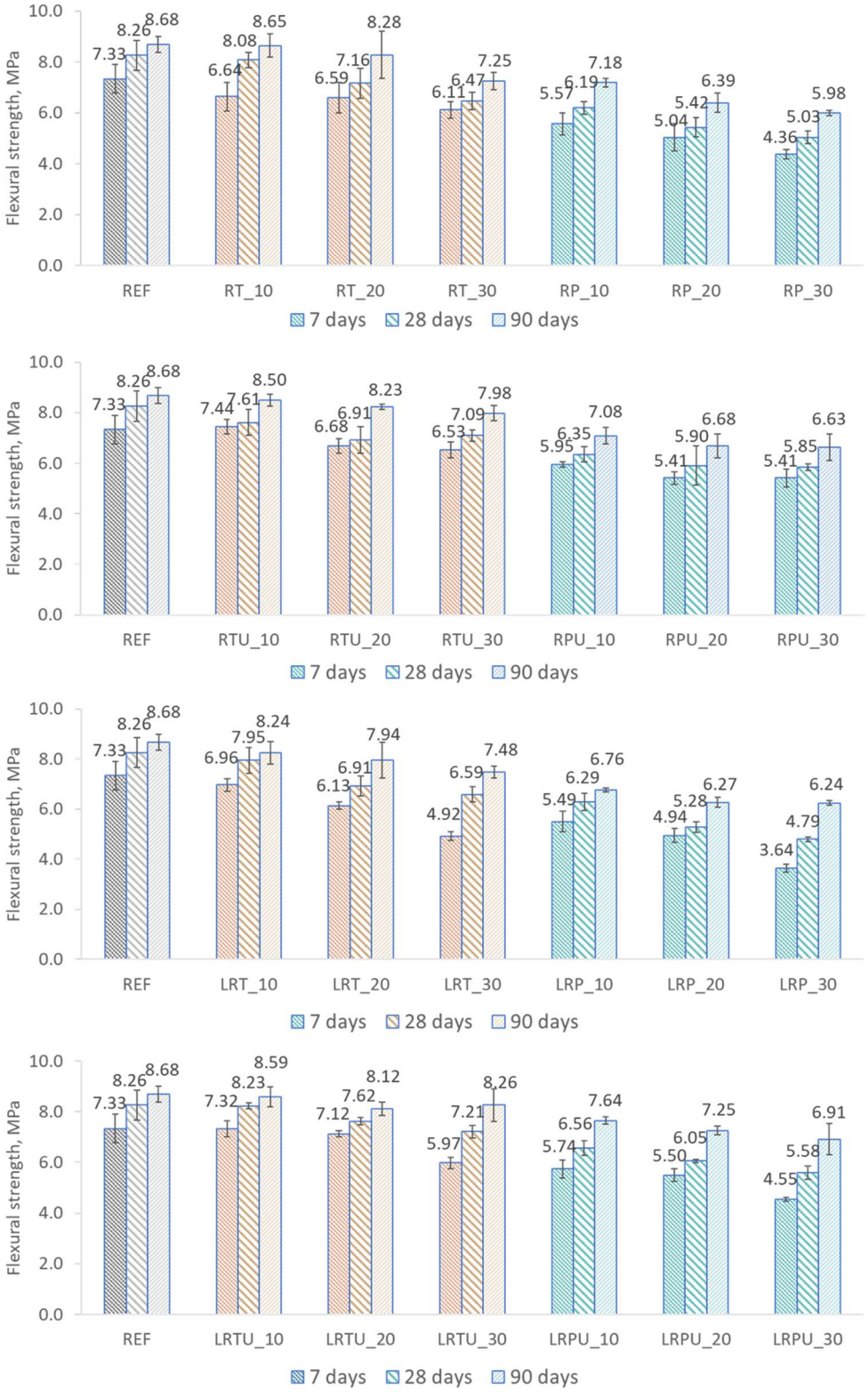

Fig. 4.10. Flexural strength of mortar specimens.

In contrast, the replacement of cement with porcelain powder substantially reduced the flexural strength of cement mortars. Similar to terracotta powders, the fineness of the porcelain powders

did not impact the flexural strength, and the inclusion of limestone filler only reduced strength during the early stages of curing.

The compressive strength of the samples provides insights into cement hydration and pozzolanic reactions. Generally, a higher compressive strength is expected with greater hydration extent, which typically increases with longer curing time. Fig. 4.11 displays the compressive strengths of both the reference and blended cement mortars after 7, 28, and 90 days of curing. The SAI values, shown in Fig. 4.12, provide a clear comparison between the strength of the OPC control mortar and the blended mortars. Over time, the SAI values of all specimens containing ceramic powders increase, indicating longer compressive strength development compared to the reference specimen. This can be attributed to the occurrence of pozzolanic reactions, which primarily take place during the later stages of hydration.

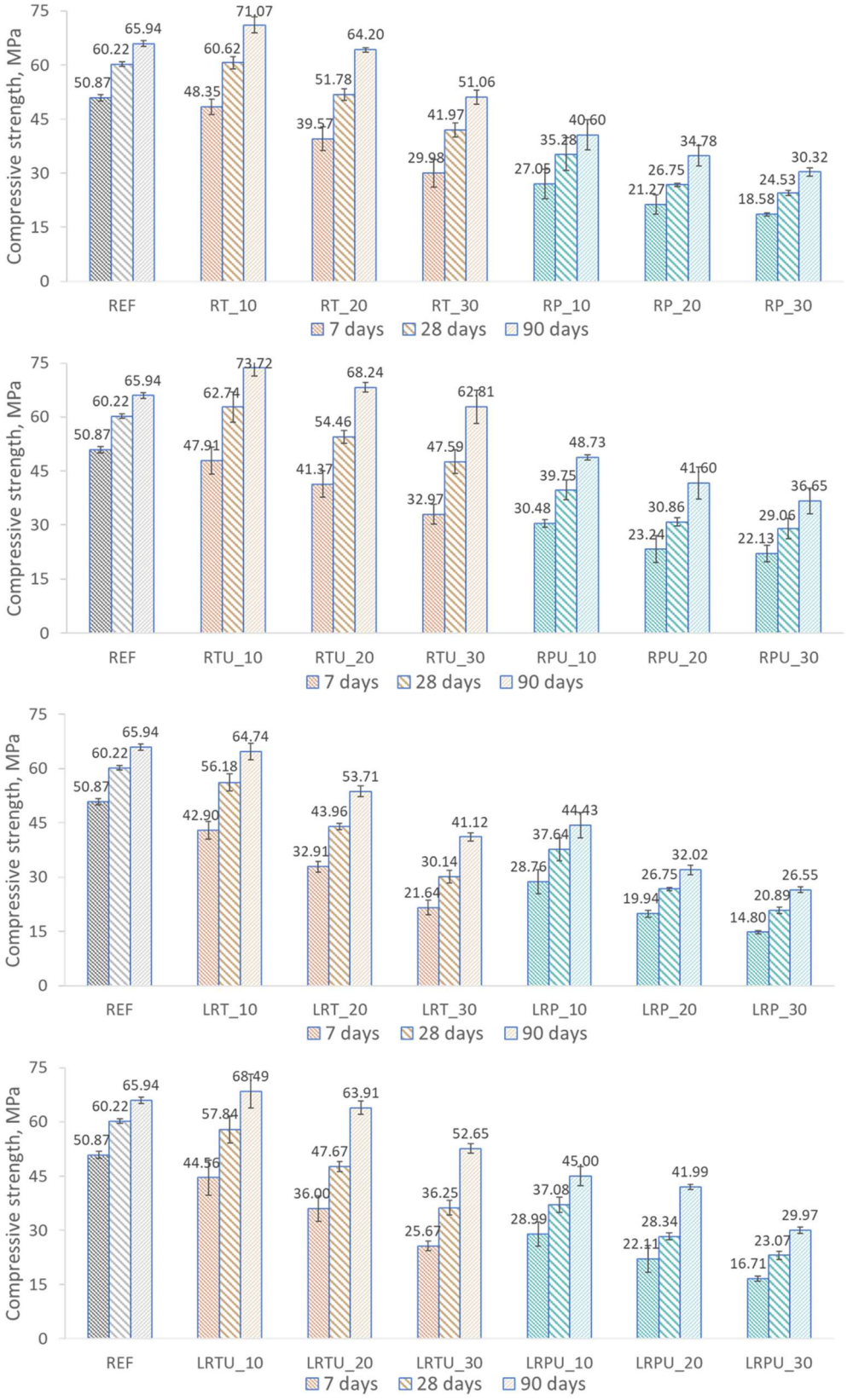

Fig. 4.11. Compressive strength of mortar specimens.

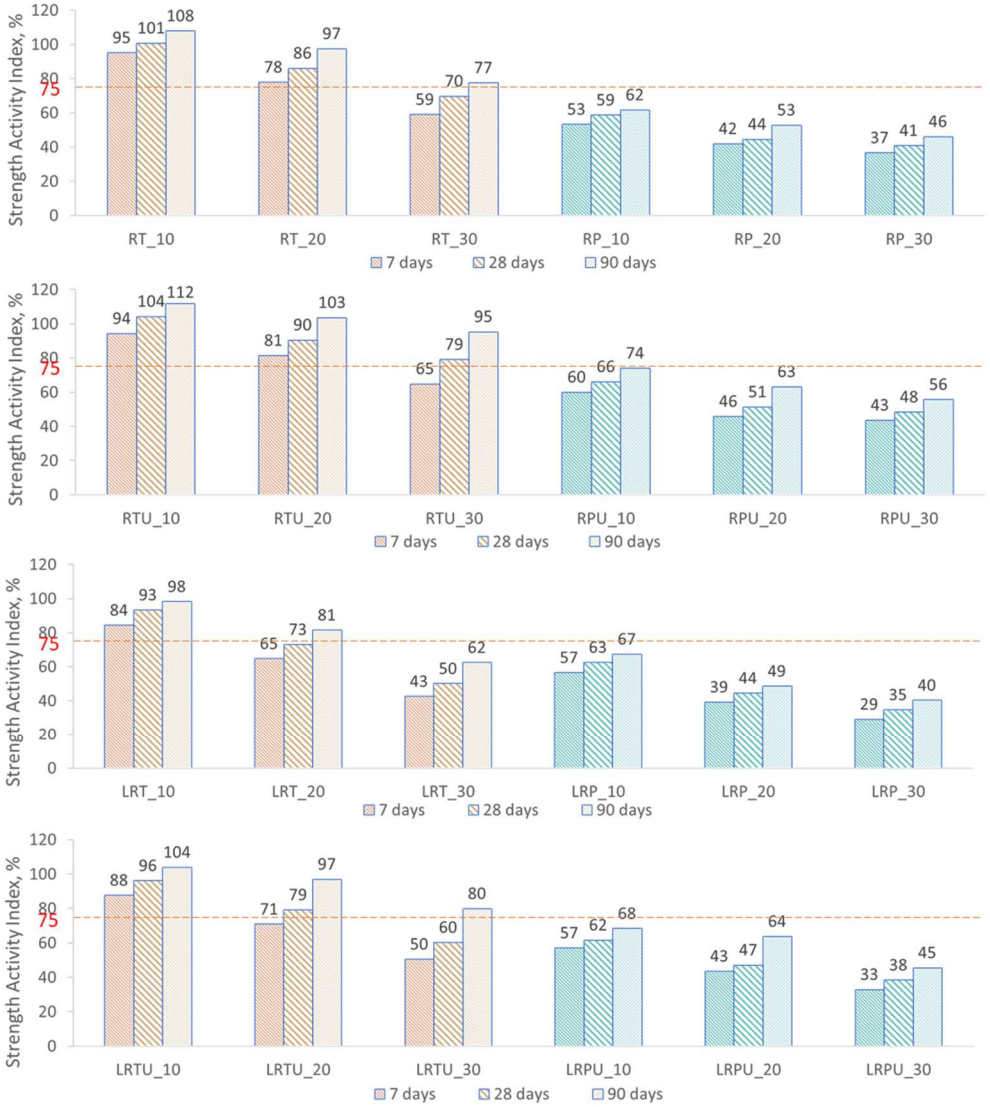

Fig. 4.12. Strength Activity Indices of mortar specimens.

The strength development is primarily attributed to the formation of hydration products, such as calcium silicate hydrate (C-S-H) and calcium aluminate hydrate (C-A-H) [190], and in the case of limestone-ceramic specimens, the carboaluminate hydrates. At 7 days, the reference specimen achieves the highest compressive strength among the 25 mixes of cement mortars, reaching 50.87 MPa. This is expected since the control mortar contains the highest concentration of reactive calcium silicates that react extensively with water during primary hydration. After 28 days, the strength of mortars containing 10% terracotta powders without limestone filler reaches the strength of the reference specimen of 60.22 MPa and is 60.62 and 62.74 for RT_10 and RTU_10, respectively. After 90 days of curing, the strength of RT_10, RTU_10, and RTU_20 specimens surpass that of the control sample (65.94 MPa), with values of 71.07 MPa, 73.72 MPa and 68.24 MPa, respectively. Moreover, the strength of RT_20 and RTU_30 samples nearly match that of the reference, measuring 64.20 MPa and 62.81 MPa, respectively. These results indicate

that a substitution rate of 20% OPC by terracotta powder is close to an optimum choice to produce high-strength mortar. Similar substitution rates for ceramic powder have been reported in other studies [87, 90 - 92, 198, 199], to achieve comparable mechanical properties to those of OPC.

Regarding the limestone filler, the addition of LF reduced the strength of samples compared to those containing only ceramic powders. This indicates a low pozzolanic activity of ceramics compared to traditional calcined clay, making them unsuitable for use in the LC3-50 design. However, samples LRT_10 and LRTU_10, with an OPC substitution rate of 15%, as well as sample LRTU_20, with an OPC substitution rate of 30%, exhibit fairly good strength, reaching 64.74 MPa, 68.49 MPa and 63.91 MPa, respectively, after 90 days of curing. This makes it possible to use terracotta powders in the manufacturing of LC3 with lower substitution rates. Nevertheless, all samples with porcelain powders showed unsatisfactory strength.

Based on the results obtained, it can be concluded that the following samples comply with the requirements of the EN 197-1 standard [13] for cement strength:

– Strength class 52.5: RT_10, RTU_10, RTU_20, LRT_10, LRTU_10.

– Strength class 42.5: RTU_30, LRT_20, LRTU_20.

– Strength class 32.5: RT_30, RP_10, RPU_10, LRTU_30, LRP_10, LRPU_10.

In general, the results of the compressive strength of samples containing porcelain powders differ significantly from the findings of other researchers who reported satisfactory strength values for mortars containing up to approximately 20% porcelain powder [91, 190, 191, 196, 201]. The SAI calculations shown in Fig. 4.12 demonstrate that the strength of samples RP_10 and RPU_10 is only 53% and 60% of the reference mortar strength after 7 days of curing, and 62% and 74% after 90 days of curing, respectively. For samples with 30% RP and RPU, these values are 37% and 43% after 7 days and 46% and 56% after 90 days. Such results indicate that the investigated porcelain powders are not suitable for use as SCM in cement production. According to the ASTM C311 standard [153], a material can be considered a pozzolanic SCM if a mortar with a cement substitution rate of 20% exhibits an SAI of at least 75% after 7 and 28 days of curing. The examined terracotta powders, regardless of their fineness, meet this requirement, while the samples containing porcelain powders do not reach the 75% threshold even at a substitution rate of 10% after 90 days of curing.

The analysis of the mineralogical composition of pastes containing terracotta and porcelain presented in Fig. 4.8 and Table 4.2, revealed no significant difference between samples

containing these different types of ceramics. Therefore, such striking differences in the strength of the samples cannot be explained by the composition of the cement matrix and the difference in the reactivity of ceramic powders. To identify the reasons for the low strength of samples with porcelain, it is necessary to compare the microstructure of samples with terracotta and porcelain powders.

4.5.5. Microstructure of mortar specimens

Upon examining the SEM micrographs at a magnification of 200x, as shown in Fig. 4.13, it becomes evident that the mortar sample containing 20% RPU exhibits a considerably more porous structure compared to the sample containing RTU. At a magnification of 1000x, it becomes also apparent that the microstructure of the sample with porcelain powder is looser and contains a higher number of micropores. As previously mentioned, the X-ray diffraction analysis of paste samples containing 20% RTU and RPU (Fig. 4.8, Table 4.2) did not reveal significant differences in their mineralogy, indicating that the cement matrix of both samples is quite similar. Thus, it can be concluded that the substantial decrease in strength observed in mortars with porcelain powders, as opposed to mortars with terracotta powders, is primarily attributed not to differences in their hydration, but rather to variations in their porosity caused by other reason, which will be discussed in the section 4.5.7.

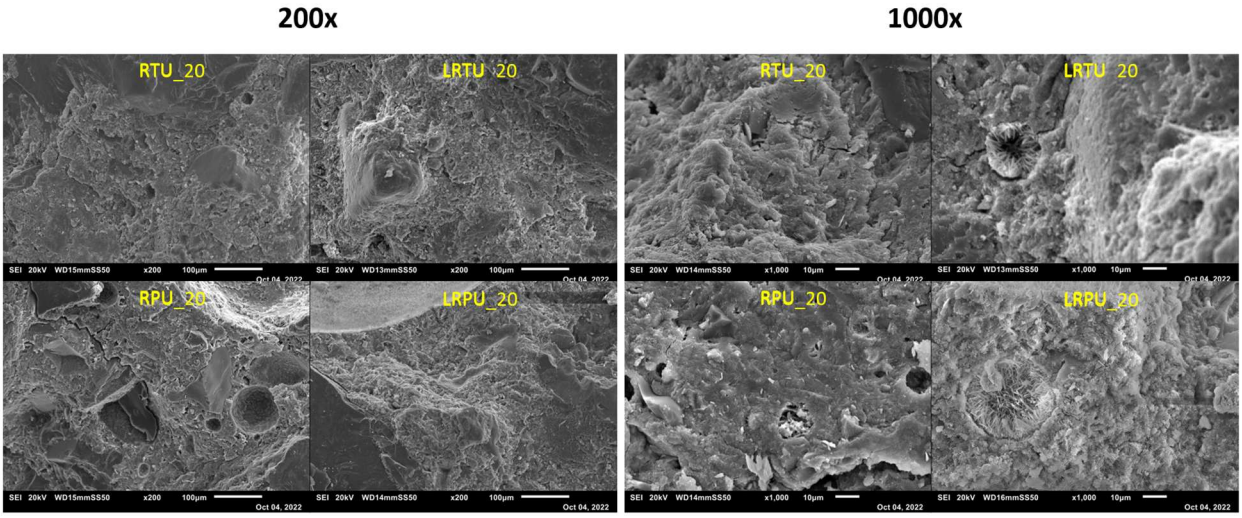

Fig. 4.13. SEM pictures of mortars with 20% of ceramic powders after 90 days of curing at magnification of 200x (left) and 1000x (right).

The microstructure analysis of samples LRTU_20 and LRPU_20 at a magnification of 200x did not exhibit noticeable differences. However, at a magnification of 1000x, it can be observed that the

pores in both samples are filled with ettringite crystals, with larger pores apparent in the LRPU_20 sample. Matschei et al. [223] explain the formation of secondary ettringite in carbonate-rich systems through the displacement of sulphate from Afm by carbonate, leading to the formation of monocarboaluminate and hemicarboaluminate. The sulphate released in this process contributes to the formation of additional ettringite, which likely fills the pores. The presence of mono- and hemicarboaluminate peaks in the X-ray diffraction pattern given in Fig. 4.8 supports this explanation.

Considering these observations, it is evident that further comprehensive investigations are necessary to study the long-term strength and microstructure development of LC3 samples beyond 90 days of curing, as well as the durability aspects of concrete structures using the new binder. The filling of pores with ettringite crystals can potentially enhance the properties of hydrated cement; however, the extensive delayed crystal growth can create internal stresses and lead to the formation of microcracks. Therefore, a more detailed examination is warranted to gain insights into these phenomena.

4.5.6. Capillary absorption measurement

The results of the capillary absorption test on specimens containing 20% ceramic powders after 90 days of curing align with the observations from the SEM micrographs. Fig. 4.14 illustrates that the addition of limestone filler decreases the absorption of the samples, indicating a reduction in open porosity. This reduction is attributed to the filling of pores with secondary ettringite crystals, as revealed by the SEM results. Furthermore, it is evident that the fineness of the ceramic powders influences the capillary absorption of the mortars, with finer powders leading to lower absorption. This suggests that finer powders have a more favourable impact on the microstructure of the cement mortar, primarily due to the filler effect and the increased availability of pozzolanic particles for reactions during cement hydration.

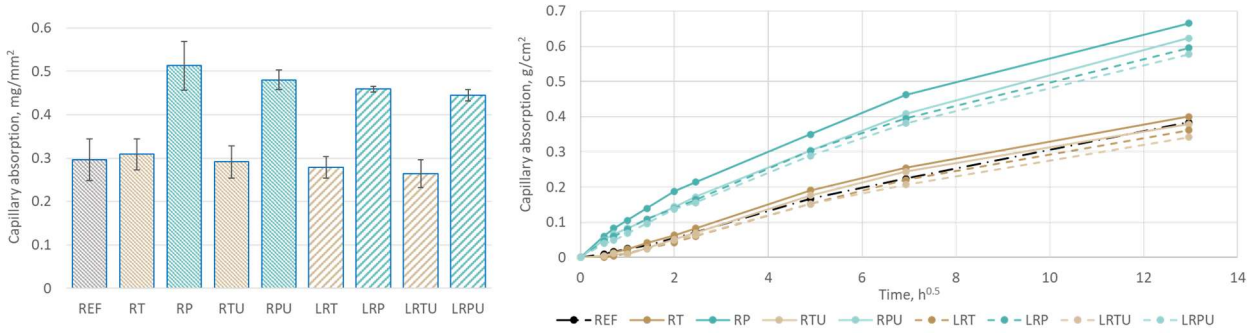

Fig. 4.14. Capillary absorption of reference OPC mortar and specimens containing 20% ceramic powders after 90 days of curing and 7 days of immersion in water.

Samples containing porcelain powders exhibit significantly higher absorbance compared to samples with terracotta powders, confirming the SEM findings of higher porosity in mortars with porcelain. Additionally, it should be noted that the samples containing terracotta powders show comparable to the reference sample capillary absorption. Other authors report a decrease of capillary absorption of samples containing ceramic powders due to pozzolanic reactions and the filler effect, which leads to pore refinement and compaction of the microstructure [89, 194, 198, 199].

4.5.7. Discussion of the reasons for the high porosity of mortars containing porcelain powders

Based on observations, it was found that cement mortar samples containing porcelain powders had significantly higher porosity compared to samples containing terracotta powders. Since the mineralogical composition of pastes containing terracotta and porcelain did not show significant differences, it can be assumed that the porcelain used in the study contained air-entraining agents. Such agents are substances like resins, fats, fatty acids, and surfactants that create stable foam when mixed with water [224].

The material under study was sanitary porcelain and faience, collected directly during demolition and repair work after prolonged use, without being washed before mixing with cement. It can be assumed that during lifespan the porcelain was contaminated with various surfactants, including soaps, shampoos, and cleaning products, which gradually penetrated the cracks in glazes and pores in ceramics, as well as remained on the surface of tiles and sanitary ware. Indeed, during the mixing of cement mortars containing porcelain powders, excessive bubble formation was

observed, which was not observed when mixing mortars with terracotta powders (Fig. 4.15(a) and Fig. 4.15(b)).

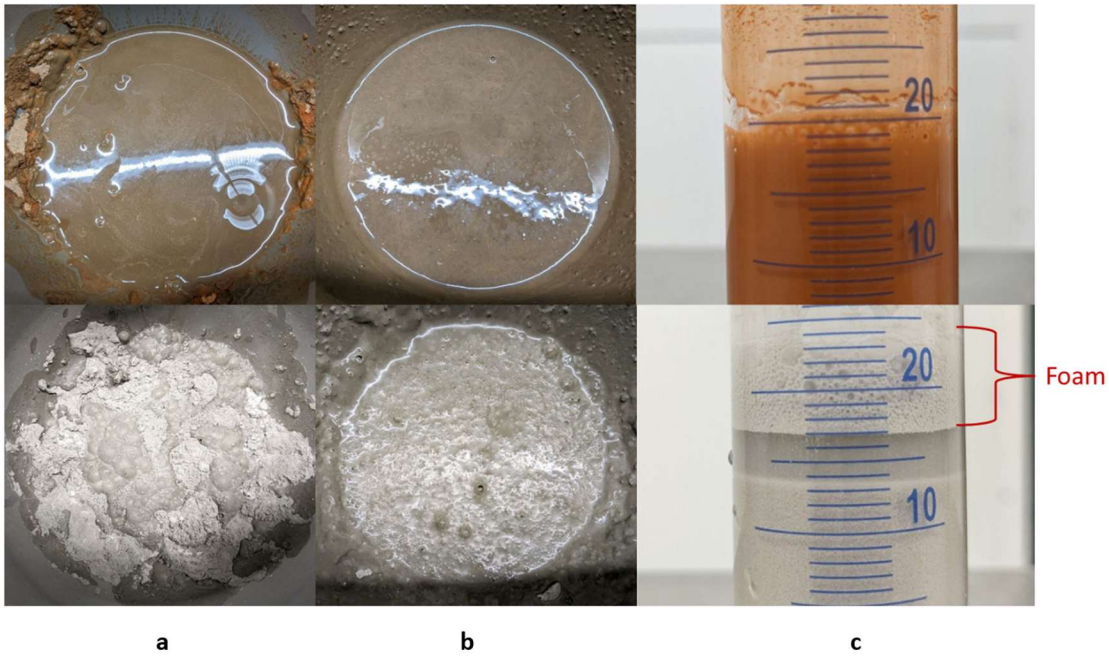

Fig. 4.15. Foam formation: a – after contact of cement-ceramic mix with water, b – after mixing of cement-ceramic mix with water for 30 s, c – after shaking of ceramic powders with water for 30 s.

To confirm the presence of surfactants in porcelain powders, a simple foaming test was performed [225]. In this test, 6 g of RPU and RTU powders were mixed with 15 ml of water and shaken for 30 seconds. After the manipulation, a small number of large bubbles, which disappeared after a few seconds, formed on the surface of the mixture with RTU. On the other hand, a stable foam, which disappeared only after a day, formed on the surface of the mixture with RPU (Fig. 4.15(c)). This confirms the presence of air-entraining agents in the used porcelain, which significantly deteriorated the mechanical properties of cement mortars, which was not observed by other researchers.

To further confirm this theory and assess the effectiveness of porcelain powder purification in improving the mechanical properties of cement mortar, thermal purification of ultrafine porcelain powder (RPU) was conducted in a muffle furnace at 500 °C for 2 hours. Subsequently, cement mortar samples were prepared following the above-described scheme with a substitution rate of 20%. The results of strength tests after 7 and 28 days of curing, as shown in Fig. 4.16, demonstrated a noticeable improvement in the mechanical properties of the mortar specimens. Thus, on the 7th day, the flexural strength increased from 5.41 MPa for the mortar with untreated porcelain powder (RPU) to 6.61 MPa for the sample with calcined porcelain powder (RPU500). By the 28th day, this value had increased from 5.90 MPa to 7.47 MPa. The compressive strength after

7 days of curing increased from 23.24 MPa to 42.67 MPa, corresponding to SAI values of 46% and 84%, respectively. After 28 days of curing, the compressive strength increased from 30.86 MPa to 53.92 MPa, corresponding to SAI values of 51% and 90%.

Fig. 4.16. Flexural and compressive strength and Strength Activity Indices of mortar specimens containing 20% untreated and calcined ultrafine porcelain powders.

These results can infer that the calcination of porcelain powder at 500 °C for 2 hours eliminates organic surfactants, rendering the powder suitable for use as a pozzolanic SCM since specimens containing 20% calcined ultrafine porcelain powder meet the SAI requirement of 75%. It means that the contamination of sanitary ware and tiles with surfactants during their use necessitates pre-washing and drying or calcination of the material before it can be used in the production of blended cement for normal use. However, these procedures require a substantial amount of water and energy, which contradicts the goals of eco-cement production. Nonetheless, since air-entraining agents are introduced into the cement mass during the production of cellular concrete, it can be assumed that sanitary porcelain without pre-treatment can be used as a SCM for the manufacture of this type of building material. However, comprehensive studies on the properties of the new cellular concrete are necessary to validate this assumption.

4.6. Conclusions

This study presents an assessment of the feasibility of using various types of ceramic demolition waste, including terracotta roof tiles and sanitary porcelain, as alternatives to calcined clay in eco-cement production. The chemical and mineralogical composition of the investigated materials aligns with typical terracotta and porcelain, making them representative of these ceramic types. The analysis has highlighted the nuanced factors influencing the comparative assessment, including the presence of impurities and the powder fineness. The following conclusions can be drawn from the obtained results:

(1) Both ceramic waste materials display a chemical composition abundant in pozzolanic oxides, namely SiO_2, Al_2O_3, and Fe_2O_3, accounting for 76.72% in terracotta and 85.74% in porcelain. Their mineralogical characteristics align with typical red and white ceramics. Terracotta powders had finer granulometry than porcelain powders due to differences in material hardness.

(2) Despite having a higher amorphous phase and pozzolanic oxide content, porcelain powders exhibited weaker pozzolanic behaviour than terracotta powders. According to the Chapelle test results, terracotta powders bound 505 and 618 mg $Ca(OH)_2$ for RT and RTU, respectively, while porcelain powders bound 395 and 443 mg $Ca(OH)_2$ for RP and RPU, respectively. This lower reactivity can be attributed to the lower specific surface area of porcelain powders and the high firing temperature.

(3) The substitution of up to 20% of OPC with terracotta powders had a minimal impact on the strength of the mortars. The SAI at 90 days of curing was 97% for RT_20 and 103% for RTU_20, indicating their potential as SCMs. However, the inclusion of porcelain powder significantly reduced the strength of the specimens, with the maximum SAI at 90 days of curing being 62% for RP_10 and 74% for RPU_10, rendering them unsuitable as SCMs.

(4) The incorporation of limestone filler led to a reduction in strength compared to samples containing only ceramic powders. Nevertheless, LC3 samples containing terracotta powders with up to a 30% substitution rate of OPC demonstrated relatively strong performance, achieving a SAI of 81% for LRT_20 and 97% for LRTU_20 after 90 days of curing. This suggests the potential for utilizing terracotta powders in the production of LC3 with lower substitution rates. However, all specimens containing porcelain powders exhibited inadequate mechanical properties, with the maximum SAI at 90 days of curing being 67% for LRP_10 and 68% for LRPU_10.

(5) The porous microstructure and poor mechanical properties of mortars containing porcelain powders are attributed to the presence of surfactants in sanitary porcelain, which was proved by foam-formation test.

(6) SEM microstructure analysis of LC3 specimens after 90 days of curing showed the presence of secondary ettringite crystals in the pores of all samples.

(7) The calcination of sanitary porcelain powder contaminated with surfactants at 500 °C leads to its purification and improves the compression strength of mortars with 20% waste powder from 23.24 MPa to 42.67 MPa after 7 days of curing and from 30.86 MPa to 53.92 MPa after 28 days of curing.

These findings offer valuable insights for the cement and processing industries regarding the treatment and application of different ceramic demolition waste materials in eco-cement production, including blended pozzolanic cements and LC3 formulations. Moreover, this research has unveiled promising avenues for further study, including the analysis of cement mixtures containing different ceramic powders in terms of their durability, long-term strength development, and microstructure characteristics at advanced stages of curing. Additionally, it is important to conduct economic and environmental assessments related to the purification of porcelain waste for its integration into cement production processes. Since the comparative assessment presented in this study is influenced by various factors, including the source and type of ceramic waste, pre- and post-grinding preparation, powder fineness and resulting surface area, future statistical research should delve into these factors to enhance the understanding of their impact on properties of final binder, contributing to the ongoing evolution of eco-cement production.

Chapter 5: Durability of cement mortars containing fine demolition wastes as supplementary cementitious materials

Abstract

The study addresses the durability performance of cementitious mortars containing 20% recycled powders derived from construction and demolition waste, specifically concrete screenings, mixed screenings, and slurries from the washing of recycled aggregates. Uncalcined and thermally activated at 500°C, the powders were evaluated for their potential as supplementary cementitious materials. Key durability parameters analyzed include freeze-thaw resistance, fire resistance and sulfuric acid corrosion resistance, along with capillary absorption and drying shrinkage. Analysis of Variance (ANOVA) was used to assess the influences of various factors on the durability properties. The results demonstrate that the type of waste has a significant impact on the durability of mortars, with ceramic-containing specimens exhibiting superior performance in comparison to those comprising pure concrete powders. Capillary absorption emerged as an important factor for resistance to extreme temperatures. Furthermore, the findings of this study demonstrate that thermal activation of waste powders does not enhance the durability parameters, and that drying shrinkage shows no significant impact on durability. This study fills a knowledge gap in the durability of cementitious materials incorporating recycled powders and highlights the potential of ceramic-containing powders in sustainable cement production.

5.1. Introduction

In recent years, the generation of construction and demolition waste (CDW) has been steadily increasing due to population growth and urbanization. This inert waste has found successful application as recycled coarse and fine aggregates [226 - 230], nevertheless the presence of cement mortar adhering to recycled aggregates significantly diminishes their quality. Addressing this issue through polishing and washing operations gives rise to the generation of secondary waste materials, such as screening fines or washing mud. These materials are characterised by their fine granulometry, which renders them unsuitable for use as aggregates [231]. To mitigate

this challenge, researchers are exploring the potential of recycled concrete powders (RCP) as supplementary cementitious materials (SCMs) to partially replace cement clinker and reduce carbon footprint of cement production [67, 129, 232, 233]. Among these, the use of thermally activated concrete powders has shown significant promise, as thermal treatment partially restores the hydraulic properties of the powders through the decomposition of portlandite and C-S-H gel [83, 144, 234, 235].

Despite numerous studies on the use of CDW as SCMs in eco-cement production, the majority of these studies have focused on the fresh and mechanical properties of the resulting binders. However, there is currently a lack of research addressing their durability characteristics, which are critical for practical applications. The effective utilization of recycled concrete powders requires a comprehensive understanding of their ability to withstand adverse environmental conditions.

Most publications on the durability of cementitious materials incorporating rehydrated RCP focus on resistance to chloride penetration and, to a lesser extent, carbonation. Researchers from the University of Lisbon investigated chloride migration and carbonation in concrete specimens containing RCP activated at 650°C in amounts ranging from 5% to 100% of Portland cement. They concluded that the durability of concrete with rehydrated RCP is comparable to conventional Portland cement concrete due to its refined pore structure [236, 237]. Similar findings were reported by Cantero et al. [238], who observed enhanced chloride and carbonation resistance in concrete specimens with 10% uncalcined RCP. Hu et al. [239] demonstrated that mortars with 50% RCP calcined at 800°C achieved resistance to chloride penetration comparable to reference specimens. However, contrasting results were found in the study by Xu et al. [240], where concrete made with 100% RCP activated at 650°C exhibited reduced durability due to increased porosity. Sun et al. [241] observed that the incorporation of 30% and 50% uncalcined waste powders into cement mortar specimens resulted in increased chloride penetration due to matrix loosening caused by inert particles. Similar results were reported by Ma et al. [242] for concrete specimens. However, heat treatment of the recycled powders improved chloride penetration resistance, although it remained lower than that of the reference sample. Wu et al. [243] investigated concrete specimens containing a blend of uncalcined recycled concrete powder and recycled ceramic brick powder. Their findings indicated that recycled powders positively affect chloride penetration resistance, while their positive impact on carbonation resistance persists only when the cement substitution rate is limited to 15%. Furthermore, Gao et al. [244] reported that the degree of carbonation in cement mortars increases as the substitution level of Portland cement by uncalcined RCP rises.

Meanwhile, critical durability parameters such as freeze-thaw resistance, fire resistance, and sulfuric acid corrosion resistance of cementitious materials containing RCP remain largely underexplored.

Algourdin et al. investigated the resistance of mortar specimens containing recycled powders activated at 500°C to high-temperature exposure [149] and freeze-thaw cycles [245]. Their findings revealed that after exposure to 200°C, the mechanical properties of the mortar samples remained virtually unchanged. However, a significant loss of strength occurred upon exposure to 500°C, with the strength loss decreasing in proportion to the degree of Portland cement substitution by thermally activated recycled powders increased. Additionally, following 100 freeze-thaw cycles at temperatures ranging from -20°C to +20°C, all specimens exhibited an increase in compressive strength due to ongoing hydration, and the mass loss of recycled cement specimens was comparable to that of the reference specimen.

Rocha et al. [67] conducted a comprehensive literature review on the use of RCP as SCMs, identifying only three studies that investigated freeze-thaw resistance [244, 246, 247]. All of these studies focused on uncalcined recycled powders and reported a decline in freeze-thaw resistance of materials containing RCPs, attributed to microstructure loosening.

Belkadi et al. [248] investigated cement mortars with 10%, 15%, and 20% uncalcined RCP and observed a decline in sulfuric acid corrosion resistance with increasing cement replacement levels attributed to the porous nature of the recycled powder, irregular morphology, and poor adhesion.

Thus, it is evident that the durability parameters of cement containing thermally activated RCPs, such as resistance to freeze-thaw during seasonal changes in the temperate zone, fire resistance in case of fire and resistance to corrosion by sulfuric acid formed in wastewater as a result of the vital activity of microorganisms and in drops of acid rain, have not yet been studied.

Although capillary absorption and drying shrinkage are not durability properties in themselves, they are important indicators that can influence durability properties indirectly. High capillary absorption usually indicates higher porosity and permeability, which can make a material more vulnerable to durability issues like chemical attack, freeze-thaw damage, or reinforcement corrosion. On the other hand, larger regular air voids can act as pressure relief inclusions, allowing expanding ice to move into these voids, which reduces internal pressure and mitigates freeze-thaw damage [249]. Excessive shrinkage also indicates higher permeability, as it can lead to the development of cracks that compromise durability by allowing the ingress of harmful agents. These two properties have been relatively well described in the context of RCP use. While

the effect of increasing RCP content on capillary absorption is generally agreed upon, with studies usually showing an increase in capillary absorption [236, 237, 240, 242, 250], the results regarding the effect on drying shrinkage are contradictory. Some studies suggest that recycled powders reduce shrinkage due to lower reactivity, reduced gel pore content, and higher particle hardness [241, 251], while others report an increase in drying shrinkage due to higher porosity [252, 253].

This study extends the research results published earlier [254] by examining the durability performance of cementitious mortars containing 20% recycled powders derived from screening of recycled concrete aggregates, recycled mixed aggregates and mud from recycled mixed aggregates washing, both untreated and thermally activated at 500°C. Durability parameters such as freeze-thaw resistance, fire resistance, and sulfuric acid corrosion resistance were analysed alongside drying shrinkage and capillary absorption. The significance of this work lies in addressing the critical knowledge gap regarding the durability of cementitious materials incorporating recycled CDW powders, particularly after thermal activation, a field with limited prior research. Notably, this study is one of the first to explore the use of mixed powders containing ceramic particles, an area that has received little to no attention in existing literature.

5.2. Materials

In this study, three types of fine demolition waste provided by the Belgian company Tradecowall were used for the preparation of mortar specimens. Tradecowall processes inert waste into recycled coarse and fine aggregates, involving several screening stages that separate the aggregates into different fractions. Substandard fractions from this screening process, which are unsuitable as aggregates, are stored on-site as final waste. Additionally, the washing of recycled aggregates generates wash mud, which is also stored on-site.

The three types of demolition waste fines utilized were:

- Concrete Screening Waste (CS): This consisted of concrete fines mixed with minor impurities, including metal reinforcement debris.
- Mixed Screening Waste (MS): This comprised approximately 60% concrete and 40% ceramics, glass, and stones, with minor impurities of organic materials such as wood, bitumen, polymers, and fabrics. The ceramic debris in MS originated from unseparated demolition waste and was not compositionally controlled. However, it predominantly

consisted of ceramic bricks, wall and floor tiles, with potential contributions from roof tiles and, to a lesser extent, sanitary porcelain.

- Washing Mud (WM): This was a dark grey mass resulting from the aggregates washing process.

The waste materials underwent drying at 105°C until reaching constant mass, followed by a two-stage crushing process. Preliminary crushing was done using a jaw crusher, and final crushing employed an impact mill with a 2 mm mesh bottom sieve. Post-crushing, the materials were sieved using a 125 µm mesh sieve, resulting in two fractions: 0/125 µm and 0.125/2 mm . Only the 0/125 µm fraction was used in this study. The powders dried at 105°C were labelled as CS105, MS105, and WM105 for concrete screenings, mixed screenings, and washing mud respectively.

Subsequently, these materials were calcined in a muffle furnace at 500°C for 2 hours with a heating rate of 10°C/min and allowed to cool naturally in a closed furnace. The calcined powders were labelled as CS500, MS500 and WM500 for concrete screenings, mixed screenings, and washing mud respectively.

For the preparation of mortar specimens, the following additional materials were used: Portland cement CEM I 52.5 R provided by the French manufacturer Vicat, CEN Standard Sand conforming to EN 196-1 [150] and tap water. Table 5.1 provides the chemical composition and the key physical properties of the raw materials utilized in this study.

Table 5.1. Chemical and physical properties of the powders used in the study.

Property	CEM I	CS	MS	WM
SiO_2 (mass-%)	16.07	28.42	41.94	44.60
Al_2O_3 (mass-%)	3.91	5.90	8.10	9.42
Fe_2O_3 (mass-%)	3.58	4.12	5.51	5.83
CaO (mass-%)	66.72	33.29	21.24	17.76
MgO (mass-%)	1.45	1.63	1.11	1.37
TiO_2 (mass-%)	0.37	0.45	0.77	0.81
MnO (mass-%)	0.08	0.12	0.11	0.11
Na_2O (mass-%)	0.26	0.35	0.47	0.30
K_2O (mass-%)	1.18	1.25	2.15	2.30
P_2O_5 (mass-%)	0.39	0.17	0.44	0.34

Property	CEM I	CS	MS	WM
SO_3 (mass-%)	3.88	0.80	2.56	1.27
*LOI (mass-%)**	2.10	23.50	15.60	15.90
Specific gravity before calcination (g/cm³)	3.045	2.444	2.547	2.509
Specific gravity after calcination at 500°C (g/cm³)	—	2.527	2.591	2.613
Blaine SSA before calcination (cm²/g)	5418	5620	5316	5436
Blaine SSA after calcination at 500°C (cm²/g)	—	5539	5049	5105

* Loss on ignition at 950 °C

The mineralogical composition of MS and WM was predominantly quartz, whereas CS contained both quartz and calcite in equal proportions. Calcite was also present in MS and WM, albeit in smaller quantities compared to CS, with WM exhibiting the lowest calcite content. Furthermore, the significant amounts of feldspars and muscovite were identified in all the examined wastes, with WM showing the highest concentration of these minerals. In terms of mineralogical differences, MS did not contain dolomite, in contrast to CS and WM. Similarly, gypsum was absent in CS, distinguishing it from the other two wastes. Notably, CS was the only waste that included clay minerals, specifically chlorites.

5.3. Experimental methods

5.3.1. Compressive strength

The compressive strength of the mortars containing demolition wastes were assessed using 40x40x160 mm mortar bars, prepared according to ISO 679:2009 [152]. The water-to-binder (w/b) and sand-to-binder (s/b) ratios for all mixtures were fixed at 0.5 and 3, respectively. A 20% substitution rate for Portland cement, performed by mass, was chosen, based on the optimal results from previous studies [79, 82, 127, 131, 255, 256]. The composition of the mortar mixtures is summarized in Table 5.2.

Table 5.2. Composition of mortar mixtures (values in grams).

Mix	CEM I	CS105	MS105	WM105	CS500	MS500	WM500	Sand	Water
REF	450	0	0	0	0	0	0	1350	225
CS105	360	90	0	0	0	0	0	1350	225
MS105	360	0	90	0	0	0	0	1350	225
WM105	360	0	0	90	0	0	0	1350	225
CS500	360	0	0	0	90	0	0	1350	225
MS500	360	0	0	0	0	90	0	1350	225
WM500	360	0	0	0	0	0	90	1350	225

The specimens were cured in a moisture chamber at 20°C for 28 days before testing. The compressive strength test was conducted according to ISO 679:2009 [152] on six specimens of each mortar type. For the graphs, the average values of six measurements, along with the standard deviation, were used.

5.3.2. Capillary absorption

The capillary absorption measurement was conducted in accordance with the EN 480-5 standard [257]. Three specimens of each mortar type were prepared for testing. After 28 days of curing, the specimens were dried at 50°C until they reached a constant mass. The specimens were then weighed to determine their mass before adsorption. Each specimen was immersed in water to a depth of 5 mm with a 40x40 mm edge resting on a support, ensuring this edge was freely exposed to water. The container was then sealed with a lid in order to prevent evaporation.

Measurements were taken at the following time intervals: 0.25, 0.5, 1, 2, 4, 6, 24, 48, and 168 hours. At each interval, the specimens were removed from the water, blotted with a paper napkin and weighed to determine the mass with absorbed water. The water level in the container was consistently maintained at a height of 5 mm.

The capillary absorption (C_a) in g/mm^2 for each time period was calculated using the formula:

$$C_a = \frac{M - M_0}{1600} \quad (11)$$

where M_0 is the mass of the dry specimen in g, M is the mass of the specimen with absorbed water in g and 1600 is the surface of the exposed edge in mm^2.

For the graphs, the average values of three measurements, along with the standard deviation, were used.

5.3.3. Drying shrinkage

The drying shrinkage test was conducted following the EN 12617-4 standard [258] on three specimens of each mortar type, with modifications to the measurement duration and frequency. Cement mortar samples were poured into 40x40x160 mm moulds equipped with integrated attachment pins at both ends. After 24 hours, the specimens were removed from the moulds and placed on the ball-bearing rollers of a Shrinkage Measuring Device Type C from Testing Bluhm & Feuerherdt GmbH (Fig. 5.1). Shrinkage measurements were taken using a digital displacement gauge with a conical contact tip, featuring LVDT displacement sensors (measuring range: 5 mm, resolution: 0.31 µm, accuracy: 0.2 µm). The gauge was positioned on one end of the specimen to monitor time-dependent volume contraction by measuring changes in length. The opposite end was horizontally constrained by a fixed pin. Measurements were recorded every 2 hours for a duration of 90 days using a Schleibinger Geräte signal processor. Additionally, the environmental conditions, including temperature and relative humidity, were continuously monitored throughout the test to ensure accurate data collection.

Fig. 5.1. Drying shrinkage measurement device.

5.3.4. Freeze-thaw resistance

Currently, there is no standardized procedure for evaluating the freeze-thaw resistance of mortar specimens. Therefore, a custom methodology was implemented. To measure freeze-thaw resistance, 40x40x160 mm specimens were dried at 50°C to a constant weight after 28 days of curing. The initial mass of each dried specimen was recorded. The specimens were then immersed in water in covered containers to prevent evaporation. These containers were placed in a freezer, cooled to -20°C at a rate of 4°C/min and maintained at this temperature for 11 hours and 50 minutes. Subsequently, the specimens were heated to +20°C at the same rate. Each freeze-thaw cycle lasted 24 hours, with the temperature regime diagram for one cycle provided in Fig. 5.2.

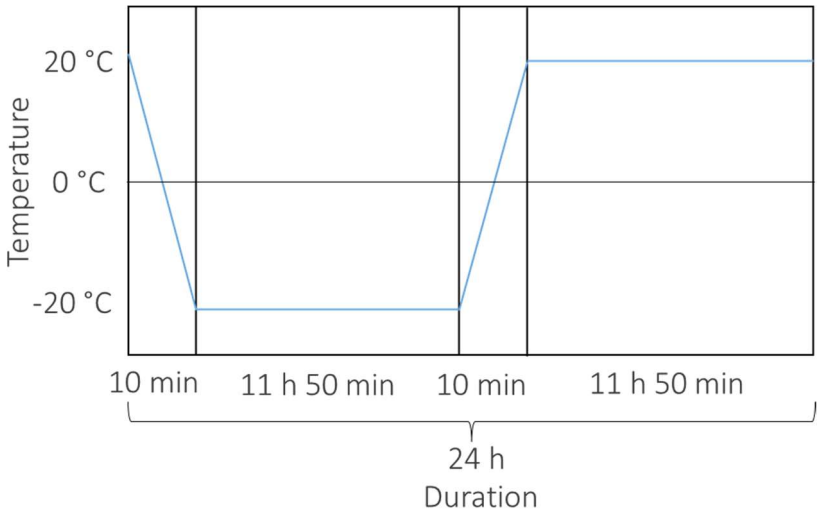

Fig. 5.2. Temperature regime of one freeze-thaw cycle.

The specimens underwent 28 freeze-thaw cycles. The selection of 28 freeze-thaw cycles aligns with previous studies assessing cementitious materials and provides a reliable comparison of different mortar formulations within a practical experimental timeframe. After completing the cycles, the specimens were dried again to a constant weight, and their final mass was recorded. The compressive strength of the specimens was then tested. Conclusions regarding the freeze-thaw resistance of the mortar specimens were drawn based on the percentage change in their mass and strength. For the analysis, the mean values of six measurements, along with the standard deviation, were used.

5.3.5. Fire resistance

Since no standardized test exists for assessing the fire resistance of mortar specimens, a custom test procedure was developed. Prior to exposure to elevated temperatures, the 40x40x160 mm mortar specimens were dried at 50°C until a constant mass was reached, at which point their initial mass was recorded. Subsequently, the samples were subjected to firing in a muffle furnace at target temperatures of 200°C, 300°C, 500°C, and 900°C for a duration of 2 hours. The heating rate was maintained at 10°C/min, while the cooling was passive in the furnace. After cooling the specimens were weighed to determine the mass loss and then subjected to compressive strength tests to assess mechanical integrity. The fire resistance of the mortar specimens was quantified by calculating the percentage change in both mass and compressive strength. For the analysis, the mean values of six measurements, along with the standard deviation, were used.

5.3.6. Sulfuric acid resistance

As no established standards exist for evaluating the sulfuric acid resistance of mortar specimens, a custom procedure was employed. The resistance to the corrosive effect of sulfuric acid was assessed using 40x40x160 mm specimens after 28 days of curing. Initially, the specimens were dried at 50°C until reaching a constant mass, and their initial mass was recorded. The specimens were then immersed in plastic containers containing a 1% (0.1 M) H_2SO_4 solution for 90 days. To prevent neutralization, the acid solution was renewed every 30 days.

After the 90-day immersion period, the specimens were rinsed with tap water and dried again at 50°C to a constant weight. The final mass and compressive strength of the corroded specimens were measured. The rate of sulfuric acid corrosion resistance of the mortars was assessed by expressing the mass and strength change as percentages. For the analysis, the mean values of six measurements, along with the standard deviation, were used.

5.3.7. Statistical analysis

Analysis of Variance (ANOVA) is a statistical tool used to analyse the collected data. In this research, ANOVA was employed to determine if there are statistically significant influences of different parameters on the durability features of the mortar specimens. The R programming language was used for data analysis. The factors included waste type, thermal treatment of waste powders, capillary adsorption and shrinkage. These factors were analysed in relation to the following responses: freeze-thaw resistance, fire resistance and sulfuric acid corrosion resistance. The analysis was organized in this way to comprehensively assess the durability of the cementitious material under various environmental conditions. Freeze-thaw resistance, fire resistance, and sulfuric acid resistance were chosen as dependent variables because they represent key durability challenges for cement-based materials in real-world applications. The four independent factors: waste type, thermal treatment of waste, capillary adsorption, and shrinkage, were selected because they are expected to significantly influence these durability properties. Waste type and thermal treatment affect the microstructure and chemical composition of the material, while capillary adsorption and shrinkage impact its porosity and mechanical stability.

The statistical significance of each factor's effect on durability properties was determined using the p-value. A p-value represents the probability of making an error when rejecting the null

hypothesis, which assumes that the variable is not dependent on the factor. Thus, the smaller the p-value, the stronger the evidence of a relationship. In this study, a significance level of 0.05 was chosen, which is a widely accepted threshold in engineering and material science research. A stricter threshold could reduce Type I errors but might overlook meaningful effects due to increased Type II errors. Conversely, a more lenient threshold would increase the risk of false positives. If a p-value is below 0.05, there is strong evidence to reject the null hypothesis and conclude that the factor has a statistically significant influence on the durability property. Conversely, p-values above 0.05 suggest that the factor's effect is not statistically significant, implying that any observed variations may be due to random chance rather than a true relationship.

5.4. Results and discussion

5.4.1. Compressive strength

Fig. 5.3 presents the compressive strength values of the tested mortar specimens after 28 days of curing, compared to the reference Portland cement mortar. All investigated materials exhibited lower mechanical properties than the reference specimen (60.2 MPa). However, thermal treatment resulted in a slight improvement in the strength of the mortars. Thus, the compressive strength values for the mortars containing CS105, MS105, and WM105 were 50.2 MPa, 49.6 MPa, and 47.8 MPa respectively, while for the mortars with CS500, MS500, and WM500, these values were 53.5 MPa, 52.3 MPa, and 51.4 MPa, respectively.

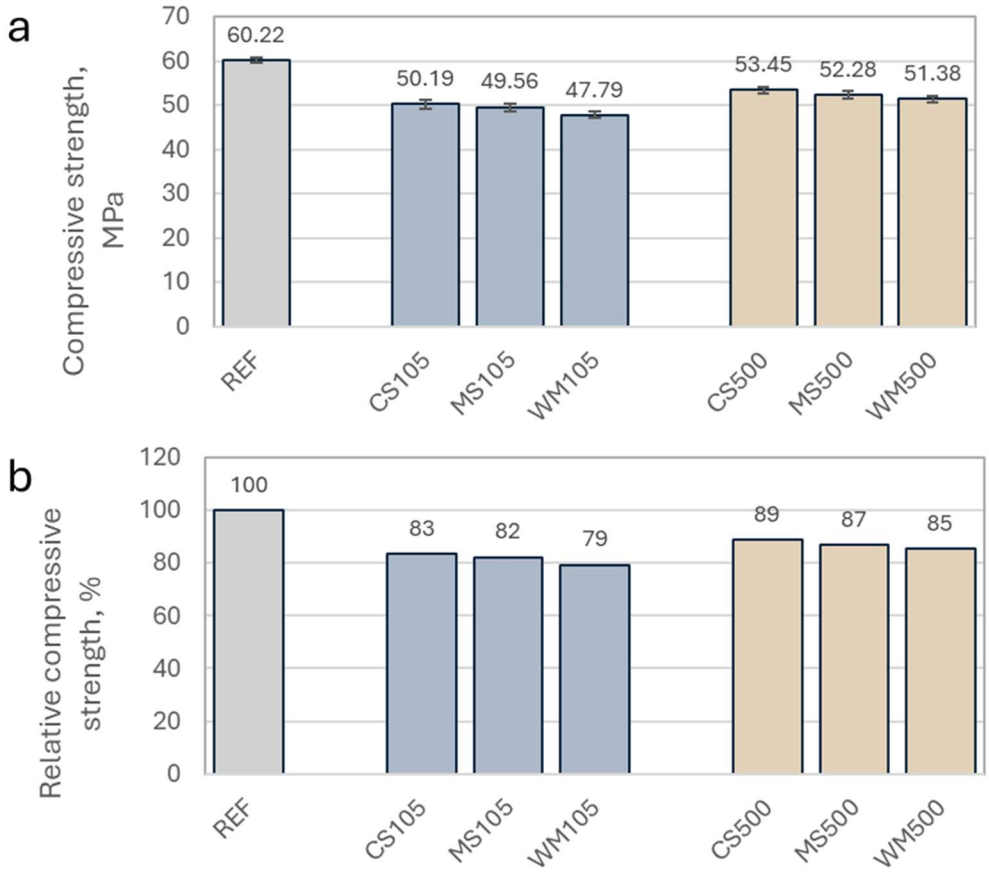

Fig. 5.3. Compressive strength of mortars containing 20% demolition waste powders after 28 days of curing: (a) absolute values; (b) relative values.

Nevertheless, all samples met the strength requirement set by the European standard EN 197-1 [13] for blended cement, corresponding to a strength class of 42.5 MPa. A more detailed discussion of the effect of thermally treated demolition waste powders on the strength of cement mortar can be found in the previous study [254]. In the current study, the compressive strength values after 28 days of curing are used to compare the strength loss of the mortars after the durability tests.

5.4.2. Capillary absorption

Fig. 5.4 presents the capillary water absorption curves for the investigated mortar specimens. The reference specimen, which contained no waste powders, exhibited the lowest absorption throughout the measurement period. The thermal activation of demolition waste powders resulted in reduced capillary absorption in all specimens. Notably, the mortar containing 20% CS500 showed a similar absorption level to the reference specimen with a value of 0.004 g/mm^2,

while without thermal activation this value was 0.005 g/mm^2. This reduction can be attributed to the increased reactivity of the thermally activated recycled powders, leading to matrix densification and reduced porosity. However, thermal activation had a smaller effect on the capillary absorption of specimens containing MS and WM, remaining at a level of around 0.005 g/mm^2 for all specimens. This can be explained by the lower content of hydrated cement in these samples compared to CS.

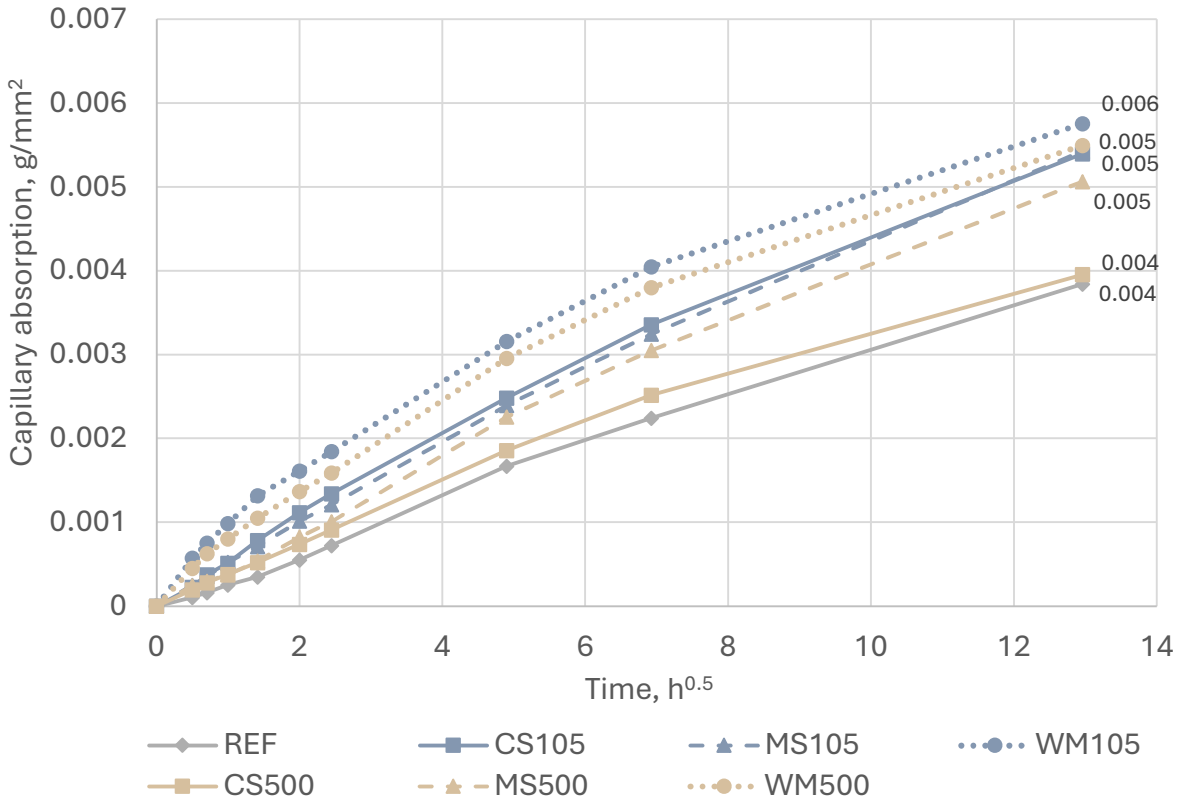

Fig. 5.4. Capillary absorption of mortars containing 20% demolition waste powders.

Fig. 5.5 compares absorption values after 7 days. It can be seen that the capillary absorption results align with the compressive strength test outcomes. Higher absorption corresponds to higher porosity, which in turn explains the lower mechanical strength observed in these specimens. These findings are consistent with the observations of Sun et al. [149] and Carriço et al. [252], who reported an increase in water absorption in cement mortar specimens with higher demolition waste powder content that correlated with compressive strength. They attributed this to the increased open porosity caused by the inherent porosity of the recycled concrete particles.

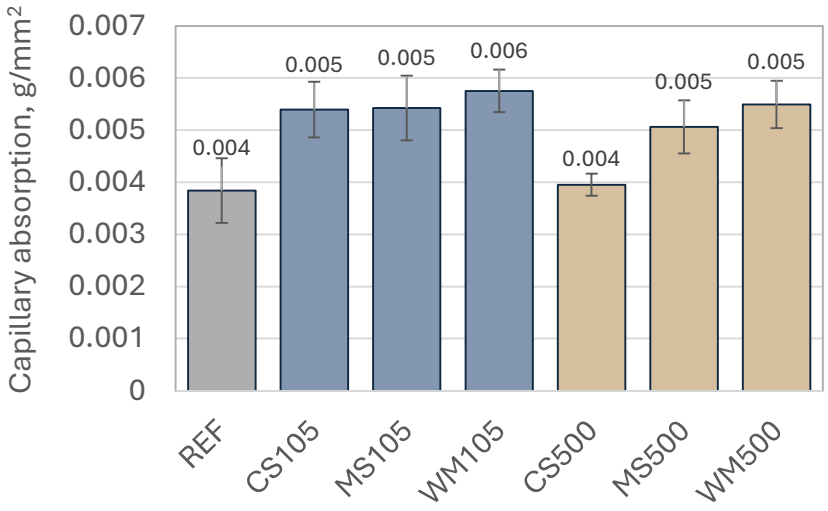

Fig. 5.5. Capillary absorption of mortars containing 20% demolition waste powders after 7 days of contact with water.

5.4.3. Drying shrinkage

Fig. 5.6 presents the drying shrinkage curves of cement mortar specimens over a 90-day period. The drying shrinkage of all specimens increased rapidly during the first 10 days, followed by a slower rate of increase over the next two months, ultimately stabilizing. The data indicate that specimens containing thermally activated powders exhibited lower shrinkage compared to those with non-calcined powders. Among the specimens, those containing MS demonstrated the lowest final shrinkage, even surpassing the reference sample, both before and after thermal activation. This observation aligns with findings from other researchers, who reported reduced drying shrinkage in specimens containing ceramic particles due to their pozzolanic activity [89, 259].

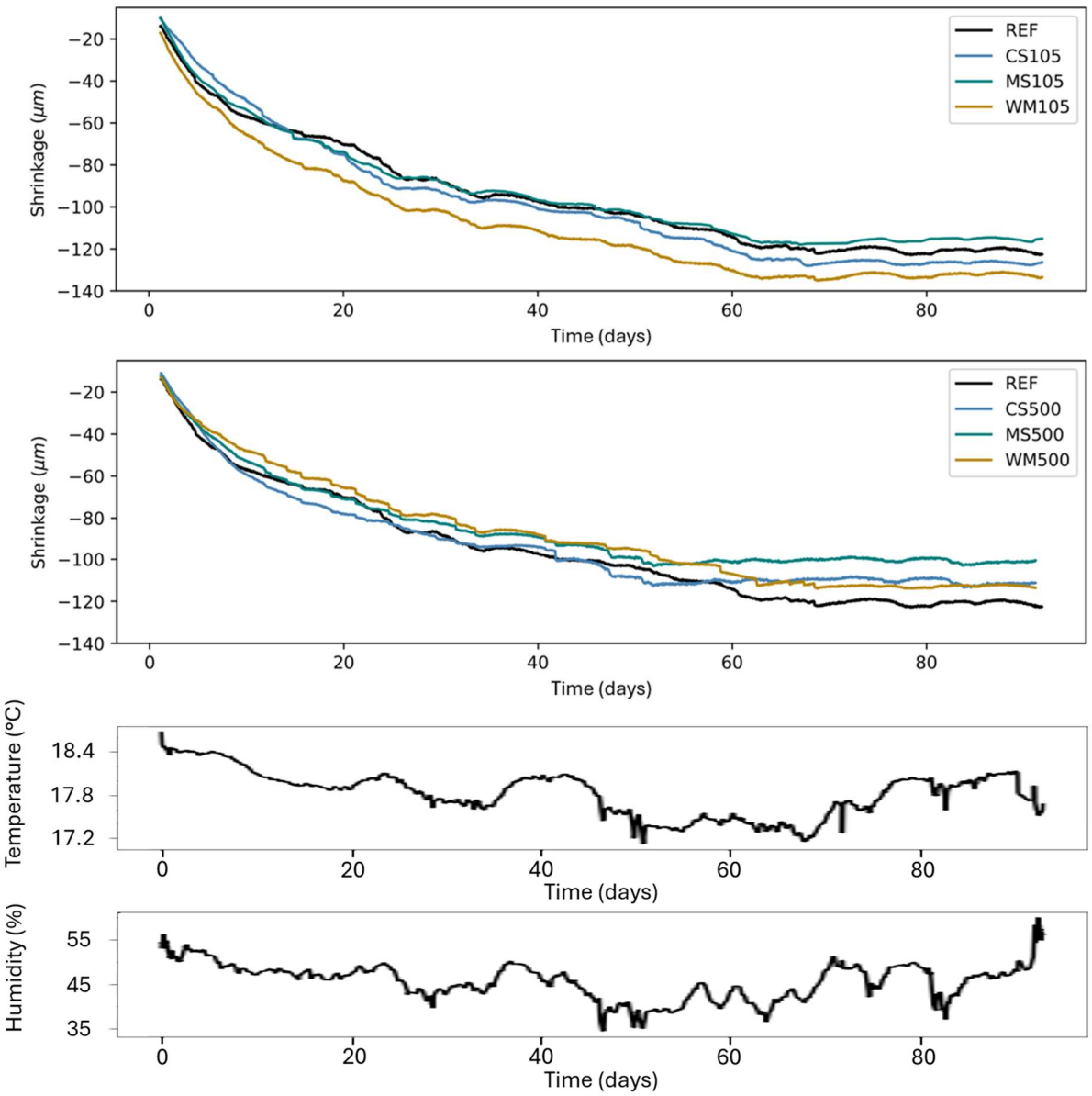

Fig. 5.6. Drying shrinkage of mortars containing 20% demolition waste powders.

At 90 days, the shrinkage values for CS105, MS105, and WM105 were 126 μm/m, 115 μm/m, and 134 μm/m, respectively. For CS500, MS500, and WM500, the values were 112 μm/m, 100 μm/m, and 112 μm/m, respectively. This reduction in shrinkage in mortars with thermally treated powders can be attributed to microstructural improvements resulting from the increased reactivity of the SCMs and the removal of organic impurities, as reported previously [254].

Interestingly, the REF specimens, despite lower capillary adsorption, exhibited higher drying shrinkage than those with thermally treated waste powders. Other researchers have found that drying shrinkage is more strongly related to pore size than to total pore volume. Zhang et al. [261] demonstrated that the smaller the pore diameter in a cementitious material, the higher its drying shrinkage. According to Schiller et al. [261], gel pores between C-S-H layers, which have no effect

on capillary absorption in cement materials, play the primary role in drying shrinkage. This suggests that incorporating partially dehydrated recycled cement containing C-S-H dehydration products different from Portland cement phases will affect shrinkage behaviour due to different morphology. Moreover, in a prior study on the investigated materials [254], it was shown that hydration products form within the larger pores of CS500, MS500, and WM500 samples, which may also contribute to reduced shrinkage in samples containing thermally activated powders.

5.4.4. Freeze-thaw resistance

The freeze-thaw resistance of cement mortar specimens was assessed by evaluating the mass loss (Fig. 5.7) and compressive strength loss (Fig. 5.8) after repeated freezing and thawing cycles. The results indicate that, overall, thermal activation of recycled powders does not significantly enhance the freeze-thaw resistance of the mortars. The mass loss was 1.07±0.02% for REF, 1.28±0.05%, 0.93±0.12% and 1.04±0.00% for CS105, MS105 and WM105, respectively, and 1.34±0.08%, 1.28±0.03% and 1.42±0.24% for CS500, MS500 and WM500, respectively. The strength loss values were 8.49±2.27%, 4.38±2.09% and 5.25±1.63% for specimens containing 20% of CS105, MS105 and WM105, respectively, while for samples incorporating CS500, MS500 and WM500, the strength loss values were 6.03±2.45%, 4.72±1.88% and 6.47±3.13%, respectively.

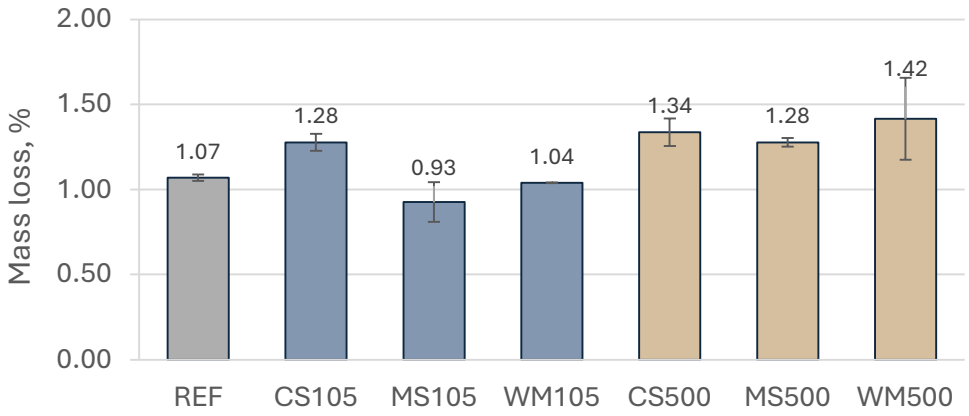

Fig. 5.7. Mass loss of mortars containing 20% demolition waste powders after 28 freeze-thaw cycles.

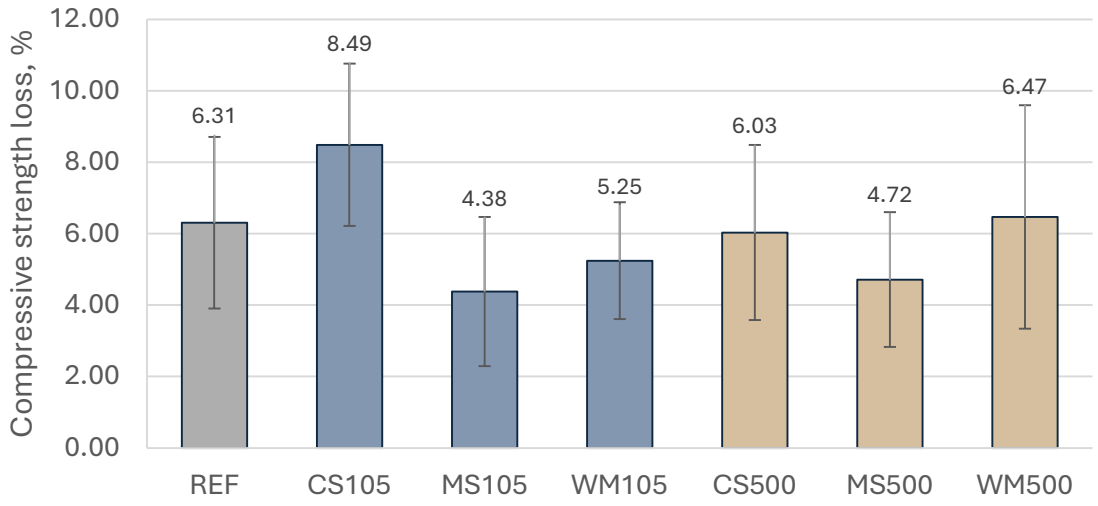

Fig. 5.8. Compressive strength loss of mortars containing 20% demolition waste powders after 28 freeze-thaw cycles.

A correlation between mass loss and strength loss is observed, as higher material degradation due to freeze-thaw cycles leads to a greater reduction in mechanical integrity. This relationship arises because mass loss results from surface scaling and microstructural damage, which in turn compromises the mortar's ability to bear loads. However, the variations in mass and strength loss among different specimens suggest that the composition of recycled powders influences the extent of deterioration.

Considering the associated measurement errors, it can be concluded that the freeze-thaw resistance of all specimens is comparable to that of the reference mortar, which exhibited a strength loss of 6.31±2.40%. Specimens containing MS105 and MS500 demonstrated slightly lower mass and strength losses after 28 freeze-thaw cycles, suggesting a potential positive influence of pozzolanic ceramic particles on the frost resistance of cement mortars.

Although freeze-thaw resistance is influenced by the open porosity of cement mortars, here no clear correlation is observed between the capillary absorption behaviour and the observed mass and strength losses. This suggests the involvement of additional parameters that significantly affect the frost resistance of the materials. As highlighted by Rhardane et al. [262], freeze-thaw resistance is also influenced by factors such as presence of ions in the pore solution and the composition of the cement paste. Furthermore, the pore size distribution plays a critical role, with larger pores contributing to improved freeze-thaw resistance by providing space for water expansion during freezing [263, 264]. As shown in Fig. 5.9, specimens MS105 and MS500, which exhibited the highest freeze-thaw resistance, contain the greatest number of macropores. Additionally, the thermal treatment of waste powders results in pore enlargement.

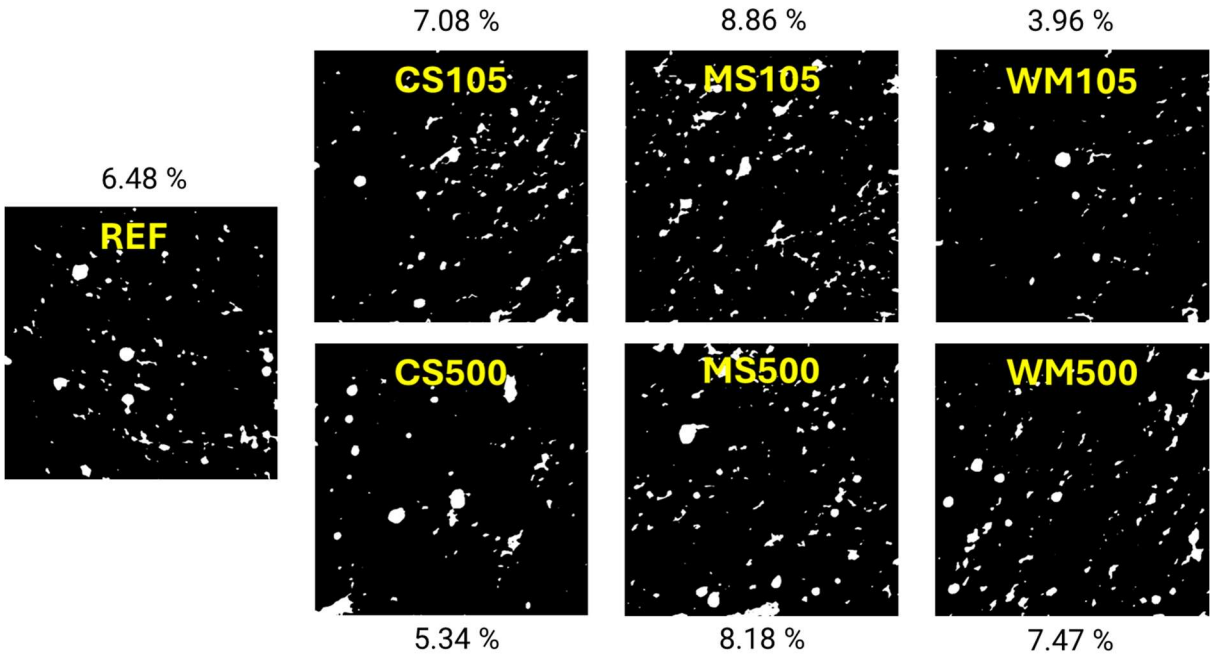

Fig. 5.9. Contrast-enhanced macropore distribution in mortars cross-sections.

5.4.5. Fire resistance

Fig. 5.10 illustrates the mass loss of the specimens after exposure to 200°C, 300°C, 500°C, and 900°C. At 200°C, all specimens exhibited a mass loss of less than 1%, mainly attributed to the decomposition of gypsum, ettringite, and partial degradation of the C-S-H gel, leading to water release. At 300°C, the continued decomposition of the C-S-H gel resulted in an approximate mass loss of 1% across all mortars. When fired at 500°C, the decomposition of the C-S-H gel persisted, accompanied by the initiation of portlandite decomposition, also involving water removal. At this stage, the specimens lost between 2.2% and 2.6% of their mass. Finally, at 900°C, the complete decomposition of both C-S-H gel and portlandite occurred, together with the decomposition of calcite with release of carbon dioxide. The mass loss at this temperature ranged from 4.6% to 5.0%. Overall, no significant differences were observed in the mass loss between the different mortar specimens.

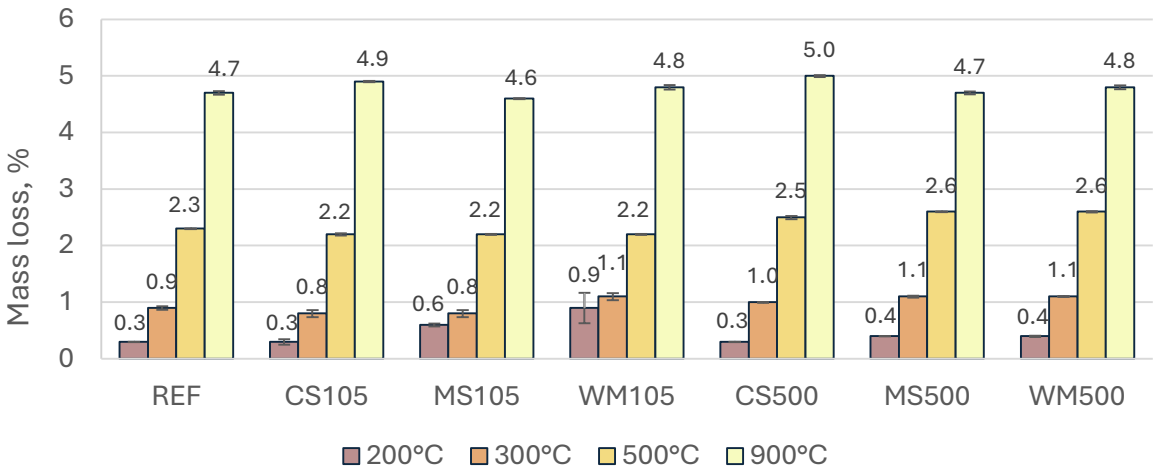

Fig. 5.10. Mass loss of mortars containing 20% demolition waste powders after firing at 200°C, 300°C, 500°C and 900°C.

Fig. 5.11 presents the compressive strength loss of the mortar specimens after exposure to 200°C, 300°C, 500°C, and 900°C. At 200°C, the change in strength was clearly dependent on the type of waste used in the cement mortar. Thus, the strength loss of specimens containing CS105 and CS500 was 7.8% and 3.9%, respectively, while specimens containing WM105 and WM500 showed strength gains of 5.6% and 14.4%, respectively. At 300°C, the strength of WM500-containing specimens increased by 6.0%, while all other specimens experienced a loss in strength ranging from 10.0% for MS500 to 22.0% for CS105. The strength gain in WM-containing specimens can be attributed to autoclave processes which forms calcium silicates and aluminates due to the higher content of pozzolanic oxides in WM (Table 1). In addition, WM powders contained fewer sulphates, which are prone to decomposition at these temperatures compared to MS.

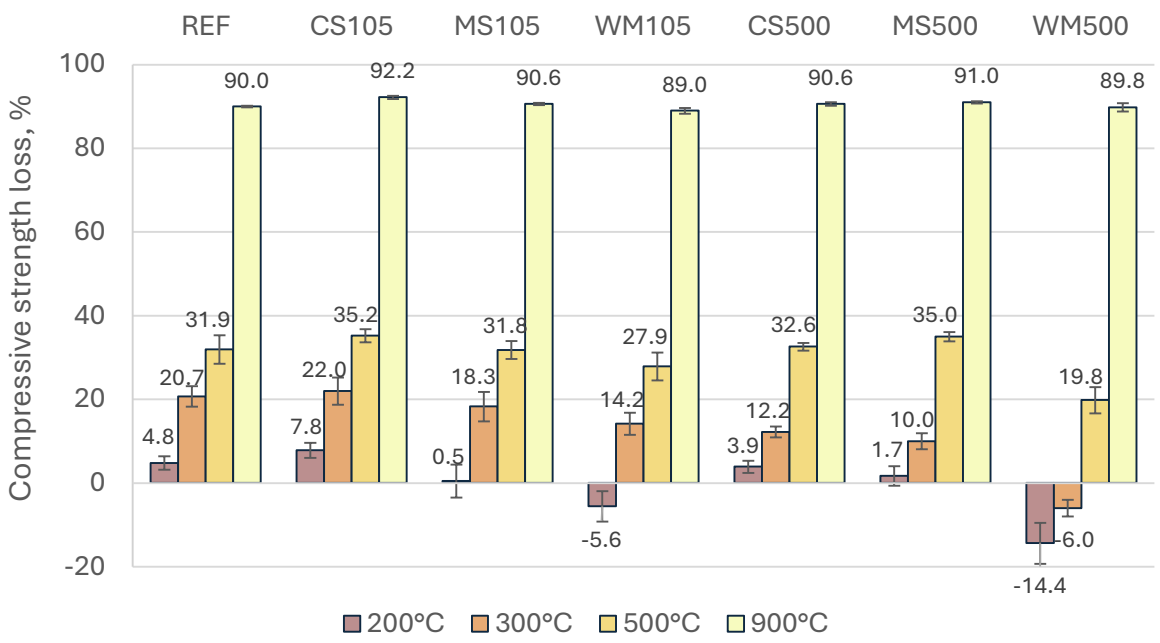

Fig. 5.11. Compressive strength loss of mortars containing 20% demolition waste powders after firing at 200°C, 300°C, 500°C and 900°C.

At 500°C, all specimens exhibited a compression strength loss. Mortars containing WM105 and WM500 had the lowest compression strength losses of 27.9% and 19.8% respectively, indicating better performance. Other specimens experienced strength losses ranging from 31.8% to 35.2%. At this temperature, visible cracks appeared on the surfaces of all mortar bars. After exposure to 900°C, almost all compressive strength was lost, with strength losses ranging from 89.0% for WM105 to 92.2% for CS105. The surfaces of the specimens were riddled with cracks, and white inclusions of free lime formed by the decomposition of portlandite and calcite were visible.

While mass loss is mainly associated with the decomposition of hydration products and the release of chemically bound water and carbon dioxide, strength loss is more strongly influenced by microstructural changes, crack formation, and phase transformations. The differences in strength loss between mortars, despite similar mass loss values, suggest that the composition of waste materials plays a significant role in determining mechanical stability at elevated temperatures, particularly through pozzolanic activity, sulphate content, and the formation of new cementitious phases during heating.

Specimens containing CS105 showed slightly lower fire resistance than the reference specimen. However, the results demonstrate an improved fire resistance in WM-containing mortars. This improved performance can be explained by the chemical and mineralogical composition of the waste:

– WM and MS contain muscovite, a refractory mineral.
– WM has a lower calcite content.
– WM has the highest content of pozzolanic oxides, and a lower sulphate content compared to MS.

Additionally, a correlation between fire resistance (Fig. 5.11) and capillary absorption (Fig. 5.5) can be observed. Indeed, porous materials provide better thermal insulation due to pores and voids filled with air, which is poor conductor of heat. The coefficient of thermal expansion (CTE) of the wastes used also plays an important role in the fire resistance of cement mortars [265, 266].

5.4.6. Sulfuric acid resistance

The resistance of mortar specimens to sulfuric acid corrosion was evaluated based on changes in mass (Fig. 5.12) and compressive strength loss (Fig. 5.13). Interestingly, all specimens gained mass after exposure, as also reported by Cao et al. [267]. The mass gain is primarily attributed to the reaction of calcium-containing compounds in cementitious materials with sulphate ions from sulfuric acid, forming gypsum ($CaSO_4 \cdot 2H_2O$) and ettringite ($3CaO \cdot Al_2O_3 \cdot 3CaSO_4 \cdot 32H_2O$) according to formulas (12) and (13). These compounds accumulate in the upper layer of the mortar, resulting in a mass increase.

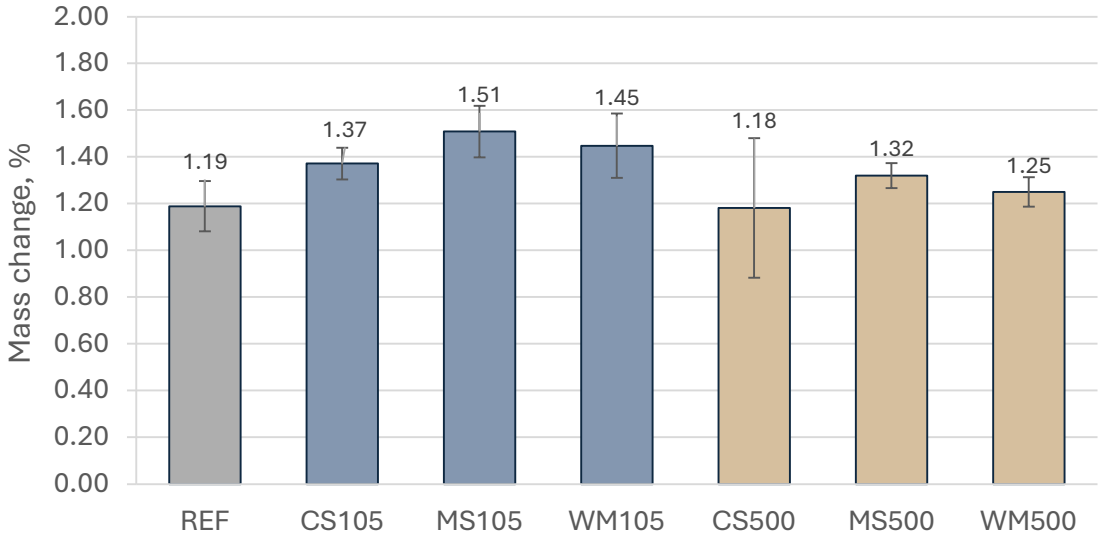

Fig. 5.12. Mass change of mortars containing 20% demolition waste powders after exposure to sulfuric acid solution.

$$Ca(OH)_2 + H_2SO_4 = CaSO_4 \cdot 2H_2O \quad (12)$$

$$3CaO \cdot Al_2O_3 \cdot 12H_2O + 3(CaSO_4 \cdot 2H_2O) + 14H_2O = 3CaO \cdot Al_2O_3 \cdot 3CaSO_4 \cdot 32H_2O \quad (13)$$

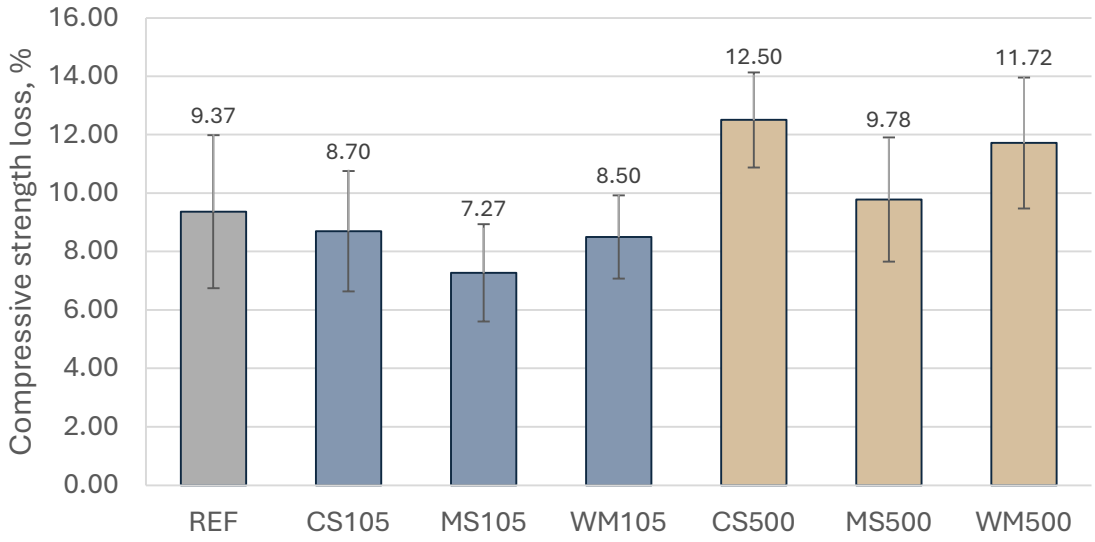

Fig. 5.13. Compressive strength loss of mortars containing 20% demolition waste powders after exposure to sulfuric acid solution.

The mass gain of specimens with recycled powders was comparable to the reference specimen (1.19%), with CS105, MS105, and WM105 showing mass increases of 1.37%, 1.51%, and 1.45%, respectively. Thermal treatment of the powders slightly reduced the weight gain, with CS500, MS500, and WM500 exhibiting gains of 1.18%, 1.32%, and 1.25%, respectively. However, change in mass alone is not a reliable indicator of corrosion resistance because it reflects both the addition of sulphate (SO_4^{2-}) and hydrogen (H^+) ions and the leaching of calcium (Ca^{2+}) and aluminium (Al^{3+}) ions from the mortar, as highlighted by Cao et al. [266] and Khan et al. [268]. The extent of these processes also depends on the acid concentration and immersion duration. The higher the concentration of sulfuric acid and the longer the exposure time, the greater the leaching processes and the degradation of the cement material [269 - 271].

Compressive strength loss provided a clearer picture of the acid resistance of the mortars. Specimens containing uncalcined waste powders exhibited slightly lower strength loss than the reference mortar (9.37%), with CS105, MS105, and WM105 showing losses of 8.70%, 7.27%, and 8.50%, respectively. In contrast, thermal treatment increased the sensitivity of the mortars to acid attack, resulting in higher strength losses for CS500, MS500, and WM500 (12.50%, 9.78%, and 11.72%, respectively). This heightened sensitivity is likely due to increased reactivity of the reactivated powders combined with the relatively higher porosity of the mortars and the formation of additional C-S-H gel during hydration, as reported in prior study [254].

Interestingly, an inverse relationship between mass gain and strength loss was observed, with specimens exhibiting higher mass gain tending to retain more compressive strength. This can be attributed to the formation of gypsum and ettringite, which, despite their expansive nature, partially fill voids in the upper layers and temporarily limit further acid penetration into the material.

Among all specimens, those containing MS powders showed the lowest loss of strength despite having the highest mass gain. This behaviour can be attributed to the chemical inertness of the ceramic particles in MS mortars. Ceramic particles, consisting of crystalline or semi-crystalline aluminosilicates, are highly stable in acidic environments, unlike more reactive cement phases such as calcium hydroxide and C-S-H gel. The inert ceramic particles resist dissolution when exposed to sulfuric acid, thereby minimizing internal degradation.

Thus, the acid reacts with calcium-bearing phases in the surrounding cement paste, leading to localized formation of gypsum and ettringite near the surface or in voids. These expansive reaction products increase the specimen's mass due to their high molecular weight and cause the structural damage of the surface layers. The presence of ceramic particles in the cement matrix reduces overall the reactivity and improves the resistance to acid penetration. This explains why MS mortars exhibit superior performance under acidic conditions, with lower strength loss and mass changes compared to other specimens.

5.4.7. Statistical analysis

The statistical approach of multifactor Analysis of Variance (ANOVA) helps in examining the relationships between multiple factors and dependent variables. In this study, ANOVA was applied to evaluate how freeze-thaw resistance, fire resistance and resistance to H_2SO_4 corrosion were influenced by four independent factors: waste type, thermal treatment of waste, capillary adsorption and shrinkage. This method is particularly advantageous for assessing differences across multiple groups and for minimizing the influence of random errors. The results of statistical analysis, conducted using R software, are presented in Table 5.3. The p-values highlight the degree of significance for each factor's effect on durability properties, with values below 0.05 indicating statistically significant dependencies.

Table 5.3. ANOVA results.

Dependent Variable	Independent Factor	Sum Sq[1]	Mean Sq[2]	F-value[3]	p-value[4]
Freeze-thaw resistance	Waste type	25.07	12.53	4.92	**0.033**
	Thermal treatment	0.32	0.32	0.13	0.732
	Capillary adsorption	19.42	19.42	7.62	**0.020**
	Shrinkage	4.91	4.91	1.93	0.195
Fire resistance	Waste type	$4.88 \cdot 10^{11}$	$2.44 \cdot 10^{11}$	12.91	**0.002**
	Thermal treatment	$8.83 \cdot 10^{8}$	$8.83 \cdot 10^{8}$	0.05	0.833
	Capillary adsorption	$3.31 \cdot 10^{11}$	$3.31 \cdot 10^{11}$	17.51	**0.002**
	Shrinkage	$1.30 \cdot 10^{9}$	$1.30 \cdot 10^{9}$	0.07	0.798
H_2SO_4 resistance	Waste type	16.37	8.18	3.91	*0.056*
	Thermal treatment	40.68	40.68	19.43	**0.001**
	Capillary adsorption	1.22	1.22	0.58	0.463
	Shrinkage	7.81	7.81	3.73	*0.082*

[1]Sum Sq (Sum of Squares) – the total variation in the dependent variable explained by each independent factor.

[2]Mean Sq (Mean Square) – the Sum of Squares divided by the degrees of freedom, representing the average variation caused by each factor.

[3]F-value – the ratio of the Mean Square of the factor to the Mean Square of the residual error, used to determine statistical significance.

[4]p-value – the probability of obtaining the observed results under the null hypothesis.

After conducting ANOVA to identify significant differences among group means (waste types), Tukey's post hoc test (Table 5.4) was employed to determine which specific group pairs differed significantly. While ANOVA identifies whether there is a significant effect of a factor overall, it does not indicate which groups differ from each other. This test controls for Type I error across multiple comparisons by adjusting p-values, ensuring robust and reliable results.

Table 5.4. Tukey post hoc test results.

Dependent Variable	Comparison	Difference[1]	Lower CI[2]	Upper CI[3]	p-value[4]
Freeze-thaw resistance	MS – CS	-2.89	-5.41	-0.36	**0.026**
	WM – CS	-1.54	-4.07	0.98	0.262
	WM – MS	1.35	-1.18	3.87	0.350
Fire resistance	MS – CS	-298864.2	-516467.2	-81261.3	**0.009**

Dependent Variable	Comparison	Difference[1]	Lower CI[2]	Upper CI[3]	p-value[4]
	WM – CS	-383975.7	-601578.6	-166372.8	**0.002**
	WM – MS	-85111.5	-302714.4	132491.5	0.551
H_2SO_4 resistance	MS – CS	-2.24	-4.53	0.05	*0.055*
	WM – CS	-0.55	-2.84	1.74	0.794
	WM – MS	1.69	-0.60	3.98	0.156

[1]Difference – the mean difference between the two groups.

[2]Lower CI (Lower Confidence Interval) – the lower bound of the confidence interval for a 95% confidence level.

[3]Upper CI (Upper Confidence Interval) – the upper bound of the confidence interval for a 95% confidence level.

[4]p-value – the probability of observing the obtained results under the null hypothesis.

For freeze-thaw resistance, both factors, the waste type (p=0.033) and the capillary adsorption (p=0.020), exhibited statistically significant effects, while the factor thermal treatment (p=0.732) had no statistically significant impact. Post hoc analysis further identified a significant difference between MS and CS (p=0.026), suggesting that the freeze-thaw resistance of MS-based specimens is superior. However, no significant differences were observed between WM and the other types.

Similarly, for fire resistance, waste type (p=0.002) and capillary adsorption (p=0.002) demonstrated highly significant effects, while thermal treatment (p=0.833) had no statistically significant impact. Post hoc analysis revealed that CS exhibited significantly lower fire resistance compared to MS (p=0.009) and WM (p=0.002), while no significant difference was observed between WM and MS.

In terms of resistance to H_2SO_4 corrosion, thermal treatment (p=0.001) was found to have a highly significant influence, while waste type (p=0.056) showed a near-significant trend. Capillary adsorption (p=0.463) did not exhibit a statistically significant effect. Tukey post hoc comparisons showed no significant differences between the waste types, although MS and CS approached significance (p=0.055), indicating a potential difference.

Shrinkage did not exhibit a statistically significant effect on any of the analysed durability parameters. The dependence on drying shrinkage was not revealed in this experiment, likely because the mechanisms of resistance to temperature changes and acids are complex and depend on more factors than just microcracks. Other parameters, such as differences in hydration products and macroporosity, appear to play a greater role in influencing durability under the conditions tested. It is possible that with longer test durations, the influence of shrinkage-related cracking would become more apparent.

5.5. Conclusions

The study investigated the effects of incorporating thermally activated and non-activated demolition wastes as SCMs in cement mortars on durability properties, including freeze-thaw resistance, sulfuric acid resistance and fire resistance. Based on the findings, the following conclusions can be drawn:

(1) The reference specimen showed the lowest capillary absorption, while thermal activation reduced this parameter in all specimens, with a smaller effect observed in those containing MS and WM compared to CS.

(2) Thermal activation of waste powders reduced the drying shrinkage of mortar specimens. The REF specimen exhibited higher drying shrinkage compared to those containing thermally activated waste powders, likely due to the presence of gel pores in the C-S-H gel matrix and the growth of hydration products in the larger pores of mortars with rehydrated waste powders.

(3) Thermal activation of recycled powders had no significant effect on the frost resistance of mortars, whereas the type of waste material did. No visually clear correlation was observed between capillary absorption and freeze-thaw resistance, suggesting the involvement of additional influencing factors. However, statistical analysis confirmed a significant dependence of freeze-thaw resistance on both the waste type and capillary absorption, while thermal treatment showed no statistically significant impact.

(4) Fire resistance was strongly influenced by the type of waste used in the cement mortar and porosity, but it was not affected by the thermal treatment of the waste. Mortars containing WM exhibited the highest fire resistance, attributed to the chemical and mineralogical composition of the waste.

(5) Thermal activation of waste powders reduced the sulfuric acid corrosion resistance of the mortars due to the increased reactivity of the activated powders.

Overall, the findings demonstrate that the type of waste has a significant impact on the durability properties of cement mortars. Specimens containing ceramic particles consistently outperformed those with pure concrete waste and even the reference mortar, underscoring their potential as a sustainable alternative in cementitious materials production. The influence of capillary absorption on both freeze-thaw and fire resistance highlights the critical role of porosity and air voids in improving thermal insulation. However, thermal treatment of the wastes did not

improve the durability of the mortars and, in the case of sulfuric acid resistance, actually reduced it.

While this research does not delve into the detailed processes occurring under the influence of aggressive environmental factors, it provides valuable insights into the potential durability of cement materials containing different CDWs. However, a more detailed investigation into the mineralogical and microstructural changes during heating, cooling and acid expose is required for a definitive explanation of the research findings.

Chapter 6: Durability assessment of cement mortars with recycled ceramic powders

Abstract

Although substantial knowledge exists regarding the use of ceramic powders as pozzolanic supplementary cementitious materials, a notable gap remains in the literature concerning the durability properties of cement with ceramics. This research aims to address this gap by evaluating the effects of ceramic powders on mortar durability, specifically focusing on resistance to freeze–thaw, high temperatures and 1 % sulphuric acid. The study also investigates the use of recycled ceramic demolition waste as a replacement for calcined clay in Limestone Calcined Clay (LC3) formulations. This research demonstrates the potential of using ceramic waste to enhance mortar durability. The results show significant improvements in freeze-thaw resistance, with strength losses of 1.91% to 2.61% for modified mortars, compared to 6.31% for the reference mortar. Fire resistance also improves, with strength gains of up to 13.9% at 200°C for LC3 mortars with ceramic powder. At 500°C, strength losses ranged from 2.8% to 31.9%, with ceramic-containing mortars showing better performance than the reference. At 900°C, substantial strength losses occurred across all mixes (72.0% to 90.0%), with mortars containing ultrafine ceramic powder showing the best resistance. Resistance to 1% sulphuric acid is enhanced, with strength losses decreasing from 9.37% in the reference mortar to 1.38% in LC3 mortar with ceramic powder.

6.1. Introduction

6.1.1. Literature review

The utilisation of binders incorporating ceramic powder as a pozzolanic component has a long historical precedent, with evidence tracing back to ancient civilisations. In Ancient Rome lime-based mortars mixed with ground ceramic materials, particularly brick dust, were extensively

employed in construction. This practice was especially widespread in regions where natural pozzolanic materials, such as volcanic ash, were scarce or unavailable [92, 272].

Numerous studies confirm the pozzolanic properties of ceramic powders and support their suitability as supplementary cementitious materials (SCMs) for the production of CO_2-reduced cements. For instance, Partarch et al. [91] measured the amount of lime fixed by cement pastes containing 25 wt.% ceramic bricks, tiles, and sanitary ware, and confirmed the superior pozzolanic activity of bricks compared to other ceramic materials. Silveira et al. [273] confirmed the pozzolanic nature of waste sanitary ware using isothermal calorimetry, thermogravimetric analysis, electrical conductivity, and strength activity index. Kannan et al. [274] applied the Frattini test to cements containing 20% and 40% waste ceramics, demonstrating their pozzolanic reactivity at both 28 and 90 days. The study by Gonçalves et al. [275] reported lower strength in mortars containing brick powder compared to those with metakaolin at the same packing density, leading to the conclusion that brick powder has lower pozzolanic activity. Although the pozzolanic reactivity of ceramic powders is generally lower than that of conventional calcined clays such as metakaolin, it remains comparable to that of fly ash, which is widely used as a pozzolanic SCM in blended cements. Thus, Pang et al. [276], after testing the pozzolanic properties of ceramic polishing powder, fly ash, and blast furnace slag using the Rapid, Reliable, and Relevant (R3) method in accordance with ASTM C1879–20, observed a similarity in pozzolanic activity between ceramics and fly ash.

Experimental investigations have demonstrated that the partial replacement of ordinary Portland cement (OPC) with finely ground ceramic waste enables the development of more sustainable binders with reduced environmental impact. Most research indicates that the optimal replacement level is in the range of 20 – 25 % by mass. At this dosage, the compressive strength of mortars and concretes incorporating ceramic powders tends to match or surpass that of conventional OPC-based materials, though this improvement is typically observed only at later curing ages, beyond 28 days. Thus, Ebrahimi et al. [259] investigated the strength development of mortars with ceramic waste powders at 28, 56, and 90 days, and observed an increase in strength compared to OPC when the cement replacement rate was up to 20%. Faldessai et al. [277] found that the maximum 28-day compressive strength of concrete containing ceramic waste was achieved at a replacement rate of 25 %, resulting in a 14.89 % reduction in production cost compared to ordinary concrete. El-Dieb and Kanaan [278] proposed an optimal substitution rate of 10–20 % for the best balance between strength and workability, but noted that higher ceramic powder content is required to improve durability. However, Pang et al. [276] concluded that the

inclusion of more than 25 % ceramic powder increases autogenous shrinkage, which may negatively affect durability.

Microstructural analyses have shown that the inclusion of ceramic powders enhances the density and compactness of the cementitious matrix. Silveira et al. [273], Kannan et al. [274] and Tremiño et al. [279] attribute the improvement to both the formation of additional calcium silicate hydrate (C–S–H) through pozzolanic reactions and the filler effect, in which fine ceramic particles occupy voids within the paste, resulting in pore refinement. As a result, mortars and concretes containing ceramic powders typically exhibit reduced total porosity and improved microstructural integrity, which in turn enhance their mechanical performance and durability.

While numerous studies have explored the rheological and mechanical behaviour of cements incorporating ceramic powders as SCMs, research on their durability performance remains limited. The available literature is sparse, offering only insights into a narrow range of durability aspects. In particular, most of the existing studies focus almost exclusively on permeability and resistance to chloride ingress, with virtually no attention given to other critical durability parameters.

Meena et al. [280], in their review, cite only a limited number of studies investigating the durability of cements containing ceramic powders as SCMs. Moreover, these few studies predominantly focus on permeability and resistance to chloride ingress, while other essential aspects of durability are largely neglected. In particular, no research has been reported on the performance of ceramic-SCM systems under extreme temperature conditions, such as high-temperature exposure or freezing. One of the few available studies addressing thermal durability is that of AlArab et al. [281], who performed freeze–thaw resistance tests on mortars incorporating porcelain powder. Their results indicated a reduction in frost resistance with increasing porcelain powder content, which they attributed to an increase in the overall porosity of the mortar matrix. Conversely, Kulovaná et al. [282] observed very good frost resistance in samples containing ceramic powder. These differences in results may stem from the types of ceramics used. The porcelain is fired at higher temperatures than the bricks and roof tiles studied by Kulovaná et al., which promotes the recrystallization of metakaolin into mullite. This transformation reduces pozzolanic activity, resulting in a less dense matrix and lower freeze–thaw resistance.

All durability studies conducted to date have consistently shown that the incorporation of ceramic powders in cementitious materials leads to improved resistance to chemical aggression. El-Dieb et al. [278] found that the addition of 40% ceramic powder reduced chloride ion penetration at 28 days by 83% compared to ordinary concrete. Kannan et al. [274] obtained

similar results, reporting an 89% reduction in chloride penetration at 28 days with a 40% replacement level. The results of Wang et al. [283] indicate that a 40% ceramic powder content reduces chloride penetration at 28 days by approximately 72%. Chen et al. [194], however, reported a 27.3% reduction in chloride penetration at a 10% substitution rate, with lower effectiveness observed at higher replacement levels. Tremiño et al. [279] reported a noticeable decrease in chloride diffusion after 4 years in mortar containing 20% brick powder compared to OPC mortar. including chlorides. Kulovaná et al. [282] reported excellent resistance of concrete containing 20% ceramic powder to magnesium and ammonium chloride solutions with concentrations of 17.76 and 2.97 g/L, respectively, as well as to a sodium sulphate solution (14.79 g/L) and a hydrochloric acid solution (10^{-3} mol/L). Zita et al. [284] demonstrated that concrete containing 24% ceramic powder exhibited a ≥48% reduction in the chloride diffusion coefficient compared to Portland cement concrete and showed good performance against sulphate attack in a 0.352 mol/L Na_2SO_4 solution. Mohammadhosseini et al. [285] investigated cement mortars incorporating 40% ceramic powder as a cement replacement and 100% recycled ceramic fine aggregate. After 18 months of curing in a 5% NaCl solution, the average penetration depth in the ceramic-containing mortar was 67% lower compared to that in OPC mortar. Exposure to a 5% Na_2SO_4 solution for up to 18 months resulted in compressive strength reductions of 41.1% and 16.8% for OPC and ceramic mortars, respectively.

According to the cited sources, this enhanced durability is primarily attributed to the improvement in the microstructure of the cement matrix, particularly the refinement of the pore structure. Additionally, the improved resistance to chemical attacks is also explained by the reduced presence of portlandite ($Ca(OH)_2$) in the system due to its consumption during pozzolanic reactions. Ikotun et al. [286], in their review, highlight the limited research on the durability of cementitious materials incorporating ceramic SCMs. However, the available studies indicate that durability properties are improved due to matrix densification resulting from pozzolanic reactions.

Recently, considerable attention has been paid to ternary calcined clay–limestone–cement (LC3) binders, developed by the EPFL research team (Switzerland) and successfully tested in industrial trials in Cuba and India [39]. Mañosa et al. [287] conducted an extensive bibliographic analysis, highlighting the growing interest in LC3 research. This blended cement formulation, combining Portland cement with metakaolin and limestone filler, is attractive due to its excellent chemical resistance and potential for significant energy savings and reduced CO_2 emissions as noted by Ijas et al. [288] and by Sharma et al. [289] in their extensive reviews.

While ceramic powders have been extensively studied in binary cement systems, their application in ternary LC3 systems remains largely unexplored. Binary systems (cement + ceramic and cement + limestone) typically show improvement in mechanical properties at relatively low cement replacement rate, whereas ternary LC3 systems (cement + ceramic + limestone) offer potential improvement at higher replacement through synergetic effect and calcium carboaluminates formation [206]. However, no studies have directly compared the durability performance of these two approaches.

De Matos et al. [290] investigated the rheological and mechanical properties of LC3 in which natural calcined clay was partially or completely replaced by ceramic waste powder. The results showed that the ceramic powder exhibited reactivity, albeit less than that of natural calcined clay. The formulations containing ceramic powder demonstrated slightly lower strength but improved flowability compared to those with calcined clay. Overall, both partial and complete replacement of natural calcined clay with ceramic waste powder proved to be an effective strategy for controlling the rheological properties of fresh LC3 and produced cements that met standard strength classes.

Mohit et al. [206] explored the mechanical strength and ASR of cement-ceramic-limestone mixtures. The optimal formulation of 65% cement, 20% ceramic powder, and 15% limestone filler showed compressive strengths within about 3% of the reference OPC mortar at all curing ages, while reducing ASR expansion by approximately 55%.

Marangu [291] examined the effects of 3% sulphuric acid attack on hydrated LC3 cement mortars containing 30% waste ceramic bricks as a substitute for calcined clay and 15% limestone filler. The study concluded that LC3 cement using waste ceramic bricks demonstrated improved mechanical properties and markedly higher resistance to sulphuric acid attack compared to OPC.

6.1.2. Scope, novelty and relation to previous work

As shown in the literature review, existing studies on the durability of blended cements with ceramic SCMs have primarily focused on chemical resistance, especially chloride penetration, while the effects of extreme temperatures remain largely unexplored. A similar gap exists for LC3 systems, and no published studies appear to have examined the durability of ternary cement–ceramics–limestone filler systems.

The present study addresses this gap by evaluating the durability of mortars with reduced Portland cement clinker content through the incorporation of recycled ceramics used both as pozzolanic SCM in binary systems and as substitute for calcined clay in LC3-type binders. The work focuses on durability criteria that are underrepresented in the literature for ceramic waste binders, including freeze–thaw resistance, thermal degradation, and sulphuric acid attack. It also provides a direct comparison between binary and LC3-type mortars, an approach rarely found in existing research. Furthermore, the study adapts the LC3 concept by substituting recycled ceramic demolition waste for industrial calcined clay, offering a more practical and energy-efficient alternative.

This work forms part of a larger project on the valorisation of demolition wastes as SCMs. It is related the earlier study [292], which investigated pozzolanic activity, microstructure, rheology and mechanical properties of mortars with waste terracotta and sanitary porcelain powders. In this study, only terracotta powder was considered, because, unlike porcelain, it exhibited significant pozzolanic activity and enhanced mortar strength. Both particle size fractions, <125 µm and <63 µm, demonstrated good performance, with an optimal cement replacement level of 20%, which was selected for further investigation. The current paper provides original durability data, which are critical for assessing the feasibility of these binders in practice, given that low durability and incapacity to resist aggressive environments can lead to premature structural failure.

While some basic material property data from [292] are repeated for context in Materials and Method section, all durability test results given in Results and Discussion section and related interpretations in this work are original. This separation was necessary to maintain focus and ensure that each paper met the length and scope expectations of a research article, while together they provide a comprehensive assessment of ceramic waste as a sustainable SCM.

This research demonstrates a circular economy approach to construction materials, where end-of-life ceramic products from demolition are transformed into value-added supplementary cementitious materials, simultaneously addressing waste management challenges and cement industry decarbonization.

6.2. Materials and methods

6.2.1. Materials

Ceramic roof tile waste was recovered from a landfill site located in Luxembourg. To simulate a process with minimal environmental impact and energy consumption, the waste was not pre-treated and was dried under natural conditions. The collected material was initially reduced to fragments of approximately 30 mm using a hammer and further processed with a jaw crusher to reduce particle size. Subsequently, the material was subjected to dry grinding in an impact mill fitted with a 2 mm mesh bottom screen. Two granulometric fractions were then prepared by sieving: particles passing through a 125 µm mesh were classified as fine ceramic powder (RT), while those passing through a 63 µm mesh were designated as ultrafine ceramic powder (RTU).

In addition to the processed ceramic waste, the materials employed in the mortar specimens design included Portland cement CEM I 52.5 R and limestone filler (LF), as well as CEN Standard Sand in accordance with EN 196-1 [150], and tap water. CEM I 52.5 R was selected because it contains no additives other than gypsum and provides rapid strength development, making it suitable for laboratory investigations. The physical properties of the powdered raw materials and pozzolanic activity of ceramic powders measured by Chapelle test are presented in Table 6.1. The granulometric composition of the used materials are given in the Fig. 6.1. All these data were previously assessed in detail in the earlier study and are presented here for context, serving as a reference point for interpreting the observed durability performance of mortars containing terracotta powder.

Table 6.1. Physical properties and pozzolanic activity of the powdered materials [292].

Property	CEM I	RT	RTU	LF
Specific gravity (g/cm^3)	3.05	2.42	2.42	2.70
Blaine SSA (cm^2/g)	5418	5239	6249	10465
$Ca(OH)_2$ fixed (mg/g)*	-	505	618	-

CEM I – cement; RT – fine terracotta powder; RTU – ultrafine terracotta powder; LF – limestone filler; SSA – specific surface area.

*The minimum fixed $Ca(OH)_2$ value indicating pozzolanic properties is 436 mg/g of material [165]; for metakaolin, the minimum value is 700 mg/g [207].

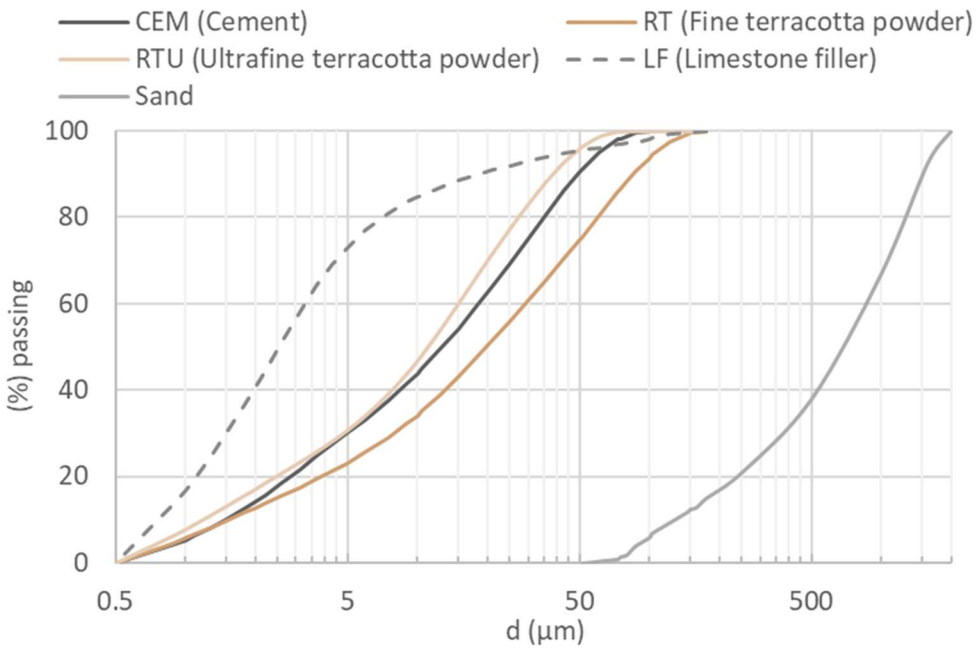

Fig. 6.1. Particle size distribution of the used materials [292].

The ceramic waste exhibited a combined content of silica, alumina, and iron oxides amounting in sum to 76.72%, exceeding the minimum threshold of 70% specified by the ASTM C618 [208] standard for pozzolanic materials. The complete chemical composition of the waste terracotta, cement, and limestone is provided in Table 6.2.

Table 6.2. Chemical composition in mass-% of the powdered materials [292].

Oxide	CEM I	Terracotta	Limestone
SiO_2	16.07	50.64	8.54
Al_2O_3	3.91	17.66	1.96
Fe_2O_3	3.58	8.42	1.06
CaO	66.72	10.32	47.68
MgO	1.45	1.51	1.81
TiO_2	0.37	1.08	0
MnO	0.08	0.19	0
Na_2O	0.26	0.39	0.12
K_2O	1.18	3.37	0.37
P_2O_5	0.39	0.23	0

Oxide	CEM I	Terracotta	Limestone
SO_3	3.88	3.28	0.1
*LOI **	2.10	2.90	38.36

* Loss on ignition at 950 °C

The main mineralogical phases of the waste ceramics were predominantly presented by quartz, feldspars, and an amorphous phase. The minor phases were presented by hematite and gypsum [292].

6.2.2. Packing density

To assess the particle packing density of cement mortars, a modified Andersen and Andersen (A&A) method was employed [293]. This approach evaluates how closely the particle size distribution (PSD) of the studied mixture approximates an ideal theoretical distribution that provides maximum packing density.

First, the cumulative PSD of each mortar mixture was calculated from the weighted contributions of its individual components given in the Figure 1 according to the following equation:

$$P_i^{Mixture} = \frac{a \cdot P_i^{CEM} + b \cdot P_i^{RT} + c \cdot P_i^{RTU} + d \cdot P_i^{LF} + e \cdot P_i^{Sand}}{a+b+c+d+e}, \quad (14)$$

where Pi is the cumulative percentage of particles corresponding to point i (CEM is cement; RT is fine terracotta powder; RTU is ultrafine terracotta powder; LF is limestone filler); a, b, c, d are the mass fractions of the corresponding components in the binder (a+b+c+d=1); e is the mass fraction of sand in the total mixture (e=3).

The ideal PSD was then generated using the A&A model:

$$P_i^{Ideal} = \frac{D_i^q - D_{min}^q}{D_{max}^q - D_{min}^q} \cdot 100, \quad (15)$$

where Di is the particle size corresponding to point i; Dmin and Dmax are the minimum and maximum particle sizes in the system; q is the distribution modulus. In this study, q=0.37 was used, consistent with values reported in the literature for achieving optimal packing [294-296].

To evaluate the packing quality of the mortar mixtures, the degree of similarity S between the real PSD and the ideal PSD was calculated using the following equation:

$$S = \frac{1}{n}\sum_{i=1}^{n}\left(1 - \frac{\left|P_i^{Ideal} - P_i^{Mixture}\right|}{P_i^{Ideal}}\right), \quad (16)$$

where n is the number of particle size intervals considered.

A similarity score S closer to 1 indicates that the particle size distribution of the mixture closely matches the ideal distribution, suggesting higher packing density.

6.2.3. Preparation of mortar specimens

Experimental testing was carried out on 40 × 40 × 160 mm prismatic mortar specimens prepared in accordance with ISO 679:2009 [152]. All mixes were designed with constant water-to-binder and sand-to-binder ratios of 0.5 and 3.0, respectively. In the reference and ceramic powder-based mortars, 20% of the Portland cement was replaced by mass. For the LC3-type formulations, a 30% binder replacement was adopted, consisting of 20% terracotta powder combined with 10% limestone filler. Mortar constituents were mixed in a laboratory mixer following the sequence specified in ISO 679:2009. The fresh mortar was placed in oiled prismatic moulds in two layers, each compacted using a jolting table. After casting, the moulds were covered with a glass sheet for 24 hours, after which the specimens were demoulded, covered with a plastic film to prevent moisture loss, and stored at 20 °C for 28 days before testing.

The full mix proportions and mean compressive strength of mortars at 28 and 90 days of curing are presented in Table 6.3. The compressive strength of the mortars was previously assessed in detail in the earlier study and is presented here for context, serving as a reference point for evaluating strength losses after the durability tests. The specimens preparation flowchart is shown in Fig. 6.2.

Table 6.3. Mix designs, fresh densities and compressive strength of mortars [292].

Mix	CEM I (kg/m^3)	RT (kg/m^3)	RTU (kg/m^3)	LF (kg/m^3)	Sand (kg/m^3)	Water (kg/m^3)	ρ_{fresh} (kg/m^3)	f_{cm},28d (MPa)	f_{cm},90d (MPa)
REF	475	0	0	0	1426	238	2139	60.2	65.9
RT	371	93	0	0	1390	232	2084	51.8	64.2
RTU	378	0	94	0	1417	236	2125	54.5	68.2
LRT	323	92	0	46	1384	231	2075	44.0	53.7
LRTU	322	0	92	46	1380	230	2070	47.7	63.9

Columns: CEM I – cement; RT – fine terracotta powder; RTU – ultrafine terracotta powder; LF – limestone filler; ρ_{fresh} – density of the fresh mortar; f_{cm},28d – mean compressive strength at 28 days of curing; f_{cm},90d – mean compressive strength at 90 days of curing.
Rows: REF – reference mortar; RT – mortar with fine terracotta powder; RTU – mortar with ultrafine terracotta powder; LRT – LC3 mortar with fine terracotta powder; LRTU – LC3 mortar with ultrafine terracotta powder.

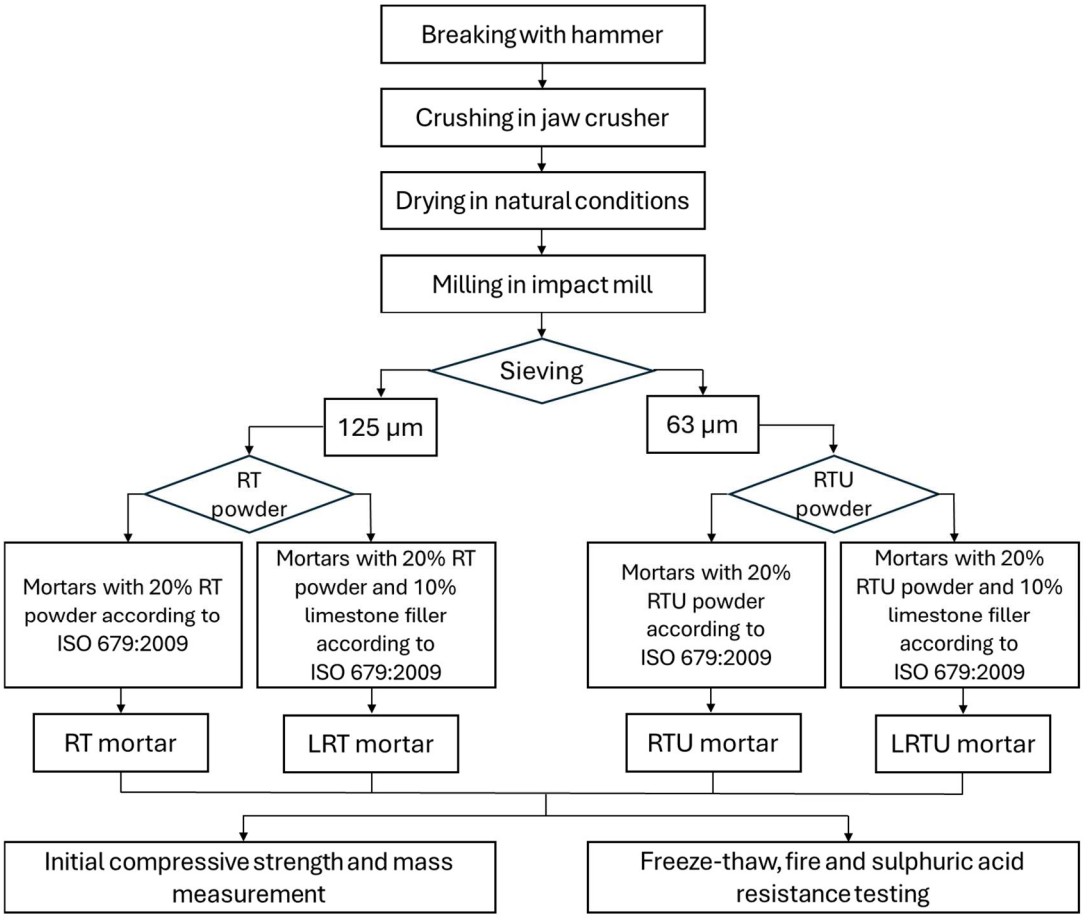

Fig. 6.2. Specimens preparation flowchart.

6.2.4. Capillary absorption

European standard EN 480 5 [257] was used for the capillary absorption measurement. Three prismatic samples were prepared for each formulation and subjected to testing after a 28 day curing period. Prior to testing, all specimens were oven dried at 50 °C until mass stabilisation was achieved, after which their dry masses were recorded. This drying temperature was chosen to prevent the decomposition of cement hydration products, which begins to occur at temperatures close to 100 °C. Dried specimens were positioned vertically with a 40 × 40 mm face in contact with water, to be plunged at 5 mm depth, as illustrated in Fig. 6.3. The 5 mm water depth was

marked directly on the specimens. During testing, the water level was visually aligned with these marks and maintained to ensure a consistent immersion depth. To minimise evaporation, the container was sealed during the test.

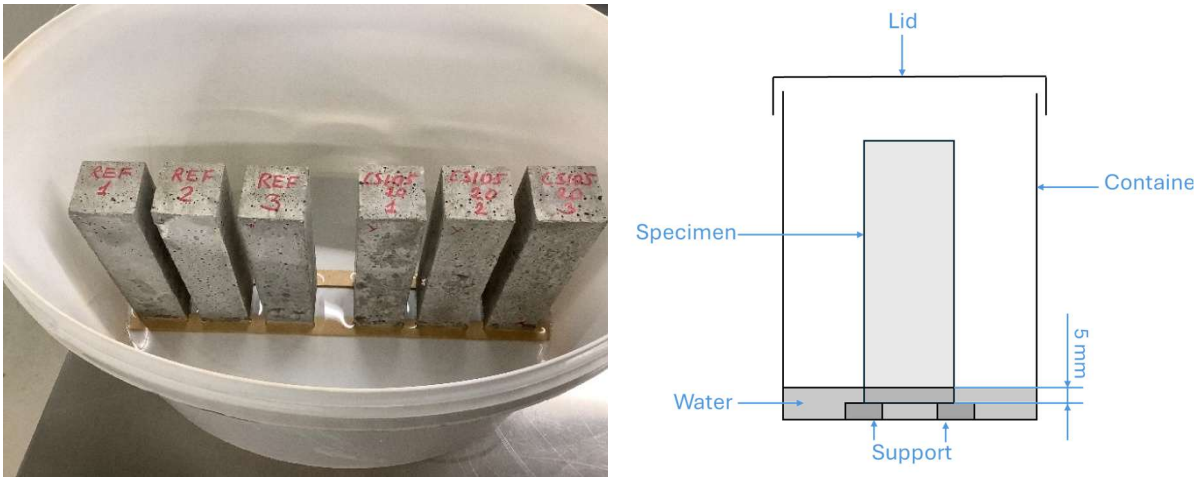

(a) (b)

Fig. 6.3. Experimental arrangement for the capillary water uptake test: (a) Specimens setup during testing; (b) Schematic representation of the arrangement.

Mass gain due to water uptake was recorded after 0.25, 0.5, 1, 2, 4, 6, 24, 48 and 168 hours of testing. Before each weighing, excess water was gently removed from the surface with absorbent material.

The capillary absorption coefficient (Ca), expressed in g/mm^2, was calculated using the following equation:

$$C_a = \frac{M - M_0}{1600}, \quad (17)$$

where M_0 is the initial dry mass (g), M is the mass after water absorption (g), and 1600 mm^2 is the surface area of the immersed face.

For data analysis and graphical presentation in Section 6.3.2. Capillary Absorption, mean values and standard deviations derived from three specimens per mixture are reported.

6.2.5. Drying shrinkage

Drying shrinkage was evaluated in accordance with EN 12617-4 [258], with modifications introduced to the measurement schedule and overall test duration. Three prismatic specimens (40 × 40 × 160 mm) were prepared per mortar type, cast in moulds equipped with embedded

metal pins at both ends to enable length change monitoring. After 24 hours of curing, the samples were demoulded and transferred onto a Type C Shrinkage Measurement System (Testing Bluhm & Feuerherdt GmbH), as depicted in Fig. 6.4.

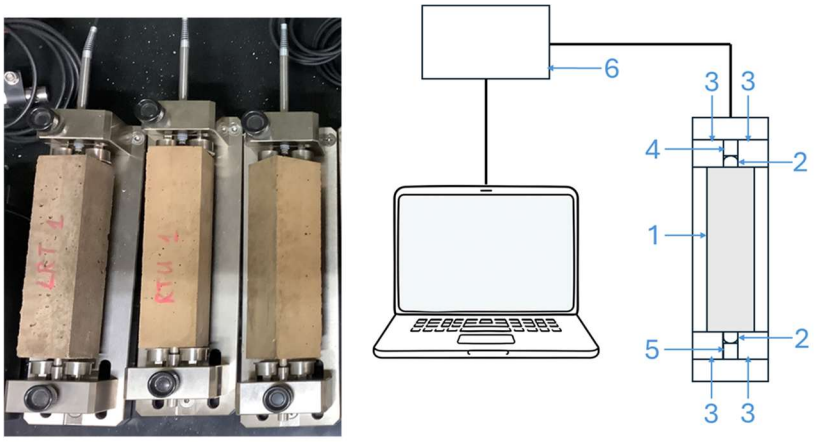

Fig. 6.4. Schematic of the apparatus used for drying shrinkage measurements.

Length variations were recorded using a digital displacement sensor fitted with LVDT transducers (accuracy: 0.2 µm; resolution: 0.31 µm; range: 5 mm) and a conical contact tip. One end of the specimen remained horizontally fixed against a reference pin, while the displacement gauge contacted the opposite end to detect axial deformation over time. Shrinkage readings were taken at 2-hour intervals over a 90-day period using a signal processing unit from Schleibinger Geräte.

Throughout the test, relative humidity and ambient temperature were recorded.

6.2.6. Freeze-thaw resistance

A non-standardized protocol [297] was employed to comparatively evaluate the durability of mortar specimens in freeze–thaw conditions. Prismatic samples (40 × 40 × 160 mm), previously cured for 28 days, were dried in a drying cabinet at 50 °C until mass stabilization and weighed to determine dry mass before durability testing. Following this, specimens were submerged in water inside sealed containers and put to a programmable freezing unit.

The specimens were cooled to -20 °C, held at this temperature for 11 hours 50 minutes, and then warmed back up to +20 °C. The cooling and heating rate was 4 °C per minute. The duration of one complete cycle was 24 hours. A total of 28 cycles were applied, consistent with previous research on cement-based materials, to balance experimental feasibility and sensitivity to performance differences among mixtures.

Upon completion of the cycling sequence, the specimens were redried to a constant mass and reweighed. Compressive strength was then measured for each mortar type. Resistance to freeze–thaw action was quantified as the change in mass and strength before and after exposure, expressed as a percentage.

Average values from six specimens were reported along with corresponding standard deviations. Since there is no established method for calculating the standard deviation of a percentage value derived from two independent sets of measurements, a cross-combination approach was applied. Specifically, all possible pairwise combinations between the pre- and post-exposure specimens were used to compute 36 individual strength loss percentages (6 × 6 combinations). The standard deviation of these values was then calculated to represent the spread. While this approach inevitably leads to a higher standard deviation due to capturing all potential differences between independent specimens, it reflects the natural scatter in compressive strength results and allows for a more comprehensive representation of variability in the derived loss values.

6.2.7. Fire resistance

Before testing, the initial mass of the samples was measured, then placed in a muffle furnace and heated to 200 °C, 300 °C, 500 °C, or 900 °C for 2 hours. The temperature increase rate was 10 °C per minute, and the samples cooled down naturally in a closed furnace chamber. The weight of the samples was measured immediately after cooling to ambient temperature to assess the degree of degradation. Fire resistance was evaluated by calculating the reduction in mass and mechanical strength after exposure, expressed as a percentage.

For each thermal condition and mortar type, six replicate specimens were tested. The results are presented as average values with corresponding standard deviations, following the statistical procedure described previously for freeze–thaw resistance evaluation.

6.2.8. Sulphuric acid resistance

After 28 days of curing, cement mortar specimens measuring 40 × 40 × 160 mm were dried in a drying chamber at 50 °C until the stabilization of mass, which was then measured before immersion of the specimens in a 1 % sulphuric acid solution for 90 days. Every 30 days, the solution was renewed to maintain constant acidity throughout the test.

At the end of the exposure period, mortar bars were rinsed with tap water, dried in a drying chamber at 50 °C to remove moisture, weighed, and tested for compressive strength.

Resistance to sulfuric acid was expressed as percentage changes in weight and strength, calculated relative to initial values. Analysis was performed on six replicates per mortar formulation, with mean values and standard deviations reported following the approach described for freeze–thaw resistance tests.

6.2.9. Statistical analysis

Multivariate analysis of variance (MANOVA) was employed in this study to evaluate the influence of multiple independent variables on a set of durability-related response variables simultaneously. This statistical technique is particularly appropriate when several dependent variables are interrelated, allowing for a more comprehensive understanding of their collective variation. In this case, compressive strength losses after freeze-thaw, high temperatures and 1 % sulphuric acid exposure are interrelated because they are all influenced by common material characteristics such as microstructure, porosity, and binder composition, which govern the material's behaviour under various environmental stressors. For instance, higher porosity or altered binder composition can simultaneously affect frost, fire and acid corrosion resistances. Thus, MANOVA provides a way to evaluate the combined effects on these durability indicators, offering a more holistic view than separate univariate tests.

The analysis was conducted in the R programming environment. The dependent variables included freeze-thaw resistance, fire resistance at four temperature levels and sulphuric acid resistance. These variables were selected as key indicators of mortar durability under various aggressive environmental conditions.

The independent variables considered were the specific surface area of the raw material powders, the presence or absence of limestone filler, drying shrinkage, and capillary absorption. These factors were chosen based on their expected impact on the microstructure, porosity, and overall stability of the cementitious matrix.

Statistical significance was assessed using p-values derived from the multivariate test statistics. While a significance threshold of 0.05 is commonly used, the main focus here was on comparing the p-values of different factors to determine which independent variables had the most substantial effect on the combined durability parameters. Smaller p-values indicate stronger

evidence against the null hypothesis, suggesting significant multivariate effect of the factor on the durability outcomes. Factors with p-values greater than 0.05 indicate weaker effects or no significant impact. By comparing these p-values, it was possible to assess the relative influence of each independent variable on the overall durability, highlighting their distinct contributions.

6.3. Results and discussion

6.3.1. Packing density

The calculated packing densities for the different binder systems, determined using the modified Andersen and Andersen method and expressed in similarity score, are summarized in Fig. 6.5.

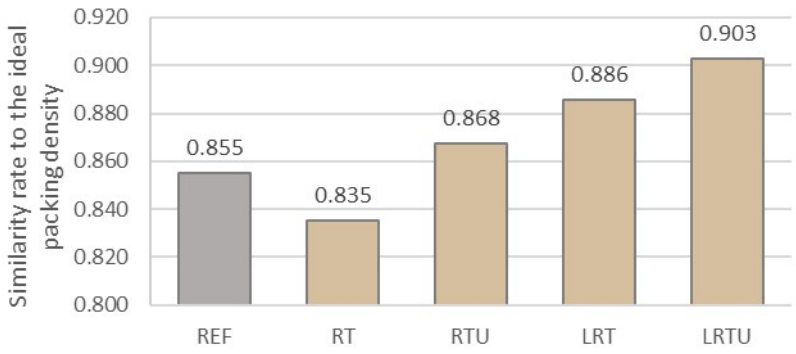

Fig. 6.5. Packing densities of the mortar mixtures: REF – reference mortar; RT – mortar with fine terracotta powder; RTU – mortar with ultrafine terracotta powder; LRT – LC3 mortar with fine terracotta powder; LRTU – LC3 mortar with ultrafine terracotta powder.

The RT system, containing fine terracotta powder, displayed a slightly reduced packing density (0.835), suggesting that the particle size distribution of this ceramic powder does not completely complement that of cement. By contrast, the use of ultrafine terracotta powder led to a notable increase in packing density (0.868). This enhancement can be attributed to the ability of finer particles to effectively occupy voids between coarser grains, thus improving the overall packing structure.

A further increase was observed in systems incorporating limestone filler. The LRT binder, contained limestone filler and fine terracotta powder, achieved a packing density of 0.886. The LRTU system, where the ultrafine ceramic powder was used, reached the highest packing density of all tested mixtures (0.903). These results clearly demonstrate that combining powders of

different particle size ranges significantly enhances the packing efficiency. The synergy between the particle size distributions of sand, cement and ceramic and limestone powders promotes the formation of a denser granular skeleton, reducing interparticle voids and enhancing material compactness, which is expected to improve durability.

6.3.2. Capillary absorption

The capillary absorption behaviour of the tested mortar mixtures is illustrated in Fig. 6.6 and Fig. 6.7. Among all specimens, the mortar incorporating fine terracotta powder RT exhibited the highest water uptake, reaching 0.0040 ± 0.00052 g/mm^2 after 7 days, which may be explained by the lower specific surface area of the RT powder, resulting in a more porous microstructure. The RTU specimen showed a capillary absorption of 0.0039 ± 0.00038 g/mm^2, identical to that of the reference mortar (0.0039 ± 0.00064 g/mm^2). The addition of limestone filler led to a modest yet consistent decrease in water absorption in both corresponding mortars. Specifically, the LRT specimen showed an absorption of 0.0037 ± 0.00038 g/mm^2, while the LRTU mortar exhibited the lowest value at 0.0035 ± 0.00053 g/mm^2. This reduction is likely due to the improved packing density associated with the finest granulometry of the limestone powder, which enhanced matrix densification and led to a decrease in porosity. However, the differences in absorption values across all mixtures fall within the range of experimental variability, as indicated by the overlapping standard deviations. Therefore, despite a general trend of reduced absorption with denser particle packing, these differences may be considered statistically insignificant.

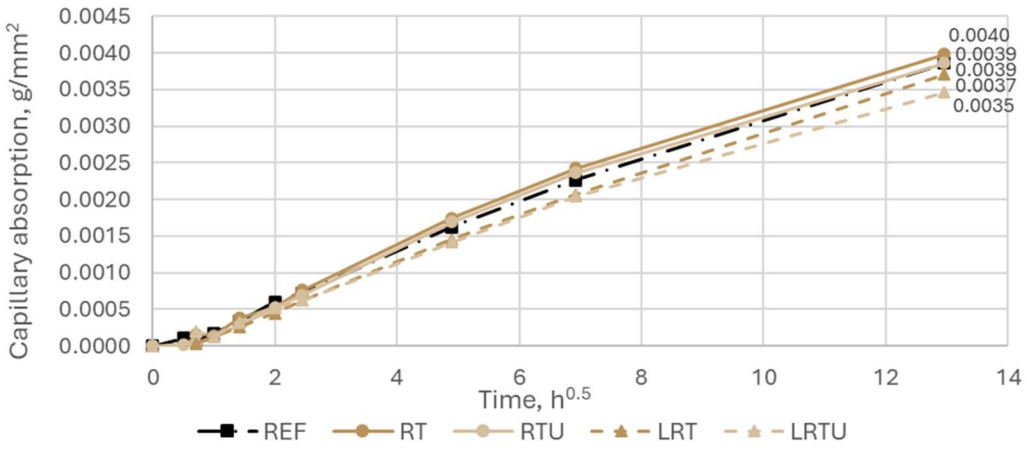

Fig. 6.6. Capillary absorption of mortar specimens: REF – reference mortar; RT – mortar with fine terracotta powder; RTU – mortar with ultrafine terracotta powder; LRT – LC3 mortar with fine terracotta powder; LRTU – LC3 mortar with ultrafine terracotta powder.

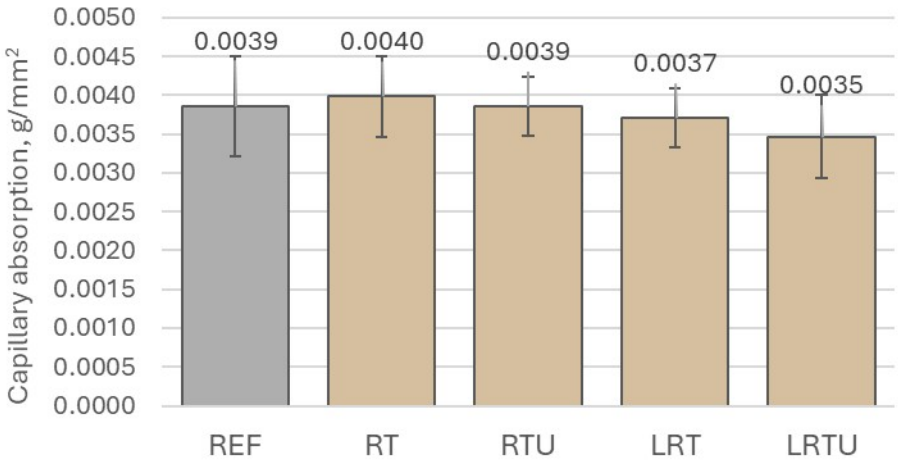

Fig. 6.7. Capillary absorption of mortar specimens after 7 days of contact with water: REF – reference mortar; RT – mortar with fine terracotta powder; RTU – mortar with ultrafine terracotta powder; LRT – LC3 mortar with fine terracotta powder; LRTU – LC3 mortar with ultrafine terracotta powder.

Although both the compressive strength (Table 6.3) and capillary water absorption results demonstrated improvement with the use of ceramic powders possessing a higher specific surface area, no clear correlation was observed between compressive strength and water absorption. Notably, the reference mortar, despite exhibiting the highest compressive strength, showed greater capillary absorption than the LRT and LRTU mortars, which exhibited lower strength values. This phenomenon can be attributed to the mechanically weaker binder matrix in the specimens containing ceramic waste powders, particularly in the LC3-based mortars, despite the improvement in particle packing density. In systems incorporating ceramic powders and limestone, the pozzolanic activity and the formation of carboaluminate phases are slower processes relative to the hydration of clinker phases [18]. Therefore, despite a denser structure, the percolation of strong chemical bonds within the matrix remains incomplete at 28 days, leading to comparatively lower mechanical strength but reduced capillary sorptivity. Other researchers have also reported results indicating no direct correlation between the compressive strength and water absorption of samples containing ceramic powders [298, 299]. Pacheco-Torgal and Jalali [299] attribute this to enhanced hydration during water absorption testing, resulting from the additional water supply.

6.3.3. Drying shrinkage

Drying shrinkage refers to the volume reduction of hardened cementitious materials as they lose moisture to the surrounding environment. This phenomenon primarily occurs due to water loss from the gel pores, which are extremely fine pores (typically <10 nm) within the C-S-H gel, which constitutes the primary strength-giving phase in hydrated cementitious systems. As water evaporates from these nanoscale pores, internal stresses develop within the matrix, leading to volumetric contraction and microcracks formation.

Fig. 6.8 illustrates the development of drying shrinkage in the mortars throughout the 90-day test duration. Drying shrinkage increased rapidly up to about 10 days, slowed between 10 and 30 days, continued at a lower rate until approximately 50 days, and then stabilised. This trend can be explained by initial rapid moisture evaporation from the cement matrix and accelerated hydration, followed by gradual pore refinement due to hydration product formation, which reduced moisture loss. As available water became depleted, shrinkage development decelerated and eventually ceased, consistent with the mechanisms reported by Nasir et al. [300].

Throughout the testing duration, the LC3-type mortar specimens exhibited the lowest drying shrinkage. The RT curve closely matched the reference sample curve for approximately two months, after which it displayed slightly lower shrinkage, although remaining very close. The RTU curve followed the reference and RT curves up to around 20 days, subsequently exhibiting reduced shrinkage until the end of the experiment. Similar trends have been noted by other authors, who documented decreased shrinkage in mixtures with ceramic components [259, 278].

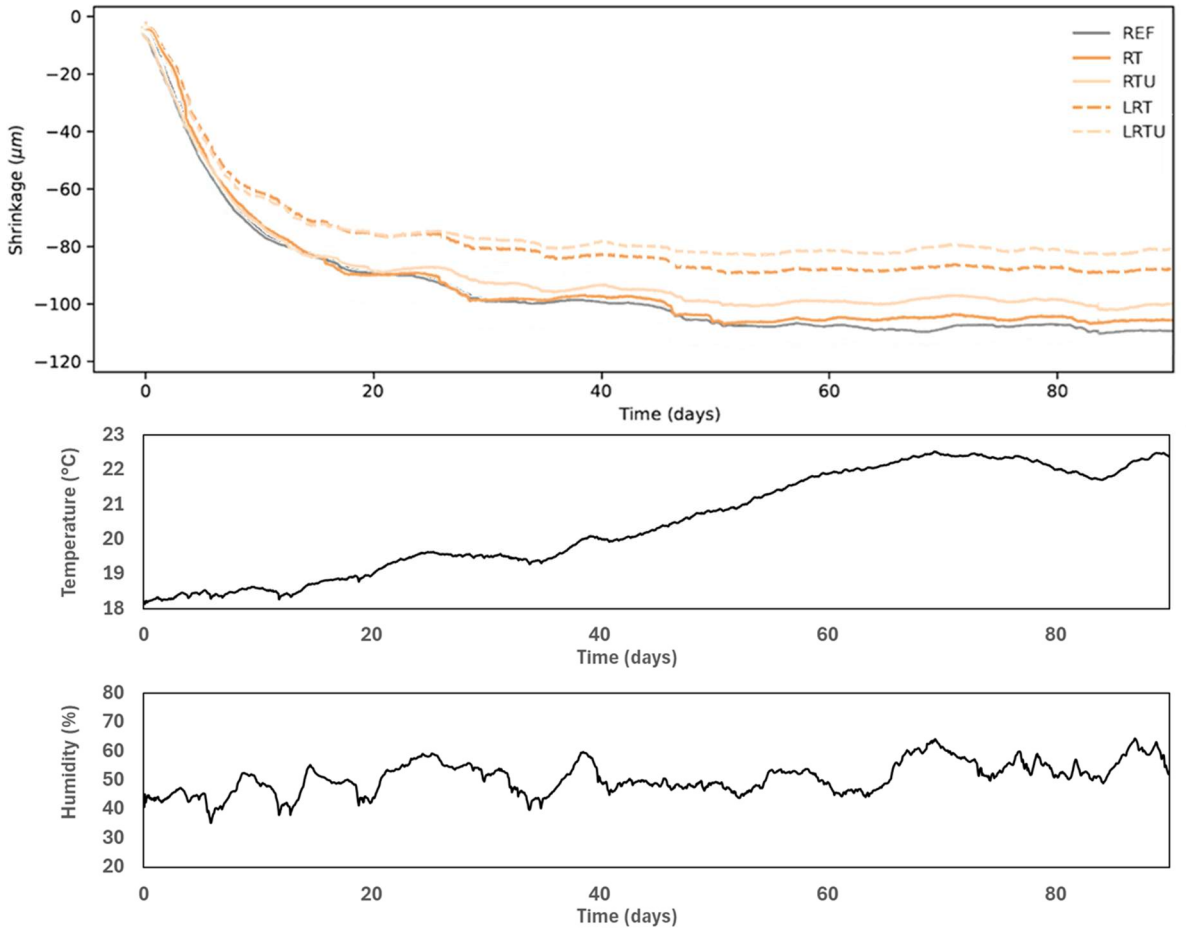

Fig. 6.8. Shrinkage development in mortars during 90-day drying period: REF – reference mortar; RT – mortar with fine terracotta powder; RTU – mortar with ultrafine terracotta powder; LRT – LC3 mortar with fine terracotta powder; LRTU – LC3 mortar with ultrafine terracotta powder.

After 90 days of drying, the shrinkage values recorded for the REF, RT, RTU, LRT, and LRTU specimens were 112 μm/m, 105 μm/m, 100 μm/m, 88 μm/m, and 80 μm/m, respectively. The observed shrinkage decrease, particularly in RTU- and limestone-containing mixtures, is likely linked to enhanced particle packing due to the finer granulometry of the ultrafine ceramic powder and limestone filler.

Fine limestone particles act as fillers, occupying spaces between cement grains. By optimising the particle size distribution and enhancing packing density, limestone fillers reduce matrix porosity. Moreover, because limestone partially replaces clinker without significantly contributing to additional C-S-H formation, it does not substantially increase the fine gel pore volume.

Interestingly, despite exhibiting lower capillary absorption, the REF specimens showed slightly higher drying shrinkage than the RT specimens. This can be explained by the fact that drying

shrinkage is mainly influenced by the gel pore network [301], while the mechanism of capillary absorption in cementitious materials is very complex and depends not only on pore size, but also on pore connectivity and swelling due to the interaction of the C–S–H gel with water [302, 303]. Therefore, a material can exhibit low absorption but still experience significant shrinkage if the gel pore volume remains relatively high.

6.3.4. Freeze-thaw resistance

The freeze-thaw resistance results, expressed as mass loss and compressive strength loss after 28 cycles, are presented in Fig. 6.9 and Fig. 6.10. The results demonstrated a clear improvement in the mortars incorporating ceramic waste powders compared to the reference mortar. The REF specimen exhibited a mass loss of 1.07% and a strength loss of 6.31%, whereas the modified mortars (RT, RTU, LRT, and LRTU) showed significantly lower values. The best performance was observed for RTU and LRTU specimens, which exhibited mass losses of 0.33% and 0.34%, and strength losses of 1.91% and 1.93%, respectively.

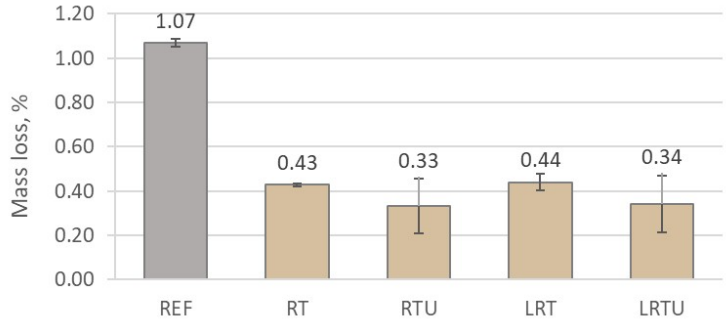

Fig. 6.9. Mass loss of mortars after 28 freeze-thaw cycles: REF – reference mortar; RT – mortar with fine terracotta powder; RTU – mortar with ultrafine terracotta powder; LRT – LC3 mortar with fine terracotta powder; LRTU – LC3 mortar with ultrafine terracotta powder.

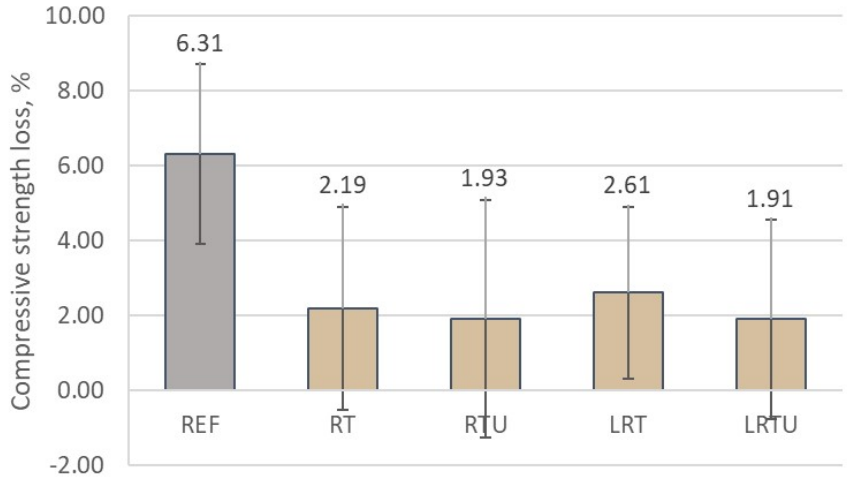

Fig. 6.10. Compressive strength loss of mortars after 28 freeze-thaw cycles: REF – reference mortar; RT – mortar with fine terracotta powder; RTU – mortar with ultrafine terracotta powder; LRT – LC3 mortar with fine terracotta powder; LRTU – LC3 mortar with ultrafine terracotta powder.

It seems that increasing the fineness of the ceramic powder positively affects the resistance of the mortars to freeze–thaw cycles. However, considering the relatively high measurement uncertainties (standard deviations), the absence of a definitive effect of powder fineness cannot be entirely excluded. The addition of limestone filler did not appear to exert a substantial influence on freeze-thaw resistance under the testing conditions.

A correlation was observed between the compressive strength (Table 6.3) and the subsequent freeze-thaw performance of the modified mortars. Specimens that achieved higher early-age compressive strengths generally exhibited smaller decreases in mass and mechanical strength after freeze-thaw test. This observation suggests that a stronger matrix better resists the internal stresses generated by the expansion of freezing water within the pore structure.

Nevertheless, the REF specimen, despite having the highest initial strength, showed significantly greater mass and strength losses than the modified specimens. Given that the REF mortar also exhibited the highest drying shrinkage, it may be inferred that shrinkage-induced microcracking contributed to its reduced durability. Therefore, drying shrinkage emerges as an important factor influencing freeze-thaw resistance, alongside compressive strength and capillary adsorption. Its role has been specifically highlighted and investigated by Miao et al. [304].

Moreover, the continuous immersion of specimens in water during the freeze-thaw cycles likely provided a favourable environment for pozzolanic reactions to occur in the mortars containing ceramic powders. Pozzolanic reactions between the reactive aluminosilicate phases in the ceramic waste and the calcium hydroxide released during cement hydration require the presence

of water to progress. The prolonged availability of moisture during the durability testing could have facilitated further formation of additional calcium silicate hydrate and other secondary binding phases. This late-stage reaction would contribute to further densification of the matrix, refinement of the pore structure, and a consequent increase in durability. Additionally, the formation of new hydration products may have partially sealed existing microcracks and pores, promoting self-healing phenomena that further improved the resistance of the mortars to freeze-thaw damage.

Thus, freeze-thaw resistance can be regarded as a multifactorial property, influenced by water permeability, initial matrix strength, shrinkage-induced microcracks, and the extent of pozzolanic reactions. Additional factors such as the ionic composition of the pore solution, the differential thermal expansion coefficients of mortar constituents, and the overall composition of the cementitious matrix also affect freeze-thaw behaviour [262].

6.3.5. Fire resistance

Mass changes of mortars following heating at 200 °C, 300 °C, 500 °C, and 900 °C are presented in Fig. 6.11. Mass loss showed no notable variation at moderate temperatures (up to 500 °C) among all specimens, except for RTU. At 200 °C, the mass loss of the REF, RT, LRT, and LRTU specimens was approximately 0.3 %, primarily associated with the dehydration of gypsum and ettringite, as well as the initial degradation of calcium silicate hydrates. At 300 °C, mass loss increased to between 0.9 % and 1.2 %, attributed to the decomposition of the calcium silicate hydrates. At 500 °C, mass loss reached values between 2.1 % and 2.4 % for the REF, RT, LRT, and LRTU specimens, corresponding to the onset of portlandite dissociation and further degradation of the C-S-H. The RTU mortar consistently exhibited slightly greater mass loss at each stage: 0.6% at 200 °C, 1.4% at 300 °C and 2.7% at 500 °C.

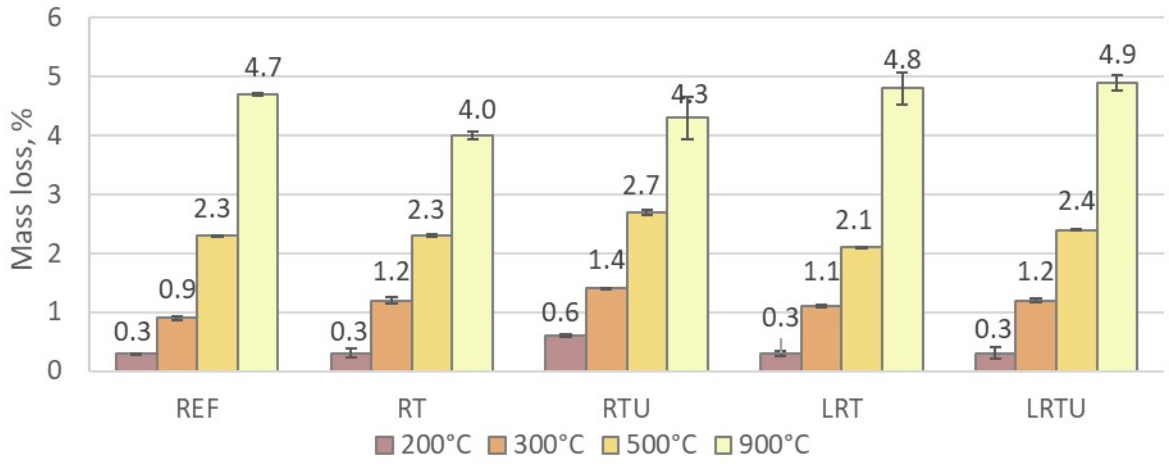

Fig. 6.11. Mass loss of mortars after exposure to elevated temperatures: REF – reference mortar; RT – mortar with fine terracotta powder; RTU – mortar with ultrafine terracotta powder; LRT – LC3 mortar with fine terracotta powder; LRTU – LC3 mortar with ultrafine terracotta powder.

Heating at 900 °C is associated with the full decomposition of C–S–H, portlandite and calcite with consequent CO2 release. The corresponding mass losses were 4.7 %, 4.0 %, 4.3 %, 4.8 %, and 4.9 % for REF, RT, RTU, LRT, and LRTU, respectively.

The residual compressive strength values after thermal treatment are presented on Fig. 6.12. The influence of ceramic SCMs was particularly evident at temperatures up to 300 °C. Upon heating to 200 °C and 300 °C, the reference specimen exhibited strength losses of 4.8 % and 20.7 %, respectively. In contrast, the RT, RTU, LRT, and LRTU specimens demonstrated strength gains of 11.7 %, 13.0 %, 13.1 %, and 13.9 % at 200 °C, respectively. The results at this temperature show a clear correlation with the drying shrinkage measurements, which is expected, as both phenomena are influenced by microstructural changes induced by water evaporation. At 300 °C, the RT, RTU, and LRTU specimens continued to exhibit strength gains of 3.7 %, 6.7 %, and 4.0 %, respectively, while the LRT specimen showed only a minor strength loss of 1.7 %. The observed strength enhancement at moderate temperatures is attributed to the acceleration of pozzolanic reactions, which are thermally activated. Similar phenomenon has been reported in [305 – 307] and in the review by Chong et al. [308], where it is explained by the increase in self-autoclaving, which in turn accelerates the rate of hydration of cement phases and pozzolanic reactions. These reactions promote the formation of additional cementitious phases and contribute to matrix densification, thereby improving mechanical performance.

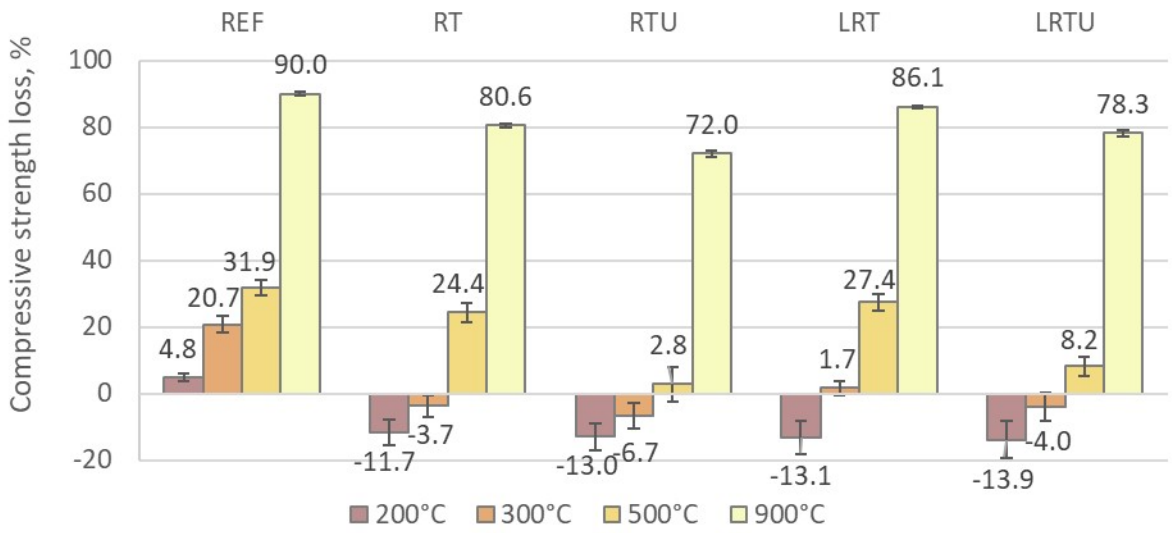

Fig. 6.12. Compressive strength changes of mortars after exposure to elevated temperatures: REF – reference mortar; RT – mortar with fine terracotta powder; RTU – mortar with ultrafine terracotta powder; LRT – LC3 mortar with fine terracotta powder; LRTU – LC3 mortar with ultrafine terracotta powder.

At 500 °C, all specimens exhibited strength losses: 31.9 %, 24.4 %, 2.8 %, 27.4 %, and 8.2 % for REF, RT, RTU, LRT, and LRTU, respectively, indicating superior performance for specimens incorporating the ultrafine ceramic powder (RTU). After exposure to 900 °C, substantial strength losses were observed across all mixes: 90.0 %, 80.6 %, 72.0 %, 86.1 %, and 78.3 %, respectively. The best fire resistance was again recorded in the mortars containing RTU. The severe strength losses at 900 °C result from the water-releasing decomposition of calcium hydroxide and calcium silicate hydrates, CO_2-releasing calcite decomposition, recrystallization of calcium silicates into wollastonite and the resulting cracking [101]. Ceramic-modified mortars retain more strength because the fired ceramic particles remain stable due to their quartz and feldspar content, whereas LC3 mixes are partly penalized by limestone decomposition, as also confirmed by Lin et al. [101]. Nevertheless, the LC3-type mortars still outperformed the reference specimen in terms of fire resistance. Visual observations further supported these findings: as shown in Figure 6.13, specimens containing ceramic powders exhibited fewer and finer surface cracks after exposure to 900 °C, whereas the OPC-based reference specimen displayed numerous wide cracks.

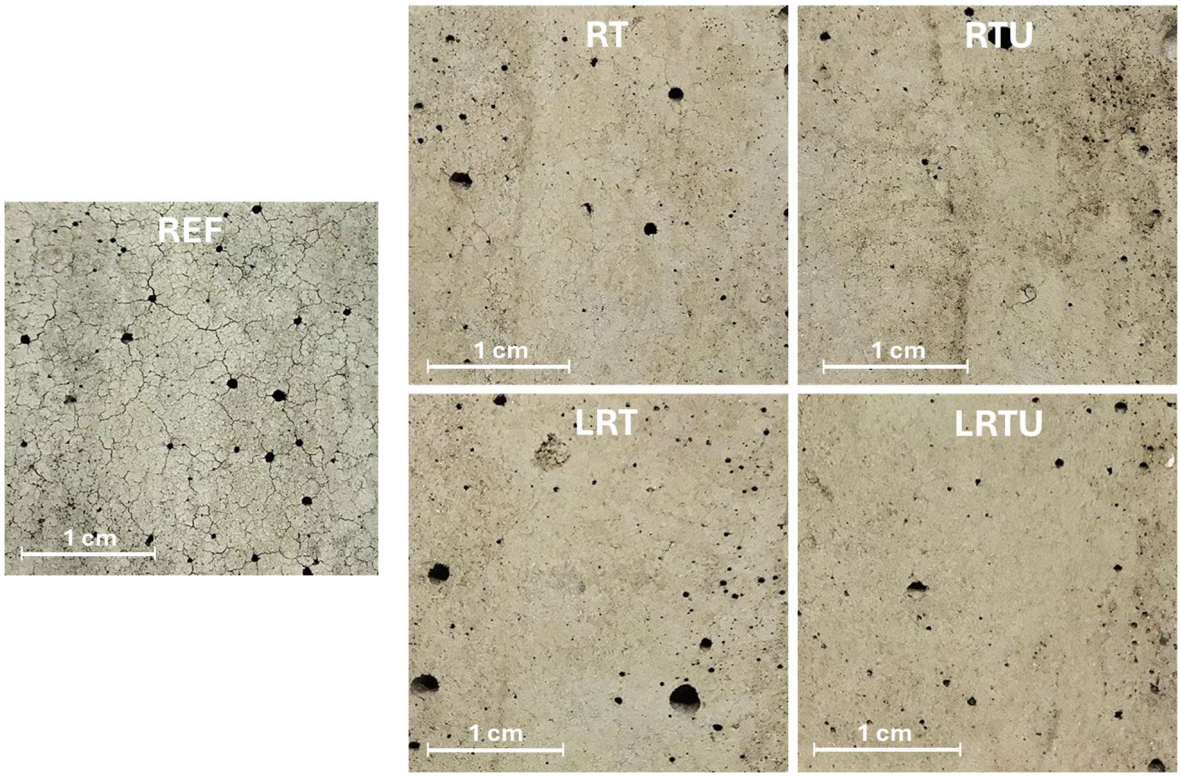

Fig. 6.13. Surface texture of the mortar specimens after exposure at 900 °C: (a) Reference mortar; (b) Mortars with ceramic powders: RT – mortar with fine terracotta powder; RTU – mortar with ultrafine terracotta powder; LRT – LC3 mortar with fine terracotta powder; LRTU – LC3 mortar with ultrafine terracotta powder.

It is important to note that while thermal decomposition, such as dehydration and decarbonation, largely governs mass loss, while the changes of mechanical strength are influenced mostly by crack development due to phase transformations and microstructural alterations. The comparable mass loss observed across all mortars, regardless of notable differences in residual strength. This suggests that internal characteristics such as mineralogical composition and pozzolanic reactivity, leading to the additional cementitious phases formation, play a critical role in high-temperature mechanical stability.

Moreover, the same pattern was observed in fire resistance (Fig. 6.12) and freeze–thaw resistance (Fig. 6.10), indicating that both durability aspects may be influenced by shared properties, including porosity [95, 100] and differences in thermal expansion coefficients between constituents [96, 97].

6.3.6. Sulphuric acid resistance

The behaviour of the 28-day mortars under sulphuric acid exposure was investigated through mass variation and compressive strength retention after 90 days of immersion in a 1% H_2SO_4 solution as shown on Fig. 6.14 and Fig. 6.15. Contrary to typical degradation trends, all formulations exhibited a net increase in mass. This phenomenon can be attributed to the ingress and reaction of sulphate ions with calcium-rich hydration products, causing the crystallisation of expansive secondary phases such as gypsum and ettringite. These compounds tend to precipitate within the outer pore network, resulting in a measurable gain in sample weight.

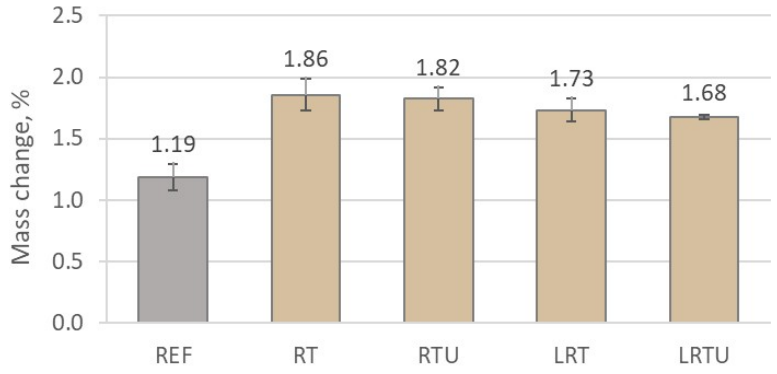

Fig. 6.14. Mass change of mortar specimens after exposure to sulphuric acid solution: REF – reference mortar; RT – mortar with fine terracotta powder; RTU – mortar with ultrafine terracotta powder; LRT – LC3 mortar with fine terracotta powder; LRTU – LC3 mortar with ultrafine terracotta powder.

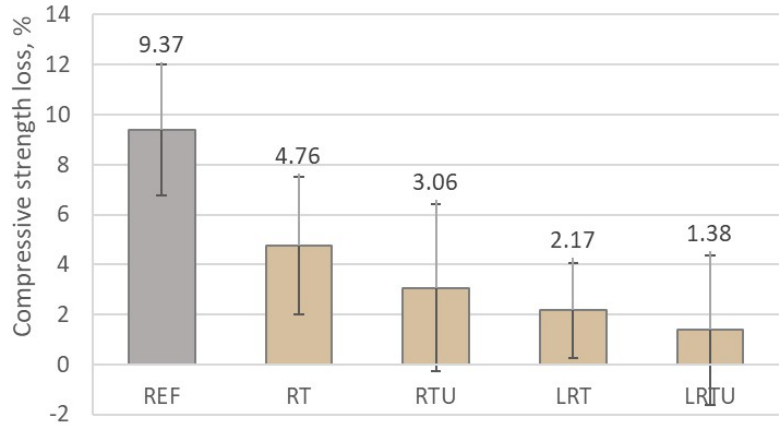

Fig. 6.15. Loss in compressive strength of mortar specimens after immersion in sulphuric acid solution: REF – reference mortar; RT – mortar with fine terracotta powder; RTU – mortar with ultrafine terracotta powder; LRT – LC3 mortar with fine terracotta powder; LRTU – LC3 mortar with ultrafine terracotta powder.

The specimens containing ceramic waste powders demonstrate a greater mass gain compared to the OPC mortar, showed mass gain of 1.19 %, with RT, RTU, LRT and LRTU achieving values of 1.86 %, 1.82 %, 1.73 % and 1.68 %, respectively. This greater mass gain may be attributed to the improved retention of the solid structure in the modified mortars after acid exposure. In OPC mortar, the higher content of portlandite, which dissolves readily under acidic conditions, promotes surface erosion and material loss, thereby reducing the net mass gain.

Changes in specimen mass are not always indicative of long-term performance in aggressive environments. The concurrent processes of ion exchange, including the incorporation of hydrogen and sulphate ions and the leaching of aluminium and calcium ions from the matrix, complicate interpretation [267, 268]. The balance between these opposing mechanisms is governed by the exposure conditions, particularly acid concentration and duration [269 – 271].

In contrast to mass gain, the residual compressive strength provides a more reliable indicator of chemical durability. Notably, mortars containing ceramic additions exhibited superior strength retention compared to the control mix. While the reference suffered a 9.37% reduction in compressive strength, values for the alternative binders ranged from 4.76% (RT) to as low as 1.38% (LRTU). Similar results were reported by other researchers [273, 309], who explained this improvement by pore refinement. It may also be attributed to the consumption of portlandite during pozzolanic reactions, which reduces the amount of acid-sensitive phases within the mortar, as observed in the case of sulphate attack [284].

Notably, specimens containing limestone filler exhibited the lowest strength losses. Additionally, an increase in the fineness of the ceramic powder further enhanced resistance to sulphuric acid attack. This can be explained by the improved pozzolanic reactivity of ultrafine powders, the greater portlandite-forming components dilution by higher clinker substitution in LC3-type mortars, and the reduction in permeability due to improved packing density.

6.3.7. Statistical analysis

The multivariate analysis of variance MANOVA approach enabled the assessment of the extent to which each independent variable influences the durability outcomes, providing a clearer understanding of their relative contributions. While graphical comparisons indicated that all independent variables had an effect on the durability parameters, MANOVA allowed for a more precise quantification of the magnitude and statistical significance of each factor's influence.

The results of the multivariate analysis of variance are summarised in Table 6.4. The Pillai's trace values and associated F-statistics demonstrate notable differences in the strength of the effects exerted by each independent factor on the set of dependent durability variables.

Table 6.4. MANOVA results.

Independent factor	Df[1]	Pillai[2]	Approx F[3]	Num Df[4]	Den Df[5]	Pr(>F)[6]
Finess	1	0.994	385.80	3	7	$3.91 \cdot 10^{-8}$
Limestone filler	1	0.9739	86.90	3	7	$6.66 \cdot 10^{-6}$
Packing density	1	0.9297	30.84	3	7	$2.09 \cdot 10^{-4}$
Capillary adsorption	1	0.9730	83.95	3	7	$7.49 \cdot 10^{-6}$
Shrinkage	1	0.9663	66.94	3	7	$1.61 \cdot 10^{-5}$

[1]*Df* – Degrees of freedom associated with the independent factor.

[2]*Pillai* – Pillai's trace statistic, a multivariate test statistic indicating the proportion of explained variance; higher values suggest a stronger multivariate effect.

[3]*Approx F* – Approximate F-value, used to test the statistical significance of the multivariate effect; calculated based on the Pillai trace.

[4]*Num Df* – Numerator degrees of freedom for the F-distribution, related to the number of dependent variables.

[5]*Den Df* – Denominator degrees of freedom for the F-distribution, related to the residuals in the multivariate model.

[6]*Pr(>F)* – p-value reflects the chance of the observed F-statistic under the null hypothesis; values below 0.05 suggest statistical significance.

In MANOVA, Pillai's trace is a test statistic used to evaluate how much variation in the combined dependent variables can be attributed to each independent factor. The closer the value is to 1 (or higher, in the case of multiple levels), the stronger the effect. The approximate F-value measures the strength of the relationship and is used to test the statistical significance of this effect. A higher F-value generally means a more pronounced impact of the factor. The p-value indicates whether this effect is likely to be genuine or due to random chance; values below 0.05 are typically considered statistically significant. Together, these statistics help determine not only whether a factor has an effect, but how strong and reliable that effect is.

Below is an interpretation of the results showing the influence of each parameter ranked in order of decreasing effect size.

Among the analysed factors, ceramic powder fineness exerted the strongest multivariate effect (Pillai = 0.994, Approx. F = 385.80, $p = 3.91 \times 10^{-8}$), indicating an overwhelmingly dominant influence. This result underscores the critical role of particle size and surface area of pozzolan in affecting the durability characteristics of cementitious composites.

Limestone filler also exhibited a very strong effect (Pillai = 0.9739, Approx. F = 86.90, p = 6.66×10^{-6}), confirming its significant multivariate contribution. Although slightly lower than the influence of fineness, the effect of limestone filler was still pronounced, highlighting its relevance in modifying the hydration process and microstructural development.

Capillary adsorption demonstrated a similarly strong and statistically significant multivariate influence (Pillai = 0.9730, Approx. F = 83.95, p = 7.49×10^{-6}), which suggests that this parameter has a considerable impact on overall durability performance, likely due to its role in both chemical degradation and freeze-thaw damage mechanisms.

Shrinkage also displayed a strong and statistically significant multivariate effect (Pillai = 0.9663, Approx. F = 66.94, p = 1.61×10^{-5}), supporting the notion that volumetric instability introduces internal microcracking, which can compromise durability over time.

Finally, packing density showed a notable effect as well (Pillai = 0.9297, Approx. F = 30.84, p = 2.09×10^{-4}), indicating that more efficiently packed granular structures contribute meaningfully to the durability of the composites. This influence is attributed to improved matrix densification and reduced porosity.

A multivariate analysis of variance was conducted as a complementary tool to assess the combined influence of several mixture parameters on the durability-related properties of mortars. Given the relatively small dataset (n = 15), the statistical analysis remains limited in terms of formal inference. These findings should be considered preliminary and warrant validation with larger experimental designs.

While the MANOVA analysis provides valuable insights into factor interactions, the relatively small dataset (n = 15) limits the statistical power for detecting subtle effects. The significant factors identified ($p < 0.05$) represent robust effects that emerge despite the sample size constraints. These findings should be considered preliminary and warrant validation with larger experimental designs.

6.4. Conclusions

The results of this study provide direct evidence of the practical durability of mortars incorporating ceramic demolition waste, supporting its adoption in construction practice. The following conclusions were drawn:

(1) Capillary absorption and drying shrinkage were reduced with increased ceramic powder fineness and limestone filler incorporation, due to enhanced matrix compaction. After 7 days, the lowest water uptake (0.0035 g/mm^2) was observed for LRTU, compared to 0.0039 g/mm^2 for the reference. Shrinkage after 90 days decreased from 112 µm/m (REF) to 80 µm/m (LRTU).

(2) Freeze–thaw resistance improved in all modified mortars, with compressive strength losses reduced from 6.31 % (REF) to between 1.91 % and 2.61 % in the alternative mixes. Increased ceramic powder fineness positively affected freeze–thaw resistance, while limestone filler had minimal impact under the tested conditions.

(3) Mortars with ceramic powders demonstrated superior fire resistance, with strength gains at 200 °C and 300 °C attributed to thermally accelerated pozzolanic reactions. At 300 °C, the reference mortar lost 20.7 % strength, while mortar with ultrafine ceramic powder gained 6.7 %. The addition of limestone filler slightly reduced fire resistance due to carbonate decomposition, but LC3-type mortars still outperformed the reference at temperatures up to 900 °C, where the reference lost 90 % of strength compared to 72.0–86 .1% for modified mortars.

(4) Resistance to sulphuric acid improved with ceramic powder incorporation, further enhanced by limestone filler. Strength losses decreased from 9.37 % in REF to 1.38 % in LRTU, attributed to reduced permeability and portlandite dilution.

(5) Statistical analysis (MANOVA) confirmed ceramic powder fineness as the most significant factor influencing durability (Pillai's trace = 0.994, $p = 3.91\times10^{-8}$), followed by limestone filler (0.9739, $p = 6.66\times10^{-6}$) and packing density (0.9297, $p = 2.09\times10^{-4}$). Capillary absorption and shrinkage had significant but weaker effects.

In general, ceramic powders enhance mortar durability, with fineness being a key parameter. These findings have important practical implications:

– For standards development. The superior durability of ceramic-modified mortars supports the inclusion of ceramic waste in cement standards, with recommended replacement levels of 20% for binary systems and 30% (comprising 20% ceramic and 10% limestone) for LC3 formulations.

- For reduction of the cement industry's carbon footprint. Since ceramic waste and limestone filler do not require thermal processing, replacing 20–30% of cement clinker may lead to a comparable reduction (20–30%) in CO_2 emissions. However, an accurate assessment requires a life cycle analysis that accounts for the energy consumption associated with waste separation, transportation, and grinding.
- For waste management. Each tonne of cement produced could incorporate 200 kg of ceramic waste, diverting it from landfills and contributing to more sustainable waste utilization.
- For practical applications. Given their reduced shrinkage and permeability, improved freeze–thaw resistance, superior fire resistance, and better chemical durability, the tested blended cements can be particularly suited for use in structural and non-structural masonry units, renders, repair mortars, and concretes exposed to aggressive environments, especially where both thermal stability and durability against moisture and chemical attack are required. However, further more detailed and industrial-scale investigations are crucial before large-scale implementation.

6.5. Limitations and outlook

This study provides an overall assessment of the durability performance of cements with ceramic SCMs. However, to achieve a more comprehensive understanding of the underlying degradation mechanisms, further investigations focusing on micro-structural and compositional changes during exposure to aggressive environments are necessary. Such analyses, including techniques like SEM and XRD, would elucidate the evolution of hydration products, phase transformations, and crack development, thereby strengthening the interpretation of durability outcomes.

The strength improvement observed in mortars with ceramic powder up to 300 °C, together with their reduced cracking at higher temperatures compared to the reference mortar, highlights the need for XRD analysis to identify the formation and decomposition of phases, and SEM/EDS to monitor crack development and locate the most vulnerable phases. In addition, XRD and SEM/EDS analyses of the outer layers of specimens exposed to sulphuric acid, conducted at specific intervals during immersion, would allow tracking of ettringite and gypsum formation and the associated stress development.

Future research integrating these microstructural insights with performance testing will contribute to optimizing ceramic-based supplementary cementitious materials for sustainable cement applications.

Chapter 7: General discussion

7.1. Comparison of different demolition waste types

7.1.1. Comparison of chemical compositions

To evaluate the potential reactivity and classify the nature of the studied waste materials, their simplified oxide compositions were plotted on the ternary CaO-SiO_2-Al_2O_3 diagram (Fig. 7.1). This approach enables a visual comparison of their principal chemical characteristics.

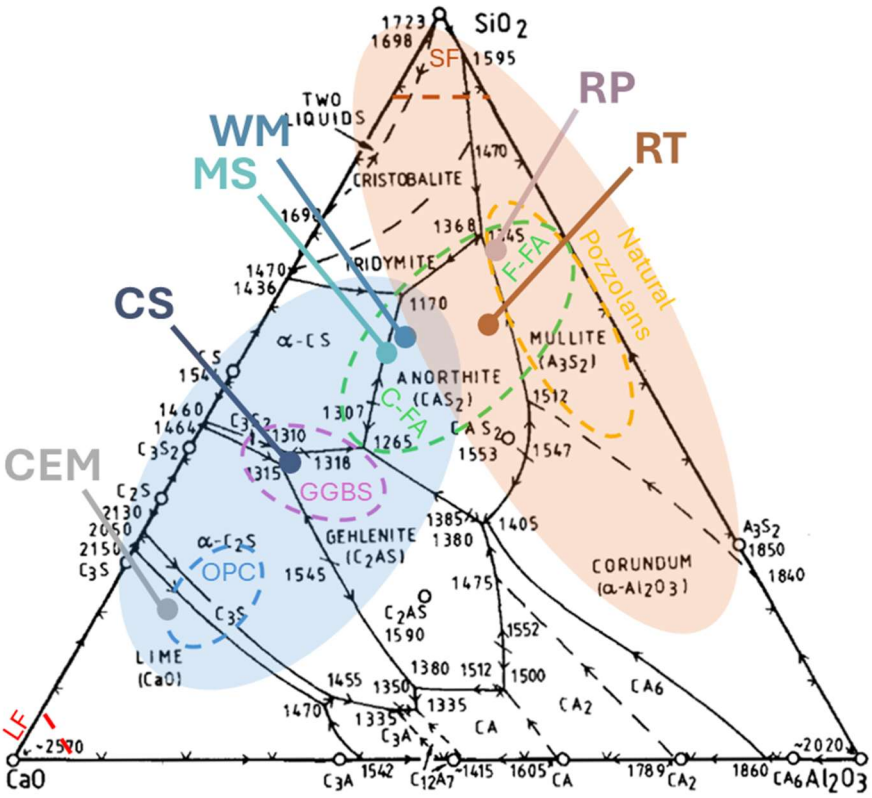

Fig. 7.1. Arrangement of the investigated materials on the ternary CaO-SiO_2-Al_2O_3 diagram.

Positioning the materials within this compositional space allows for a graphical distinction between those with hydraulic potential (typically rich in CaO and located in the lower left region) and those with pozzolanic potential (typically low in CaO and high in SiO_2 and/or Al_2O_3, located in the upper and right sectors). Such positioning helps to assess whether a material's chemical composition is compatible with hydraulic or pozzolanic reactions. In addition, it provides a

preliminary indication of the types of mineral phases the material composition is thermodynamically related to.

By plotting the recalculated equivalent compositions of the studied wastes on the diagram, their similarity to classical materials, such as blast furnace slag, fly ash, silica fume, and natural pozzolans, can be visually assessed. This facilitates clearer comparison and interpretation of their potential role in blended cement systems.

In the diagram shown in Fig. 7.1, the blue-shaded region represents compositions of hydraulic materials, while the orange region corresponds to pozzolanic materials.

CS (Concrete Screening Wastes) are positioned within the hydraulic region, close to the typical composition of blast furnace slags. CS is characterized by a relatively high CaO content, along with moderate amounts of SiO_2 and Al_2O_3.

MS (Mixed Screening Wastes) and WM (Recycled Aggregate Washing Mud) lie near the boundary between the hydraulic and pozzolanic regions but remain within the hydraulic field. This is attributed to the presence of ceramic particles rich in silica and alumina. Their close positioning implies compositional similarity, although WM contains slightly more SiO_2 and Al_2O_3.

RT (Recycled Terracotta) and RP (Recycled Porcelain) are located within the pozzolanic zone due to low CaO content and higher proportions of silica and alumina. Such compositions are characteristic of ceramics and Class F fly ash. However, both ceramic materials contain slightly less Al_2O_3 than conventional natural pozzolans, such as calcined clays (metakaolin). RP is richer in silica and alumina compared to RT and lies within the mullite field, while RT falls in the anorthite feldspar field. In Chapter 4, "Using ceramic demolition wastes for CO_2-reduced cement production," the presence of mullite in RP and its absence in RT is attributed to differences in firing temperatures. However, their respective positions on the ternary diagram suggest that variations in chemical composition may also explain this difference.

7.1.2. Compliance of investigated materials with EN 197-1, EN 197-6, and ASTM C 618 standards

Table 7.1 summarizes the compliance of the investigated waste-based powders and binders with the requirements of the European standard EN 197-1 for blended cements, the American standard ASTM C 618–15 for pozzolanic materials and EN 197-6 for concrete fines.

Table 7.1. Compliance of the investigated waste materials with EN-107-1 and ASTM C 618-15 standards.

Standard	Parameter	Requirement	RT	RTU	RP	RPU	CS105	CS500	MS105	MS500	WM105	WM500
EN-197-1	SO_3 (final cement)	≤3.5%	***3.8%****	***3.8%****	3.2%	3.2%	3.3%	3.3%	***3.6%****	***3.7%****	3.4%	3.4%
EN-197-1	LOI (final cement)	≤5%	2.3%	2.3%	2.0%	2.0%	***6.4%***	5.0%	4.8%	3.6%	4.9%	3.9%
EN-197-1	Initial setting time	≥75 min	215 min	215 min	190 min	180 min	220 min	215 min	230 min	210 min	230 min	205 min
EN-197-1	28 days strength	≥32.5 MPa	51.8 MPa	54.5 MPa	***26.8 MPa***	***30.9 MPa***	50.2 MPa	53.5 MPa	49.6 MPa	52.3 MPa	47.8 MPa	51.4 MPa
ASTM C 618–15	SiO_2+Al_2O_3+Fe_2O_3	≥70%	76.7%	76.7%	85.7%	85.7%						
ASTM C 618–15	SO_3	≤4%	3.3%	3.3%	0.2%	0.2%						
ASTM C 618–15	LOI	≤10%	2.9%	2.9%	1.7%	1.7%						
ASTM C 618–15	>45 μm	≤34%	29.5%	7.0%	***39.8%***	15.4%						
ASTM C 618–15	SAI 7 days	≥75%	78%	81%	***42%***	***46%***						
ASTM C 618–15	SAI 28 days	≥75%	86%	90%	***44%***	***51%***						
ASTM C 618–15	Water demand	Max 15%>REF	3.6%	5.5%	-3.9%	1.6%						

**The excessive SO_3 content in the final binder is due to the high SO_3 content in CEM I (3.9%). The SO_3 content in all wastes did not exceed 3.3%.*

All binders satisfied the initial setting time requirement of EN 197-1 (≥75 minutes). The compressive strength criterion (≥32.5 MPa at 28 days) was met by all binders except those incorporating recycled porcelain (RP and RPU), which exhibited lower strength (26.8 and 30.9 MPa, respectively). This reduction is attributed to the presence of surfactant contaminants in porcelain waste, as discussed in Chapter 4.

The loss on ignition (LOI) values of all binders complied with the EN 197-1 limit of ≤5%, except CS105 (6.4%), which slightly exceeded the threshold. However, the SO_3 content in the final binders, containing mixed screening waste and terracotta powders slightly exceeded the EN 197-1 limit of 3.5%. This excess is not due to the waste materials themselves but results from the high SO_3 level in the reference CEM I cement (3.9%) used in the blends. The SO_3 content of all waste powders was below 3.3%, and their contribution to the total sulphate content in the binder is considered acceptable.

Regarding ASTM C 618–15, both ceramic materials (RT and RP) fulfilled the key compositional requirement of ≥70% combined SiO_2, Al_2O_3, and Fe_2O_3. Their LOI and SO_3 contents were also well within permissible limits. Terracotta waste showed excellent pozzolanic reactivity, with strength activity indices (SAI) at 7 and 28 days exceeding 75%. In contrast, RP and RPU demonstrated insufficient pozzolanic activity (SAI < 51%), again due to the presence of surfactants. Additionally, particle fineness for RP did not meet the ASTM requirement of ≤34% particle with size >45 μm.

In the case of EN 197-6, which governs the use of concrete fines in cement production, only concrete screening waste (CS) is eligible for assessment, as it originates solely from crushed concrete. The other concrete-based powders (MS, WM) include mixed demolition waste and contain more than 10% non-concrete constituents and are therefore excluded under the standard.

CS met the sulphate content limit of <2.0% for concrete fines, with a measured SO_3 content of 0.8%. However, the clay content, estimated at approximately 5% of chlorites, exceeded the EN 197-6 threshold of 1.2%. For final cements incorporating 20% concrete fines, EN 197-6 requires the total SO_3 to remain below 4%, which was met in all CS-containing blends (3.3%). Other standard criteria, such as chloride content and organic matter, could not be evaluated in this study due to the lack of testing.

Overall, the findings demonstrate that most studied waste materials conform to the relevant compositional and performance standards. Terracotta demolition waste exhibits good pozzolanic properties and mechanical performance. Porcelain waste requires pretreatment for surfactant removal. The research showed that the presence of approximately 40% ceramic particles in concrete waste does not negatively affect the mechanical properties of the final cement and even contributes to improved durability. Therefore, the current exclusion of ceramic-containing waste in EN 197-6 appears overly restrictive. A revision of the standard, or the development of supplementary criteria for mixed demolition waste, would better reflect the realities of urban waste recycling and promote more sustainable material use in cementitious systems.

7.1.3. Comparison of mortars properties

Table 7.2 presents the main characteristics of mortar specimens incorporating various SCMs at a 20% replacement level. The data include physical properties (packing density and capillary absorption), pozzolanic activity, drying shrinkage, compressive strength at different ages, and durability performance under freeze-thaw cycles, fire exposure, and sulfuric acid attack. These parameters will be used in the subsequent MANOVA analysis to assess the influence of different factors on mortars strength development and durability.

Table 7.2. Key properties of mortars with various recycled powders.

Property	**REF**	**CS105**	**MS105**	**WM105**	**CS500**	**MS500**	**WM500**	**RT**	**RTU**
Packing density	0.855	0.832	0.824	0.838	0.83	0.821	0.823	0.835	0.868
Pozzolanic activity, mg/g	-	216	326	249	306	395	353	505	618
Shrinkage, μm	-122	-126	-115	-133	-111	-101	-114	-105	-100
Capillary absorption, g/mm^2	0.0038	0.0054	0.0054	0.0058	0.004	0.0051	0.0055	0.0041	0.0038
7 days strength, MPa	50.87	38.98	39.15	37.93	41.65	41.01	41.08	39.57	41.37
28 days strength, MPa	60.22	50.19	49.56	47.79	53.45	52.28	51.38	51.78	54.46
90 days strength, MPa	65.94	55.84	56.1	53.09	59.47	57.88	56.44	64.2	68.24
Freeze-thaw strength loss, %	6.3	8.5	4.4	5.3	6	4.7	6.5	2.2	1.9
H_2SO_4 strength loss, %	9.3	8.7	7.3	8.5	12.5	9.8	11.7	4.8	3
200 °C strength loss, %	4.8	7.8	0.5	-5.6	3.9	1.7	-14.4	-11.7	-13
300 °C strength loss, %	20.7	22	18.3	14.2	12.2	10	-6	-3.7	-6.7
500 °C strength loss, %	31.9	35.2	31.8	27.9	32.6	35	19.8	24.4	28
900 °C strength loss, %	90	92.2	90.6	89	90.6	91	89.8	80.6	72

Packing density

The highest packing density was observed in the specimen RTU, which contains ultrafine terracotta powder. This is attributed to the superior fineness and granulometric distribution of this powder, which enhances particle packing and reduces interparticle voids. The mortars with other SCMs demonstrated relatively similar packing densities, slightly lower than that of the reference mortar (REF), likely due to their coarser particle size distributions.

Pozzolanic activity

The pozzolanic activity values depend on the content of ceramic particles and their fineness in the investigated materials. The ultrafine ceramic powder RTU exhibited the highest pozzolanic activity, followed by RT; both are rich in reactive aluminosilicates, with RTU characterized by higher fineness than RT. Among the concrete-based SCMs, mixed MS and WM powders showed minor activity due to the presence of ceramic phases in their composition. Finally, CS powders exhibited the lowest pozzolanic activity, which is attributed to their low silica and alumina content. Calcination moderately enhanced the pozzolanic activity of the demolition waste powders, likely due to the removal of organic matter and improved surface exposure of reactive components.

Capillary absorption

Capillary absorption values were lowest for CS500, RT, and RTU, approaching those of the REF mortar. This suggests relatively low open porosity and refined pore structure, likely resulting from the hydraulic or pozzolanic activity of these additives. In contrast, mortars incorporating uncalcined concrete-based powders exhibited higher capillary absorption, probably due to their inertness and insufficient microstructural densification.

Drying shrinkage

Shrinkage measurements revealed that mortars incorporating ceramic powders RT and RTU, as well as mixed concrete-ceramic powders MS105 and MS500, exhibited the lowest drying shrinkage. This effect can be attributed to the pozzolanic activity of these materials, which contributes to pore structure refinement, reduces the proportion of gel pores due to C-S-H gel modification, and lowers capillary tension during drying. In contrast, mortars containing uncalcined concrete-based waste powders, CS105 and WM105, showed the highest shrinkage, likely due to their lower reactivity and higher porosity, which facilitates moisture loss.

Compressive strength

The reference mortar exhibited the highest 7-day compressive strength due to the hydraulic activity of Portland cement. At early age, the strength ranking was REF > CS500 > RTU > WM500 > MS500 > RT > MS105 > CS105 > WM105, illustrating the contribution of both hydraulic reactivity and packing density. At 28 days, the development of pozzolanic reactions became evident: REF > RTU > CS500 > MS500 > RT > WM500 > CS105 > MS105 > WM105. By 90 days, pozzolanic reactions dominated the strength profile, with RTU surpassing REF, followed by RT > CS500 > MS500 > WM500 > MS105 > CS105 > WM105. Mortars containing uncalcined concrete-based powders consistently showed lower strengths at all ages, confirming their limited reactivity. In contrast, specimens with pozzolanic terracotta-based SCMs demonstrated significant strength gain over time.

Freeze-thaw resistance

Mortars incorporating ceramic-containing powders RT, RTU, and MS105 demonstrated improved freeze-thaw resistance, which may be attributed to better microstructure due to pozzolanic reactions and better compatibility in the coefficient of thermal expansion (CTE) between the cementitious matrix and the fine aggregates. Mortars with other concrete-based powders exhibited resistance comparable to that of the reference specimen, regardless of whether the powders were thermally activated.

Fire resistance

Fire resistance analysis revealed strength gains at temperatures up to 300 °C in specimens WM500, RT, and RTU. For RT and RTU, this behaviour is attributed to the enhancement of pozzolanic reactions at elevated temperatures. The strength gain observed in WM500 may be related to its specific mineralogical composition, particularly the presence of alumina-rich phases; however, further investigation of the microstructural and compositional changes during heating is necessary to confirm this. At higher temperatures (500–900 °C), RT and RTU maintained the highest residual strengths, whereas CS105 exhibited the most severe degradation. The superior thermal performance of terracotta- and washing mud-based mortars is likely associated with their high content of refractory oxide Al_2O_3, which enhances thermal stability, as well as improved compatibility in the coefficient of thermal expansion.

Sulfuric acid resistance

Sulfuric acid resistance followed the order RTU > RT > MS105 > WM105 > CS105 > REF > MS500 > WM500 > CS500. Ceramic-containing mortars showed enhanced resistance due to portlandite consumption during pozzolanic reactions and the formation of a denser matrix. Thermal activation of concrete-based wastes reduced acid resistance, possibly due to increased reactivity and basicity.

Overall, terracotta SCMs, particularly the ultrafine powder (RTU), demonstrated the most promising performance across all evaluated criteria. These materials contribute not only to long-term strength development but also to enhanced durability against thermal and chemical stresses, indicating their suitability as effective SCMs for sustainable cementitious systems.

7.1.4. Comprehensive statistical analysis

Factors influencing compressive strength development

To identify the key factors influencing compressive strength development at different curing ages, a multivariate analysis of variance (MANOVA) was performed using compressive strengths at 7, 28, and 90 days as the dependent variables. The independent variables included waste type, packing density, drying shrinkage, capillary absorption and pozzolanic activity of the additives.

The results given in the Table 7.3 demonstrate that waste type had a statistically significant effect on the compressive strength profile (Pillai's trace = 1.563, $p = 1.95\times10^{-5}$), indicating that the nature of the SCM, whether concrete, mixed concrete-ceramic, washing mud, or terracotta, substantially influences strength development over time. This confirms the critical role of SCM composition in both early and long-term mechanical performance.

Table 7.3. MANOVA results for the effect of different parameters on compressive strength development.

Independent factor	Df[1]	Pillai[2]	Approx F[3]	Num Df[4]	Den Df[5]	Pr(>F)[6]
Waste type	3	1.563	5.807	9	48	$1.95 \cdot 10^{-5}$
Packing density	1	0.044	0.212	3	14	0.89
Pozzolanic activity	1	0.935	67.417	3	14	$5.41 \cdot 10^{-7}$
Shrinkage	1	0.891	38.203	3	14	0.03
Capillary adsorption	1	0.457	3.921	3	14	$1.46 \cdot 10^{-8}$

[1]*Df* – Degrees of freedom associated with the independent factor.

[2]*Pillai* – Pillai's trace statistic, a multivariate test statistic indicating the proportion of explained variance; higher values suggest a stronger multivariate effect.

[3]*Approx F* – Approximate F-value, used to test the statistical significance of the multivariate effect; calculated based on the Pillai trace.

[4]*Num Df* – Numerator degrees of freedom for the F-distribution, related to the number of dependent variables.

[5]*Den Df* – Denominator degrees of freedom for the F-distribution, related to the residuals in the multivariate model.

[6]*Pr(>F)* – p-value indicating the probability of observing the given F-value under the null hypothesis; lower values (typically < 0.05) indicate statistically significant effects.

Pozzolanic activity emerged as the most influential factor (Pillai's trace = 0.935, p = 5.41×10^{-7}), reflecting its strong contribution to strength gain through secondary hydration reactions. Similarly, drying shrinkage was also a significant predictor (Pillai's trace = 0.891, p = 0.03), suggesting a possible relationship between microstructural evolution and mechanical behaviour. The relationship between shrinkage and strength may also result from the densifying effect of pozzolanic reactions, which reduces shrinkage and improves strength simultaneously.

Capillary absorption also had a statistically significant effect (Pillai's trace = 0.457, p = 1.46×10^{-8}) since pore structure refinement, as reflected in reduced water uptake, contributes positively to compressive strength.

In contrast, packing density showed no significant influence on strength development (Pillai's trace = 0.044, p = 0.89). This result is likely due to the limited variability in particle size distribution among the analysed mortars, which resulted in only minor differences in packing density and, consequently, minimal impact on strength-related parameters.

Factors influencing durability performance

To assess the combined influence of different compositional and physical parameters on durability performance, a multivariate analysis of variance was conducted using six dependent variables: residual compressive strengths after freeze-thaw tests, exposure to sulfuric acid and thermal

exposure at 200, 300, 500, and 900 °C. The independent variables included waste type, packing density, drying shrinkage, capillary absorption, pozzolanic activity, and compressive strengths at 7, 28, and 90 days. The results are presented in Table 7.4.

Table 7.4. MANOVA results for the effect of different parameters on durability performance.

Independent factor	Df[1]	Pillai[2]	Approx F[3]	Num Df[4]	Den Df[5]	Pr(>F)[6]
Waste type	3	2.816	25.519	18	30	$1.98 \cdot 10^{-13}$
Packing density	1	0.479	1.225	6	8	0.38
Pozzolanic activity	1	0.991	145.500	6	8	$1.01 \cdot 10^{-7}$
Shrinkage	1	0.982	74.356	6	8	$1.40 \cdot 10^{-6}$
Capillary adsorption	1	0.956	29.105	6	8	$5.14 \cdot 10^{-5}$
7 days strength	1	0.846	7.330	6	8	0.01
28 days strength	1	0.830	6.528	6	8	0.01
90 days strength	1	0.961	32.726	6	8	$3.31 \cdot 10^{-5}$

[1]*Df* – Degrees of freedom associated with the independent factor.

[2]*Pillai* – Pillai's trace statistic, a multivariate test statistic indicating the proportion of explained variance; higher values suggest a stronger multivariate effect.

[3]*Approx F* – Approximate F-value, used to test the statistical significance of the multivariate effect; calculated based on the Pillai trace.

[4]*Num Df* – Numerator degrees of freedom for the F-distribution, related to the number of dependent variables.

[5]*Den Df* – Denominator degrees of freedom for the F-distribution, related to the residuals in the multivariate model.

[6]*Pr(>F)* – p-value indicating the probability of observing the given F-value under the null hypothesis; lower values (typically < 0.05) indicate statistically significant effects.

The analysis revealed that waste type had a highly significant multivariate effect on durability-related properties (Pillai's trace = 2.816, $p = 1.98 \times 10^{-13}$). This indicates that the nature of the SCM strongly influences performance under aggressive conditions such as freeze-thaw cycles, sulfuric acid attack, and high-temperature exposure. This result highlights the importance of material composition and mineralogical characteristics in durability-related behaviour.

Among the continuous predictors, pozzolanic activity had the strongest effect (Pillai's trace = 0.991, $p = 1.01 \times 10^{-7}$), suggesting that increased pozzolanic reactivity significantly improves the material's resistance to environmental degradation. This is consistent with the known role of pozzolanic reactions in refining pore structure and reducing portlandite content.

Drying shrinkage was also a significant factor (Pillai's trace = 0.982, $p = 1.40 \times 10^{-6}$), supporting the idea that microstructural integrity and internal stresses developed during drying are closely linked to long-term durability. Shrinkage reflects the material's potential for increased permeability and susceptibility to cracking.

Similarly, capillary absorption (Pillai's trace = 0.956, $p = 5.14\times10^{-5}$) was significantly associated with durability outcomes. This result underscores the role of open porosity and water transport mechanisms in determining the resistance of mortars to aggressive media and thermal stress.

The inclusion of compressive strengths at 7, 28, and 90 days as independent variables yielded statistically significant effects. Among these, long-term strength at 90 days (Pillai's trace = 0.961, $p = 3.31\times10^{-5}$) showed the strongest correlation with durability performance, highlighting its greater importance likely due to ongoing microstructural development via pozzolanic reactions and formation of stable hydration products. The strengths at 7 and 28 days exhibited similar levels of significance (Pillai's trace = 0.846 and 0.830, p = 0.01 for both) and are considered equally relevant predictors of durability in the earlier stages.

In contrast, packing density did not show a significant multivariate effect (Pillai's trace = 0.479, p = 0.38). This result is likely due to the relatively narrow range of particle size distributions in the tested mortars, leading to only minor differences in packing behaviour. Consequently, its influence on durability was overshadowed by more relevant parameters such as pozzolanic reactivity, open porosity, and strength development.

It is also noteworthy that ANOVA assessing the effect of drying shrinkage on the durability of mortars containing concrete-based wastes did not reveal any statistically significant relationship (Table 5.3). In contrast, MANOVA that included both concrete-based and ceramic powders indicated a strong influence of shrinkage on durability-related properties (Table 7.4). Furthermore, when the analysis was limited to ceramic powders only (Table 6.4), the observed effect of shrinkage on durability was smaller than in the combined analysis of all powder types. This suggests that drying shrinkage is not an isolated factor but is strongly correlated with other independent variables, such as chemical reactivity, powders fineness or porosity. As a result, its effect on durability becomes evident only when these interdependent factors are considered together, as in multivariate analysis (MANOVA). In univariate analysis (ANOVA), where variables are examined individually, such combined effects remain undetected.

7.2. Review of recent research

Since the publication of the articles comprising this dissertation, a significant number of studies have been published by other researchers on the use of demolition waste in the production of CO_2-reduced cement, indicating the sustained interest of the scientific community in this topic.

Kim and Ubysz [310] explored the thermal activation of recycled concrete powder for partial cement replacement. They found that treatment at 800 °C resulted in the greatest improvements in mechanical properties, water absorption, and shrinkage resistance. However, overall performance declined with increasing OPC substitution rates and recycling cycles. Additionally, the authors estimated that concrete incorporating recycled powder treated at 800 °C could reduce the global warming potential by 5–22% compared to conventional concrete, although thermal activation may raise production costs.

Gholizadeh-Vayghan et al. [311] concluded that thermal treatment of recycled pastes above 350 °C was detrimental, as highly reactive powders interfered with the early hydration of major clinker phases. In particular, premature gypsum depletion before the peak of C_3S hydration led to higher levels of crystalline ettringite and AFm, which hindered hydrate formation and microstructure development, causing early setting and slower strength gain. Furthermore, the hydration products of recycled pastes appeared to have limited contribution to mechanical strength.

In contrast, Zanovello and Angulo [312] reported that dehydration at temperatures above 650 °C significantly reduced initial reactivity. Their findings suggest that, in terms of mechanical and environmental performance, the optimal activation range lies between 400 °C and 600 °C.

Xi et al. [313] investigated microstructural and phase transformations in thermally treated materials and their effects on hydration activity. They observed that incomplete decomposition of hydration products occurred up to 450 °C, while transformation of α-SiO_2 to β-SiO_2 at 1000 °C caused particle agglomeration, adversely affecting hydration and strength. The optimal activation temperature was identified as 750 °C, at which C–S–H transforms into α'L-C_2S, a more reactive form compared to its β and γ counterparts.

Similarly, Chen et al. [314] found 700 °C to be the most effective activation temperature. They also concluded that chemical activation using sodium hydroxide, sodium sulphate, or water glass had minimal impact on the reactivity of recycled concrete.

Zhai et al. [315] demonstrated that incorporating fly ash alongside recycled cement powders enhanced the performance of mortars through the formation of a new monocarbonate phase. They observed that replacing 10% of OPC with recycled powder notably reduced drying shrinkage, while higher replacement levels led to a looser microstructure and increased shrinkage. Life cycle analysis indicated reductions of 11.05% in cost and 15.33% in CO_2 emissions with 10% OPC substitution.

De Lima et al. [316] improved the properties of cementitious mixtures by combining CDW powders with metakaolin. Using 15–30% CDW and 35–20% metakaolin ensured effective pore refinement, lower water absorption, and maintained compressive strength at approximately 40 MPa.

Wei et al. [317] combined thermal activation at 700 °C with ultrafine grinding of recycled powders. This approach improved mechanical performance by promoting the formation of additional C–S–H and a minor amount of carboaluminate phases.

Zanovello et al. [318] enhanced paste performance not by increasing the fineness of recycled powders but by using micronized Portland cement. The resulting engineered recycled cement achieved early and late compressive strengths comparable to conventional OPC, despite containing only 20 wt% clinker. Moreover, thermal activation was performed at just 500 °C, and the carbon footprint was 40% lower than that of LC3.

Klemczak et al. [319] studied the use of recycled foam concrete, with and without microcapsules, as a partial cement replacement at 20% and 40% levels. Pastes with recycled foam concrete exhibited higher water demand, delayed setting, reduced hydration heat, lower strength, and increased shrinkage. The presence of microcapsules exacerbated these effects. However, thermal treatment at 750 °C mitigated or eliminated the adverse impacts of microcapsules, significantly increasing strength while also raising shrinkage and water demand, limiting practical applicability.

Subramanian et al. [320] found that recycled brick powder enhanced cement–sand adhesion due to its abrasive surface. They estimated that ceramic powder mixtures could reduce CO_2 emissions and energy consumption by 18% and 19%, respectively.

Koňáková et al. [321] examined ternary binders composed of 45% calcium aluminate cement, 40% reactive alumina, and 15% brick dust. The incorporation of ceramic powder in systems with reactive alumina enhanced strength despite increased porosity, indicating a synergistic effect. In a subsequent study [322], they evaluated the thermal behaviour of these composites with different proportions up to 1400 °C, confirming excellent durability. The combination of ceramics with reactive

alumina enabled the formation of high-temperature phases such as gehlenite, mullite and hibonite, contributing to thermal stability.

Despite growing interest, studies on the durability of binders containing CDW powders remain limited. Wei et al. [323] conducted freeze–thaw tests on concrete containing recycled powder, both untreated and thermally activated at 700 °C. Concrete with activated powder endured a higher number of freeze–thaw cycles than that with untreated material.

Getachew et al. [324] reported that mortars with recycled concrete powder activated at 700 °C exhibited superior resistance to sulphate attack after 90 days of curing, attributed to lower porosity and reduced alkali content.

Dehghani et al. [325] evaluated concrete paving blocks containing 10–30% ceramic waste as cement replacement. After 28 freeze–thaw cycles, mass loss was reduced by 40% in mixtures with 30% ceramic powder. Abrasion resistance remained largely unaffected. Life cycle analysis revealed that this mixture reduced impacts on water depletion, water consumption, freshwater ecotoxicity, and climate change by 24.65%, 23.57%, 20.04%, and 19.41%, respectively. These reductions were mainly attributed to decreased cement use during raw material sourcing.

Tawfik et al. [326] produced high-performance concrete using waste ceramic tile and brick powders. The optimal formulation involved 5% brick powder and 10% tile powder. However, sulphate resistance declined, possibly due to increased porosity.

In summary, there is no consensus yet on the optimal activation temperature for recycled concrete waste, underscoring the need for continued research and standardised methodologies. Moreover, the durability properties of binders incorporating demolition waste remain insufficiently studied, and comprehensive life cycle assessments are still lacking.

Chapter 8: Conclusion

8.1. Summary of key findings

This research explored the potential of various CDWs as supplementary cementitious materials for producing CO_2-reduced cements. Through a series of experimental studies, the chemical and physical characteristics of several CDW types, as well as their influence on the mortars properties, were systematically assessed. Particular attention was given to their pozzolanic reactivity, hydration behaviour, durability performance, and suitability for use in binary and LC3-type binders. The key findings and implications derived from this work are summarised below.

1. All tested CDW powders, except sanitary porcelain, are suitable for use as SCMs, as confirmed by their strength activity indices and compliance with standards requirements. Ultrafine terracotta powder demonstrated the highest effectiveness as an SCM due to its pozzolanic reactivity. However, the pozzolanic reactivity of waste ceramic powders is insufficient for complete replacement of calcined clay in LC3-50 formulation. Nevertheless, ultrafine terracotta powder can be used effectively in formulations with a lower level of clinker substitution. Sanitary porcelain, by contrast, contains surfactants that negatively affect strength and microstructure, and requires purification, for example by calcination at 500 °C, to become suitable for use.
2. Thermal activation at 500 °C slightly improves the reactivity of concrete-based CDWs, such as screening fines and wash mud. The presence of ceramic admixtures in concrete wastes did not influence their performance either before or after thermal activation; however, their content at 40% in CDW was insufficient to impart significant pozzolanic properties.
3. Thermal treatment of concrete-based powders does not improve durability and may even reduce acid resistance due to increased chemical reactivity and basicity. However, the presence of ceramic inclusions has a positive effect on drying shrinkage and durability properties.
4. Ceramic waste powders enhance the durability of cement mortars by improving resistance to freeze–thaw cycles, sulfuric acid attack, and high temperatures. These improvements are

attributed to the formation of pozzolanic reaction products that densify the matrix. The increasing ceramic powder fineness and addition of lime filler further strengthens this effect.

5. Mortars containing ceramic powders, as well as those with washing mud, which has the highest aluminium oxide content among the concrete-based CDWs, exhibited increased strength after exposure to temperatures up to 300 °C. In the case of ceramic powders, this is clearly explained by autoclave-like conditions that accelerate pozzolanic reactions. However, to accurately determine the mechanisms responsible for strength gain in mortars with washing mud, further investigation of their composition and microstructural changes during heating is required.
6. Statistical analysis confirmed that compressive strength and durability performance are primarily influenced by waste type and pozzolanic activity, while drying shrinkage and capillary absorption also have significant, though secondary, effects.

8.2. Contribution to the field

This research advances the scientific understanding of the potential use of real-world construction and demolition waste as supplementary cementitious materials for the production of CO_2-reduced cements. It contributes to the field in several key ways:

1. It provides a comparative evaluation of diverse real CDW types, including concrete screening fines, mixed screening fines, mud from recycled aggregate washing, terracotta roof tiles, and sanitary porcelain, highlighting their suitability, limitations, and required pre-treatment methods for use as SCMs in both binary and LC3-type binders.
2. It addresses existing research gaps by assessing the durability properties of binders containing CDWs under various aggressive conditions.
3. It applies statistical analysis to identify the dominant factors affecting strength and durability, confirming the critical roles of waste type and pozzolanic activity.

Together, these findings support the development of eco-efficient cementitious systems incorporating CDWs, contribute to the formulation of quality criteria for recycled powders, and promote sustainable resource utilization in the construction industry.

8.3. Practical implications

The findings of this research provide several insights that can inform practical applications in recycling, cement and construction industries:

1. Concrete-based CDWs can be effectively used to produce eco-cements for applications with moderate mechanical and durability performance requirements, such as non-structural elements, pavements, blocks, or screeds.
2. In such applications, there is no need to separate concrete waste from ceramic inclusions, simplifying the recycling process and reducing pre-treatment costs.
3. Pure ceramic powders are suitable for the production of high-strength and durable binders, provided that they are ground to a very fine granulometry to ensure sufficient pozzolanic reactivity.
4. When using separated ceramic waste types, such as sanitary porcelain, there is a risk of contamination with substances like surfactants. This highlights the need for quality control and purification procedures before integration into cementitious systems.
5. The use of CDWs as SCMs offers substantial environmental benefits, including the reduction of CO_2 emissions, diversion of waste from landfills, and conservation of natural raw materials such as limestone and clay.

8.4. Limitations and future research directions

Due to the limited time frame of the study, the present work provides only a preliminary evaluation of the feasibility of using various CDWs, including concrete screening fines, mixed screening fines, mud from recycled aggregate washing, terracotta roofing tiles, and sanitary porcelain, as SCMs in CO_2-reduced cement systems. While the obtained results are promising, several limitations remain, and further in-depth research is required to validate and expand upon the findings. In particular, the following research directions are suggested:

1. Long-term studies incorporating advanced microstructural techniques such as differential thermal and thermogravimetric analysis, X-ray diffraction, and scanning electron microscopy at various stages of exposure to aggressive environments are essential to monitor

degradation pathways, pozzolanic activity evolution, and the formation or transformation of hydration products.

2. As the formation of free lime becomes a risk when reactivating concrete waste at temperatures exceeding 500 °C, it is essential to evaluate the durability and long-term strength development of binders incorporating concrete waste treated at different activation temperatures.
3. A full cradle-to-grave life cycle assessment, including both midpoint and endpoint indicators, should be conducted to quantify the environmental and economic advantages of using CDW-based binders. Particular attention should be paid to the trade-offs introduced by thermal activation and additional processing steps, such as grinding and purification, which may offset CO_2 savings.
4. The current study is limited to paste and mortar scales. Further work should address the behaviour of these alternative binders in concrete formulations, particularly regarding binder–aggregate interactions, interfacial transition zone characteristics, shrinkage, cracking resistance, and mechanical performance under various curing regimes.
5. As it was found, sanitary ceramics can contain surfactants that may significantly increase porosity. Research into low-cost, scalable purification technologies, such as mild calcination or washing, is needed to ensure the chemical stability of ceramic waste-derived powders.
6. The potential synergistic behaviour between calcined clays and ceramic CDW should be explored further to develop more effective LC3 formulations. Studies should focus on determining optimal mixing ratios, assessing the impact on rheology, strength development and durability.
7. The substitution of conventional limestone filler in LC3 systems with finely ground concrete CDW powders presents a potential route for increasing recycled content. However, their impact on packing density, water demand, early hydration, mechanical and durability properties must be thoroughly evaluated.
8. Given the high variability in CDW composition and the potentially beneficial effects of ceramic particles on cement performance, future studies should aim to expand classification criteria and performance-based specifications for recycled powders. This includes reconsidering upper thresholds for ceramic constituents, which are typically

classified as contaminants, and incorporating granulometric parameters to better reflect material performance.

9. Finally, pilot-scale trials and industrial case studies are essential to assess the real-world applicability of CDW-based SCMs. This includes their handling, processing, performance in structural and non-structural elements, and overall feasibility within existing supply chains and regulatory frameworks.

List of figures

List of tables

References

[1] S.A. Miller, A. Horvath, P.J.M. Monteiro, Readily implementable techniques can cut annual CO_2 emissions from the production of concrete by over 20%, Environ. Res. Lett. 11 (2016) 074029, DOI 10.1088/1748-9326/11/7/074029.

[2] D. Cheng, D.M. Reiner, F. Yang, C. Cui, J. Meng, Y. Shan, Y. Liu, S. Tao, D. Guan, Projecting future carbon emissions from cement production in developing countries, Nat. Commun. 14 (2023) 8213, https://doi.org/10.1038/s41467-023-43660-x.

[3] R. Maddalena, J.J. Roberts, A. Hamilton, Can Portland cement be replaced by low-carbon alternative materials? A study on the thermal properties and carbon emissions of innovative cements, J. Clean. Prod. 186 (2018) 933-942, https://doi.org/10.1016/j.jclepro.2018.02.138.

[4] J. Södje, No cement production without refractories, in: H. Pöllmann (Ed.), Cementitious Materials, De Gruyter, Berlin, 2017, pp. 445-480. DOI 10.1515/9783110473728-016.

[5] M. Voldsund, S.O. Gardarsdottir, E. De Lena, J.E. Pérez-Calvo, A. Jamali, D. Berstad, C. Fu, M. Romano, S. Roussanaly, R. Anantharaman, H. Hoppe, D. Sutter, M. Mazzotti, M. Gazzani, G. Cinti, K. Jordal, Comparison of technologies for CO_2 capture from cement production—Part 1: Technical evaluation, Energies. 12 (2019) 559, https://doi.org/10.3390/en12030559.

[6] M.S. Imbabi, C. Carrigan, S. McKenna, Trends and developments in green cement and concrete technology, Int. J. Sustain. Built Environ. 1 (2012) 194-216, https://doi.org/10.1016/j.ijsbe.2013.05.001.

[7] J. Farfan, M. Fasihi, C. Breyer, Trends in the global cement industry and opportunities for long-term sustainable CCU potential for Power-to-X, J. Clean. Prod. 217 (2019) 821-835, https://doi.org/10.1016/j.jclepro.2019.01.226.

[8] Global Carbon Budget (2024) – with major processing by Our World in Data. "Annual CO_2 emissions from cement – GCB" [dataset]. Global Carbon Project, "Global Carbon Budget" [original data]. Retrieved February 3, 2025 from https://ourworldindata.org/grapher/annual-co2-cement.

[9] E. Worrell, L. Price, N. Martin, C. Hendriks, L.O. Meida, Carbon dioxide emissions from the global cement industry, Annu. Rev. Energy Environ. 26 (2001) 303–329, https://doi.org/10.1146/annurev.energy.26.1.303.

[10] M. Schneider, The cement industry on the way to a low-carbon future, Cem. Concr. Res. 124 (2019) 105792, https://doi.org/10.1016/j.cemconres.2019.105792.

[11] K.L. Scrivener, V.M. John, E.M. Gartner, Eco-efficient cements: Potential economically viable solutions for a low-CO2 cement-based materials industry, Cem. Concr. Res. 114 (2018) 2-26, https://doi.org/10.1016/j.cemconres.2018.03.015.

[12] P. Stemmermann, New CO2-reduced cementitious systems, in: H. Pöllmann (Ed.), Cementitious Materials, De Gruyter, Berlin, 2017, pp. 333-352, DOI 10.1515/9783110473728-012.

[13] EN 197-1:2011, Cement – Part 1: Composition, specifications and conformity criteria for common cements.

[14] B. Lothenbach, K. Scrivener, R.D. Hooton, Supplementary cementitious materials, Cem. Concr. Res. 41 (2011) 1244-1256, https://doi.org/10.1016/j.cemconres.2010.12.001.

[15] H.F.W. Taylor, Cement Chemistry, Academic Press, London, 1990.

[16] R. Siddique, M.I. Khan, Supplementary Cementing Materials, Springer, Berlin, 2011, DOI 10.1007/978-3-642-17866-5.

[17] R. Snellings, G. Mertens, J. Elsen, Supplementary Cementitious Materials, Rev. Mineral. Geochem. 74 (2012) 211–278, https://doi.org/10.2138/rmg.2012.74.6.

[18] J. Skibsted, R. Snellings, Reactivity of supplementary cementitious materials (SCMs) in cement blends, Cem. Concr. Res. 124 (2019) 105799, https://doi.org/10.1016/j.cemconres.2019.105799.

[19] R. Lewis, L. Sear, P. Wainwright, R. Ryle, Cementitious additions, in: J. Newman, B.S. Choo (Eds.), Advanced Concrete Technology Set, Elsevier, Oxford, 2003, pp. 3/3-3/66, https://doi.org/10.1016/B978-0-7506-5686-3.X5246-X.

[20] W. Kurdowski, Cement and Concrete Chemistry, Springer, 2014, DOI 10.1007/978-94-007-7945-7.

[21] M. Moranville-Regourd, S. Kamali-Bernard, Cements Made from Blastfurnace Slag, in: P.C. Hewlett, M. Liska (Eds.), Lea's Chemistry of Cement and Concrete (Fifth Edition), Butterworth-Heinemann, 2019, pp. 469-507, https://doi.org/10.1016/B978-0-08-100773-0.00010-1.

[22] P.K. Gahlot, S.S. Sankhla, K.K. Saini, Use of GGBS as partial replacement of cement in concrete while using Master REHO Build 823PQ, Int. J. Eng. Adv. Technol. 9 (2020) 4323-4329, DOI: 10.35940/ijeat.C6523.029320.

[23] B. Pacewska, I. Wilińska, Usage of supplementary cementitious materials: advantages and limitations, J. Therm. Anal. Calorim. 142 (2020) 371–393, https://doi.org/10.1007/s10973-020-09907-1.

[24] B. Klemczak, M. Batog, Heat of hydration of low-clinker cements, J. Therm. Anal. Calorim. 123 (2016) 1351–1360, https://doi.org/10.1007/s10973-015-4782-y.

[25] Ç. Yalçınkaya, O. Çopuroğlu, Hydration heat, strength and microstructure characteristics of UHPC containing blast furnace slag, J. Build. Eng. 34 (2021) 101915, https://doi.org/10.1016/j.jobe.2020.101915.

[26] K. Tang, S. Millard, G. Beattie, Early-age heat development in GGBS concrete structures, Proc. Inst. Civ. Eng. Struct. Build. 168 (2015) 541-553, https://doi.org/10.1680/stbu.14.00089.

[27] J. Sun, K.H. Kong, C.Q. Lye, S.T. Quek, Effect of ground granulated blast furnace slag on cement hydration and autogenous healing of concrete, Constr. Build. Mater. 315 (2022) 125365, https://doi.org/10.1016/j.conbuildmat.2021.125365.

[28] P.C.R.A. Abrão, F.A. Cardoso, V.M. John, Efficiency of Portland-pozzolana cements: Water demand, chemical reactivity and environmental impact, Constr. Build. Mater. 247 (2020) 118546, https://doi.org/10.1016/j.conbuildmat.2020.118546.

[29] M.J. McCarthy, T.D. Dye, Pozzolanas and Pozzolanic Materials, in: P.C. Hewlett, M. Liska (Eds.), Lea's Chemistry of Cement and Concrete (Fifth Edition), Butterworth-Heinemann, 2019, pp. 363-467, https://doi.org/10.1016/B978-0-08-100773-0.00009-5.

[30] R. Cai, Z. Tian, H. Ye, Z. He, S. Tang, The role of metakaolin in pore structure evolution of Portland cement pastes revealed by an impedance approach, Cem. Concr. Compos. 119 (2021) 103999, https://doi.org/10.1016/j.cemconcomp.2021.103999.

[31] J. Feng, J. Sun, P. Yan, The influence of ground fly ash on cement hydration and mechanical property of mortar, Adv. Civ. Eng. 2018 (2018) 4023178, https://doi.org/10.1155/2018/4023178.

[32] R.U.D. Nassar, S. Room, Comparison of the performance of class-C and class-F fly ash concrete mixtures produced with crushed stone sand, Mater. Today Proc. (2023), https://doi.org/10.1016/j.matpr.2023.03.510.

[33] R. Rumman, M.S. Alam, Does wood fly ash (WFA) have pozzolanic property? A study on low- and high-temperature partially burnt WFA compared to classes C and F coal fly ash (CFA), Constr. Build. Mater. 471 (2025) 140700, https://doi.org/10.1016/j.conbuildmat.2025.140700.

[34] L. Black, Low clinker cement as a sustainable construction material, in: J.M. Khatib (Ed.), Sustainability of Construction Materials, 2nd ed., Woodhead Publ., 2016, pp. 415–457, https://doi.org/10.1016/B978-0-08-100370-1.00017-2.

[35] R. Lewis, P. Fidjestøl, Microsilica as an Addition, in: P.C. Hewlett, M. Liska (Eds.), Lea's Chemistry of Cement and Concrete (Fifth Edition), Butterworth-Heinemann, 2019, pp. 509-535, https://doi.org/10.1016/B978-0-08-100773-0.00011-3.

[36] G. Moir, Cements, in: J. Newman, B.S. Choo (Eds.), Advanced Concrete Technology Set, Elsevier, Oxford, 2003, pp. 1/3-1/45, https://doi.org/10.1016/B978-0-7506-5686-3.X5246-X.

[37] D.A. Silva, H.R. Wenk, P.J.M. Monteiro, Comparative investigation of mortars from Roman Colosseum and cistern, Thermochim. Acta 438 (2005) 35–40, https://doi.org/10.1016/j.tca.2005.03.003.

[38] J.M. Khatib, O. Baalbaki, A.A. ElKordi, Metakaolin, in: R. Siddique, P. Cachim (Eds.), Waste and Supplementary Cementitious Materials in Concrete, Woodhead Publ., 2018, pp. 493–511, https://doi.org/10.1016/B978-0-08-102156-9.00015-8.

[39] K. Scrivener, F. Martirena, S. Bishnoi, S. Maity, Calcined clay limestone cements (LC3), Cem. Concr. Res. 114 (2018) 49–56, https://doi.org/10.1016/j.cemconres.2017.08.017.

[40] M.C.G. Juenger, R. Snellings, S.A. Bernal, Supplementary cementitious materials: New sources, characterization, and performance insights, Cem. Concr. Res. 122 (2019) 257–273, https://doi.org/10.1016/j.cemconres.2019.05.008.

[41] B.L. Damineli, R.G. Pileggi, B. Lagerblad, V.M. John, Effects of filler mineralogy on the compressive strength of cementitious mortars, Constr. Build. Mater. 299 (2021) 124363, https://doi.org/10.1016/j.conbuildmat.2021.124363.

[42] T. Oey, A. Kumar, J.W. Bullard, N. Neithalath, G. Sant, The filler effect: The influence of filler content and surface area on cementitious reaction rates, J. Am. Ceram. Soc. 96 [6] (2013) 1978–1990, https://doi.org/10.1111/jace.12264.

[43] K.L. Scrivener, P. Juilland, P.J.M. Monteiro, Advances in understanding hydration of Portland cement, Cem. Concr. Res. 78, Part A (2015) 38–56, https://doi.org/10.1016/j.cemconres.2015.05.025.

[44] M. Aqel, D. Panesar, Physical and chemical effects of limestone filler on the hydration of steam cured cement paste and mortar, Rev. ALCONPAT 10 (2) (2020) 191–205, https://doi.org/10.21041/ra.v10i2.481.

[45] L. Zongshou, X. Weihong, C. Wie, Cementitious Materials Science, De Gruyter, 2019.

[46] S. Mindess, Sustainability of concrete, in: S. Mindess (Ed.), Developments in the Formulation and Reinforcement of Concrete, 2nd ed., Woodhead Publ., 2019, pp. 3–17, https://doi.org/10.1016/B978-0-08-102616-8.00001-0.

[47] P.J.M. Monteiro, G. Geng, D. Marchon, J. Li, P. Alapati, K.E. Kurtis, M.J. Abdolhosseini Qomi, Advances in characterizing and understanding the microstructure of cementitious materials, Cem. Concr. Res. 124 (2019) 105806, https://doi.org/10.1016/j.cemconres.2019.105806.

[48] V.M. John, B.L. Damineli, M. Quattrone, R.G. Pileggi, Fillers in cementitious materials — Experience, recent advances and future potential, Cem. Concr. Res. 114 (2018) 65–78, https://doi.org/10.1016/j.cemconres.2017.09.013.

[49] F. Zunino, K. Scrivener, The reaction between metakaolin and limestone and its effect in porosity refinement and mechanical properties, Cem. Concr. Res. 140 (2021) 106307, https://doi.org/10.1016/j.cemconres.2020.106307.

[50] Eurostat, Waste statistics, Statistics Explained, European Commission, 2024. https://ec.europa.eu/eurostat/statistics-explained/index.php?title=Waste_statistics (accessed 18 April 2025).

[51] E. Vazquez (Ed.), Progress of Recycling in the Built Environment: Final Report of the RILEM Technical Committee 217-PRE, Springer, 2013, DOI 10.1007/978-94-007-4908-5.

[52] F. Pacheco-Torgal, V.W.Y. Tam, J.A. Labrincha, Y. Ding, J. de Brito (Eds.), Handbook of Recycled Concrete and Demolition Waste, Woodhead Publishing, Cambridge, 2013.

[53] M. Pepe, A Conceptual Model for Designing Recycled Aggregate Concrete for Structural Applications, Springer, 2015, DOI 10.1007/978-3-319-26473-8.

[54] C. Medina Martinez, I.F. Sáez del Bosque, G. Medina, M. Frías, M.I. Sánchez de Rojas, Fillers and additions from industrial waste for recycled aggregate concrete, in: P.O. Awoyera, C. Thomas, M.S. Kirgiz (Eds.), The Structural Integrity of Recycled Aggregate Concrete Produced with Fillers and Pozzolans, Woodhead Publ., 2022, pp. 105–143, https://doi.org/10.1016/B978-0-12-824105-9.00012-3.

[55] A.E.B. Cabral, Concrete with construction and demolition wastes (CDW), in: F. Pacheco-Torgal, S. Jalali, J. Labrincha, V.M. John (Eds.), Eco-Efficient Concrete, Woodhead Publ., 2013, pp. 340–367, https://doi.org/10.1533/9780857098993.3.340.

[56] M.S. Kırgız, Water requirement for recycled concrete, in: P.O. Awoyera, C. Thomas, M.S. Kırgız (Eds.), The Structural Integrity of Recycled Aggregate Concrete Produced with Fillers and Pozzolans, Woodhead Publ., 2022, pp. 253–272, https://doi.org/10.1016/B978-0-12-824105-9.00005-6.

[57] EN 12620:2002+A1:2008, Aggregates for Concrete.

[58] F. Agrela, P. Alaejos, C. Thomas, J. Rueda, R.V. Silva, J. Moreno-Juez, M.A. Sanjuán, J. de Brito, M.I. Sánchez de Rojas, Normative review and necessary advances to promote the use of recycled aggregates and by-products in cement-based materials, in: J. de Brito, C. Thomas, C. Medina, F. Agrela (Eds.), Waste and Byproducts in Cement-Based Materials, Woodhead Publ., 2021, pp. 735–776, https://doi.org/10.1016/B978-0-12-820549-5.00001-2.

[59] Y. Villagrán-Zaccardi, E. Sosa, L. Carrizo, C. Zega, Use of recycled fines from waste concrete as an admixture in new concrete, in: P.O. Awoyera, C. Thomas, M.S. Kırgız (Eds.), The Structural Integrity of Recycled Aggregate Concrete Produced with Fillers and Pozzolans, Woodhead Publ., 2022, pp. 39–65, https://doi.org/10.1016/B978-0-12-824105-9.00020-2.

[60] B. González-Fonteboa, F. Lopez Gayarre, J. Vera-Agulló, M. Casado, C. Medina, Real-scale applications of waste in cement-based materials in building, in: J. de Brito, C. Thomas, C. Medina, F. Agrela (Eds.), Waste and Byproducts in Cement-Based Materials, Woodhead Publ., 2021, pp. 681–713, https://doi.org/10.1016/B978-0-12-820549-5.00014-0.

[61] A. Juan-Valdés, J. García-González, M.I. Guerra-Romero, J. Ma Morán-del Pozo, R. Martínez-García, Macroscopic mechanical characterization of self-compacting recycled concrete mixed with natural lime filler, in: P.O. Awoyera, C. Thomas, M.S. Kırgız (Eds.), The Structural Integrity of Recycled Aggregate Concrete Produced with Fillers and Pozzolans, Woodhead Publ., 2022, pp. 303–322, https://doi.org/10.1016/B978-0-12-824105-9.00016-0.

[62] P.O. Awoyera, P. Perumal, K. Ohenoja, I. Mansouri, Upcycling CO2 for enhanced performance of recycled aggregate concrete and modeling of properties, in: P.O. Awoyera, C. Thomas, M.S. Kırgız (Eds.), The Structural Integrity of Recycled Aggregate Concrete Produced with Fillers and Pozzolans, Woodhead Publ., 2022, pp. 349–364, https://doi.org/10.1016/B978-0-12-824105-9.00017-2.

[63] H.M. Magbool, Utilisation of ceramic waste aggregate and its effect on Eco-friendly concrete: A review, J. Build. Eng., 47 (2022) 103815, https://doi.org/10.1016/j.jobe.2021.103815.

[64] S. Ray, M. Haque, M.N. Sakib, A.F. Mita, M.D.M. Rahman, B.B. Tanmoy, Use of ceramic wastes as aggregates in concrete production: A review, J. Build. Eng., 43 (2021) 102567, https://doi.org/10.1016/j.jobe.2021.102567.

[65] M.V.A. Florea, Z. Ning, H.J.H. Brouwers, Smart crushing of concrete and activation of liberated concrete fines, Report, Eindhoven University of Technology, Department of the Built Environment, Unit Building Physics and Services, 2012.

[66] P.O. Awoyera, M.S. Kırgız, Mineralogy and interfacial transition zone features of recycled aggregate concrete, in: P.O. Awoyera, C. Thomas, M.S. Kırgız (Eds.), The Structural Integrity of Recycled Aggregate Concrete Produced with Fillers and Pozzolans, Woodhead Publ., 2022, pp. 243–251. https://doi.org/10.1016/B978-0-12-824105-9.00013-5.

[67] J.H.A. Rocha, R. Dias Toledo Filho, The utilization of recycled concrete powder as supplementary cementitious material in cement-based materials: A systematic literature review, J. Build. Eng., 76 (2023) 107319, https://doi.org/10.1016/j.jobe.2023.107319.

[68] Y. Yang, Z. Kang, B. Zhan, P. Gao, Q. Yu, J. Wang, W. Zhao, Y. Zhang, W. Bi, C. Yang, A short review on the application of recycled powder in cement-based materials: Preparation, performance and activity excitation, Buildings 12 (2022) 1568, https://doi.org/10.3390/buildings12101568.

[69] L. De Brabandere, V. Grigorjev, P. Van den Heede, H. Nachtergaele, K. Degezelle, N. De Belie, Using fines from recycled high-quality concrete as a substitute for cement, Sustainability 17 (2025) 1506, https://doi.org/10.3390/su17041506.

[70] S. Li, J. Liu, C. Yu, et al., Study on the performance of ternary blended cement with calcined clay and recycled concrete powder, Low-carbon Mater. Green Constr. 2 (2024) 4, https://doi.org/10.1007/s44242-024-00035-9.

[71] M. Soomro, V.W.Y. Tam, M. Shigeishi, N.N. Kencanawati, T. Namihira, K. Kalinowska, Quality improvement of recycled aggregate, in: V.W.Y. Tam, M. Soomro, A.C.J. Evangelista (Eds.), Recycled Concrete, Woodhead Publishing, 2023, pp. 161–194, https://doi.org/10.1016/B978-0-323-85210-4.00004-7.

[72] H. Wu, C. Liu, Y. Zhao, G. Chen, J. Gao, Elucidating the role of recycled concrete powder in low-carbon ultra-high performance concrete (UHPC): Multi-performance evaluation, Constr. Build. Mater. 441 (2024) 137520, https://doi.org/10.1016/j.conbuildmat.2024.137520.

[73] Y.A. Villagrán-Zaccardi, A.T.M. Marsh, M.E. Sosa, C.J. Zega, N. De Belie, S.A. Bernal, Complete re-utilization of waste concretes – Valorisation pathways and research needs, Resour. Conserv. Recycl. 177 (2022) 105955, https://doi.org/10.1016/j.resconrec.2021.105955.

[74] C.-S. Poon, S. Azhar, M. Anson, Y.-L. Wong, Strength and durability recovery of fire-damaged concrete after post-fire-curing, Cem. Concr. Res. 31 (2001) 1307–1318, https://doi.org/10.1016/S0008-8846(01)00582-8.

[75] C. Wang, C. Chazallon, S. Braymand, P. Hornych, Thermogravimetric analysis (TGA) for characterization of self-cementation of recycled concrete aggregates in pavement, Thermochim. Acta 733 (2024) 179680, https://doi.org/10.1016/j.tca.2024.179680.

[76] Q. Zhang, G. Ye, E. Koenders, Investigation of the structure of heated Portland cement paste by using various techniques, Constr. Build. Mater. 38 (2013) 1040–1050, https://doi.org/10.1016/j.conbuildmat.2012.09.071.

[77] J.A. Bogas, S. Real, A. Carriço, J.C.C. Abrantes, M. Guedes, Hydration and phase development of recycled cement, Cem. Concr. Compos. 127 (2022) 104405, https://doi.org/10.1016/j.cemconcomp.2022.104405.

[78] C. Alonso, L. Fernandez, Dehydration and rehydration processes of cement paste exposed to high temperature environments, J. Mater. Sci. 39 (2004) 3015–3024, https://doi.org/10.1023/B:JMSC.0000025827.65956.18.

[79] A. Carriço, S. Real, J.A. Bogas, M.F.C. Pereira, Mortars with thermo activated recycled cement: Fresh and mechanical characterisation, Constr. Build. Mater. 256 (2020) 119502, https://doi.org/10.1016/j.conbuildmat.2020.119502.

[80] J.A. Bogas, A. Carriço, A.J. Tenza-Abril, Microstructure of thermoactivated recycled cement pastes, Cem. Concr. Res. 138 (2020) 106226, https://doi.org/10.1016/j.cemconres.2020.106226.

[81] R. Serpell, F. Zunino, Recycling of hydrated cement pastes by synthesis of α'H-C_2S, Cem. Concr. Res. 100 (2017) 398–412, https://doi.org/10.1016/j.cemconres.2017.08.001.

[82] J.A. Bogas, A. Carriço, M.F.C. Pereira, Mechanical characterization of thermal activated low-carbon recycled cement mortars, J. Clean. Prod. 218 (2019) 377–389, https://doi.org/10.101/10.1016/j.jclepro.2019.01.325.

[83] A. Carriço, J.A. Bogas, M. Guedes, Thermoactivated cementitious materials – A review, Constr. Build. Mater. 250 (2020) 118873, https://doi.org/10.1016/j.conbuildmat.2020.118873.

[84] P. Boch, J.-C. Niepce (Eds.), Ceramic Materials: Processes, Properties and Applications, ISTE, Chippenham, 2007, DOI:10.1002/9780470612415.

[85] European Commission, Reference Document on Best Available Techniques in the Ceramic Manufacturing Industry, 2007.

[86] J.V. de Almeida, Ceramics, in: M. Gonçalves, F. Margarido (Eds.), Materials for Construction and Civil Engineering, Springer, Cham, 2015, pp. 303–334, https://doi.org/10.1007/978-3-319-08236-3_7.

[87] L.A. Pereira-de-Oliveira, J.P. Castro-Gomes, P.M.S. Santos, The potential pozzolanic activity of glass and red-clay ceramic waste as cement mortars components, Constr. Build. Mater. 31 (2012) 197–203, https://doi.org/10.1016/j.conbuildmat.2011.12.110.

[88] L. Li, W. Liu, Q. You, M. Chen, Q. Zeng, Waste ceramic powder as a pozzolanic supplementary filler of cement for developing sustainable building materials, J. Clean. Prod. 259 (2020) 120853, https://doi.org/10.1016/j.jclepro.2020.120853.

[89] A. Alsaif, Utilization of ceramic waste as partially cement substitute – A review, Constr. Build. Mater. 300 (2021) 124009, https://doi.org/10.1016/j.conbuildmat.2021.124009.

[90] J. Shao, J. Gao, Y. Zhao, X. Chen, Study on the pozzolanic reaction of clay brick powder in blended cement pastes, Constr. Build. Mater. 213 (2019) 209–215, https://doi.org/10.1016/j.conbuildmat.2019.03.307.

[91] A.M. Pitarch, L. Reig, A.E. Tomás, G. Forcada, L. Soriano, M.V. Borrachero, J. Payá, J.M. Monzó, Pozzolanic activity of tiles, bricks and ceramic sanitary-ware in eco-friendly Portland blended cements, J. Clean. Prod. 279 (2021) 123713, https://doi.org/10.1016/j.jclepro.2020.123713.

[92] A.E. Lavat, M.A. Trezza, M. Poggi, Characterization of ceramic roof tile wastes as pozzolanic admixture, Waste Manag. 29 (2009) 1666–1674, https://doi.org/10.1016/j.wasman.2008.10.019.

[93] J. Golden, E. Gomes, A. Roy, Y.T. Su, De La Concorde Overpass Bridge Collapse: Analysis of a Historical Failure, Technical Report, 2018, https://doi.org/10.13140/RG.2.2.17401.01129.

[94] W. Yang, The Issues and Discussion of Modern Concrete Science, Springer, Berlin, Heidelberg, 2015, https://doi.org/10.1007/978-3-662-47247-7.

[95] J.H. Keyser, Scaling of Concrete by Frost Action, in: E.G. Swenson (Ed.), Performance of Concrete: Resistance of Concrete to Sulphate and Other Environmental Conditions. A Symposium in Honour of Thorbergur Thorvaldson, University of Toronto Press, Toronto, 1968, pp. 230–244, https://doi.org/10.3138/9781487584092-014.

[96] S. Mindess, Resistance of Concrete to Destructive Agencies, in: P.C. Hewlett, M. Liska (Eds.), Lea's Chemistry of Cement and Concrete (Fifth Edition), Butterworth-Heinemann, 2019, pp. 251–283, https://doi.org/10.1016/B978-0-08-100773-0.00006-X.

[97] J.Y.R. Liew, M.-X. Xiong, B.-L. Lai, Design of Steel-Concrete Composite Structures Using High Strength Materials, Elsevier Inc., 2021, https://doi.org/10.1016/C2019-0-05474-X .

[98] U. Wickström, A very simple method for estimating temperature in fire exposed concrete structures, Technical Report, Swedish National Testing Institute, 1986.

[99] K. Horová, T. Jána, F. Wald, Temperature heterogeneity during travelling fire on experimental building, Adv. Eng. Softw. 62–63 (2013) 119–130, https://doi.org/10.1016/j.advengsoft.2013.05.001.

[100] M. Jedidi, Effect of temperature rise caused by fire on the physical and mechanical properties of concrete, Insight - Civ. Eng. 7 (2024) 319, https://doi.org/10.18282/ice.v7i1.319.

[101] R.-S. Lin, Y. Han, X.-Y. Wang, Macro–meso–micro experimental studies of calcined clay limestone cement (LC3) paste subjected to elevated temperature, Cem. Concr. Compos. 116 (2021) 103871, https://doi.org/10.1016/j.cemconcomp.2020.103871.

[102] J.J. Hamilton, G.O. Handegord, The performance of ordinary Portland cement concrete in prairie soils of high sulphate content, in: E.G. Swenson (Ed.), Performance of Concrete: Resistance of Concrete to Sulphate and Other Environmental Conditions. A Symposium in Honour of Thorbergur Thorvaldson, University of Toronto Press, Toronto, 1968, pp. 135–158, https://doi.org/10.3138/9781487584092-010.

[103] B. Mather, Field and laboratory studies of the sulphate resistance of concrete, in: E.G. Swenson (Ed.), Performance of Concrete: Resistance of Concrete to Sulphate and Other Environmental Conditions. A Symposium in Honour of Thorbergur Thorvaldson, University of Toronto Press, Toronto, 1968, pp. 66–76, https://doi.org/10.3138/9781487584092-005.

[104] F.M. Lea, Some studies on the performance of concrete structures in sulphate-bearing environments, in: E.G. Swenson (Ed.), Performance of Concrete: Resistance of Concrete to Sulphate and Other Environmental Conditions. A Symposium in Honour of Thorbergur Thorvaldson, University of Toronto Press, Toronto, 1968, pp. 56–65, https://doi.org/10.3138/9781487584092-004.

[105] G.J. Verbeck, Field and laboratory studies of the sulphate resistance of concrete, in: E.G. Swenson (Ed.), Performance of Concrete: Resistance of Concrete to Sulphate and Other Environmental Conditions. A Symposium in Honour of Thorbergur Thorvaldson, University of Toronto Press, Toronto, 1968, pp. 113–124, https://doi.org/10.3138/9781487584092-008.

[106] L.A. López Ruiz, X. Roca Ramón, S. Gassó Domingo, The circular economy in the construction and demolition waste sector – A review and an integrative model approach, J. Clean. Prod. 248 (2019) 119238, https://doi.org/10.1016/j.jclepro.2019.119238.

[107] M. Menegaki, D. Damigos, A review on current situation and challenges of construction and demolition waste management, Curr. Opin. Green Sustain. Chem. 13 (2018) 8–15, https://doi.org/10.1016/j.cogsc.2018.02.010.

[108] A. Adessina, A. Ben Fraj, J.-F. Barthélémy, Improvement of the compressive strength of recycled aggregate concretes and relative effects on durability properties, Constr. Build. Mater. 384 (2023) 131447, https://doi.org/10.1016/j.conbuildmat.2023.131447.

[109] H. Wu, R. Hu, D. Yang, Z. Ma, Micro-macro characterizations of mortar containing construction waste fines as replacement of cement and sand: A comparative study, Constr. Build. Mater. 383 (2023) 131328, https://doi.org/10.1016/j.conbuildmat.2023.131328.

[110] Z. Ma, J. Shen, C. Wang, H. Wu, Characterization of sustainable mortar containing high-quality recycled manufactured sand crushed from recycled coarse aggregate, Cem. Concr. Compos. 132 (2022) 104629, https://doi.org/10.1016/j.cemconcomp.2022.104629.

[111] L. Bogoviku, D. Waldmann, Experimental investigations on the interfacial bond strength of the adhered mortar paste to the new mortar paste in a recycled concrete matrix, Constr. Build. Mater. 347 (2022), 128509, https://doi.org/10.1016/j. conbuildmat.2022.128509.

[112] B. Luo, D. Wang, E. Mohamed, The process of optimizing the interfacial transition zone in ultra-high performance recycled aggregate concrete through immersion in a water glass solution, Mater. Lett. 338 (2023), 134056, https://doi.org/10.1016/j. matlet.2023.134056.

[113] B.J. Zhan, D.X. Xuan, C.S. Poon, K.L. Scrivener, Characterization of interfacial transition zone in concrete prepared with carbonated modeled recycled concrete aggregates, Cem. Concr. Res. 136 (2020), 106175, https://doi.org/10.1016/j. cemconres.2020.106175.

[114] G.C. Lee, H.B. Choi, Study on interfacial transition zone properties of recycled aggregate by micro-hardness test, Constr. Build. Mater. 40 (2013) 455–460, https://doi.org/10.1016/j.conbuildmat.2012.09.114.

[115] W. Li, J. Xiao, Z. Sun, S. Kawashima, S.P. Shah, Interfacial transition zones in recycled aggregate concrete with different mixing approaches, Constr. Build. Mater. 35 (2012) 1045–1055, https://doi.org/10.1016/j. conbuildmat.2012.06.022.

[116] V.M. Raman, J., Ramasamy, V., Various treatment techniques involved to enhance the recycled coarse aggregate in concrete: A review, Mater. Today:. Proc. 45 (7) (2021) 6356–6363, https://doi.org/10.1016/j.matpr.2020.10.935.

[117] A.A. Bahraq, J. Jose, M. Shameem, M. Maslehuddin, A review on treatment techniques to improve the durability of recycled aggregate concrete: Enhancement mechanisms, performance and cost analysis, J. Build. Eng. 55 (2022), 104713, https://doi.org/10.1016/j.jobe.2022.104713.

[118] V.W.Y. Tam, M. Soomro, A.C.J. Evangelista, Quality improvement of recycled concrete aggregate by removal of residual mortar: A comprehensive review of approaches adopted, Constr. Build. Mater. 288 (2021), 123066, https://doi.org/10.1016/j.conbuildmat.2021.123066.

[119] C.M.M.A. Silva, M.M.L. Pereira, V.M.S. Capuzzo, J. de Brito, Concrete produced with recycled concrete aggregate exposed to treatment methods, Case Stud. Constr. Mater. 18 (2023) e01938.

[120] B. Zhang, Y. Feng, J. Xie, W. Chen, Z. Xue, G. Zhao, Y. Li, J. Li, J. Yang, Compressive behaviour and microstructures of concrete incorporating pretreated recycled powder/aggregates: The coupling effects of calcination and carbonization, J. Build. Eng. 68 (2023), 106158, https://doi.org/10.1016/j.jobe.2023.106158.

[121] Y. Li, T. Fu, R. Wang, Y. Li, An assessment of microcracks in the interfacial transition zone of recycled concrete aggregates cured by CO2, Constr. Build. Mater. 236 (2020), 117543, https://doi.org/10.1016/j.conbuildmat.2019.117543.

[122] L. Li, Q. Liu, T. Huang, W. Peng, Mineralization and utilization of CO2 in construction and demolition wastes recycling for building materials: A systematic review of recycled concrete aggregate and recycled hardened cement powder, Sep. Purif. Technol. 298 (2022), 121512, https://doi.org/10.1016/j.seppur.2022.121512.

[123] H. Zhang, W. Liu, X. Lin, S. Su, B. Zhao, To ameliorate the performance of recycled aggregate concrete (RAC) by pre-treating aggregate in sulfoaluminate cement slurry and water glass solution, J. Build. Eng. 44 (2021), 103364, https://doi.org/10.1016/j.jobe.2021.103364.

[124] A.S. Alqarni, H. Abbas, K.M. Al-Shwikh, Y.A. Al-Salloum, Treatment of recycled concrete aggregate to enhance concrete performance, Constr. Build. Mater. 307 (2021), 124960, https://doi.org/10.1016/j.conbuildmat.2021.124960.

[125] World Economic Forum Shaping the Future of Construction: A Breakthrough in Mindset and Technology 2016 http://www3.weforum.org/docs/WEF_Shaping_the_Future_of_Construction_full_report__.pdf.

[126] P.R. de Matos, R.D. Sakata, L. Onghero, V.G. Uliano, J. de Brito, C.E.M. Campos, P. J.P. Gleize, Utilization of ceramic tile demolition waste as supplementary cementitious material: an early-age investigation, J. Build. Eng. 38 (2021) 1–12, https://doi.org/10.1016/j.jobe.2021.102187.

[127] M.V.A. Florea, Z. Ning, H.J.H. Brouwers, Activation of liberated concrete fines and their application in mortars, Constr. Build. Mater. 50 (2014) 1–12, https://doi.org/10.1016/j.conbuildmat.2013.09.012.

[128] Z. He, A. Shen, H. Wu, W. Wang, L. Wang, C. Yao, J. Wu, Research progress on recycled clay brick waste as an alternative to cement for sustainable construction materials, Constr. Build. Mater. 274 (2021) 1–13, https://doi.org/10.1016/j.conbuildmat.2020.122113.

[129] S.K. Kaliyavaradhan, T.C. Ling, K.H. Mo, Valorization of waste powders from cement-concrete life cycle: a pathway to circular future, J. Clean. Prod. 268 (2020) 1–25, https://doi.org/10.1016/j.jclepro.2020.122358.

[130] Y.J. Kim, Y.W. Choi, Utilization of waste concrete powder as a substitution material for cement, Constr. Build. Mater. 30 (2012) 500–504, https://doi.org/10.1016/j.conbuildmat.2011.11.042.

[131] T.C.F. Oliveira, B.G.S. Dezen, E. Possan, Use of concrete fine fraction waste as a replacement of Portland cement, J. Clean. Prod. 273 (2020) 1–9, https://doi.org/10.1016/j.jclepro.2020.123126.

[132] Z. Prosek, V. Nezerka, R. Hlůzek, J. Trejbal, P. Tesarek, Karraa, G.,, Role of lime, fly ash, and slag in cement pastes containing recycled concrete fines, Constr. Build. Mater. 201 (2019) 702–714, https://doi.org/10.1016/j.conbuildmat.2018.12.227.

[133] M. Frías, S. Martínez-Ramírez, R. Vigil de la Villa, L. Fernandez-Carrasco, R. García, Reactivity in cement pastes bearing fine fraction concrete and glass from construction and demolition waste: Microstructural analysis of viability, Cem. Concr. Res. 148 (2021), 106531, https://doi.org/10.1016/j.cemconres.2021.106531.

[134] F.N. Costa, D.V. Ribeiro, Reduction in CO2 emissions during production of cement, with partial replacement of traditional raw materials by civil construction waste (CCW), J. Clean. Prod. 276 (2020) 1–11, https://doi.org/10.1016/j.jclepro.2020.123302.

[135] D. Gastaldi, F. Canonico, L. Capelli, L. Buzzi, E. Boccaleri, S. Irico, An investigation on the recycling of hydrated cement from concrete demolition waste, Cem. Concr. Compos. 61 (2015) 29–35, https://doi.org/10.1016/j.cemconcomp.2015.04.010.

[136] D. Oh, T. Noguchi, R. Kitagaki, H. Choi, Proposal of demolished concrete recycling system based on performance evaluation of inorganic building materials manufactured from waste concrete powder, Renew. Sust. Energ. Rev. 135 (2021) 1–9, https://doi.org/10.1016/j.rser.2020.110147.

[137] J. Schoon, K. De Buysser, I. Van Driessche, N. De Belie, Fines extracted from recycled concrete as alternative raw material for Portland cement clinker production, Cem. Concr. Compos. 58 (2015) 70–80, https://doi.org/10.1016/j.cemconcomp.2015.01.003.

[138] S. Zhutovsky, A. Shishkin, Recycling of hydrated Portland cement paste into new clinker, Constr. Build. Mater. 280 (2021) 1–8, https://doi.org/10.1016/j.conbuildmat.2021.122510.

[139] S.A. Miller, V.M. John, S.A. Pacca, A. Horvath, Carbon dioxide reduction potential in the global cement industry by 2050, Cem. Concr. Res. 114 (2018) 115–124, https://doi.org/10.1016/j.cemconres.2017.08.026.

[140] L. Bogoviku, D. Waldmann, Modelling of mineral construction and demolition waste dynamics through a combination of geospatial and image analysis, J. Environ. Manag. 282 (2021) 1–14, https://doi.org/10.1016/j.jenvman.2020.111879.

[141] F. Splittgerber, A. Mueller, Inversion of the cement hydration as a new method for identification and/or recycling, 11th ICCC, 2003, DOI: 10.13140/2.1.2201.3766.

[142] S. Lim, P. Mondal, Micro- and nano-scale characterization to study the thermal degradation of cement-based materials, Mater Charact 92 (2014) 15–25, https://doi.org/10.1016/j.matchar.2014.02.010.

[143] X. Shi, Q. Cai, C. Qi, L. Zhang, X. Lu, W. Zhou, B. Zhao, Co-utilization of reactivated cement pastes with coal gangue, Constr. Build. Mater. 270 (2021), 121423, https://doi.org/10.1016/j.conbuildmat.2020.121423.

[144] L. Xu, J. Wang, K. Li, S. Lin, M. Li, T. Hao, Z. Ling, D. Xiang, T. Wang, A systematic review of factors affecting properties of thermal-activated recycled cement, Resour. Conserv. Recycl. 185 (2022), 106432, https://doi.org/10.1016/j.resconrec.2022.106432.

[145] S. Real, A. Carriço, J.A. Bogas, M. Guedes, Influence of the Treatment Temperature on the Microstructure and Hydration Behavior of Thermoactivated Recycled Cement Materials 13 18 3937.

[146] J. Wang, M. Mu, Y. Liu, Recycled cement, Constr. Build. Mater. 190 (2018) 1124–1132, https://doi.org/10.1016/j.conbuildmat.2018.09.181.

[147] Z. Shui, D. Xuan, H. Wan, B. Cao, Rehydration reactivity of recycled mortar from concrete waste experienced to thermal treatment, Constr. Build. Mater. 22 (2008) 1723–1729, https://doi.org/10.1016/j.conbuildmat.2007.05.012.

[148] L. Alarcon-Ruiz, G. Platret, E. Massieu, A. Ehrlacher, The use of thermal analysis in assessing the effect of temperature on a cement paste, Cem. Concr. Res. 35 (2005) 609–613, https://doi.org/10.1016/j.cemconres.2004.06.015.

[149] N. Algourdin, B. Sy Hung, Z. Mesticou, A. Si Larbi, Effects of high temperature on mechanical behaviour and physicochemical properties of recycled mortars and its components, Constr. Build. Mater. 248 (2020) 118554.

[150] EN 196-1, Methods of testing cement — Part 1: Determination of strength.

[151] EN 196-3, Methods of testing cement — Part 3: Determination of setting times and soundness.

[152] ISO 679:2009, Cement — Test methods — Determination of strength.

[153] ASTM C311/C311M, Standard Test Methods for Sampling and Testing Fly Ash or Natural Pozzolans for Use in Portland-Cement Concrete.

[154] L. Zhang, Y. Ji, G. Huang, J. Li, Y. Hu, Modification and enhancement of mechanical properties of dehydrated cement paste using ground granulated blast-furnace slag, Constr. Build. Mater. 164 (2018) 525–534, https://doi.org/10.1016/ j.conbuildmat.2017.12.232.

[155] Z. Wan, T. He, N. Chang, R. Yang, H. Qiu, Effect of silica fume on shrinkage of cement-based materials mixed with alkali accelerator and alkali-free accelerator, J. Mater. Res. Technol. 22 (2023) 825–837, https://doi.org/10.1016/j.jmrt.2022.11.110.

[156] T. Dorn, O. Blask, D. Stephan, Acceleration of cement hydration – A review of the working mechanisms, effects on setting time, and compressive strength development of accelerating admixtures, Constr. Build. Mater. 323 (2022), 126554, https://doi.org/10.1016/j.conbuildmat.2022.126554.

[157] H. Uchikawa, S. Uchida, K. Ogawa, S. Hanehara, Influence of CaSO4.2H20, CaSO4.1/2H20 and CaSO4 on the initial hydration of clinker having different burning degree, Cem. Concr. Res. 14 (1984) 645–656, https://doi.org/10.1016/0008-8846(84)90027-9.

[158] G. Tzouvalas, N. Dermatas, S. Tsimas, Alternative calcium sulfate-bearing materials as cement retarders: Part I, Anhydrite. Cem. Concr. Res. 34 (2004) 2113–2118, https://doi.org/10.1016/j.cemconres.2004.03.020.

[159] Z. Ding, J. Chen, S. Zheng, Y. Hu, Y. Fang, Influence of anhydrite on the properties and microstructure of aluminophosphate cement, Materials 15 (2022) 7005, https://doi.org/10.3390/ma15197005.

[160] K. Elert, P. Bel-Anzue, M. Burgos-Ruiz, Influence of calcination temperature on hydration behavior, strength, and weathering resistance of traditional gypsum plaster, Constr. Build. Mater. 367 (2023), 130361, https://doi.org/10.1016/j.conbuildmat.2023.130361.

[161] A. Vimmrova, J. Krejsova, L. Scheinherrova, M. Dolezelova, M. Keppert, Changes in structure and composition of gypsum paste at elevated temperatures, J. Therm. Anal. Calorim. 142 (2020) 19–28, https://doi.org/10.1007/s10973-020-09528-8.

[162] R.A. Berenguer, A.P.B. Capraro, M.H. Farias de Medeiros, A.M.P. Carneiro, R.A. De Oliveira, Sugar cane bagasse ash as a partial substitute of Portland cement: effect on mechanical properties and emission of carbon dioxide, J. Environ. Chem. Eng. 8 (2020) 1–7, https://doi.org/10.1016/j.jece.2020.103655.

[163] R. Berenguer, N. Lima, L. Pinto, E. Monteiro, Y. Povoas, R. Oliveira, N.B.D. Lima, Cement-based materials: Pozzolanic activities of mineral additions are compromised by the presence of reactive oxides, J. Build. Eng. 41 (2021) 1–14, https://doi.org/10.1016/j.jobe.2021.102358.

[164] M. Heikal, M.E.A. Zaki, S.M. Ibrahim, Characterization, hydration, durability of nano-Fe2O3-composite cements subjected to sulphates and chlorides media, Constr. Build. Mater. 269 (2021) 1–16, https://doi.org/10.1016/j. conbuildmat.2020.121310.

[165] Raverdy, M., Brivot, F., Paillere, A. M., Dron, R., 1980. Appréciation de l'activité pouzzolanique des constituants secondaires. 7th Int. Congr. Chem. Cem. [in French], 36 – 41.

[166] S. Tsivilis, E. Chaniotakis, E. Badogiannis, G. Pahoulas, A. Ilias, A study on the parameters affecting the properties of Portland limestone cements, Cem. Concr. Compos. 21 (1999) 107–116, https://doi.org/10.1016/S0958-9465(98)00031-6.

[167] P. Pliya, D. Cree, Limestone derived eggshell powder as a replacement in Portland cement mortar, Constr. Build. Mater. 95 (2015) 1–9, https://doi.org/10.1016/j.conbuildmat.2015.07.103.

[168] M. Saraya, Study physico-chemical properties of blended cements containing fixed amount of silica fume, blast furnace slag, basalt and limestone, a comparative study, Constr. Build. Mater. 72 (2014) 104–112, https://doi.org/10.1016/j.conbuildmat.2014.08.071.

[169] A.H. Ali, A.M. Kandeel, A.S. Ouda, Hydration Characteristics of Limestone Filled Cement Pastes, Chem. Mater. Res. 5 (2013) 68–73. https://core.ac.uk/downloa d/pdf/234666405.pdf.

[170] M. Meziani, N. Leklou, O. Amiri, N. Chelouah, Physical and mechanical studies on binary blended Portland cements containing mordenite-rich tuff and limestone filler, Mater. Tech. 107 (2019) 1–12, https://doi.org/10.1051/mattech/2019021.

[171] M.S. Hemalatha, M. Santhanam, Characterizing supplementary cementing materials in blended mortars, Constr. Build. Mater. 191 (2018) 440–459, https://doi.org/10.1016/j.conbuildmat.2018.09.208.

[172] European Cement Research Academy (ECRA), 2017. Evaluation of the energy performance of cement kilns in the context of co-processing. Technical Report. https://cembureau.eu/media/oyahklgk/12042-ecra-energy-performance-cement-kilns-2017-10-15.pdf.

[173] J.S. Damtoft, J. Lukasik, D. Herfort, D. Sorrentino, E.M. Gartner, Sustainable development and climate change initiatives, Cem. Concr. Res. 38 (2008) 115–127, https://doi.org/10.1016/j.cemconres.2007.09.008.

[174] Cavalett, O., Cherubini, F., Olsson, O., 2021. Deployment of bio-CCS in the cement sector: an overview of technology options and policy tools. Report. International Energy Agency (IEA) Bioenergy. https://www.ieabioenergy.com/wp-content/uploads/2022/03/bio-CCS-in-the-cement-sector.pdf.

[175] Tokheim, L.A., Mathisen, A., Oi, L.E., Jayarathna, C., Eldrup, N., Gautestad, T., 2019. Combined calcination and CO2 capture in cement clinker production by use of electrical energy. Trondheim CCS Conference – CO2 Capture, Transport and Storage. TCCS-10 Trondheim, Norway.

[176] R.M. Andrew, Global CO_2 emissions from cement production, 1928–2018, Earth Syst. Sci. Data. 11 (2019) 1675–1710, https://doi.org/10.5194/essd-11-1675-2019.

[177] I. Etxebarria, M. Veneranda, I. Costantini, N. Prieto-Taboada, A. Larrañaga, C. Marieta, B. De Nigris, A. Martellone, V. Amoretti, G. Arana, J.M. Madariaga, K. Castro, Testing the volcanic material burying Pompeii as pozzolanic component for compatible conservation mortars, Case Stud. Constr. Mater. 18 (2023) e02194, https://doi.org/10.1016/j.cscm.2023.e02194.

[178] F. Marra, A. Danti, M. Gaeta, The volcanic aggregate of ancient Roman mortars from the Capitoline Hill: Petrographic criteria for identification of Rome's “pozzolans” and historical implications, J. Volcanol. Geotherm. Res. 308 (2015) 113-126, https://doi.org/10.1016/j.jvolgeores.2015.10.007.

[179] H. Goldsworthy, M. Zhu, Mortar studies towards the replication of Roman concrete, Archaeometr 51(6) (2009) 932-946, https://doi-org.proxy.bnl.lu/10.1111/j.1475-4754.2009.00450.x.

[180] F. Marra, M. Anzidei, A. Benini, E. D'Ambrosio, M. Gaeta, G. Ventura, A. Cavallo, Petro-chemical features and source areas of volcanic aggregates used in ancient Roman maritime concretes, J. Volcanol. Geotherm. Res. 328 (2016) 59-69, https://doi.org/10.1016/j.jvolgeores.2016.10.005.

[181] B.B Sabir, S. Wild, J. Bai, Metakaolin and calcined clays as pozzolans for concrete: a review, Cem. Concr. Compos. 23(6) (2001) 441-454, https://doi.org/10.1016/S0958-9465(00)00092-5.

[182] N.J. Coleman, W.R. Mcwhinnie, The solid state chemistry of metakaolin-blended ordinary Portland cement, J. Mater. Sci. 35 (2000) 2701–2710, https://doi.org/10.1023/A:1004753926277.

[183] Q. Wan, F. Rao, S. Song, Reexamining calcination of kaolinite for the synthesis of metakaolin geopolymers - roles of dehydroxylation and recrystallization, J. Non-Cryst. Solids. 460 (2017) 74-80, https://doi.org/10.1016/j.jnoncrysol.2017.01.024.

[184] E. Navratilova, P. Rovnanikova, Pozzolanic properties of brick powders and their effect on the properties of modified lime mortars, Constr. Build. Mater. 120 (2016) 530-539, https://doi.org/10.1016/j.conbuildmat.2016.05.062.

[185] A.T. Bakera, M.G. Alexander, Use of metakaolin as supplementary cementitious material in concrete, with focus on durability properties, RILEM Tech. Lett. 4 (2019) 89-102, http://dx.doi.org/10.21809/rilemtechlett.2019.94.

[186] C.B. Carter, M.G. Norton, Ceramic Materials: Science and Engineering, Springer, New York, 2007.

[187] E. Asensio, C. Medina, M. Frias, M.I. Sanchez de Rojas, Characterization of ceramic-based construction and demolition waste: use as pozzolan in cements, J. Am. Ceram. Soc. 99(12) (2016) 4121–4127, https://doi.org/10.1111/jace.14437.

[188] S. Wild, A. Gailius, H. Hansen, L. Pederson, J. Szwabowski, Pozzolanic properties of a variety of European clay bricks, Build. Res. Inf., 25(3) (1997) 170-175, https://doi.org/10.1080/096132197370435.

[189] E. Vejmelkova, D. Konakova, M.Cachova, M. Zaleska, P. Svora, M. Keppert, P. Rovnanikova, R.Cerny, High-strength concrete based on ternary binder with high pozzolan content, Struct. Concr. 19(5) (2018) 1258–1267, https://doi.org/10.1002/suco.201700173.

[190] E. Lasseuguette, S. Burns, D. Simmons, E. Francis, H.K. Chai, V. Koutsos, Y. Huang, Chemical, microstructural and mechanical properties of ceramic waste blended cementitious systems, J. Clean. Prod., 211 (2019) 1228-1238, https://doi.org/10.1016/j.jclepro.2018.11.240.

[191] F. Andreola, L. Barbieri, I. Lancellotti, M.C. Bignozzi, F. Sandrolini, New blended cement from polishing and glazing ceramic sludge, Int. J. Appl. Ceram., 7(4) (2010) 546-555, https://doi.org/10.1111/j.1744-7402.2009.02368.x.

[192] P.R. de Matos, L.R. Prudencio, A.L. de Oliveira, F. Pelisser, P.J.P. Gleize, Use of porcelain polishing residue as a supplementary cimentitious material in self-compacting concrete, Constr. Build. Mater. 193 (2018) 623-630, https://doi.org/10.1016/j.conbuildmat.2018.10.228.

[193] J.M. Ortega, V. Letelier, C. Solas, G. Moriconi, M.A. Climent, I. Sanchez, Long-term effects of waste brick powder addition in the microstructure and service properties of mortars, Constr. Build. Mater. 182 (2018) 691-702, https://doi.org/10.1016/j.conbuildmat.2018.06.161.

[194] X. Chen, D. Zhang, S. Cheng, X. Xu, C. Zhao, X. Wang, Q. Wu, X. Bai, Sustainable reuse of ceramic waste powder as a supplementary cementitious material in recycled aggregate concrete: Mechanical properties, durability and microstructure assessment, J. Build. Eng. 52 (2022) 104418, https://doi.org/10.1016/j.jobe.2022.104418.

[195] C.M. Carvalho, N.P. Barbosa, U.T. Bezerra, T.B. Simas, Red ceramic industry residues: Used to produce Portland cement, Case Stud. Constr. Mater. 13 (2020) e00449, https://doi.org/10.1016/j.cscm.2020.e00449.

[196] P.C. Jacoby, F. Pelisser, Pozzolanic effect of porcelain polishing residue in Portland cement, J. Clean. Prod. 100 (2015) 84-88, http://dx.doi.org/10.1016/j.jclepro.2015.03.096.

[197] P. Jain, R. Gupta, S. Chaudhary, A literature review on the effect of using ceramic waste as supplementary cementitious material in cement composites on workability and compressive strength, Mater. Today: Proc. 65(2) (2022) 871-876, https://doi.org/10.1016/j.matpr.2022.03.453.

[198] R.D. Toledo Filho, J.P. Goncalves, B.B. Americano, E.M.R. Fairbairn, Potential for use of crushed waste calcined-clay brick as a supplementary cementitious material in Brazil, Cem. Concr. Res. 37(9) (2007) 1357-1365, http://dx.doi.org/10.1016/j.cemconres.2007.06.005.

[199] A. Heidari, D. Tavakoli, A study of the mechanical properties of ground ceramic powder concrete incorporating nano-SiO2 particles, Constr. Build. Mater. 38 (2013) 255-264, http://dx.doi.org/10.1016/j.conbuildmat.2012.07.110.

[200] L.R. Steiner, A.M. Bernardin, F. Pelisser, Effectiveness of ceramic tile polishing residues as supplementary cementitious materials for cement mortars, SM&T 4 (2015) 30-35, http://dx.doi.org/10.1016/j.susmat.2015.05.001.

[201] L.G. Li, Z.Y. Zhuo, A.K.H. Kwan, T.S. Zhang, D.G. Lu, Cementing efficiency factors of ceramic polishing residue in compressive strength and chloride resistance of mortar, Powder Technol. 367 (2020) 163-171, https://doi.org/10.1016/j.powtec.2020.03.050.

[202] A. Abreu, S.H.L. da Silva, R. Schneider, A. Bail, Effects for partial replacement of Portland cement by low water absorption porcelain insulator, Materialia 24 (2022) 101488, https://doi.org/10.1016/j.mtla.2022.101488.

[203] G. Baronio, L. Binda, Study of the pozzolanicity of some bricks and clays, Constr. Build. Mater. 11(1) (1997) 41-46, https://doi.org/10.1016/S0950-0618(96)00032-3.

[204] S. Mohammed, Processing, effect and reactivity assessment of artificial pozzolans obtained from clays and clay wastes: A review, Constr. Build. Mater. 140 (2017) 10-19, https://doi.org/10.1016/j.conbuildmat.2017.02.078.

[205] F. Pacheco-Torgal, S. Jalali, Reusing ceramic wastes in concrete, Constr. Build. Mater. 24(5) (2010) 832-838, https://doi.org/10.1016/j.conbuildmat.2009.10.023.

[206] M. Mohit, H. Haftbaradaran, H.T. Riahi, Investigating the ternary cement containing Portland cement, ceramic waste powder, and limestone, Constr. Build. Mater. 369 (2023) 130596, https://doi.org/10.1016/j.conbuildmat.2023.130596.

[207] NF P18–513 (2012): Addition for concrete - Metakaolin - Specifications and conformity criteria, AFNOR – Association Française de Normalisation.

[208] ASTM C618: Standard specification for coal fly ash and raw or calcined natural pozzolan for use in concrete.

[209] M. Keppert, E. Vejmelkova, P. Bezdicka, M. Dolezelova, M. Cachova, L. Scheinherrova, J. Pokorny, M. Vysvaril, P. Rovnanikova, R. Cerny, Red-clay ceramic powders as geopolymer precursors: Consideration of amorphous portion and CaO content, Appl. Clay Sci. 161 (2018) 82-89, https://doi.org/10.1016/j.clay.2018.04.019.

[210] D. Konakova, V. Pommer, M. Jerman, M. Keppert, R. Cerny, E. Vejmelkova, Utilization of ceramic powder, calcined shale and sintered mullite as partial replacements of calcium aluminate cement, Constr. Build. Mater. 326 (2022) 126824, https://doi.org/10.1016/j.conbuildmat.2022.126824.

[211] Y.F. Chen, M.C. Wang, M.H. Hon, Phase transformation and growth of mullite in kaolin ceramics, J. Eur. Ceram. 24(8) (2004) 2389-2397, https://doi-org.proxy.bnl.lu/10.1016/S0955-2219(03)00631-9.

[212] J. Martin-Marquez, A.G. De la Torre, M.A.G. Aranda, J.M. Rincon, M. Romero, Evolution with Temperature of crystalline and amorphous phases in porcelain stoneware, J. Am. Ceram. Soc. 92(1) (2009) 229-234, https://doi.org/10.1111/j.1551-2916.2008.02862.x.

[213] F. Chargui, M. Hamidouche, H. Belhouchet, Y. Jorand, R. Doufnoune, G. Fantozzi, Mullite fabrication from natural kaolin and aluminium slag, Bol. Soc. Esp. Ceram. Vidr. 57(4) (2018) 169-177, https://doi-org.proxy.bnl.lu/10.1016/j.bsecv.2018.01.001.

[214] M. Fugazzotto, G. Cultrone, P. Mazzoleni, G. Barone, Suitability of ceramic industrial waste recycling by alkaline activation for use as construction and restoration materials, Ceram. Int. 49(6) (2023) 9465-9478, https://doi.org/10.1016/j.ceramint.2022.11.111.

[215] A.L. Campinho Paes, L.C.G. Botelho, G. de Castro Xavier, C.M. Fontes Vieira, A.R.G. Azevedo, S.N. Monteiro, Ground waste ceramic brick effect at different times on mortar, J. Mater. Res. Technol. 24 (2023) 3513-3523, https://doi-org.proxy.bnl.lu/10.1016/j.jmrt.2023.03.191.

[216] F. Puertas, I. Garcia-Diaz, A. Barba, M.F. Gazulla, M. Palacios, M.P. Gomez, S. Martinez-Ramirez, Ceramic wastes as alternative raw materials for Portland cement clinker production, Cem. Concr. Compos. 30(9) (2008) 798-805, https://doi.org/10.1016/j.cemconcomp.2008.06.003.

[217] M. Raverdy, F. Brivot, A.M. Paillere, R. Dron, Appréciation de l'activité pouzzolanique des constituants secondaires. 7th Int. Congr. Chem. Cem. (1980) 36-41 (in French).

[218] M.G. Medeiros, W.C. Nadaleti, J.C. Rocha, M. Cheriaf, P.J.P. Gleise, A.B. de Castilhos, A cleaner material production by the incorporation of the rockwool waste into portland cement matrices, J. Clean. Prod. 293 (2021) 126059, https://doi.org/10.1016/j.jclepro.2021.126059.

[219] V.M. Pereira, R.H. Geraldo, R. Baldusco, G. Camarini, Porcelain waste from electrical insulators in self-leveling mortar: Materials characterization and properties, J. Build. Eng. 61 (2022) 105297, https://doi.org/10.1016/j.jobe.2022.105297.

[220] J.P. Bigas and J.L. Gallias, Effect of fine mineral additions on granular packing of cement mixtures, Mag. Concr. Res. 54(3) (2002) 155-164, https://doi.org/10.1680/macr.2002.54.3.155.

[221] A. Lecomte, J.M. Mechling, C. Diliberto, Compaction index of cement paste of normal consistency, Constr. Build. Mater. 23(10) (2009) 3279-3286, https://doi-org.proxy.bnl.lu/10.1016/j.conbuildmat.2009.05.005.

[222] B. Luzu, R. Trauchessec, A. Lecomte, Packing density of limestone calcined clay binder, Powder Technol. 408 (2022) 117702, https://doi-org.proxy.bnl.lu/10.1016/j.powtec.2022.117702.

[223] T. Matschei, B. Lothenbach, F.P. Glasser, The AFm phase in Portland cement, Cem. Concr. Res. 37(2) (2007) 118-130, https://doi.org/10.1016/j.cemconres.2006.10.010.

[224] H.A. Shah, Q. Yuan, S. Zuo, Air entrainment in fresh concrete and its effects on hardened concrete-a review, Constr. Build. Mater. 274 (2021) 121835, https://doi.org/10.1016/j.conbuildmat.2020.121835.

[225] M.K. Memon, K.A. Elraies, M.I.A. Al-Mossawy, Surfactant screening to generate strong foam with formation water and crude oil, J. Petrol. Explor. Prod. Technol. 11 (2021) 3521–3532, https://doi.org/10.1007/s13202-021-01251-w.

[226] S.N. Abbas, M.I. Qureshi, Influence on the durability properties of concrete after incorporating different types of recycled aggregates: A review, Prog. Eng. Sci. 1 (2024) 100026, https://doi.org/10.1016/j.pes.2024.100026.

[227] L. Wu, Z. Sun, Y. Cao, Modification of recycled aggregate and conservation and application of recycled aggregate concrete: A review, Constr. Build. Mater. 431 (2024) 136567, https://doi.org/10.1016/j.conbuildmat.2024.136567.

[228] F. Muhammad, M. Harun, A. Ahmed, N. Kabir, H.R. Khalid, A. Hanif, Influence of bonded mortar on recycled aggregate concrete properties: A review, Constr. Build. Mater. 432 (2024) 136564, https://doi.org/10.1016/j.conbuildmat.2024.136564.

[229] A. Hasheminezhad, D. King, H. Ceylan, S. Kim, Comparative life cycle assessment of natural and recycled aggregate concrete: A review, Sci. Total Environ. 950 (2024) 175310, https://doi.org/10.1016/j.scitotenv.2024.175310.

[230] C.M. Nwakaire, S.P. Yap, C.C. Onn, C.W. Yuen, H.A. Ibrahim, Utilisation of recycled concrete aggregates for sustainable highway pavement applications; a review, Constr. Build. Mater. 235 (2020) 117444, https://doi.org/10.1016/j.conbuildmat.2019.117444.

[231] R.P. Neupane, N.R. Devi, T. Imjai, A. Rajput, T. Noguchi, Cutting-edge techniques and environmental insights in recycled concrete aggregate production: A comprehensive review, RCR Advances, 25 (2025) 200241, https://doi.org/10.1016/j.rcradv.2024.200241.

[232] A.O. Tanash, K. Muthusamy, F.M. Yahaya, M.A. Ismail, Potential of recycled powder from clay Brick, sanitary Ware, and concrete waste as a cement substitute for Concrete: An overview, Constr. Build. Mater. 401 (2023) 132760, https://doi.org/10.1016/j.conbuildmat.2023.132760.

[233] C. Martin, E. Manu, P. Hou, S. Adu-Amankwah, Circular economy, data analytics, and low carbon concreting: A case for managing recycled powder from end-of-life concrete, Resour. Conserv. Recycl. 198 (2023) 107197, https://doi.org/10.1016/j.resconrec.2023.107197.

[234] M. Zanovello, R. Baldusco, V.M. John, S.C. Angulo, Strength-porosity correlation and environmental analysis of recycled Portland cement, Resour. Conserv. Recycl. 190 (2023) 106763, https://doi.org/10.1016/j.resconrec.2022.106763.

[235] Y. Zheng, X. Xi, H. Liu, C. Du, H. Lu, A review: Enhanced performance of recycled cement and CO2 emission reduction effects through thermal activation and nanosilica incorporation, Constr. Build. Mater. 422 (2024) 135763, https://doi.org/10.1016/j.conbuildmat.2024.135763.

[236] A. Carriço, S. Real, J.A. Bogas, Durability performance of thermoactivated recycled cement concrete, Cem. Concr. Compos. 124 (2021) 104270, https://doi.org/10.1016/j.cemconcomp.2021.104270.

[237] J.A. Bogas, A. Carriço, S. Real, Durability of concrete produced with recycled cement from waste concrete, Mater. Today Proc. 58 (2022) 1149-1154, https://doi.org/10.1016/j.matpr.2022.01.280.

[238] B. Cantero, M. Bravo, J. de Brito, I.F.S. del Bosque, C. Medina, Assessment of the Permeability to Aggressive Agents of Concrete with Recycled Cement and Mixed Recycled Aggregate, Appl. Sci. 11 (2021) 3856, https://doi.org/10.3390/app11093856.

[239] R. Hu, C. Wang, J. Shen, Z. Ma, Chloride transport and thermoactivated modification of sustainable cement-based materials with high-content waste concrete powder, J. Mater. Res. Technol. 23 (2023) 4012-4031, https://doi.org/10.1016/j.jmrt.2023.02.048.

[240] L. Xu, J. Wang, X. Hu, B. Ran, T. Wu, X. Zhou, Y. Xiong, Physical performance, durability, and carbon emissions of recycled cement concrete and fully recycled concrete, Constr. Build. Mater. 447 (2024) 138128, https://doi.org/10.1016/j.conbuildmat.2024.138128.

[241] C. Sun, L. Chen, J. Xiao, A. Singh, J. Zeng, Compound utilization of construction and industrial waste as cementitious recycled powder in mortar, Resour. Conserv. Recycl. 170 (2021) 105561, https://doi.org/10.1016/j.resconrec.2021.105561.

[242] Z. Ma, P. Yao, D. Yang, J. Shen, Effects of fire-damaged concrete waste on the properties of its preparing recycled aggregate, recycled powder and newmade concrete, J. Mater. Res. Technol. 15 (2021) 1030-1045, https://doi.org/10.1016/j.jmrt.2021.08.116.

[243] Y. Wu, C. Liu, H. Liu, H. Hu, C. He, L. Song, W. Huang, Pore structure and durability of green concrete containing recycled powder and recycled coarse aggregate, J. Build. Eng. 53 (2022) 104584, https://doi.org/10.1016/j.jobe.2022.104584.

[244] Y. Gao, X. Cui, N. Lu, S. Hou, Z. He, C. Liang, Effect of recycled powders on the mechanical properties and durability of fully recycled fiber-reinforced mortar, J. Build. Eng. 45 (2022) 103574, https://doi.org/10.1016/j.jobe.2021.103574.

[245] N. Algourdin, Q.N.A. Nguyen, Z. Mesticou, A. Si Larbi, Durability of recycled fine mortars under freeze–thaw cycles, Constr. Build. Mater. 291 (2021) 123330, https://doi.org/10.1016/j.conbuildmat.2021.123330.

[246] C. Sun, L. Chen, J. Xiao, J. Zuo, H. Wu, Effects of eco powders from solid waste on freeze-thaw resistance of mortar, Constr. Build. Mater. 333 (2022) 127405, https://doi.org/10.1016/j.conbuildmat.2022.127405.

[247] S. Li, J. Gao, Q. Li, X. Zhao, Investigation of using recycled powder from the preparation of recycled aggregate as a supplementary cementitious material, Constr. Build. Mater. 267 (2021) 120976, https://doi.org/10.1016/j.conbuildmat.2020.120976.

[248] A.A. Belkadi, O. Kessal, A. Berkouche, A. Noui, S.E. Daguiani, M. Dridi, S. Benaniba, T. Tayebi, Experimental investigation into the potential of recycled concrete and waste glass powders for improving the sustainability and performance of cement mortars properties, Sustain. Energy Technol. Assess. 64 (2024) 103710, https://doi.org/10.1016/j.seta.2024.103710.

[249] O. Onuaguluchi, N. Banthia, Entrained air and freeze-thaw durability of concrete incorporating nano-fibrillated cellulose (NFC), Cem. Concr. Compos. 150 (2024) 105582, https://doi.org/10.1016/j.cemconcomp.2024.105582.

[250] J. Kim, N. Nciri, A. Sicakova, N. Kim, Characteristics of waste concrete powders from multi-recycled coarse aggregate concrete and their effects as cement replacements, Constr. Build. Mater. 398 (2023) 132525, https://doi.org/10.1016/j.conbuildmat.2023.132525.

[251] H. Wu, C. Wang, Z. Ma, Drying shrinkage, mechanical and transport properties of sustainable mortar with both recycled aggregate and powder from concrete waste, J. Build. Eng. 49 (2022) 104048, https://doi.org/10.1016/j.jobe.2022.104048.

[252] A. Carriço, J.A. Bogas, S. Real, M.F.C. Pereira, Shrinkage and sorptivity of mortars with thermoactivated recycled cement, Constr. Build. Mater. 333 (2022) 127392, https://doi.org/10.1016/j.conbuildmat.2022.127392.

[253] H. Wu, J. Gao, C. Liu, X. Luo, G. Chen, Combine use of 100% thermoactivated recycled cement and recycled aggregate for fully recycled mortar: Properties evaluation and modification, J. Clean. Prod. 450 (2024) 141841, https://doi.org/10.1016/j.jclepro.2024.141841.

[254] A. Tokareva, S. Kaassamani, D. Waldmann, Fine demolition wastes as Supplementary cementitious materials for CO2 reduced cement production, Constr. Build. Mater. 392 (2023) 131991, https://doi.org/10.1016/j.conbuildmat.2023.131991.

[255] D. Qian, R. Yu, Z. Shui, Y. Sun, C. Jiang, F. Zhou, M. Ding, X. Tong, Y. He, A novel development of green ultra-high performance concrete (UHPC) based on appropriate application of recycled cementitious material, J. Clean. Prod. 261 (2020) 121231, https://doi.org/10.1016/j.jclepro.2020.121231.

[256] Z. Duan, S. Hou, J. Xiao, B. Li, Study on the essential properties of recycled powders from construction and demolition waste, J. Clean. Prod. 253 (2020) 119865, https://doi.org/10.1016/j.jclepro.2019.119865.

[257] EN 480-5:2005, Admixtures for concrete, mortar and grout – Test methods – Part 5: Determination of capillary absorption.

[258] EN 12617-4:2002, Products and systems for the protection and repair of concrete structures - Test methods - Part 4: Determination of shrinkage and expansion.

[259] M. Ebrahimi, A. Eslami, I. Hajirasouliha, M. Ramezanpour, K. Pilakoutas, Effect of ceramic waste powder as a binder replacement on the properties of cement- and lime-based mortars, Constr. Build. Mater. 379 (2023) 131146, https://doi.org/10.1016/j.conbuildmat.2023.131146.

[260] L. Zhang, X. Qian, T. Lin, S. Ruan, D. Yan, K. Qian, Is early drying shrinkage still determined by the mesopore content? A case study of cement paste with minerals, J. Build. Eng. 50 (2022) 104187, https://doi.org/10.1016/j.jobe.2022.104187.

[261] P. Schiller, M. Wahab, T. Bier, H.-J. Mögel, A model for elucidating the contributions of meso- and macropores to water sorption and strain in cementitious materials, Cem. Concr. Res. 151 (2022) 106589, https://doi.org/10.1016/j.cemconres.2021.106589.

[262] A. Rhardane, S.A.H. Sleiman, S.Y. Alam, F. Grondin, A quantitative assessment of the parameters involved in the freeze–thaw damage of cement-based materials through numerical modelling, Constr. Build. Mater. 272 (2021) 121838, https://doi.org/10.1016/j.conbuildmat.2020.121838.

[263] O. Keleştemur, S. Yildiz, B. Gökçer, E. Arici, Statistical analysis for freeze–thaw resistance of cement mortars containing marble dust and glass fiber, Mater. Des. 60 (2014) 548-555, https://doi.org/10.1016/j.matdes.2014.04.013.

[264] A.E. Richardson, K.A. Coventry, S. Wilkinson, Freeze/thaw durability of concrete with synthetic fibre additions, Cold Reg. Sci. Technol. 83–84 (2012) 49-56, https://doi.org/10.1016/j.coldregions.2012.06.006.

[265] D. Cree, M. Green, A. Noumowé, Residual strength of concrete containing recycled materials after exposure to fire: A review, Constr. Build. Mater. 45 (2013) 208-223, https://doi.org/10.1016/j.conbuildmat.2013.04.005.

[266] C.J. Zega, A.A. Di Maio, Recycled concrete made with different natural coarse aggregates exposed to high temperature, Constr. Build. Mater. 23 (2009) 2047-2052, https://doi.org/10.1016/j.conbuildmat.2008.08.017.

[267] R. Cao, J. Yang, G. Li, F. Liu, M. Niu, W. Wang, Resistance of the composite cementitious system of ordinary Portland/calcium sulfoaluminate cement to sulfuric acid attack, Constr. Build. Mater. 329 (2022) 127171, https://doi.org/10.1016/j.conbuildmat.2022.127171.

[268] H.A. Khan, A. Castel, M.S.H. Khan, A.H. Mahmood, Durability of calcium aluminate and sulphate resistant Portland cement based mortars in aggressive sewer environment and sulphuric acid, Cem. Concr. Res. 124 (2019) 105852, https://doi.org/10.1016/j.cemconres.2019.105852.

[269] E. Rozière, A. Loukili, R.El Hachem, F. Grondin, Durability of concrete exposed to leaching and external sulphate attacks, Cem. Concr. Res. 39 (2009) 1188-1198, https://doi.org/10.1016/j.cemconres.2009.07.021.

[270] L. Gu, T. Bennett, P. Visintin, Sulphuric acid exposure of conventional concrete and alkali-activated concrete: Assessment of test methodologies, Constr. Build. Mater. 197 (2019) 681-692, https://doi.org/10.1016/j.conbuildmat.2018.11.166.

[271] A.H. Saputra, M. Shohibi, M. Kubouchi, Effect of Fly Ash Fortification in the Manufacture Process of Making Concrete towards Characteristics of Concrete in Sulfuric Acid Solution, Makara J. Technol. 19/3 (2015) 133-140, https://doi.org/10.7454/mst.v19i3.3045.

[272] C. Rispoli, A. De Bonis, V. Guarino, S.F. Graziano, C. Di Benedetto, R. Esposito, V. Morra, P. Cappelletti, The ancient pozzolanic mortars of the thermal complex of Baia (Campi Flegrei, Italy), Constr. Build. Mater. 40 (2019) 143–154. https://doi.org/10.1016/j.culher.2019.05.010.

[273] V.A.L. Silveira, D.S. de Resende, A.C.S. Bezerra, Sanitary ware waste in eco-friendly Portland blended cement: Potential use as supplementary cementitious material, CEMENT 19 (2025) 100126. https://doi.org/10.1016/j.cement.2024.100126.

[274] D.M. Kannan, S.H. Aboubakr, A.S. El-Dieb, M.M. Reda Taha, High performance concrete incorporating ceramic waste powder as large partial replacement of Portland cement, Constr. Build. Mater. 144 (2017) 35–41. https://doi.org/10.1016/j.conbuildmat.2017.03.115.

[275] J.P. Gonçalves, L.M. Tavares, R.D. Toledo Filho, E.M.R. Fairbairn, Performance evaluation of cement mortars modified with metakaolin or ground brick, Constr. Build. Mater. 23 (2009) 1971–1979. https://doi.org/10.1016/j.conbuildmat.2008.08.027.

[276] L. Pang, H. Liang, D. Zhang, K. Fang, Combining thermodynamic modeling and experiments to characterize the effect of ceramic polishing powder in cement-based materials, Constr. Build. Mater. 438 (2024) 137215. https://doi.org/10.1016/j.conbuildmat.2024.137215.

[277] K. Faldessai, S. Lawande, A. Kelekar, R. Gurav, S. Kakodkar, Utilization of ceramic waste as a partial replacement for cement in concrete manufacturing, Mater. Today Proc. (2023) in press. https://doi.org/10.1016/j.matpr.2023.06.453.

[278] A.S. El-Dieb, D.M. Kanaan, Ceramic waste powder: An alternative cement replacement—Characterization and evaluation, Sustain. Mater. Technol. 17 (2018) e00063. https://doi.org/10.1016/j.susmat.2018.e00063.

[279] R.M. Tremiño, T. Real-Herraiz, V. Letelier, J.M. Ortega, Four-years influence of waste brick powder addition in the pore structure and several durability-related parameters of cement-based mortars, Constr. Build. Mater. 306 (2021) 124839. https://doi.org/10.1016/j.conbuildmat.2021.124839.

[280] R.V. Meena, J.K. Jain, H.S. Chouhan, A.S. Beniwal, Use of waste ceramics to produce sustainable concrete: A review, Cleaner Mater. 4 (2022) 100085. https://doi.org/10.1016/j.clema.2022.100085.

[281] A. AlArab, B. Hamad, J.J. Assaad, Strength and durability of concrete containing ceramic waste powder and blast furnace slag, J. Mater. Civ. Eng. 34 (2022) 04031. https://doi.org/10.1061/(ASCE)MT.1943-5533.0004031.

[282] T. Kulovaná, E. Vejmelková, M. Keppert, P. Rovnaníková, Z. Keršner, R. Černý, Mechanical, durability and hygrothermal properties of concrete produced using Portland cement-ceramic powder blends, Struct. Concr. 17 (2016) 105–115. https://doi.org/10.1002/suco.201500029.

[283] S. Wang, V.T. Nguyen, Z. Xiu, W. Han, Test research on the effect of waste ceramic polishing powder on the compressive strength and chloride penetration resistance of seawater concrete, Constr. Build. Mater. 386 (2023) 131590. https://doi.org/10.1016/j.conbuildmat.2023.131590.

[284] S.V. Zito, G.P. Cordoba, E.F. Irassar, V.F. Rahhal, Durability of eco-friendly blended cements incorporating ceramic waste from different sources, J. Sustain. Cement-Based Mater. 12 (2022) 13–23. https://doi.org/10.1080/21650373.2021.2010242.

[285] H. Mohammadhosseini, N.H.A.S. Lim, M.M. Tahir, et al., Effects of waste ceramic as cement and fine aggregate on durability performance of sustainable mortar, Arab. J. Sci. Eng. 45 (2020) 3623–3634. https://doi.org/10.1007/s13369-019-04198-7.

[286] K. Faldessai, S. Lawande, A. Kelekar, R. Gurav, S. Kakodkar, Utilization of ceramic waste as a partial replacement for cement in concrete manufacturing, Mater. Today Proc. (2023) in press. https://doi.org/10.1016/j.matpr.2023.06.453.

[287] J. Mañosa, A. Calderón, R. Salgado-Pizarro, A. Maldonado-Alameda, J.M. Chimenos, Research evolution of limestone calcined clay cement (LC3), a promising low-carbon binder – A comprehensive overview, Heliyon 10 (2024) e25117. https://doi.org/10.1016/j.heliyon.2024.e25117.

[288] N. Ijaz, W.-M. Ye, Z. ur Rehman, Z. Ijaz, M.F. Junaid, Global insights into micro-macro mechanisms and environmental implications of limestone calcined clay cement (LC3) for sustainable construction applications, Sci. Total Environ. 907 (2024) 167794. https://doi.org/10.1016/j.scitotenv.2023.167794.

[289] M. Sharma, S. Bishnoi, F. Martirena, K. Scrivener, Limestone calcined clay cement and concrete: A state-of-the-art review, Cem. Concr. Res. 149 (2021) 106564. https://doi.org/10.1016/j.cemconres.2021.106564.

[290] P.R. de Matos, G. Doerner, S. da Silva Nazário, J. da Silva Andrade Neto, M. Longhi, M. Folgueras, E.D. Rodríguez, Limestone calcined clay cements (LC3) produced with iron ore tailings and ceramic waste: Hydration, mechanical performance and rheology, Constr. Build. Mater. 458 (2025) 139604. https://doi.org/10.1016/j.conbuildmat.2024.139604.

[291] J.M. Marangu, Effects of sulfuric acid attack on hydrated calcined clay–limestone cement mortars, J. Sustain. Cement-Based Mater. 10 (2020) 257–271. https://doi.org/10.1080/21650373.2020.1810168.

[292] A. Tokareva, S. Kaassamani, D. Waldmann, Using ceramic demolition wastes for CO_2-reduced cement production, Constr. Build. Mater. 426 (2024) 135980. https://doi.org/10.1016/j.conbuildmat.2024.135980.

[293] S. Indhumathi, S.P. Kumar, M. Pichumani, Reconnoitring principles and practice of modified Andreasen and Andersen particle packing theory to augment engineered cementitious composite, Constr. Build. Mater. 353 (2022) 129106. https://doi.org/10.1016/j.conbuildmat.2022.129106.

[294] T. Yin, K. Liu, D. Fan, R. Yu, Derivation and verification of multilevel particle packing model for ultra-high performance concrete (UHPC): Modelling and experiments, Cem. Concr. Compos. 136 (2023) 104889. https://doi.org/10.1016/j.cemconcomp.2022.104889.

[295] K. Liu, T. Yin, D. Fan, J. Wang, R. Yu, Multiple effects of particle size distribution modulus (q) and maximum aggregate size (Dmax) on the characteristics of ultra-high performance concrete (UHPC): Experiments and modeling, Cem. Concr. Compos. 133 (2022) 104709. https://doi.org/10.1016/j.cemconcomp.2022.104709.

[296] H.J.H. Brouwers, H.J. Radix, Self-compacting concrete: Theoretical and experimental study, Cem. Concr. Res. 35 (2005) 2116–2136. https://doi.org/10.1016/j.cemconres.2005.06.002.

[297] A. Tokareva, D. Waldmann, Durability of cement mortars containing fine demolition wastes as supplementary cementitious materials, Constr. Build. Mater. 477 (2025) 141316. https://doi.org/10.1016/j.conbuildmat.2025.141316.

[298] L. Li, P. Joseph, X. Zhang, L. Zhang, A study of some relevant properties of concrete incorporating waste ceramic powder as a cement replacement agent, J. Build. Eng. 87 (2024) 109106. https://doi.org/10.1016/j.jobe.2024.109106.

[299] F. Pacheco-Torgal, S. Jalali, Reusing ceramic wastes in concrete, Constr. Build. Mater. 24 (2010) 832–838. https://doi.org/10.1016/j.conbuildmat.2009.10.023.

[300] M. Nasir, W.O. Alimi, E.A. Oladapo, M. Imran, Z.A. Kazmi, Behavior of drying and plastic shrinkage of Portland cement concrete prepared and cured under harsh field, Dev. Built Environ. 16 (2023) 100252. https://doi.org/10.1016/j.dibe.2023.100252.

[301] C. Zhou, X. Zhang, J. Qiao, J. Feng, Q. Zeng, The deformation of C–S–H gels and its link with dynamic length change of cement pastes upon drying and resaturation, Cem. Concr. Res. 187 (2025) 107693. https://doi.org/10.1016/j.cemconres.2024.107693.

[302] P.J. McDonald, O. Istok, M. Janota, A.M. Gajewicz-Jaromin, D.A. Faux, Sorption, anomalous water transport and dynamic porosity in cement paste: a spatially localised ^{1}H NMR relaxation study and a proposed mechanism, Cem. Concr. Res. 133 (2020) 106045. https://doi.org/10.1016/j.cemconres.2020.106045.

[303] N.M. Alderete, Y.A. Villagrán Zaccardi, N. De Belie, Physical evidence of swelling as the cause of anomalous capillary water uptake by cementitious materials, Cem. Concr. Res. 120 (2019) 256–266. https://doi.org/10.1016/j.cemconres.2019.04.001.

[304] Y. Miao, W. Yu, L. Jin, L. Wang, J. Lin, Y. Li, Z. Lu, J. Jiang, Effect of shrinkage-induced initial damage on the frost resistance of concrete in cold regions, Eng. Fract. Mech. 312 (2024) 110652. https://doi.org/10.1016/j.engfracmech.2024.110652.

[305] C.-S. Poon, S. Azhar, M. Anson, Y.-L. Wong, Comparison of the strength and durability performance of normal- and high-strength pozzolanic concretes at elevated temperatures, Cem. Concr. Res. 31 (2001) 1291–1300. https://doi.org/10.1016/S0008-8846(01)00580-4.

[306] M. Heikal, Effect of temperature on the physico-mechanical and mineralogical properties of homra pozzolanic cement pastes, Cem. Concr. Res. 30 (2000) 1835–1839. https://doi.org/10.1016/S0008-8846(00)00403-8.

[307] H.E.H. Seleem, A.M. Rashad, T. Elsokary, Effect of elevated temperature on physico-mechanical properties of blended cement concrete, Constr. Build. Mater. 25 (2011) 1009–1017. https://doi.org/10.1016/j.conbuildmat.2010.06.078.

[308] R. Chong, W. Zhang, B. Yin, K.M. Liew, Evaluating next-gen sustainable cementitious materials: Unleashing the potential of LC3-based composites under high-temperature environments, J. Clean. Prod. 503 (2025) 145421. https://doi.org/10.1016/j.jclepro.2025.145421.

[309] D. Sinkhonde, R.O. Onchiri, W.O. Oyawa, J.N. Mwero, Durability and water absorption behaviour of rubberised concrete incorporating burnt clay brick powder, Cleaner Mater. 4 (2022) 100084. https://doi.org/10.1016/j.clema.2022.100084.

[310] J. Kim, A. Ubysz, Thermal activation of multi-recycled concrete powder as supplementary cementitious material for repeated and waste-free recycling, J. Build. Eng. 98 (2024) 111169. https://doi.org/10.1016/j.jobe.2024.111169

[311] A. Gholizadeh-Vayghan, G. Meza Hernandez, F.K. Kingne, J. Gu, N. Dilissen, M. El Kadi, T. Tysmans, J. Vleugels, H. Rahier, R. Snellings, Thermal reactivation of hydrated cement paste: Properties and impact on cement hydration, Materials 17 (2024) 2659. https://doi.org/10.3390/ma17112659

[312] M. Zanovello, S. Angulo, Thermoactivated recycled cement waste: optimal dehydration temperature and binder properties insights, Ambiente Construído 25 (2025) e143282. https://doi.org/10.1590/s1678-86212025000100889

[313] X. Xi, Y. Zheng, C. Du, P. Zhang, M. Sun, Study on the hydration characteristics, mechanical properties, and microstructure of thermally activated low-carbon recycled cement, Constr. Build. Mater. 447 (2024) 138042. https://doi.org/10.1016/j.conbuildmat.2024.138042.

[314] L. Chen, M. Wei, N. Lei, H. Li, Effect of chemical–thermal activation on the properties of recycled fine powder cementitious materials, Case Stud. Constr. Mater. 20 (2024) e02956. https://doi.org/10.1016/j.cscm.2024.e02956.

[315] W.-q. Zhai, R.-m. Sun, Y.-d. Xie, H.-c. Ding, Y. Su, Z.-h. He, Thermal-activated recycled cement powder synergized with fly ash as supplementary cementitious in Portland cement: Strength, microstructure and environmental benefits, Constr. Build. Mater. 474 (2025) 141018. https://doi.org/10.1016/j.conbuildmat.2025.141018.

[316] D.O. de Lima, D.S. de Lira, M. Frías Rojas, H. Savastano Junior, Assessment of the potential use of construction and demolition waste (CDW) fines as eco-pozzolan in binary and ternary cements, Constr. Build. Mater. 411 (2024) 134320. https://doi.org/10.1016/j.conbuildmat.2023.134320.

[317] M. Wei, L. Chen, N. Lei, H. Li, L. Huang, Mechanical properties and microstructures of thermally activated ultrafine recycled fine powder cementitious materials, Constr. Build. Mater. 475 (2025) 141195. https://doi.org/10.1016/j.conbuildmat.2025.141195.

[318] M. Zanovello, V.M. John, C.E. White, S.C. Angulo, Engineered blended thermoactivated recycled cement: A study on reactivity, water demand, strength-porosity, and CO2 emissions, ACS Sustain. Chem. Eng. 13 (2) (2025) 800–814. https://doi.org/10.1021/acssuschemeng.4c06567.

[319] B. Klemczak, J. Gołaszewski, G. Cygan, M. Gołaszewska, H. Jonkers, D. Zhilyaev, E.A.B. Koenders, Utilization of waste foam concrete with MPCM as a substitution material for cement in mortars, J. Build. Eng. 90 (2024) 109284. https://doi.org/10.1016/j.jobe.2024.109284.

[320] R. Subramanian, S. Vijayaprakash, Y. Subramaniyan, Y. Venkatraman, A study on the strength and durability of cement mortar featuring partial brick powder replacement: economic and sustainability implications, Matéria (Rio de Janeiro) 30 (2025) e20240792. https://doi.org/10.1590/1517-7076-RMAT-2024-0792.

[321] D. Koňáková, V. Pommer, K. Šádková, M. Záleská, M. Böhm, M. Keppert, E. Vejmelková, Heat-resistant composites based on ternary binders with a low cement content: Characterization and performance, Developments in the Built Environment 18 (2024) 100400. https://doi.org/10.1016/j.dibe.2024.100400.

[322] D. Koňáková, K. Šádková, R. Vaníčková, V. Pommer, M. Keppert, E. Vejmelková, The role of ceramic powder in sustainable thermal-resistant cement-based composites, Construction and Building Materials 487 (2025) 142095. https://doi.org/10.1016/j.conbuildmat.2025.142095.

[323] M. Wei, L. Chen, N. Lei, H. Li, L. Huang, Experimental investigation on freeze–thaw resistance of thermally activated recycled fine powder concrete, Construction and Building Materials 457 (2024) 139378. https://doi.org/10.1016/j.conbuildmat.2024.139378.

[324] E. M. Getachew, B. W. Yifru, B. T. Habtegebreal, M. D. Yehualaw, Performance evaluation of mortar with ground and thermo-activated recycled concrete cement, Cogent Engineering 11(1) (2024) 2357726. https://doi.org/10.1080/23311916.2024.2357726.

[325] O. Dehghani, A. Eslami, M. A. Mahdavipour, D. Mostofinejad, M. Ghorbani Mooselu, K. Pilakoutas, Ceramic waste powder as a cement replacement in concrete paving blocks: Mechanical properties and environmental assessment, Int. J. Pavement Eng. 25(1) (2024). https://doi.org/10.1080/10298436.2024.2370563.

[326] T. A. Tawfik, A. Sičáková, E. Kuzielová, et al., Sustainable reuse of waste ceramic tiles powder and waste brick powder as a replacement for cement on green high strength concrete properties, Innov. Infrastruct. Solut. 9 (2024) 166. https://doi.org/10.1007/s41062-024-01498-2.

Appendix

Appendix A.

Comparison of available works on the use of dehydrated cement in the production of binders.

Source	Main objective of study	Experiments	Precursor	Target temperature, °C	OPC replacement, %	Main conclusion
[40]	To check, whether the hydration of the cement is reversible to have a possibility to identify the original cement used in a concrete and for the recycling of all concrete constituents.	XRD, extraction of free lime by ethyl acetoacetate, Differential Calorimetric Analyses, compressive strength.	Laboratory made cement paste.	600, 900, 1100, 1200, 1400	100	The reactions of clinker hydration are reversible completely at the cement burning temperature, the addition of gypsum form an additional intermediary phase. Portland cement heated at 1100°C contains high amount of belite and free lime, while Portland cement with high sulfate resistance contains ye'elimite and blast furnace slag cement contains gehlenite.
[54]	Analysis of rehydration capability of concrete powder after thermal treatment.	TGA/DSC, XRD, SEM, compressive strength,	Laboratory made concrete.	200, 500, 800	100	Concrete powder heated at 500 °C consists of sand, dehydrated C–S–H, C2S, CaO, partial CH and dehydrated amorphous phase. Rehydration products have loose microstructure.

						Fly ash and OPC improves rehydration and mechanical properties of dehydrated cement.
[84]	Investigation of the cementitious characteristics and rehydration capability of dehydrated cement.	Standard consistency, setting time, compressive strength, LOI of dry rehydrated samples, SEM.	Laboratory made cement paste.	300, 400, 500, 600, 700, 800, 900	100	Rehydrated cement required more water for standard consistency and shows short setting time and rapid rehydration rate. These characteristics increase with dehydration temperature. The microstructure of the rehydrated cement is loose because of the fast formation of rehydration products occupying the internal space. The optimal dehydration temperature is 800°C.
[85]	To study the rehydration of cement pastes with different initial water/binder ratios treated at different temperatures.	XRD, SEM, standard consistency, setting time, compressive strength.	Laboratory made cement paste.	300, 400, 500, 600, 700, 800, 900	100	The water demand increases, and the setting time decreases with increasing of dehydration temperature and initial w/b ratio. Strength development of the recycled cement is attributed to the rehydration of dehydrated phases and the hydration of the initially

						unhydrated particles and depends on the dehydration temperature and initial w/b ratio. The microstructure of the rehydrated paste is loose because of the fast formation of hydration products occupying the internal spaces.
[86]	To identify factors affecting the cementitious characteristics of the dehydrated cement.	Compressive strength, statistical analysis of 9 factors influence: fineness, w/b ratio, NaOH content, OPC content, dehydration temperature, Silica Fume content, Silica Fume content in the precursor, sand residues in the precursor and clay brick residues in the precursor.	Laboratory made cement paste.	700, 750, 800	100	The following factors have the biggest influence on the strength of rehydrated cement: the degree of hydration of the precursor, the presence of silica fume in the precursor, the fineness of the dehydrated waste, and the replacement of the dehydrated cement with silica fume have a positive effect, while the presence of sand in the precursor and the high temperature of dehydration have a negative effect.
[87]	To investigate the effect of dehydrated cement particle agglomeration on its rehydration and microstructure development.	XRD, SEM, isothermal calorimetry, standard consistency, setting time, compressive strength.	Laboratory made cement paste.	650	5, 7.5, 10, 12.5, 15	Dehydrated cement has high water demand due to the water retention in the flaky layers of agglomerated particles. The optimal content

						of the dehydrated cement in the binder is 10%. Dispersed recycled cement creates additional C–S–H nucleation seeds.
[23]	To use recycled concrete powder received by a new method as Portland cement substitution.	TGA/DSC, XRD, SEM, isothermal calorimetry, flowability, flexural strength, compressive strength.	Laboratory made concrete.	500, 800	10, 20, 30	Dehydration products at 800°C are C2S and lime. The rehydration occurs in the first hour. The dehydrated cement has higher water demand. Recycled cement can be used to replace up to 20% of the OPC. Dehydrated cement has an activation effect on fly ash and ground granulated blast furnace slag.
[63]	To investigate the rehydration process of the cement with different additives (blast furnace slag, fly ash and limestone).	XRD, standard consistency, setting time, mercury intrusion porosimetry, flexural strength, compressive strength.	Laboratory made cement paste.	200, 400, 600, 800, 1000, 1200	100	Slag and fly ash do not positively affect the strength after rehydration. Samples with higher content of brownmillerite (C4AF) and lower content of larnite (C2S) have higher strength. Limestone is more suitable additive for the rehydration process than slag and fly ash.
[45]	To explain the effect of dehydration	XRD, isothermal calorimetry,	Laboratory made	699, 740, 800, 860, 901	100	Dehydration products are C2S polymorphs.

	process parameters on the hydration reactivity of the recycled cement and on the strength of pastes made with it.	compressive strength.	cement paste.			Stability and reactivity of alpha-C2S formed at lower temperatures are higher due to smaller crystallite size. Pastes made with cement dehydrated at lower temperatures have higher strengths. Optimal dehydration temperature is 740°C. Cooling rate had influence on the hydration at later ages.
[51]	Checking the possibility to produce cement which similar physical properties as OPC from a 2 - years old waste cement paste.	TGA, XRD, SEM, isothermal calorimetry, rheology measurement (shear stress, viscosity and dynamic yield stress), compressive strength.	Laboratory made cement paste.	120, 450, 750, 1150	100	Paste made of cement dehydrated at 450°C had a similar strength as OPC paste but with a poor workability. Increasing the dehydrated cement fineness and addition of blast-furnace slag improve the workability without reducing the strength.
[52]	Investigation of fresh and mechanical properties of mortars containing dehydrated mortars and concrete, analysis of influence of replacement	TGA, XRD, standard consistency, setting time, fresh density, flexural strength, compressive strength, ultrasonic pulse velocity,	Laboratory made cement paste and concrete.	350, 650	20, 50, 75, 100	Rehydrated paste showed higher efficiency than rehydrated concrete powder. Fineness of recycled cement is important. Incorporation of up to 20% of paste powder dehydrated at

	ratio, target temperature and fineness.	dynamic modulus of elasticity.				650°C does not affect the properties of mortar.
[88]	To evaluate the effects of mechanical and thermal treatment of concrete rubble on the properties of fine fraction and its potential use as a supplement of Portland cement.	TGA/DTA, XRD, SEM, isothermal calorimetry, flexural strength, compressive strength, water absorbability.	Laboratory made concrete.	288, 350, 500, 650, 712	25	Dehydrated concrete contains non-hydrated cement, calcium hydroxide, calcium oxide and dicalcium silicate. The calcination temperature had more significant effect on the rehydration of cement than the calcination time.
[47]	Microstructure development at ages up to 28 days of paste made of rehydrated cement.	TGA, XRD, isothermal calorimetry, SEM, mercury intrusion porosimetry, nitrogen adsorption, fresh density, flexural strength, compressive strength.	Laboratory made cement paste.	700	100	Dehydration product is new nesosilicate. Rehydration products at earliest age are AFm, carboaluminates, sulfoaluminates C-S-H, CH and ettringite. Paste of thermoactivated cement has high volume of hydration products and fine porosity.
[50]	Better knowledge of the cement rehydration by studying of the fresh and hardened properties of mortars with dehydrated cement.	TGA, XRD, isothermal calorimetry, standard consistency, setting time, soundness, flowability, SEM, nuclear magnetic resonance spectroscopy, flexural strength,	Laboratory made cement paste.	400, 500, 600, 800, 900	20, 50, 100	The dehydration product formed at 600-800°C is a new nesosilicate with a structure of the reactive polymorph α'L-C2S. The rehydration products are C-S-H with dimer and longer silicate chains and carbonates. The

		compressive strength.				optimal dehydration temperatures are 600-700°C. The optimal substitution rate is up to 50%.
[48]	Better understanding of the rehydration and microstructure of thermoactivated recycled cement.	TGA, XRD, standard consistency, setting time, SEM, isothermal calorimetry, nuclear magnetic resonance spectroscopy, flowability, flexural strength, compressive strength, mercury intrusion porosimetry.	Laboratory made cement paste.	400, 450, 500, 600, 650, 700, 750, 800, 900	100	Dehydration of cement at temperatures above 600°C forms C2S polymorphs. Rehydrated cement has high initial hydration heat, high water requirement and high setting time. The hydration products of thermoactivated cement and OPC are similar. The optimal dehydration temperatures are in the range 600-650°C.
[89]	Studying of hydration activity of thermally activated waste concrete powders.	Differential scanning calorimetry, XRD, SEM, flexural strength, compressive strength.	Laboratory made concrete.	200, 400, 600, 700, 800	30	Thermal treatment decreases the particle size of waste concrete powder. Free calcium oxide was formed after treatment at 800°C. Concrete powder treated at 700°C can be used as cement substitution material.
[90]	To study the use of dehydrated cement in the production of ultra-high-performance concrete. Dehydrated	XRD, isothermal calorimetry, SEM, flowability, compressive strength, shrinkage,	Laboratory made cement paste.	650	12.5, 25, 37.5, 50	Dehydrated cement can be used in the production of ultra-high-performance concrete with very dense

	cement is used to improve a compact packing structure of the concrete.	rapid chloride penetration test, mercury intrusion porosimetry, carbon footprint assessment.				microstructure. The optimal substitution rate is 25%. Using dehydrated cement can effectively reduce the CO2 emissions per unit volume of concrete and improve its performances.
[91]	Description and evaluation of the effectiveness of a new method for separation of hydrated cement and aggregates.	Qualitative image analysis, TGA, XRD, acid attack, flexural strength, compressive strength.	Laboratory made cement paste and concrete.	700	100	The method allows to obtain a recycled binder with cement content up to 80 wt% and recycled fine aggregates with cement contamination lower than 3 wt%. The mechanical strength of paste made of recycled binder was about 70% of that of OPC paste.
[92]	Characterization of the durability of concrete containing dehydrated cement.	Slump, fresh density, dry density, compressive strength, capillary absorption, oxygen permeability, rapid chloride migration, carbonation resistance tests.	Laboratory made cement paste and concrete.	650	5, 15, 30, 40, 100	Incorporation of up to 15% of the dehydrated paste or concrete resulted in similar durability to regular concrete. Using more than 30% of dehydrated concrete led to decreased durability compared to samples with recycled paste due to increased w/b. Concrete made of dehydrated cement has similar or better

						durability compared to regular concrete of the same strength class.
[93]	To evaluate the applicability of recycled cement powder for liquid radioactive waste immobilization.	XRD, compressive strength, leachability, freeze-thaw test.	Laboratory made concrete.	600	100	High water demand of dehydrated cement due to high surface area and low density. Dehydrated cement powder can be used for immobilization of liquid radioactive waste since the specimens with 3 M $CoCl_2$ and 3 M CsCl meet all the strength and leachability requirements.
[94]	To characterize the mechanical properties and shrinkage of concrete with various content of dehydrated cement and w/b ratio.	XRD, TGA, slump, fresh density, dry density, compressive strength, splitting tensile strength, ultrasonic pulse velocity, modulus of elasticity, shrinkage.	Laboratory made cement paste.	650	5, 15, 30, 40, 100	15% dehydrated cement can be added to concrete without significantly affecting workability. Dehydrated cement has high rehydration capacity. The optimum incorporation percentage is 15%, and concrete has similar or better characteristics than non-recycled concrete. The performance of recycled cement is improved by the addition of superplastisizer. Dehydrated cement also has a filler effect

						improving the concrete microstructure.
[44]	To study the co-utilization of dehydrated cement paste and coal gangue.	XRD, SEM, flowability, Fourier-transform infrared spectroscopy, compressive strength.	Laboratory made cement paste.	500, 600, 700, 800, 900	5, 10, 20, 30, 50 (mixed with coal gangue)	Dehydration products of cement paste are lime and β-C2S. Mixing it with coal gangue also creates quartz and mayenite. Adding coal gangue improves grinding of recycled cement and binder flowability. The optimum substitution rate was 30%, and the optimum calcination temperature was 800°C.
[49]	To analyse the rehydration behaviour and phase development of thermoactivated recycled cement pastes at early age.	TGA, XRD, isothermal calorimetry, SEM, nuclear magnetic resonance spectroscopy, flowability, flexural strength, compressive strength.	Laboratory made cement paste.	700	100	The fast early formation of AFm phases and carboaluminate hydrates during rehydration and high reactivity of α'H–C2S formed in dehydrated cement were confirmed. The amount of hydratable products in dehydrated cement is lower because of excess of carbonates. In the rehydrated paste the same type of C–S–H as is the OPC paste is formed.
[95]	To analyze the effects of the simultaneous replacement of	Flexural strength, compressive strength.	Demolition concrete.	400, 650, 900	5, 10, 15	The most influent parameters on the strength are the amount of the

	cement by dehydrated concrete fines and natural coarse aggregates by recycled aggregates on the mechanical properties of concrete.					recycled aggregates and the particle size of the dehydrated cement. The optimal combination of the parameters is: 20% of recycled aggregates, 5% of dehydrated at 900°C cement with a size <75 µm.
[61]	To investigate the effect of blast furnace slag on the grinding process and mechanical properties of dehydrated cement paste.	Particle size distribution, particle hardness, semi-adiabatic calorimetry, compressive strength, SEM.	Demolition concrete.	600	100 (mixed with blast furnace slag)	Blast furnace slag enhanced grinding efficiency of dehydrated cement. Recycled cement has better hydration rate than OPC in the early stage, but worse hydration in the later stage. Rehydrated cement showed low strength due to low particle hardness. Slag provides a micro-aggregate framework supporting the cementitious system with high mechanical properties.
[96]	To study the effects of retarders on properties of pastes based on dehydrated cement.	Standard consistency, setting time, compressive strength, semi-adiabatic calorimetry, SEM.	Demolition concrete.	600	100 (mixed with blast furnace slag at cement to slag ratio of 2:1)	The optimal retarder to prolong setting of the rehydrated cement and improve paste microstructure and strength is borax in an amount of 2%. Borax reacts with

						Ca2+ and aluminate in dehydrated phase forming a layer, which prevents water penetration into the cement particles.
[56]	To analyze the effects of dehydrated cement and recycled sand on the properties of cement mortar.	XRD, SEM, TGA/DSC, setting time, flowability, shrinkage, total porosity of mortars heated at 200 and 500°C, flexural and compressive strength of mortars heated at 200 and 500°C.	Demolition waste of unknown origin.	500	5, 10, 15, 20, 30, 50	The finer fraction of recycled concrete contains more reactive components than the coarser one. The addition of 10% of dehydrated cement does not have a significant effect on the workability. The optimal contents of the recycled sand and dehydrated cement for the mechanical properties of mortars are 20% and 15% respectively. Dehydrated cement increases the total porosity that decreases the heat resistance of the mortar.
Present research	To investigate the potential of fine mixed concrete-ceramic waste and mud from the recycled aggregates washing for use as SCMs and understand their behavior after	DTA/TGA, XRD, isothermal calorimetry, standard consistency, setting time, Chapelle test, compressive strength, SEM.	Concrete screening fines, mixed screening fines, mud from recycled aggregates washing.	450, 500	20	Uncalcined MS and WM, containing gypsum, increase setting time. Mortars with 20% of all three waste types had similar mechanical properties. Thermal treatment of

	thermal treatment.					waste slightly improves mortar's mechanical properties. Dehydrated at 500°C mixed wastes have weak hydraulic activity, but no pozzolanic activity.

Appendix B.

EDX microanalysis of the mineralogical phases identified by SEM: A – reference OPC mortar, B – CS500, C – MS500, D – WM500.